Conference Papers in Materials Science

International Conference on Natural Fibers—Sustainable Materials for Advanced Applications 2013

Guest Editors: Raul Fangueiro, R. Alagirusamy, Amar Mohanty, Hu Hong, and António Torres Marques

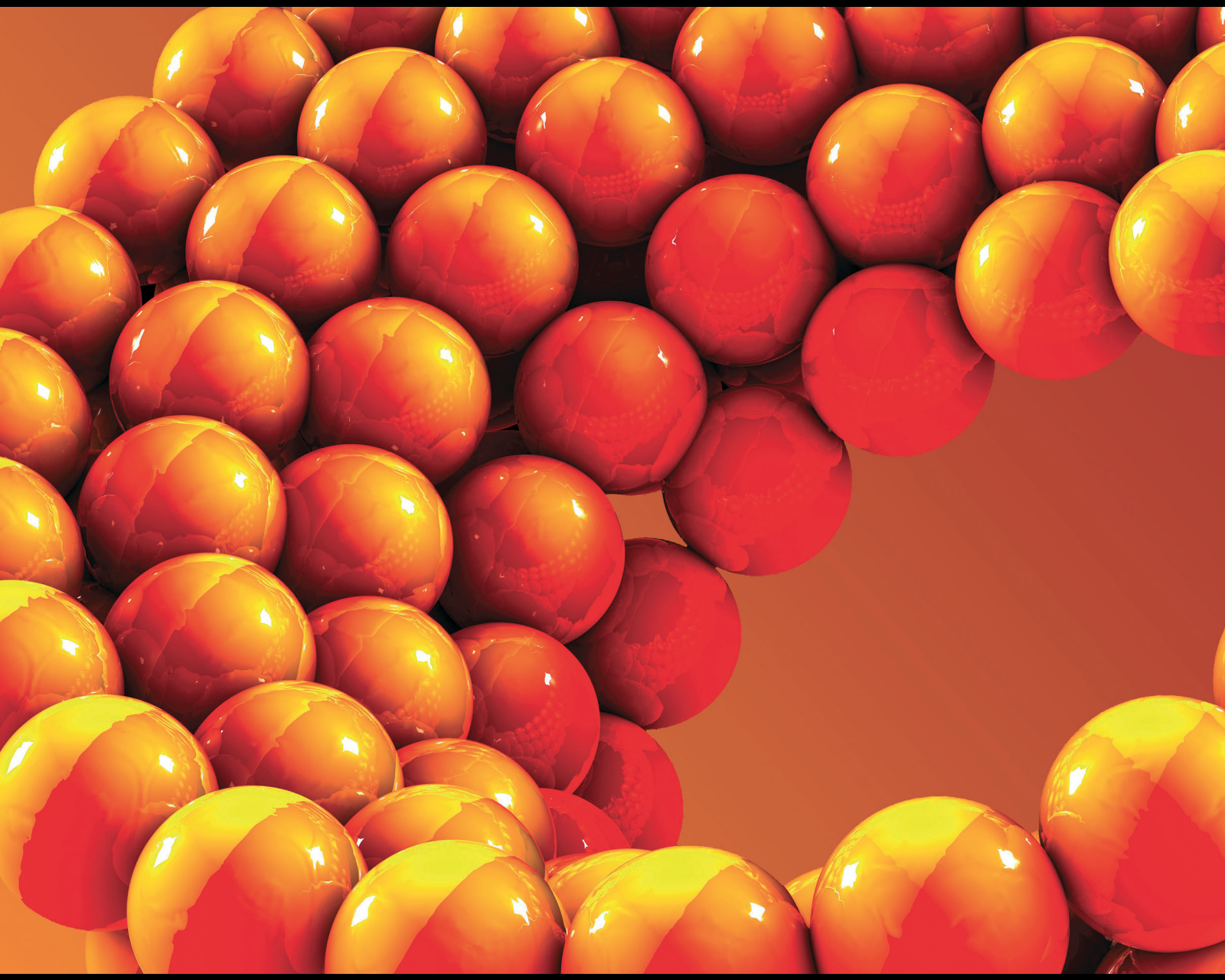

International Conference on Natural Fibers—Sustainable Materials for Advanced Applications 2013

Conference Papers in Materials Science

International Conference on Natural Fibers—Sustainable Materials for Advanced Applications 2013

Guest Editors: Raul Fangueiro, R. Alagirusamy,
Amar Mohanty, Hu Hong, and António Torres Marques

Editorial Board

Contents

Hindawi Publishing Corporation
Conference Papers in Materials Science
Volume 2013, Article ID 463790, 1 page
http://dx.doi.org/10.1155/2013/463790

Editorial

International Conference on Natural Fibers—Sustainable Materials for Advanced Applications 2013

Raul Fangueiro,[1] R. Alagirusamy,[2] Amar Mohanty,[3] Hu Hong,[4] and António Torres Marques[5]

[1] *Department of Civil Engineering, University of Minho, Guimarães, Portugal*
[2] *Department of Textile Technology, Indian Institute of Technology, Delhi, India*
[3] *Department of Plant Agriculture, School of Engineering, University of Guelph, Guelph, Canada*
[4] *Institute of Textiles and Clothing, The Hong Kong Polytechnic University, Hong Kong*
[5] *Department of Mechanical Engineering, University of Porto, Porto, Portugal*

Correspondence should be addressed to Raul Fangueiro; rfangueiro@civil.uminho.pt

Received 8 December 2013; Accepted 8 December 2013

Natural fibers are a renewable resource par excellence—they have been renewed by nature and human ingenuity for millennia. Besides, they are carbon neutral once they absorb the same amount of carbon dioxide which they produce. During processing, natural fibers generate mainly organic wastes and leave residues that can be used to generate energy or make ecological housing material. And, at the end of their life cycle, they are 100% biodegradable.

Natural fibers have widely enlarged their range of applications due to the intensive scientific and technical research undertaken by several institutes all over the world, turning these amazing materials into an alternative feasible choice for many situations in civil engineering, medicine, sports, architecture, and design, among others.

The 1st international conference on natural fibers—sustainable materials for future applications (ICNF2013) discussed all these new advances and the potential developments by bringing together companies, universities, research and technological centers, and entrepreneurs.

The proceedings of ICNF2013 are the most important scientific result of the event presenting several up-to-date papers on the following topics:

(i) animal and plant based natural fibers;

(ii) fibers produced based on natural resources—Innovative and functional natural fibers;

(iii) nanodimensional natural fibers (e.g., nanocellulose);

(iv) properties and characterization of natural fibers;

(v) new, efficient, and cost effective processes for natural fiber extraction and processing;

(vi) natural fiber modification techniques;

(vii) textile processing of natural fibers (spinning, weaving, coloration, finishing, etc.);

(viii) advanced fibrous structures based on natural fibers;

(ix) natural fiber based polymeric and cementitious composites;

(x) green composites;

(xi) applications of natural fibers in high-end sectors (civil engineering, medicine, transportation systems, sports, etc.);

(xii) innovative applications of natural fibers;

(xiii) product design with natural fibers;

(xiv) modelling and prediction of properties and behaviour.

Raul Fangueiro
R. Alagirusamy
Amar Mohanty
Hu Hong
António Torres Marques

Hindawi Publishing Corporation
Conference Papers in Materials Science
Volume 2013, Article ID 269313, 14 pages
http://dx.doi.org/10.1155/2013/269313

Conference Paper

Electrospun Nanomaterials: Biotechnology, Food, Water, Environment, and Energy

James J. Doyle,[1,2,3] Santosh Choudhari,[2] Seeram Ramakrishna,[4,5,6] and Ramesh P. Babu[2,3]

[1] *Dublin Dental School & Hospital, Trinity College Dublin, Lincoln Place, Dublin 2, Ireland*
[2] *CRANN Institute, Trinity College Dublin, Dublin 2, Ireland*
[3] *School of Physics, Trinity College Dublin, Dublin 2, Ireland*
[4] *Institute of Materials Research and Engineering, Singapore 117602*
[5] *King Saud University, Riyadh 11451, Saudi Arabia*
[6] *National University of Singapore, Center for Nanofibers and Nanotechnology, Department of Mechanical Engineering, Singapore 117576*

Correspondence should be addressed to Ramesh P. Babu; babup@tcd.ie

Received 29 April 2013; Accepted 8 September 2013

Academic Editors: R. Fangueiro and H. Hong

This Conference Paper is based on a presentation given by Seeram Ramakrishna at "International Conference on Natural Fibers—Sustainable Materials for Advanced Applications 2013" held from 9 June 2013 to 11 June 2013 in Guimarães, Portugal.

Over the past decade, electrospinning and electrospraying techniques have become affordable platform techniques for growing numbers of students, researchers, academics, and businesses around the world, producing organic and inorganic nanofibres and nanoparticles for a range of purposes. This review illustrates various advances in the science and engineering of electrospun nanomaterials and their applicability in meeting the growing needs within five crucial sectors: clean water, environment, energy, healthcare, and food. Although most of these sectors are principally dominated by synthetic polymer systems, the emergence of natural polymer and hybrid natural-synthetic electrospun polymer systems offers particular advantages. Current scientific and materials engineering advancements have resulted in highly competitive nanofibre, electrospun products, offering credible solutions to real-world applications.

1. Introduction

Electrospinning has attracted increased attention as a versatile technique, applicable to numerous organic and inorganic systems which can result in a tightly controlled size distribution of nanomaterials [1]. The resulting nanosystem can be described as highly porous network structure, with a large *surface area to volume* ratio, the dimensions of which can be easily tailored and optimised during production. It is commonly accepted that a material, which is termed *nano* in size, must possess at least one dimension of the order of 100 nm or less [2]. *Nanomaterials* can be produced in tube, wire, or particulate form and from both natural or synthetic material precursors [2, 3]. Numerous methods are employed to prepare higher volumes of nanomaterials, including chemical synthesis [4, 5], electrodeposition [6], templating [7], catalytic growth [8], chemical vapour deposition [9], and, more recently, electrospinning [10] techniques.

The electrospinning method allows for the high volume production of light weight, highly functional, nanoscale, mesh-like structures. Electrospraying is a similar technique to electrospinning, which electrostatically accelerates solution droplets onto a target, forming uniformly sized particulates or thin film coatings. The accelerated droplets can also be charged, leading to self-dispersion upon collection at the target. These *electrohydrodynamic* techniques result in a porous structure, which can be in film form as a coating or multidimensional network structure. The highly versatile

technique of electrospinning allows for the selective formation of micron to nanoscale fibrous systems by optimisation of electrostatic forces on a jet of polymer solution. In its most basic form, the electrospinning process involves placing a polymer solution in a pipette, between two electrodes, which can create potential difference in the kV regime. This large voltage then electrostatically draws the polymer solution towards a grounded target in a thin, continuous jet, leading to a deposition of a fibrous web. The resulting pore size and distribution within the web can be controlled by varying such parameters as the jet height, voltage, target type (static or rotated dynamically), and jet spindle speed. In addition to the optimisation of system parameters, advances in higher throughput electrospinning system designs continue to be developed [11–14].

Though acknowledging that the topic of electrospinning has its basis in early studies [15–17], the first filed patent based on an electrostatically controlled deposition system for plastics was in 1934 [18]. Since then in excess of 700 associated patents have been filed [19], citing Formals' core patent [18]. Overall nearly 2,500 patents associated with electrospinning have been filed for patenting [19]. Aligned with this patent trend has been an explosive increase in the number of journal publications related to electrospinning over the last 20 years [20], presented in Figure 1 with the number of citations inset. This increase has been attributed to both market and industry demands and also to the progress made in the field of nanotechnology. It is unsurprising that the number of patents granted in the same term mimics the same exponential increase over recent years. Figure 2(a) presents a graphical illustration of the number of patents granted over recent years, together with a global distribution analysis of those patents in Figure 2(b), displaying the emergence of electrospinning as a real solution to current commercial and industrial needs.

This review aims to provide a review of current electrospun nanomaterials research, processing, applications, technological limitations, and remaining challenges specific to the fields of biotechnology, food, water, environment, and energy.

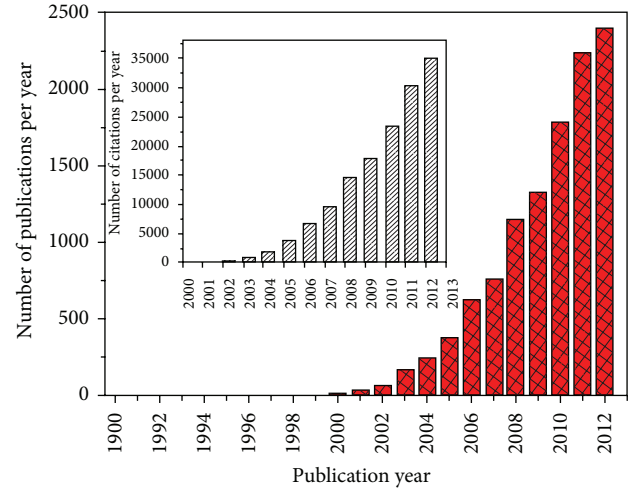

Figure 1: Graph displaying the yearly number of journal publications which include electrospinning in the concept (1990–2012). Inset: yearly number of citations for the same period.

2. Materials and Production

As described previously, electrospinning and electrospraying both involve simple *electrohydrodynamic* processing to form fibre sheets, particulates, or thin films from host solutions. The morphology of the final nanomaterial depends both on the type of polymer and solvent, under varying experimental conditions. This process can be adapted to any soluble polymers with sufficient molecular weight to electrospun. Electrospinning nanofibres will result in systems with high surface area to volume ratio, low weight, high density of pores, and high permeability with controlled, small fibre diameters. Numerous materials have been employed to produce electrospun fibres, tailored to meet the demands of specific functional requirements, including both natural and synthetic polymers, polymer blends, hybrid polymer systems, and ceramics and metals compounds [1, 21–23]. The diverse *real-world* applications have continued to steadily grow over recent years and include such areas as high performance air filters, sensors, textiles, medical wound dressing, photovoltaic cells, fuel cells, batteries, capacitors, and scaffolds for tissue engineering [1]. Figure 3 highlights some of the diverse and wide ranging potential applications and the potential applications in which natural polymers may provide a plausible solution.

In conjunction with the wide diversification of potential commercial applications, Figure 4 presents the electrospinning focussed patents granted between 1994 and 2012 in five main areas of interest to this review, highlighting the amazing versatility of electrospun polymer products. Currently there continues to be a keen focus on the biotechnology sector not only at research and development stage but also from a commercialisation viewpoint.

In conjunction with the growth in journal publications and patent filings, there are many well established companies who currently supply electrospun nanofibres to the market. A selection of current commercial suppliers of nanofibre-based commercial products is presented in Table 1.

3. Applications

Recently there has been a shift in focus from pure material fabrication towards end-use applications and appropriate functionality. Numerous overview papers have been published over recent years in the area of electrospinning [24–30]. This paper will focus on recent trends in electrospinning using various polymeric materials, emphasizing use of natural polymers specific to five main areas of interest—biotechnology, food, water, environment, and energy. Through continual progress in electrospinning techniques, we note the proliferation of coaxial, composite, and core-shell nanofibre systems with advanced functionality and the emergence of natural polymer systems as a solution to meet industrial needs.

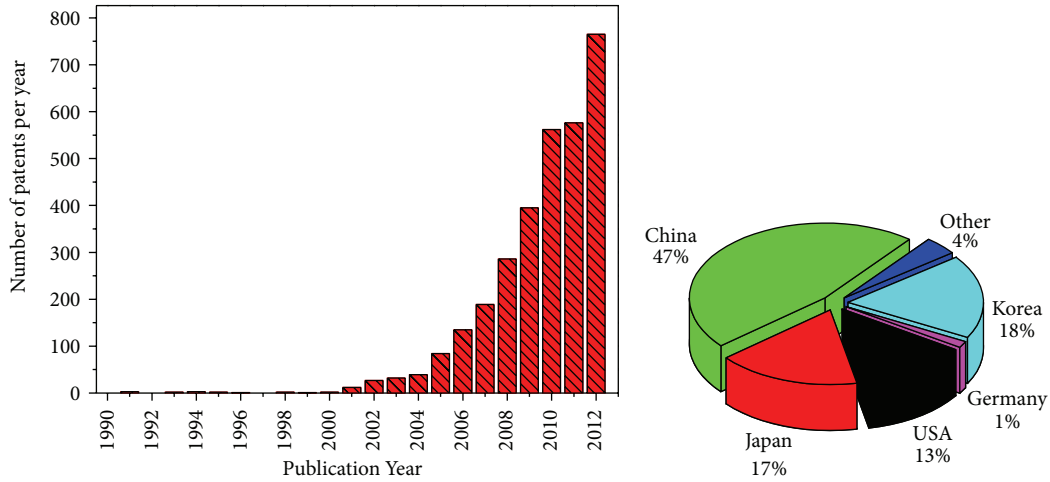

FIGURE 2: (a) Graph displaying the yearly number of patent filings which include electrospinning in the concept of 1990–2012. (b) Graph displaying the main geographical spread of the patent filings from (a) (1990–2012).

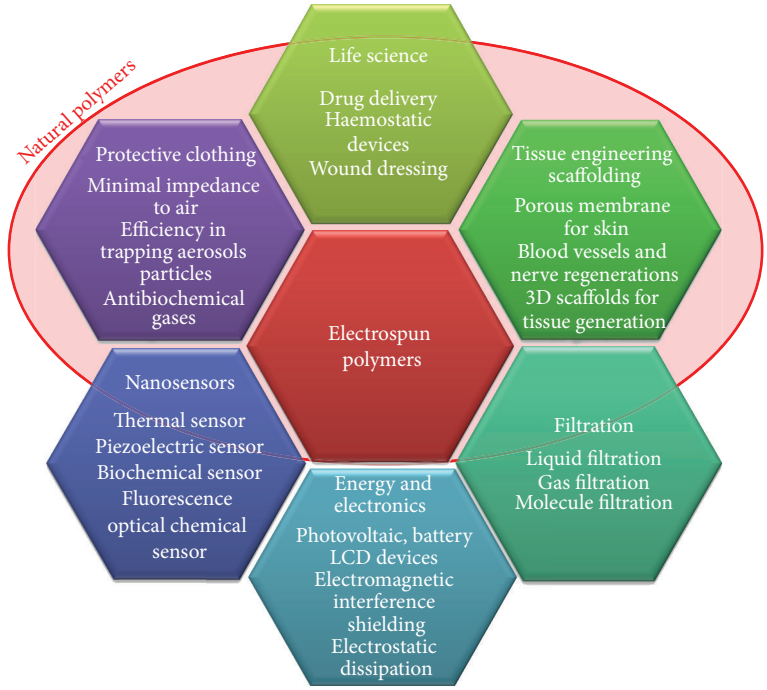

FIGURE 3: A selection of potential applications for electrospun polymer systems, highlighting the current areas of most interest for natural polymers.

However challenging the fabrication process may be for *real-world* applications, natural polymer could hold key advantages over the synthetic counterparts, such as biocompatibility, low toxicity, renewable source materials, controlled biodegradation, and, with increasing output, the possibility of lower production costs. Specific to the biotechnology sector, the ability to fabricate electrospun, naturally occurring proteins can provide cells with a physiologically relevant platform and promote a natural state of differentiation of the cellular components. Various natural proteins have been successfully electrospun to date, including silk, collagen, gelatin, and fibrinogen. Complex carbohydrate biopolymers such as polysaccharides have also been electrospun [30]. However, many natural polymers suffer from poor mechanical and thermal properties, which limit their applications. To overcome this limitation, several plausible routes have

Table 1: Selection of commercial suppliers of electrospun nanofibre-based products.

	Company Name	Country of origin	Website
1	Donaldson Company Inc.	USA	http://www.donaldson.com/
2	Espin Technologies Inc.	USA	http://www.espintechnologies.com/
3	US Global Nanospace	USA	http://www.usgn.com/
4	Finetex Technology	Republic of Korea	http://www.finetextech.com/
5	Nanoval GmbH and Co. KG	Germany	http://www.nanoval.de/
6	Japan Vilene Company Ltd.	Japan	http://www.vilene.co.jp/
7	Toray	Japan	http://www.toray.com/
8	Elamarco	Czech Republic	http://www.elmarco.cz/
9	Hills Inc.	USA	http://www.hillsinc.net/
10	Esfil Tehno	Republic of Estonia	http://www.esfiltehno.ee/

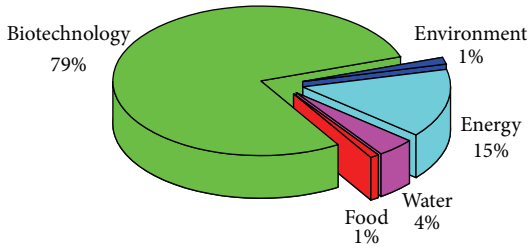

Figure 4: Chart displaying five of the main commercial applications for electrospun nanofibres, a function of overall patent filing percentage, of 1994–2012.

been proposed and hybrid synthetic-natural, electrospun copolymer systems have emerged as possible contenders to solve current commercial demands [31].

3.1. Biotechnology. Applications and products which employ polymers in the biomedical field require tight tolerance of the resulting chemical and physical properties. In the mid-1990's, research began to focus on merging nanotechnology with tissue engineering. Today the primary, practical applications include tissue and cell regeneration, surgical implants, drug delivery, and wound healing. Some common materials that have been electrospun are biodegradable synthetic polymers, such as polylactic acid, polycaprolactone, and polyglycolic acid, nonbiodegradable synthetics such as polyurethane, and natural polymers such as cellulose, collagen, and chitosan. Table 2 presents some common electrospun synthetic and natural polymers which are currently under study in this sector.

The mimicking of the extracellular matrix is the core focus of nanofibre scaffold for tissue engineering and cell growth. The use of such scaffolds has been shown to yield a cellular response that differs positively from that of traditional smooth-surfaced substrates.

In a recent review Ramakrishna et al. [27] highlighted one such publication where, in most cases, electrospun scaffolds constructed from natural occurring proteins in the extracellular matrix such as collagen allowed much better infiltration of cells into the scaffold [39]. They also referenced the work

Table 2: Table of some recently electrospun synthetic and natural polymers and the main function in the biotechnology sector.

Common Polymer	Function	Reference
Polyurethane, PU	Tissue engineering, functional biomaterial	[32]
	Biosensor	[33]
Poly(lactic acid), PLA	Tissue engineering, functional biomaterial	[34]
Poly(ε-caprolactone), *PCL*	Tissue engineering, functional biomaterial	[35]
Chitosan	Tissue engineering, functional biomaterial	[36]
Collagen	Tissue engineering, functional biomaterial	[37]
Cellulose Acetate	Biomolecule immobilization, tissue engineering, and biosensor	[38]

on stromal cells [40, 41] (including haemopoietic stem cells [42], embryonic stem cells [43], and neural progenitor cells) which have been successfully cultured onto nanofibre meshes. Recently Jin et al. [44] reported a high proliferation of human dermal fibroblast growth on *Memecylonedule* polycaprolactone nanofibres when compared to that of other plant extracts with wound healing properties such as *Indigofera aspalathoides*, *Azadirachta indica,* and *Myristica andamanica*. With an average nanofibre diameter of 487 nm, the newly formed hydrophilic, *memecylonedule* polycaprolactone nanofibre scaffolds resulted in a 394% increase in the rate of cell proliferation between days 3 and 9 of the study.

Alternative materials and biotechnology applications which have recently been studied include nylon-6/lactic acid core-shell nanofibres [45], prepared using a two-step electrospinning and surface neutralization technique. The calcium lactate coated nanofibre scaffold displayed noted osteoblast cell growth. Sheng et al. [46] investigated the electrospinning of a novel vitamin E loaded silk fibroin nanofibrous mats from an aqueous solution for cosmetic tissue regeneration applications. Additionally a review of the emerging research into novel electrospun nanofibre/hydrogel

composite systems has recently been published [47], comparing five unique approaches for creating composite scaffolds.

Collagen has several material properties that make it attractive for application in biotechnology such as biocompatibility, low antigenicity, biodegradability, low inflammatory and cytotoxic responses, high water affinity, and availability from a variety of sources. What has become evidently clear is that successful nanofibre scaffolds cannot just mimic the mechanical structure of the extracellular matrix; they must also promote a natural state of differentiation of the cellular components. A tailored, composite, nanofibre scaffold system, with the addition of proteins may be necessary to regulate and enhance cell proliferation. However the intrinsic instability of electrospun collagen needs to be addressed [48].

Composite materials have been widely investigated as potential for bone tissue engineering applications, such as alginate, chitosan, collagen, and hydroxyapatite composite systems fabricated by electrospinning [49]. This composite system was reported to lower the scaffold disintegration in 300–800 nm diameter nanofibres by 35% for 10 days in collagenase solution when compared to a collagen film. An alternative approach to fabricating collagen-based microfibre constructs was proposed via a layer-by-layer coating process onto preformed polyacrylonitrile and poly (DL-lactide-co-glycolide) microfibre bases [48]. This study looked for avoiding the use of volatile solvents during preparation and the resulting intrinsic instability of collagen. Other recent composite systems include collagen-chitosan-thermoplastic polyurethane blends, McClure et al. presented work on electrospun silk fibroin, collagen, elastin, and polycaprolactone prepared via a 3-1 input-output nozzle [50, 51], creating a trilayered structure. They investigated the effects on changing the composition of the medial and/or adventitial layers within the electrospun system, presented as architecturally mimicking the vascular wall and providing a mechanically positive match for vessel replacement.

An emerging, cost effective alternative to collagen is gelatin—a biocompatible, biodegradable, nonimmunogenic protein, and it displays many integrin binding sites for cell adhesion and differentiation [52]. Recently a series of silk fibroin/gelatin nanofibre composites (diameters varying from 99 to 244 nm) were prepared for use as vascular scaffold systems [53]. A homogeneous bead-free nanofibre system was obtained for a 70 : 30 ratio (silk : gelatin). The subsequent high biocompatibility resulted in high cell proliferation and growth and was concluded to support long-term cell adhesion. Francis et al. [54] simultaneously employed electrospinning (of gelatin) and electrospraying (of nanohydroxyapatite) to successfully form biocomposite, nanofibrous scaffold on a rotating cylinder, which were crosslinked to increase stability.

Through the simultaneous electrospinning of two different polymer solutions, the coaxial electrospinning [55] technique can produce core-shell structured nanofibres, leading to advanced material functionality. Jiang et al. [56] successfully demonstrated the ability to coaxially prepare water-soluble bioactive agents into biodegradable core-shell nanofibres with polycaprolactone (PCL) as shell and protein containing polyethylene glycol (PEG) as the core. PCL has been well studied for is flexibility, biodegradability, and relatively hydrophobic nature. Ladd et al. [57] fabricated a dual scaffold system from both poly(ε-caprolactone)/collagen and poly(l-lactide)/collagen. They reported a noncytotoxic, 452–549 nm nanofibre system with three distinctly varying mechanical properties within different regions of a continuous structure for potential in muscle-tendon junction tissue engineering. Similarly Gluck et al. [58] prepared core-polyurethane nanofibre scaffolds with a shell composite mixture of poly(ε-caprolactone) and gelatin, where the surface functionality encouraged cellular migration to the interior of the scaffold. Functional photosensitive poly(3-hexylthiophene) (P3HT) containing PCL nanofibrous scaffolds were fabricated by electrospinning, on which the rapid growth of human fibroblasts cells occurs under light simulation [59]. It was concluded that blending photosensitive polymer P3HT with PCL would aid proliferation and morphology of fibroblast under light simulation by converting the optical energy from the light into electrical energy. Figure 5 illustrates the cell density and proliferated human dermal fibroblasts with various combinations of polymer blends.

3.2. Food. The nanofibres and novel structures are produced by electrospinning process from synthetic and natural polymers enabling their use in wide area of applications such as new food ingredients, food additives, novel packaging, food sensors, and additive encapsulations [60]. The use of electrospun nanofibres in the food sector is relatively low, since most of the nanofibres produced are usually composed of nonfood grade polymers. On the other hand nanofibres produced from natural polymers have potential applications in development of high performance packaging for food, food coatings, flavour enhancement, additive encapsulation, and nutraceutical applications due to their biocompatibility and biodegradability.

Food packaging is the largest growing sector and it is an integral part of food processing and supply operations. The main objective is to maintain the quality and protection from various hazards during the transportation and until it reaches to the customer. The food industry can use electrospun nanofibres in many ways. Food packaging materials constructed from biobased and natural polymers can be used to improve the shelf time and retain the flavours in the food. Furthermore intelligent active packaging materials can be produced by this process by incorporating the biosensors into the fibres for indication of the expiration date of the food products [61]. Biobased polyester multilayer structure packaging films produced with a high barrier interlayer of electrospun zein nanofibres were recently reported [62] for food packaging applications. By incorporating the zein electrospun nanofibre in the multilayer structure by compression moulding, the oxygen barrier properties were significantly improved.

Nanoparticles produced by electrospraying have potential cost saving in confectionery industry [63]. Electrospinning process uses lesser amount of chocolate sauces and the fibres/particles produced by this process would have different texture and mouth feeling compared to bulk chocolates. This could potentially help developing new food products and help saturated confectionery markets to grow.

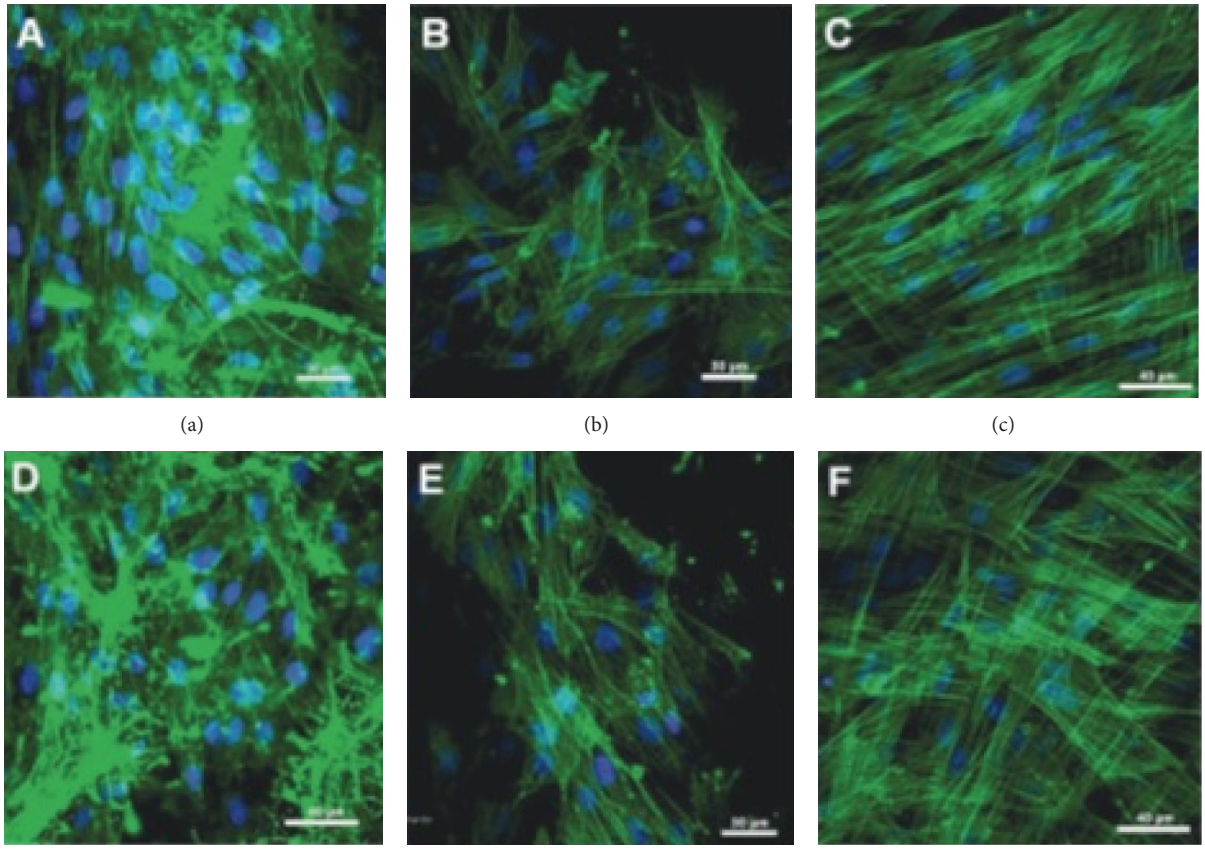

Figure 5: Laser scanning confocal microscopic (LSCM) micrographs of HDFs grown on (a) PCL/P3HT (10) (S), (b) PCL (S), (c) TCP (S), (d) PCL/P3HT (10) (NS), (e) PCL (NS), and (f) TCP (NS), expressing F-actin [59].

Fast responding biosensors are probably the most popular nanofibre application allowing fast response, higher sensitivity, and selectivity compared to current solutions. Immobilisation of tyrosinase enzyme on a glassy carbon electrode covered by a polyamidic nanofibrous membrane showed rapid detection of phenolic compounds due to nanofibre coating on the electrode [64]. Similarly electrospun nanofibres made of nylon-6 are used to detect the migration of phenolic compounds from food such as cooking oils and mineral water [65]. By incorporating electrospun nanofibres in the active packaging material, it will greatly assist regulators and enhance health and safety controls.

Electrospun nanofibres produced from natural polymers such as cellulose and proteins will find applications in food packaging applications [66]. Due to their biodegradability and biocompatibility these nanofibres have potential applications in controlled release of drugs in gastrointestinal tract. Smart electrospun nanofibres are produced from poly(N-isopropylacrylamide) (PNIPAAm) which are capable of responding to external stimuli such as temperature changes. These materials may find use in many applications, such as smart packaging of food, controlled drug delivery, and tissue engineering. Figure 6 illustrates the smart electrospun fibres which are sensitive to temperature changes.

Nanofibres are deemed part of the "nano" family, which is currently a hot topic for many food regulatory bodies, due to potential health risks related to nanoparticles which may deposit in soft tissues. Until recently there was no clear definition of what kind of nanomaterials imposes risk in the food sector. Directorate for Science, Technology, and Industry Committee for Scientific and Technological Policy recently published regulatory frame works for nano technology in food and medical products [68]. This could significantly change how nanofibres can be used for various applications in food sector.

3.3. Water. The world is facing formidable challenges in meeting rising demands of clean water resources due to extended droughts, growing industrialization, and rising population. Ninety seven percent of surface waters are oceans which are hard to make suitable for drinking because of high salt content [69].

Advances in nanotechnology could greatly help overcome the current issues of meeting the demand of clean water supplies using novel, nanostructured membranes produced by electrospinning process. Currently electrospun nanofibrous membranes (ENMs) are a very attractive and plausible

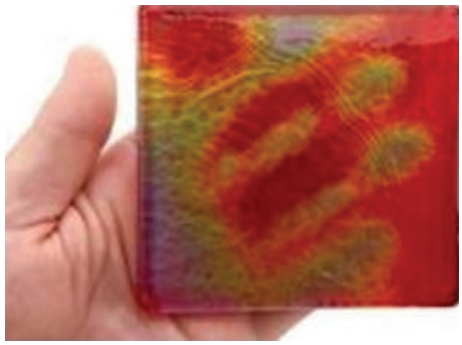

Figure 6: Smart electrospun nanofibre membranes produced PNIPAM [67].

solution in filtration technology due to their unique properties such as high porosity, micro- to nanoscaled pore sizes, interconnected open pore structure, and a large surface area per unit volume. Due to the flexibility of the electrospinning process, it is anticipated that membranes can be produced with various novel functionalities which could effectively remove salts and various toxic compounds to produce clean water for human consumption and various other day-to-day uses.

The primary function of a filtration membrane is to separate two distinct phases, preferentially regulating one phase through the membrane while simultaneously acting as a barrier to the other phase, such as suspended solids. Safe removal of waterborne pollutants is critical to clean water recovery and is an area of critical importance as the global population continues to rise to over 7 billion [70], applying severe pressure on diminishing global resources. Polymer filtration membranes are commonly prepared via the *phase inversion* method, various casting techniques, and electrospinning. Electrospun filtration membranes offer a plausible, alternative, and advantageous route for providing clean water via ease of scalability, low power consumption, and the nonusage of chemicals. Table 3 presents some common electrospun synthetic and natural polymers which are under current investigation for use in water filtration. The dimensionality of nanofibres allows for the high volume production of light weight, highly functional, nanoscale, mesh-like structures. Membrane filtration can be broadly divided into two types.

(a) The first type is micro- and ultrafiltration for the removal of larger particles, operating at low pressures with high productivity. The degree of separation process relies heavily on membrane pore dimension. Traditional polymer surfaces are hydrophobic which can lead to *membrane fouling* (issue where particulates deposit onto the membrane surface and clog the pores, leading to a degradation of the membrane performance).

(b) The second type is nanofiltration and reverse osmosis which remove dissolved salts from the aqueous system. In contract to category (a), the separation mainly occurs via diffusion through the membrane.

Table 3: Table of some recently electrospun synthetic and natural polymers and the main function in the water treatment sector.

Polymer	Function	Reference
Polyvinylidene fluoride, PVDF	Filtration membrane	[71]
Polyacrylonitrile, PAN	Filtration membrane	[72]
Poly(lactic acid), PLA	Filtration membrane, antifouling	[73]
Polyurethane	Affinity membranes	[74]
Chitosan	Filtration membrane	[75, 76]
Cellulose Acetate	Filtration membrane	[77]
Silk	Heavy metal ion recovery	[78]

In the review by Balamurugan et al. [24] reviewing the trends in air and water filtration, they highlighted reports which demonstrated that, by introducing expanded polystyrene nanofibres to conventional nanofibres, it increases the separation efficiency of the filter media by 20% [79]. They also reviewed the work by Gopal et al. [25] investigating electrospun polyvinylidene difluoride (PVDF) nanofibrous membranes for the microfiltration of varying micrometre size of polystyrene particles. The study proved the efficiency of electrospun nanofibres compared to the conventional microfiltration membranes reporting a high rejection rate of ~90% of polystyrene microparticles. Currently microglass fibres are commonly employed in the petrochemical industry for water/oil emulsion separation processing.

Together with increasing separation efficiency by nanofibre dimensionality, membranes fouling must be addressed. Recently Kaur et al. [80] blended a series of PVDF polymers with hydrophilic, surface modifying macromolecule prior to electrospinning to minimise the issue of membrane fouling. The surface modifying macromolecules were prepared from a urethane prepolymer with poly(ethylene glycol) (PEG) and poly(propylene glycol) of various average molecular weights. They also compared electrospinning to the phase inversion technique, noting that the contact angle varied significantly with technique, —0° for electrospun compared to 54° for asymmetric membrane (phase inversion technique), after blending with a PEG-based surface modifying macromolecule.

Other filtration application areas for hybrid or composite polymer systems included modified and crosslinked chitosan coupled with electrospun polyvinylidene fluoride (PVDF) [71]. This surface modified, electrospun membrane exhibited a wider operating environment range, maintaining a good flux rate and rejection efficiency of >98% in bovine serum albumin filtration tests at 0.2 MPa. This is higher than that of commercial ultrafiltration membranes (*Sepro UF, PES10*), while displaying low membrane fouling levels. Tian et al. [77] fabricated electrospun cellulose acetate nonwoven membranes, which were subsequently surface modified with poly(methacrylic acid) (PMAA) for heavy metal ion adsorption (Cu^{2+}, Hg^{2+}, Cd^{2+}). Adsorption experimental results reported that the higher initial pH value

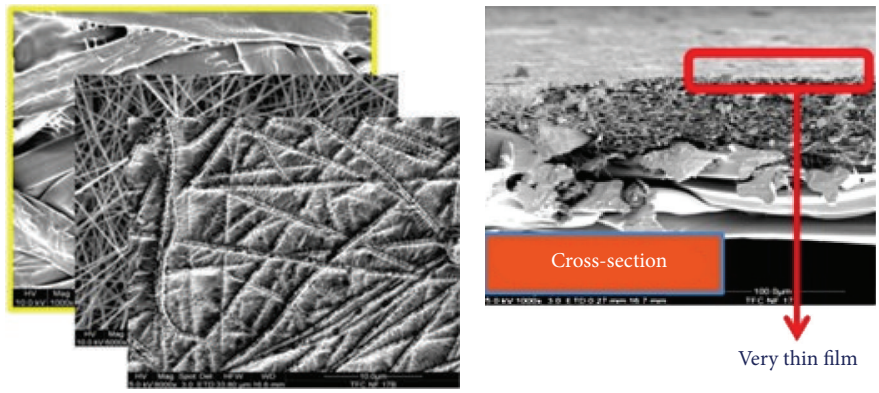

(a) (b)

Figure 7: A three-tier architecture of TFNC membrane (a) and its cross-sectional view (b) [84].

corresponded to higher adsorption capacity. Back in 2007, Ki et al. [78] fabricated silk fibroin and wool keratose/silk fibroin blended nanofibrous membranes (diameter ~200–400 nm) which reportedly exhibited an excellent performance for the adsorption of metal ions, when compared to common filter (wool sliver, filter paper). Metal ion tests were performed with Cu^{2+} as a model heavy metal ion in a stock solution. Haider et al. [81] examined the metal adsorbability of high mechanical strength, chitosan electrospun nanofibre (diameter ~235 nm) mats. They noted Cu (II) adsorption rates of roughly six times higher than reported values from chitosan microspheres, underlining the critical role played by exposure of chitosan nanofibre's functional groups to the metal ions. Pantet al. [82] prepared nylon-6 nanofibre mats containing TiO_2 nanoparticles resulting in improved mechanical strength and UV blocking ability along with antimicrobial and hydrophilic properties, for use as both protective clothing and water filtration applications.

Much research attention has been placed on multilayered electrospun composite mats for water filtration, for higher water flux and filtration efficiency. However the intrinsic properties of chitosan as a hydrophilic, water-resistant, but water-permeable coating can play a significant role in enhancing the filtration properties. Back in 2006, Yoon et al. [83] presented a paper on demonstrating a new type of high flux ultra-/nanofiltration system based on a polyacrylonitrile (PAN) electrospun nanofibrous scaffold (diameter 124–720 nm, porosity ~70%), with a thin top layer of natural chitosan—a hydrophilic, water-resistant, but water-permeable coating. They fabricated a three-tire composite membrane, coarse nanofibre PAN/fine nanofibre PAN/chitosan, observing flux rates over an order of magnitude higher than commercial nanofiltration filter (*NF 270, Dow*) after 24 h operation, while maintaining good filtration efficiency.

This work led to the fabrication of high flux thin film nanofibrous composite membranes. A three-layer composite structure of *thin film nanocomposite* (TFNC) membranes was constructed for the desalination via nanofiltration of water [84]. Figure 7 illustrates the construction and three dimensional structure of TNFC membranes prepared by electrospinning processes. Nanofiltration membranes made by this process and employed in desalination of water have shown higher permeated fluxes and less fouling than conventional membranes.

One such paper presents an interfacially polymerized polyamide barrier layer composed of varying ratios of piperazine and bipiperidine, fabricated on both PAN electrospun nanofibre scaffolds and PAN ultrafiltration membrane [85]. They conclude that the piperazine concentration played a major role in the interfacial polymerization to optimize the flux and rejection performance. Even more recently, a double-layer mat was fabricated by electrospinning a thin poly(vinyl alcohol), PVA/surface oxidized multiwalled carbon nanotube (MWNT) layer on the electrospun PAN nanofibrous substrate for use as high flux thin film nanofibrous composite membranes to separate an oil/water emulsion [86]. The incorporation of MWNTs into the PVA barrier layer could improve the water flux significantly. This mechanically robust, double-layer membrane reported a high water flux (270.1 L/m^2 h) with high rejection rate (99.5%) in oil/water emulsion separation, even at low pressures (0.1 MPa).

3.4. Environmental Applications. As mentioned in Section 3.3, a recent publication [24] reviewed trends in water and air filtrations and concluded that polymer based-nanofibres embedded with nanoparticles can replace high-efficiency particulate air filters and overcome the current limitations in the filtration of chemical contaminants. These nanoparticle impregnated nanofibre filters offer a range of advantages from filtration efficiency, protection duration, and nonselective decontamination efficiency, to final product weight reduction. However many of these novel nanofibre/nanoparticle systems require simultaneous electrospinning/electrospraying methods to fabricate a useful filter [28]. Some common electrospun synthetic and natural polymers which are employed as plausible, alternative systems in this sector are presented in Table 4.

Previously Ahn et al. [92] studied the filtration efficiency of nylon-6-based nanofibre membranes, which outperformed

already commercialized, high-efficiency particulate air filter. The key properties for high performance electrospun air filters are high filtration efficiency with low pressure drop and slow clogging of the filter during use. Amsoil [93] has introduced nanofibre technology in the form of air filtration membranes used in the auto/light truck market. The image in Figure 8 indicates the construction of air filtration membrane using electrospun nanofibres.

These air filtration membranes are highly efficient in removing the dust and have higher life time compared to cellulose-based, conventional air filtration membranes which are used currently in automotive industry.

Alternative synthetic polymers have also been well fabricated including a multi-layered nanofibre mat from polyacrylonitrile (PAN) by Zhang et al. [89]. They reported that a thin, multi-layered nanofibrous structure outperformed HEPA and military standard filters due to volume/layer compensation effects. As a gaseous filter, poly(methyl methacrylate) (PMMA) nanofibres containing the inclusion complex forming beta-cyclodextrin (β-CD) were fabricated for the removal of organic waste vapours from the environment [90]. They concluded that this nanofibre system can entrap organic vapours such as aniline, styrene, and toluene as a result of fibre surface, inclusion complexation with β-CD. Patanaik et al. [88] examined the effects of composite polyethylene oxide (PEO) nanofibrous membranes sandwiched between another nonwoven mat. They concluded that the increase in diameter of PEO nanofibres with the increased concentration has a positive impact on the filtration efficiency and pressure drop. Interestingly the composite filter media was reported to be more stable against cyclic compression when compared to membranes deposited over nonwoven mats. Wang et al. [94] electrospun polyvinyl chloride, (PVC)/polyurethane (PU) fibrous membranes composite air filters and reported filtration efficiency of the order of 99.5%, with a low pressure drop (144 Pa) performance for 300–500 nm sodium chloride aerosol particles. An optimal PVC/PU weight ratio of 8 : 2 was reported with enhanced mechanical and air permeability properties.

Even with the numerous potential advantages that nanofibres possess when compared to commercial filters, there must remain a consideration for the environmental effect via some current manufacturing routes. These often require a relatively large carbon footprint for low yield of filter material produced. Exploiting the intrinsic benefits of natural polymers, Cao et al. [91] recently reported the fabrication of jute cellulose nanowhiskers on PAN, PVA, and silica nanofibrous membrane supports. These new biobased and environmental friendly porous network materials offer an alternative route to manufacture, avoiding such issues as higher costs, lower productivity, and time efficiency and the potential need for harmful solvents.

3.5. Energy. The ever growing global demands for high-energy density electrochemical power sources have prompted a huge interest in such products as lithium- (Li-) ion batteries to exploit the high-energy density, long cycle lives, and flexible design as an effective solution [95]. This in turn has focussed huge efforts on fabricating low-cost, high capacity electrodes for such devices with long life cycles. Such work included carbon nanofibres prepared through electrospinning a blend solution of polyacrylonitrile and polypyrrole and subsequent carbonisation [96]. Without the addition of polymer binder or conductive material, these anode materials displayed high reversible capacity, improved cycle performance, relatively good rate capability and clear fibrous morphology even after 50 charge/discharge cycles. Table 5 presents some common electrospun synthetic and natural polymers which are currently under study in the energy sector. Aravindan et al. [97] recently examined NiO nanofibres to evaluate its potential as a high performance anode in Li-ion batteries. In evaluating the performance of a test cell, they reported good cycleability, exhibiting capacity retention of over 75% of reversible capacity after 100 cycles.

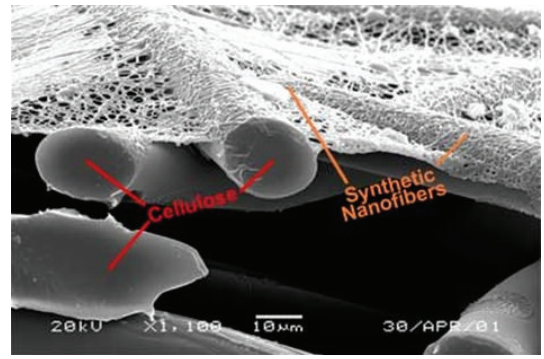

Figure 8: AMSOIL Ea air filters used for automotive industry [93].

Table 4: Table of some recently electrospun synthetic and natural polymers and the main function in the environmental sector.

Polymer	Function	Reference
Polyvinylalcohol, PVA	Air filtration	[87]
Polyethylene oxide, PEO	Air filtration	[88]
Polyacrylonitrile, PAN	Air filtration	[89]
Poly(methyl methacrylate), PMMA	Organic vapour waste, air filtration	[90]
Cellulose	Air filtration	[91]

Specific to battery cathode systems, recent work includes the preparation of $LiFePO_4$/C submicrofibre composite by a facile electrospinning method in a host poly(4-vinyl) pyridine solution. These $LiFePO_4$/C submicrofibre composites reportedly delivered discharge capacities of 132 and 138 mAh g^{-1}, with excellent cycle performance at 25 and 55°C. Electrospun fibre systems are also employed in preparing the separator layer in Li-ion batteries. Polyimide nanofibre-based membranes have been fabricated for the separators, with higher capacity, lower resistance, and higher rate of capability, compared to the Celgard membrane separator [104].

In conjunction with the electrode and separator materials, low self-discharge composite electrolytes based on porous polymer membranes are another route of increasing

Table 5: Table of some recently electrospun synthetic and natural polymers and the main function in the energy sector.

Polymer	Function	Reference
Polyacrylonitrile, PAN	Battery, fuel cell	[98]
Polyvinylidene fluoride, PVDF	Battery	[99]
	Solar cell	[100]
Polyaniline, PANI	Solar cell	[101]
Cellulose	Battery	[102, 103]

the efficiency of high-energy density electrochemical power systems. These systems also offer a positive safety aspect with good compatibility and no leakage. Raghavan et al. [105] examined polymer gel electrolytes by activating nonwoven polyacrylonitrile electrospun membranes with different liquid electrolytes. The fabricated system showed good interfacial stability, oxidation stability, good cycle performance with high initial discharge properties, and low capacity fade under continuous cycling. Other work has focussed on composite electrospun systems such as TPU/PVDF with and without in situ ceramic fillers (SiO_2 and TiO_2), resulting in superior electrochemical and mechanical performances [106, 107]. Specific to the field of supercapacitor energy storage devices, recently tubular nanofibres of vanadium pentoxide were electrospun from a phase-separated vanadium oxytrihydroxide, poly(vinylpyrrolidone) (PVP) polymer solution.

Focusing on the emerging role of natural polymers, cellulose-based battery devices have previously been fabricated and are already being used for clinic diagnosis. Lee et al. [108] prepared human urine activated paper batteries as a power source to drive the on-board biosensors for healthcare screening of urine. Baptista et al. [109] fabricated a *biobattery*, composed of an ultrathin monolithic structure of an electrospun cellulose acetate membrane. Recently blended synthetic/natural solid state electrolytes were prepared from electrospun PEO, with a novel cellulosic reinforcement material, GELPEO [102]. Good thermal stability and high tensile strength show this as a promising material for use in various electrochemical devices such as lithium ion batteries and dye sensitized solar cells. Comparable ionic conductivities were achieved for both electrospun PEO and PEO + 5 wt% GELPEO nanocomposite systems.

As a viable, green technology energy supply, fuel cells have recently attracted enormous attention. In the simplest form, fuel cells efficiently convert stored energy into electrical energy via a catalytic reaction, resulting in a high power density supply. The main types of fuel cells are proton exchange membrane fuel cells (PEMFC), direct methanol fuel cell (DMFC), solid oxide fuel cell (SOFC), phosphoric acid fuel cell (PAFC), and alkaline fuel cells (AFC). Research in these areas is growing rapidly and is discovering noted advantages when incorporating electrospun component systems. In 2010, Tamura et al. [110] fabricated electrospun aligned sulfonated polyimide nanofibres for use as proton exchange membrane. They noted significant improvement in the membrane stability along with an increase in proton conductivity of the membrane.

Investigating and optimising the electrocatalytic performance of fuel cells have led to the fabrication of such systems as platinum (Pt) nanowires, prepared by the high temperature treatment (450°C) of electrospun PVP-Pt composite fibres. The researchers noted increased electrochemical specific and mass activities. Even more recently, Guo et al. [111] fabricated an electrospun palladium nanoparticle loaded carbon nanofibre composite which exhibited enhanced electrocatalytic performance toward methanol electrooxidation. In 2011 sulfonated poly(ether sulfone) (SPES) nanofibres were prepared via electrospinning techniques and a new class of triple-layer polyelectrolyte membranes based on Nafion-filled nanofibrous webs was fabricated [112]. These systems were deemed suitable for high-performance direct methanol fuel cells. Additional published research included the electrospraying of platinum-carbon catalyst nanoparticle suspensions in Nafion-alcohol solutions over carbon paper to prepare cathodes for proton exchange membrane fuel cells [113]. This work found that the relative power density was substantially higher for any of the electrosprayed electrodes (comparing platinum loading). Chen et al. [114] prepared carbon fibre mats via a layer-by-layer electrospinning of polyacrylonitrile onto thin natural cellulose paper as a low cost and highly efficient electrode for the anode in microbial fuel cells. They concluded that much larger current densities would be obtained if you further increased the gap between the layers within the layered-carbon fibre mat. This would lead to thicker layered biofilm growth in every layer of the entire layered system.

Over recent years huge interest has been focussed on nanosized TiO_2 powders for use in photocatalysis, photocatalytic water splitting, solar energy conversions and catalytic devices. The ability to synthesize TiO_2 in different shapes and morphologies such as nanoporous structures, nanoparticles, nanotubes, nanowires, and nanofibres by various methods makes it a very interesting and versatile material. In a series of work, Veluru et al. [115] fabricated and subsequently annealed and functionalized multiwalled carbon nanotube MWNT-TiO_2 nanostructures via electrospinning and noted a dramatically enhanced hydrogen generation, primarily due to the increase in surface area of the hybrid nanostructures. Peining [116] also reported an optimum concentration of MWNTs in the TiO_2 matrix for best performance in dye-sensitized solar cells to be 0.2 wt%, with a 32% enhancement in the energy conversion efficiency.

To overcome some of the limitations of such photocatalysts as TiO_2 applied under visible light, many researchers are looking for alternative, visible light-induced photocatalysts with the appropriate band gap energy. Wu et al. [117] fabricated CdS/ZnO core-shell nanofibres via the electrospinning technique. They noted that the power conversion efficiencies of these hybrid solar cells were improved by more than 100% after the modification of CdS. Afeesh et al. [118] presented work highlighting the photocatalytic effects of a reusable, novel nematic shaped CdS-doped poly(vinyl acetate) electrospun mat. They noted no secondary pollution problem from the CdS nanoparticles. Shengyuan et al. [119] combined the two photocatalysts to form an electrospun

TiO_2-/CdS-based photoelectrode with a CoS counter electrode. They conclude that these CoS counter electrodes could be a good substitute for the expensive Pt counter electrode in CdS-sensitized nanocrystalline solar cells.

4. Conclusions

The high surface to volume ratio of the electrospun fibres makes them attractive for various applications such as high performance filters, energy generation, water filtration, and scaffolds in tissue engineering. Considering the versatility of electrospinning process the number of applications using various synthetic and natural polymers is increasing at an exponential rate in various fields. However, the use of natural polymers in various applications is relatively low compared to synthetic polymers due to incompatibility of the choice of the polymer for particular application and in some cases due to poor chemical and mechanical properties. Further developments are required to find new hybrid polymer systems based on synthetic and natural polymers that are suitable for electrospinning with improved functionalities suitable for across spectrum of applications especially food and biotechnology areas. They aim to exploit the key material advantages from both systems, whilst overcoming some of the individual limitations which have hindered the true exploitation of electrospun systems to date. As fabrication costs continue to reduce and higher volume electrospinning systems are brought on-stream, the resulting nanofibre-based products will become highly competitive alternatives to current, often out-dated, market solutions. Based on current studies it is not a surprise that electrospun nanofibres are expected to play a critically important role in many important application areas, such as water purification, renewable energy, and environmental protection in the coming years.

Acknowledgment

Dr. Ramesh Babu would like to acknowledge the support of Electrospinng COST Action MP1206.

References

[1] S. Ramakrishna, K. Fujihara, W.-E. Teo, T.-C. Lim, and Z. Ma, *An Introduction to Electrospinning and Nanofibers*, chapter 2, World Scientific Publishing, Singapore, 2005.

[2] P. J. A. Borm, D. Robbins, S. Haubold et al., "The potential risks of nanomaterials: a review carried out for ECETOC," *Particle and Fibre Toxicology*, vol. 3, no. 1, article 11, 2006.

[3] Q. Zhang, J. Q. Huang, W. Z. Qian, Y. Y. Zhang, and F. Wei, "The road for nanomaterials industry: a review of carbon nanotube production, post-treatment, and bulk applications for composites and energy storage," *Small*, vol. 9, no. 8, pp. 1237–1265, 2013.

[4] C. N. R. Rao, M. Achim, and A. K. Cheetham, Eds., *The Chemistry of Nanomaterials Synthesis, Properties and Applications*, vol. 1, John Wiley & Sons, Weinheim, Germany, 2004.

[5] C. Nitschke, S. M. O'Flaherty, M. Kröll, J. J. Doyle, and W. J. Blau, "Optical properties of zinc phthalocyanine nanoparticle dispersions," *Chemical Physics Letters*, vol. 383, no. 5-6, pp. 555–560, 2004.

[6] L. P. Bicelli, B. Bozzini, C. Mele, and L. D'Urzo, "A review of nanostructural aspects of metal electrodeposition," *International Journal of Electrochemcal Science*, vol. 3, no. 4, pp. 356–408, 2008.

[7] S. De, S. Duttaa, A. K. Patra et al., "Biopolymer templated porous TiO_2: an efficient catalyst for the conversion of unutilized sugars derived from hemicellulose," *Applied Catalysis A*, vol. 435-436, pp. 197–203, 2012.

[8] I. Stamatin, A. Morozan, A. Dumitru et al., "The synthesis of multi-walled carbon nanotubes (MWNTs) by catalytic pyrolysis of the phenol-formaldehyde resins," *Physica E*, vol. 37, no. 1-2, pp. 44–48, 2007.

[9] E. Lahiff, R. Leahy, J. N. Coleman, and W. J. Blau, "Physical properties of novel free-standing polymer-nanotube thin films," *Carbon*, vol. 44, no. 8, pp. 1525–1529, 2006.

[10] J. Doshi and D. H. Reneker, "Electrospinning process and applications of electrospun fibers," *Journal of Electrostatics*, vol. 35, no. 2-3, pp. 151–160, 1995.

[11] W.-E. Teo, R. Inai, and S. Ramakrishna, "Technological advances in electrospinning of nanofibers," *Science and Technology of Advanced Materials*, vol. 12, no. 1, Article ID 013002, 2011.

[12] S. H. Shin, O. Purevdorj, O. Castano, J. A. Planell, and H.-W. Kim, "A short review: recent advances in electrospinning for bone tissue regeneration," *Journal of Tissue Engineering*, vol. 3, no. 1, 2012.

[13] H. Alam and S. Ramakrishna, "A review on the enhancement of figure of merit from bulk to nano-thermoelectric materials," *Nano Energy*, vol. 2, no. 2, pp. 190–212, 2013.

[14] P. Raghavan, D.-H. Lim, J.-H. Ahn et al., "Electrospun polymer nanofibers: the booming cutting edge technology," *Reactive and Functional Polymers*, vol. 72, no. 12, pp. 915–930, 2012.

[15] G. M. Bose, *Recherches sur la Cause et sur la Véritable Théorie de L'électricité*, 1745.

[16] J. F. Cooley, "Apparatus for electrically dispersing fluids," U.P. Specification, 1902.

[17] W. J. Morton, "Method of dispersing fluid," U.P. Office, Editor 1902.

[18] A. Formhals, "Apparatus for producing artificial filaments from material such as cellulose acetate," Schreiber-Gastell, Richard, 1934.

[19] S. Scholar, "Electrospinning, electrospun, electrostatic spin," Patent search, 1994–2012.

[20] S. Scholar, "Electrospinning, electrospun, electrostatic spin," Journal search, 1994–2012.

[21] N. Bock, T. R. Dargaville, and M. A. Woodruff, "Electrospraying of polymers with therapeutic molecules: state of the art," *Progress in Polymer Science*, vol. 37, no. 11, pp. 1510–1551, 2012.

[22] R. P. Babu, K. O'Connor, and R. Seeram, "Current progress on bio-based polymers and their future trends," *Progress in Biomaterials*, vol. 2, no. 8, 2013.

[23] H.-S. Wang, G.-D. Fu, and X.-S. Li, "Functional polymeric nanofibers from electrospinning," *Recent Patents on Nanotechnology*, vol. 3, no. 1, pp. 21–31, 2009.

[24] R. Balamurugan, S. Sundarrajan, and S. Ramakrishna, "Recent trends in nanofibrous membranes and their suitability for air and water filtrations," *Membranes*, vol. 1, no. 3, pp. 232–248, 2011.

[25] R. Gopal, S. Kaur, Z. Ma, C. Chan, S. Ramakrishna, and T. Matsuura, "Electrospun nanofibrous filtration membrane," *Journal of Membrane Science*, vol. 281, no. 1-2, pp. 581–586, 2006.

[26] Z.-M. Huang, Y.-Z. Zhang, M. Kotaki, and S. Ramakrishna, "A review on polymer nanofibers by electrospinning and their applications in nanocomposites," *Composites Science and Technology*, vol. 63, no. 15, pp. 2223–2253, 2003.

[27] S. Ramakrishna, R. Jose, P. S. Archana et al., "Science and engineering of electrospun nanofibers for advances in clean energy, water filtration, and regenerative medicine," *Journal of Materials Science*, vol. 45, no. 23, pp. 6283–6312, 2010.

[28] M. Roso, S. Sundarrajan, D. Pliszka, S. Ramakrishna, and M. Modesti, "Multifunctional membranes based on spinning technologies: the synergy of nanofibers and nanoparticles," *Nanotechnology*, vol. 19, no. 28, Article ID 285707, 2008.

[29] W.-E. Teo and S. Ramakrishna, "Electrospun nanofibers as a platform for multifunctional, hierarchically organized nanocomposite," *Composites Science and Technology*, vol. 69, no. 11-12, pp. 1804–1817, 2009.

[30] D. B. Khadka and D. T. Haynie, "Protein- and peptide-based electrospun nanofibers in medical biomaterials," *Nanomedicine*, vol. 8, no. 8, pp. 1242–1262, 2012.

[31] J. Xie and Y.-L. Hsieh, "Ultra-high surface fibrous membranes from electrospinning of natural proteins: casein and lipase enzyme," *Journal of Materials Science*, vol. 38, no. 10, pp. 2125–2133, 2003.

[32] R. Chen, C. Huang, Q. Ke, C. He, H. Wang, and X. Mo, "Preparation and characterization of coaxial electrospun thermoplastic polyurethane/collagen compound nanofibers for tissue engineering applications," *Colloids and Surfaces B*, vol. 79, no. 2, pp. 315–325, 2010.

[33] N. Wang, K. Burugapalli, W. S. J. Halls, F. Moussy, A. Ray, and Y. Zheng, "Electrospun fibro-porous polyurethane coatings for implantable glucose biosensors," *Biomaterials*, vol. 34, no. 4, pp. 888–901, 2013.

[34] C. Gualandi, M. Govonib, L. Foroni et al., "Ethanol disinfection affects physical properties and cell response of electrospun poly(l-lactic acid) scaffolds," *European Polymer Journal*, vol. 48, no. 12, pp. 2008–2018, 2012.

[35] J. Dias and P. Bártolo, "Morphological characteristics of electrospun PCL meshes—The influence of solvent type and concentration," *Procedia CIRP*, vol. 5, pp. 216–221, 2013.

[36] V. Sencadas, D. M. Correia, A. Areias et al., "Determination of the parameters affecting electrospun chitosan fiber size distribution and morphology," *Carbohydrate Polymers*, vol. 87, no. 2, pp. 1295–1301, 2012.

[37] J. Ji, B. Bar-On, and H. D. Wagner, "Mechanics of electrospun collagen and hydroxyapatite/collagen nanofibers," *Journal of the Mechanical Behavior of Biomedical Materials*, vol. 13, pp. 185–193, 2012.

[38] R. Konwarh, N. Karak, and M. Misra, "Electrospun cellulose acetate nanofibers: the present status and gamut of biotechnological applications," *Biotechnology Advances*, vol. 31, no. 4, pp. 421–437, 2013.

[39] W.-E. Teo, W. He, and S. Ramakrishna, "Electrospun scaffold tailored for tissue-specific extracellular matrix," *Biotechnology Journal*, vol. 1, no. 9, pp. 918–929, 2006.

[40] W.-J. Li, R. Tuli, X. Huang, P. Laquerriere, and R. S. Tuan, "Multilineage differentiation of human mesenchymal stem cells in a three-dimensional nanofibrous scaffold," *Biomaterials*, vol. 26, no. 25, pp. 5158–5166, 2005.

[41] M. P. Prabhakaran, J. R. Venugopal, and S. Ramakrishna, "Mesenchymal stem cell differentiation to neuronal cells on electrospun nanofibrous substrates for nerve tissue engineering," *Biomaterials*, vol. 30, no. 28, pp. 4996–5003, 2009.

[42] K.-N. Chua, C. Chai, P.-C. Lee et al., "Surface-aminated electrospun nanofibers enhance adhesion and expansion of human umbilical cord blood hematopoietic stem/progenitor cells," *Biomaterials*, vol. 27, no. 36, pp. 6043–6051, 2006.

[43] J. Xie, S. M. Willerth, X. Li et al., "The differentiation of embryonic stem cells seeded on electrospun nanofibers into neural lineages," *Biomaterials*, vol. 30, no. 3, pp. 354–362, 2009.

[44] G. Jin, M. P. Prabhakaran, D. Kai, S. K. Annamalai, K. D. Arunachalam, and S. Ramakrishna, "Tissue engineered plant extracts as nanofibrous wound dressing," *Biomaterials*, vol. 34, no. 3, pp. 724–734, 2013.

[45] H. R. Pant, P. Risal, C. H. Park, L. D. Tijinge, Y. J. Jeong, and C. S. Kim, "Core-shell structured electrospun biomimetic composite nanofibers of calcium lactate/nylon-6 for tissue engineering," *Chemical Engineering Journal*, vol. 221, pp. 90–98, 2013.

[46] X. Sheng, L. Fan, C. He, K. Zhang, X. Mo, and H. Wang, "Vitamin E-loaded silk fibroin nanofibrous mats fabricated by green process for skin care application," *International Journal of Biological Macromolecules*, vol. 56, pp. 49–56, 2013.

[47] L. A. Bosworth, L. A. Turner, and S. H. Cartmell, "State of the art composites comprising electrospun fibres coupled with hydrogels: a review," *Nanomedicine*, vol. 9, no. 3, pp. 322–335, 2013.

[48] Y. B. Truong, V. Glattauera, K. L. Briggs, S. Zappe, and J. A. M. Ramshaw, "Collagen-based layer-by-layer coating on electrospun polymer scaffolds," *Biomaterials*, vol. 33, no. 36, pp. 9198–9204, 2012.

[49] C.-C. Yu, J. Changb, Y.-H. Lee et al., "Electrospun scaffolds composing of alginate, chitosan, collagen and hydroxyapatite for applying in bone tissue engineering," *Materials Letters*, vol. 93, pp. 133–136, 2013.

[50] M. J. McClure, D. G. Simpson, and G. L. Bowlin, "Tri-layered vascular grafts composed of polycaprolactone, elastin, collagen, and silk: optimization of graft properties," *Journal of the Mechanical Behavior of Biomedical Materials*, vol. 10, pp. 48–61, 2012.

[51] M. J. McClure, S. A. Sell, D. G. Simpson, B. H. Walpoth, and G. L. Bowlin, "A three-layered electrospun matrix to mimic native arterial architecture using polycaprolactone, elastin, and collagen: a preliminary study," *Acta Biomaterialia*, vol. 6, no. 7, pp. 2422–2433, 2010.

[52] Z.-M. Huang, Y. Z. Zhang, S. Ramakrishna, and C. T. Lim, "Electrospinning and mechanical characterization of gelatin nanofibers," *Polymer*, vol. 45, no. 15, pp. 5361–5368, 2004.

[53] S.-D. Wang, Y.-Z. Zhang, G.-B. Yin, H.-W. Wang, and Z.-H. Dong, "Fabrication of a composite vascular scaffold using electrospinning technology," *Materials Science and Engineering C*, vol. 30, no. 5, pp. 670–676, 2010.

[54] L. Francis, J. Venugopal, M. P. Prabhakaran, V. Thavasi, E. Marsano, and S. Ramakrishna, "Simultaneous electrospin-electrosprayed biocomposite nanofibrous scaffolds for bone tissue regeneration," *Acta Biomaterialia*, vol. 6, no. 10, pp. 4100–4109, 2010.

[55] Z. Sun, E. Zussman, A. L. Yarin, J. H. Wendorff, and A. Greiner, "Compound core-shell polymer nanofibers by co-electrospinning," *Advanced Materials*, vol. 15, no. 22, pp. 1929–1932, 2003.

[56] H. Jiang, Y. Hu, Y. Li, P. Zhao, K. Zhu, and W. Chen, "A facile technique to prepare biodegradable coaxial electrospun nanofibers for controlled release of bioactive agents," *Journal of Controlled Release*, vol. 108, no. 2-3, pp. 237–243, 2005.

[57] M. R. Ladd, S. J. Lee, J. D. Stitzel, A. Atala, and J. J. Yoo, "Co-electrospun dual scaffolding system with potential for muscle-tendon junction tissue engineering," *Biomaterials*, vol. 32, no. 6, pp. 1549–1559, 2011.

[58] J. M. Gluck, P. Rahgozar, N. P. Ingle et al., "Hybrid coaxial electrospun nanofibrous scaffolds with limited immunological response created for tissue engineering," *Journal of Biomedical Materials Research B*, vol. 99, no. 1, pp. 180–190, 2011.

[59] G. Jin, M. P. Prabhakaran, D. Kai, M. Kotaki, and S. Ramakrishna, "Electrospun photosensitive nanofibers: potential for photocurrent therapy in skin regeneration," *Photochemical & Photobiological Sciences*, vol. 12, no. 1, pp. 124–134, 2013.

[60] A. Fiorello, E. G. Mcdonnell, and J. D. Smith, "Indicator device having an active agent encapsulated in an electrospun nanofiber," EP1799805 A2, 2006.

[61] C. Kriegel, A. Arrechi, K. Kit, D. J. McClements, and J. Weiss, "Fabrication, functionalization, and application of electrospun biopolymer nanofibers," *Critical Reviews in Food Science and Nutrition*, vol. 48, no. 8, pp. 775–797, 2008.

[62] M. J. Fabra, A. Lopez-Rubio, and J. M. Lagaron, "High barrier polyhydroxyalcanoate food packaging film by means of nanostructured electrospun interlayers of zein," *Food Hydrocolloids*, vol. 32, no. 1, pp. 106–114, 2013.

[63] C. J. Luo, S. Loh, E. Stride, and M. Edirisinghe, "Electrospraying and electrospinning of chocolate suspensions," *Food and Bioprocess Technology*, vol. 5, no. 6, pp. 2285–2300, 2012.

[64] A. Arecchi, M. Scampicchio, S. Drusch, and S. Mannino, "Nanofibrous membrane based tyrosinase-biosensor for the detection of phenolic compounds," *Analytica Chimica Acta*, vol. 659, no. 1-2, pp. 133–136, 2010.

[65] Q. Xu, X. Yin, M. Wang et al., "Analysis of phthalate migration from plastic containers to packaged cooking oil and mineral water," *Journal of Agricultural and Food Chemistry*, vol. 58, no. 21, pp. 11311–11317, 2010.

[66] S. Wongsasulak, M. Patapeejumruswong, J. Weiss, P. Supaphol, and T. Yoovidhya, "Electrospinning of food-grade nanofibers from cellulose acetate and egg albumen blends," *Journal of Food Engineering*, vol. 98, no. 3, pp. 370–376, 2010.

[67] "Thermally sensitive smart nanofibers," http://www.nafigate.com/en/section/portal/app/news/detail/70048-thermally-sensitive-smart-nanofibers.

[68] Directorate for Science, T. a. I. and C. f. S. a. T. Policy, "Regulatory frameworks for nanotechnology in foods and medical products," Tech. Rep., Organisation for Economic Co-Operation and Development, 2013.

[69] W. G. Water facts, http://uncw.edu/troubledwaters/resource_issues.htm.

[70] UNFPA, "The state of world population 2012," 2012.

[71] Z. Zhao, J. Zheng, M. Wang, H. Zhang, and C. C. Han, "High performance ultrafiltration membrane based on modified chitosan coating and electrospun nanofibrous PVDF scaffolds," *Journal of Membrane Science*, vol. 394-395, pp. 209–217, 2012.

[72] X. Cao, M. Huanga, B. Ding, J. Yu, and G. Sun, "Robust polyacrylonitrile nanofibrous membrane reinforced with jute cellulose nanowhiskers for water purification," *Desalination*, vol. 316, pp. 120–126, 2013.

[73] A. Dasari, J. Quirós, B. Herrero, K. Boltes, E. García-Calvo, and R. Rosal, "Antifouling membranes prepared by electrospinning polylactic acid containing biocidal nanoparticles," *Journal of Membrane Science*, vol. 405-406, pp. 134–140, 2012.

[74] C. H. Bamford, K. G. Al-Lamee, M. D. Purbrick, and T. J. Wear, "Studies of a novel membrane for affinity separations. I. Functionalisation and protein coupling," *Journal of Chromatography A*, vol. 606, no. 1, pp. 19–31, 1992.

[75] M. Z. Elsabee, H. F. Naguib, and R. E. Morsi, "Chitosan based nanofibers: review," *Materials Science and Engineering C*, vol. 32, no. 7, pp. 1711–1726, 2012.

[76] T. T. T. Nguyen, O. H. Chung, and J. S. Park, "Coaxial electrospun poly(lactic acid)/chitosan (core/shell) composite nanofibers and their antibacterial activity," *Carbohydrate Polymers*, vol. 86, no. 4, pp. 1799–1806, 2011.

[77] Y. Tian, M. Wu, R. Liu et al., "Electrospun membrane of cellulose acetate for heavy metal ion adsorption in water treatment," *Carbohydrate Polymers*, vol. 83, no. 2, pp. 743–748, 2011.

[78] C. S. Ki, E. H. Gang, I. C. Um, and Y. H. Park, "Nanofibrous membrane of wool keratose/silk fibroin blend for heavy metal ion adsorption," *Journal of Membrane Science*, vol. 302, no. 1-2, pp. 20–26, 2007.

[79] C. Shin, G. G. Chase, and D. H. Reneker, "Recycled expanded polystyrene nanofibers applied in filter media," *Colloids and Surfaces A*, vol. 262, no. 1–3, pp. 211–215, 2005.

[80] S. Kaur, D. Rana, T. Matsuura, S. Sundarrajan, and S. Ramakrishna, "Preparation and characterization of surface modified electrospun membranes for higher filtration flux," *Journal of Membrane Science*, vol. 390-391, pp. 235–242, 2012.

[81] S. Haider and S.-Y. Park, "Preparation of the electrospun chitosan nanofibers and their applications to the adsorption of Cu(II) and Pb(II) ions from an aqueous solution," *Journal of Membrane Science*, vol. 328, no. 1-2, pp. 90–96, 2009.

[82] H. R. Pant, M. P. Bajgai, K. T. Nam et al., "Electrospun nylon-6 spider-net like nanofiber mat containing TiO_2 nanoparticles: a multifunctional nanocomposite textile material," *Journal of Hazardous Materials*, vol. 185, no. 1, pp. 124–130, 2011.

[83] K. Yoon, K. Kim, X. Wang, D. Fang, B. S. Hsiao, and B. Chu, "High flux ultrafiltration membranes based on electrospun nanofibrous PAN scaffolds and chitosan coating," *Polymer*, vol. 47, no. 7, pp. 2434–2441, 2006.

[84] S. Subramanian and R. Seeram, "New directions in nanofiltration applications—Are nanofibers the right materials as membranes in desalination?" *Desalination*, vol. 308, pp. 198–208, 2013.

[85] K. Yoon, B. S. Hsiao, and B. Chu, "High flux nanofiltration membranes based on interfacially polymerized polyamide barrier layer on polyacrylonitrile nanofibrous scaffolds," *Journal of Membrane Science*, vol. 326, no. 2, pp. 484–492, 2009.

[86] H. You, X. Li, Y. Yang et al., "High flux low pressure thin film nanocomposite ultrafiltration membranes based on nanofibrous substrates," *Separation and Purification Technology*, vol. 108, pp. 143–151, 2013.

[87] Y. Liu, R. Wang, H. Ma, S. B. Hsiao, and B. Chu, "High-flux microfiltration filters based on electrospun polyvinylalcohol nanofibrous membranes," *Polymer*, vol. 54, no. 2, pp. 548–556, 2013.

[88] A. Patanaik, V. Jacobs, and R. D. Anandjiwala, "Performance evaluation of electrospun nanofibrous membrane," *Journal of Membrane Science*, vol. 352, no. 1-2, pp. 136–142, 2010.

[89] Q. Zhang, J. Welch, H. Park, C.-Y. Wu, W. Sigmund, and J. C. M. Marijnissen, "Improvement in nanofiber filtration by multiple thin layers of nanofiber mats," *Journal of Aerosol Science*, vol. 41, no. 2, pp. 230–236, 2010.

[90] T. Uyar, R. Havelund, Y. Nur et al., "Cyclodextrin functionalized poly(methyl methacrylate) (PMMA) electrospun nanofibers for organic vapors waste treatment," *Journal of Membrane Science*, vol. 365, no. 1-2, pp. 409–417, 2010.

[91] X. Cao, X. Wang, B. Ding, J. Yu, and G. Sun, "Novel spider-web-like nanoporous networks based on jute cellulose nanowhiskers," *Carbohydrate Polymers*, vol. 92, no. 2, pp. 2041–2047, 2013.

[92] Y. C. Ahn, S. K. Park, G. T. Kim et al., "Development of high efficiency nanofilters made of nanofibers," *Current Applied Physics*, vol. 6, no. 6, pp. 1030–1035, 2006.

[93] http://www.amsoil.com/.

[94] N. Wang, A. Raza, Y. Si, J. Yu, G. Sun, and B. Ding, "Tortuously structured polyvinyl chloride/polyurethane fibrous membranes for high-efficiency fine particulate filtration," *Journal of Colloid and Interface Science*, vol. 398, pp. 240–246, 2013.

[95] Z. Dong, S. J. Kennedy, and Y. Wu, "Electrospinning materials for energy-related applications and devices," *Journal of Power Sources*, vol. 196, no. 11, pp. 4886–4904, 2011.

[96] L. Ji, Y. Yao, O. Toprakci et al., "Fabrication of carbon nanofiber-driven electrodes from electrospun polyacrylonitrile/polypyrrole bicomponents for high-performance rechargeable lithium-ion batteries," *Journal of Power Sources*, vol. 195, no. 7, pp. 2050–2056, 2010.

[97] V. Aravindan, V. S. Kumar, J. Sundaramurthy, W.C. Ling, S. Ramakrishna, and S. Madhavi, "Electrospun NiO nanofibers as high performance anode material for Li–ion batteries," *Journal of Power Sources*, vol. 227, pp. 284–290, 2013.

[98] S. A. Patil, S. Chigome, C. Hägerhäll, N. Torto, and L. Gorton, "Electrospun carbon nanofibers from polyacrylonitrile blended with activated or graphitized carbonaceous materials for improving anodic bioelectrocatalysis," *Bioresource Technology*, vol. 132, pp. 121–126, 2013.

[99] Z. Zhong, Q. Cao, B. Jing, X. Wang, X. Li, and H. Deng, "Electrospun PVdF-PVC nanofibrous polymer electrolytes for polymer lithium-ion batteries," *Materials Science and Engineering B*, vol. 177, no. 1, pp. 86–91, 2012.

[100] S.-H. Park, D.-H. Won, H.-J. Choi et al., "Dye-sensitized solar cells based on electrospun polymer blends as electrolytes," *Solar Energy Materials and Solar Cells*, vol. 95, no. 1, pp. 296–300, 2011.

[101] G. Ćirić-Marjanović, "Recent advances in polyaniline composites with metals, metalloids and nonmetals," *Synthetic Metals*, vol. 170, pp. 31–56, 2013.

[102] Y. A. Samad, A. Asghar, and R. Hashaikeh, "Electrospun cellulose/PEO fiber mats as a solid polymer electrolytes for Li ion batteries," *Renewable Energy*, vol. 56, pp. 90–95, 2013.

[103] A. C. Baptista, J. I. Martins, E. Fortunato, R. Martins, J. P. Borges, and I. Ferreira, "Thin and flexible bio-batteries made of electrospun cellulose-based membranes," *Biosensors and Bioelectronics*, vol. 26, no. 5, pp. 2742–2745, 2011.

[104] Y. E. Miao, G.-N. Zhu, H. Hou, Y.-Y. Xia, and T. Liu, "Electrospun polyimide nanofiber-based nonwoven separators for lithium-ion batteries," *Journal of Power Sources*, vol. 226, pp. 82–86, 2013.

[105] P. Raghavan, J. Manuel, X. Zhao, D.-S. Kim, J.-H. Ahn, and C. Nah, "Preparation and electrochemical characterization of gel polymer electrolyte based on electrospun polyacrylonitrile nonwoven membranes for lithium batteries," *Journal of Power Sources*, vol. 196, no. 16, pp. 6742–6749, 2011.

[106] N. Wu, Q. Cao, X. Wang, S. Li, X. Li, and H. Deng, "In situ ceramic fillers of electrospun thermoplastic polyurethane/poly(vinylidene fluoride) based gel polymer electrolytes for Li-ion batteries," *Journal of Power Sources*, vol. 196, no. 22, pp. 9751–9756, 2011.

[107] N. Wu, Q. Cao, X. Wang, and Q. Chen, "Study of a novel porous gel polymer electrolyte based on TPU/PVdF by electrospinning technique," *Solid State Ionics*, vol. 203, no. 1, pp. 42–46, 2011.

[108] K. B. Lee, "Urine-activated paper batteries for biosystems," *Journal of Micromechanics and Microengineering*, vol. 15, no. 9, pp. S210–S214, 2005.

[109] A. C. Baptista, J. I. Martins, E. Fortunato, R. Martins, J. P. Borges, and I. Ferreira, "Thin and flexible bio-batteries made of electrospun cellulose-based membranes," *Biosensors and Bioelectronics*, vol. 26, no. 5, pp. 2742–2745, 2011.

[110] T. Tamura and H. Kawakami, "Aligned electrospun nanofiber composite membranes for fuel cell electrolytes," *Nano Letters*, vol. 10, no. 4, pp. 1324–1328, 2010.

[111] Q. H. Guo, J. S. Huang, and T. Y. You, "Electrospun palladium nanoparticle-loaded carbon nanofiber for methanol electrooxidation," *Chinese Journal of Analytical Chemistry*, vol. 41, no. 2, pp. 210–214, 2013.

[112] M. M. Hasani-Sadrabadi, I. Shabani, M. Soleimani, and H. Moaddel, "Novel nanofiber-based triple-layer proton exchange membranes for fuel cell applications," *Journal of Power Sources*, vol. 196, no. 10, pp. 4599–4603, 2011.

[113] S. Martin, P. L. Garcia-Ybarra, and J. L. Castillo, "Electrospray deposition of catalyst layers with ultra-low Pt loadings for PEM fuel cells cathodes," *Journal of Power Sources*, vol. 195, no. 9, pp. 2443–2449, 2010.

[114] S. Chen, G. He, A. A. Carmona-Martinez et al., "Electrospun carbon fiber mat with layered architecture for anode in microbial fuel cells," *Electrochemistry Communications*, vol. 13, no. 10, pp. 1026–1029, 2011.

[115] J. B. Veluru, K. K. Manippady, M. Rajendiren et al., "Photocatalytic hydrogen generation by splitting of water from electrospun hybrid nanostructures," *International Journal of Hydrogen Energy*, vol. 38, no. 11, pp. 4324–4333, 2013.

[116] Z. Peining, A. S. Nair, Y. Shengyuan, P. Shengjie, N. K. Elumalai, and S. Ramakrishna, "Rice grain-shaped TiO_2–CNT composite—A functional material with a novel morphology for dye-sensitized solar cells," *Journal of Photochemistry and Photobiology A*, vol. 231, no. 1, pp. 9–18, 2012.

[117] S. Wu, J. Li, S.-C. Lo, Q. Tai, and F. Yan, "Enhanced performance of hybrid solar cells based on ordered electrospun ZnO nanofibers modified with CdS on the surface," *Organic Electronics*, vol. 13, no. 9, pp. 1569–1575, 2012.

[118] R. Afeesh, N. A.M. Barakat, S. S. Al-Deyab, A. Yousef, and H. Y. Kim, "Nematic shaped cadmium sulfide doped electrospun nanofiber mat: highly efficient, reusable, solar light photocatalyst," *Colloids and Surfaces A*, vol. 409, pp. 21–29, 2012.

[119] Y. Shengyuan, A. S. Nair, Z. Peining, and S. Ramakrishna, "Electrospun TiO_2 nanostructures sensitized by CdS in conjunction with CoS counter electrodes: quantum dot-sensitized solar cells all prepared by successive ionic layer adsorption and reaction," *Materials Letters*, vol. 76, pp. 43–46, 2012.

Hindawi Publishing Corporation
Conference Papers in Materials Science
Volume 2013, Article ID 578690, 4 pages
http://dx.doi.org/10.1155/2013/578690

Conference Paper

Development of Sustainable Technology to Produce Jute-Ramie Blended Textile and Its Applications

Debkumar Biswas, Anup Kumar Nandi, Syamal Kanti Chakrabarti, and Prabir Ray

Indian Jute Industries' Research Association (IJIRA), Kolkata, West Bengal 700088, India

Correspondence should be addressed to Debkumar Biswas; biswas.debkumar@gmail.com

Received 1 August 2013; Accepted 8 September 2013

Academic Editors: R. Fangueiro and H. Hong

This Conference Paper is based on a presentation given by Debkumar Biswas at "International Conference on Natural Fibers—Sustainable Materials for Advanced Applications 2013" held from 9 June 2013 to 11 June 2013 in Guimarães, Portugal.

Ramie (*Boehmeria nivea*), commonly known as China grass, is the strongest and finest plant fibre which is considered one of the valuable textile entities. Despite its unique characteristics, ramie has received reasonably less importance specially in the Indian subcontinent due to unavailability of appropriate postharvesting and processing technologies. With increase in global environmental awareness, the alternative (to cotton) cellulosic natural fibre "ramie" is gaining importance in the international textile domain. Sustainable methods and technologies which could trigger the utilization of ramie fibre are in demand worldwide. This paper will describe the developments carried out in the areas of postharvesting and spinning process of ramie. An ecofriendly degumming technology of ramie fibre has been elaborated along with suitable fibre processing route of ramie-jute blends that will bring new avenue for manufacturing jute diversified market acceptable products.

1. Introduction

The raw ramie fibre is extracted by decortication of long fibre strands or ribbons, where gummy matter is encrusted around the ultimate fibre. Decorticated ramie fibre contains 25–30% of noncellulosic gummy matter (pectic colloidal substances, i.e., gum) [1] consisting of pectins, waxes, lignin, and hemicellulose. Postharvesting technology particularly "degumming" is the most crucial aspect for successful processing of ramie fibre due to presence of gum which needs to be removed to the highest possible extent (degumming) without compromising fibre properties and performance [2]. The existing degumming technologies [3] commonly practiced in the Indian subcontinent region encounter multifold limitations including biohazard and processing difficulties. As a sustainable alternative, a user friendly degumming technology has been developed recently exploring biotechnological (enzymatic) method. A cocktail of enzymes has been judiciously formulated with market available varieties, namely, hemicellulase, pectinase and pectate lyase, and so forth, and applied on freshly decorticated ramie to get a fibre that could be transformed into valuable blended textiles.

Degummed ramie fibre is suitable for textile applications since its properties have close coherence with the aesthetics of the apparel textiles [4]. However, available varieties of ramie fibre in India are difficult to process in both "long-staple" and "short-staple" spinning systems for producing finer yarns [5–7]; as a result ramie has been losing its worth in Indian textile scenario. A wide range of fibres have been tried for blending with ramie among them jute; a lingocellulosic plant fibre abundantly produced in the Indian subcontinent region, is an important one [8]. Both the fibres inherently have some similarities in their chemical constituents and physical properties [9]. These attributes are encouraging enough to get uniform fibre blend that might actuate the smooth fibre processing as well. In the current study, ramie fibre has been efficiently blended with Jute in different blend proportions (ramie : jute—100 : 0; and 50 : 50; 20 : 80) to produce jute-ramie blended fine yarns of count range from 75 tex to 45 tex, something difficult to produce with pure

jute fibre in commercial scale [10]. Innovative processing and spinning route (combination of semiworsted and jute spinning machines) have been explored to manufacture jute-ramie blended fine yarns without much alteration in existing industrial jute spinning setup.

The jute-ramie blended fabrics are superior in quality, having the potentiality to be utilized as value added home textiles.

2. Experimental Methods

2.1. Enzymatic Degumming of Ramie. To compensate the limitations of conventional "chemical degumming" [11] technology, which represents high energy consumption and heavy release of caustic residue in effluents, an enzymatic degumming route of ramie fibre has been explored. To avoid the processing difficulties, the common method of enzyme extraction from bacterial stains has been evaded. Purified grade of substrate specific enzymes has been mixed in a fitting ratio to develop a degumming formulation. The formulation has been tried on freshly decorticated ramie to get fibres that could be processed subsequently.

Ramie requires a multifunctional enzyme system to liquefy its complex gummy matters represented majorly by hemicellulose, pectin and lignin. The formulation comprising of synergistic mixture of organic enzymes has been used for the required degumming action. Major components of the enzyme formulation are hemicellulase (xylanase, arabinase) and pectinase (pectate lyase, polygalacturonase); those are supplied by Novozymes A/S, Denmark, in purified form. Activities of enzyme formulation on the substrate have been ensured by repeated enzyme assay. The enzyme formulation has shown optimum activity in 5.0 to 5.7 pH range; to achieve such pH profile Citrate Buffer (pH 3.0–6.2) has been selected as degumming bath media.

2.1.1. Degumming Process. The bundle of freshly decorticated raw ramie fibre having 70–75% moisture has been briefly opened up by manual hackling action with combs. After that prewashing treatment has been given to the decorticated fibre with ecoemulsifier to an extent of 0.1-0.2% on the weight of fibre. Citrate Buffer solution is prepared (pH—5.5–5.7) next to prewashing process for preparation of degumming bath (MLR-1 : 5). Subsequently, the enzyme formulation, as per optimized quantity, is added to the bath (1.0% enzyme on wt. of the fibre) along with gentle stirring action. Fibre bunch is then dipped into the degumming bath and kept in the incubation system for 24 Hrs.

2.1.2. Fibre Characterization. The efficiency of the degumming process is evaluated by the estimation of residual gum content (repeated acid and alkali extraction method) remaining in degummed fibre. Fibre tensile strength (IS 7032, Part-7) and fibre fineness (IS 7032, Part-8) are measured for both raw and degummed fibres for comparative analysis. Surface characteristics of the fibres have been observed under scanning electron microscopy (SEM).

Table 1: Characterization of degummed.

Pectinase	Enzyme activity (Units/mL)		
	Jute hemicellulase	Endo, β-1-4-glucanase	Exo, β-1-4-glucanase
23000	560	360	20

Table 2: Characterization of degummed ramie fibres.

Test parameters	Raw ramie	Degummed ramie
Residual gum %	25.00	6.06
Fibre fineness (tex)	1.50	0.76
Single fibre tenacity (g/tex)	30.58	28.61
Bulk density (g/cc)	0.27	0.37

2.2. Customized Processing System for Ramie Blends. Ramie, being longer and finer natural fibre, is difficult to process and spin yarn utilizing commonly available spinning systems. Both short-staple spinning system, namely, cotton spinning and long-staple spinning process, namely, worsted spinning system have been explored for spinning of ramie yarns, although economic viability of such industrial process is difficult to attain. In search of a suitable alternative method to spin ramie blended yarns, a processing sequence has been customized which is basically a combination of jute and semiworsted spinning machinery.

Mainly four varieties of yarns, namely, 100% ramie, 50 : 50 jute-ramie, 80 : 20 jute-ramie blended, and 100% jute yarns have been developed under identical processing conditions.

2.2.1. Customized Spinning System. See Figure 2.

2.2.2. Characterization of Yarn. The quality characteristics of four varieties of ramie and jute-ramie blended yarns have been evaluated and compared with jute yarns. Tensile properties and yarn evenness properties have been evaluated in INSTRON (5500-R) and UT3 instruments.

3. Results and Conclusions

Before performing fibre degumming process, the activities of component enzymes in the formulation have been evaluated to ascertain the conjugal strength of the developed degumming formulation. It is observed (Table 1) that activity of pectinase is considerably high, and hemicellulase activity level is found to be within the desired mark.

The enzyme-based degumming formulation effectively acted on gummy substances and removed almost 75% of the inherent gum in ramie. The SEM of degummed fibre (see Figure 1 and Table 2) represents a regular and smooth surface as compared to raw fibre because of the removal of gummy matters from the fibre's outer periphery. As shown in Table 1 the fineness of ramie fibre has improved considerably without much compromise in tensile properties.

Quality parameters of developed yarns are compared with 100% ramie and 100% jute yarns, produced using identical process conditions. Gradual improvement in yarn quality

Table 3: Comparative analysis of yarn quality.

Yarn parameters	100% Ramie	50% Ramie 50% jute	20% Ramie 80% jute	100% Jute
Average yarn count (tex)	40.65	53.74	75.80	77.86
Wt. CV%	6.34	6.53	4.51	6.42
Yarn tenacity (g/tex)	13.81	9.27	7.63	7.48
Hairiness index	11.73	15.28	17.48	18.88

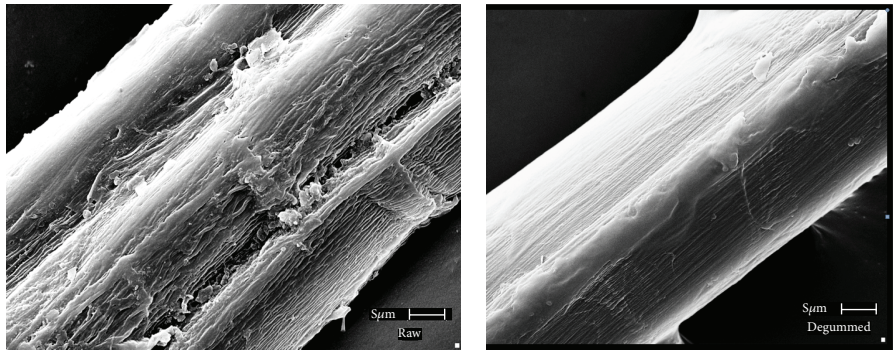

(a) (b)

Figure 1: SEM of raw and degummed ramie.

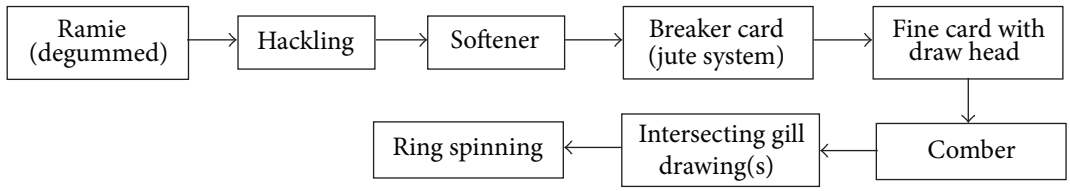

Figure 2

has been observed (Table 3) as the proportion of ramie is increased in the blends.

4. Conclusion

New sustainable approach for postharvesting processing and spinning of ramie fibre has been developed in this R&D study. The prescribed fibre degumming technology is biofriendly and the produced fibres possess adequate strength required for sustain subsequent fibre processing. The residual gum content and fineness confirm the suitability of degummed fibre in textile applications. The customized spinning line is effective for blending ramie with jute and other compatible fibres. The jute-ramie blended yarns are superior in quality and appearance and are quite suitable for development of home textiles that might add value to jute-based diversified product market.

Conflict of Interests

The authors declare that there is no conflict of interests regarding the publication of this paper. Debkumar Biswas does not have a direct financial relation that might lead to a conflict of interests to any of the authors.

Acknowledgments

The authors gratefully acknowledge the financial support of the National Jute Board, Ministry of Textiles, Government. of India. The authors also express gratitude to the Indian Jute Industry and the Indian Council of Agricultural Research (ICAR) for their help and technical support.

References

[1] P. Satya, D. Sarkar, C. S. Kar et al., "Possibilities for reducing gum content in ramie by genetic modification of pectin biosynthesis pathway," *Indian Journal of Experimental Biology*, vol. 3, no. 3, pp. 261–264, 2010.

[2] P. C. Das Gupta, K. Sen, and S. K. Sen, "Degumming of decorticated ramie for textile purposes," *Cellulose Chemistry and Technology*, vol. 10, pp. 285–291, 1976.

[3] S. N. Pandey, "Ramie fibre: Part I. Chemical composition and chemical properties. A critical review of recent developments," *Textile Progress*, vol. 39, no. 1, pp. 1–66, 2007.

[4] S. K. Chattopadhyay and M. Ahmed, "Blended Textiles for Niche Market from Natural Fibres," 2006-2007, http://www.cicr.org.in/.

[5] G. Basu and A. N. Roy, "Blending of jute with different natural fibres," *Journal of Natural Fibers*, vol. 4, no. 4, pp. 13–29, 2007.

[6] M. C. Mazumder, S. K. Sen, and P. C. Das Gupta, "Blending of ramie with jute for fine yarn production," *Indian Textile Journal*, vol. 85, p. 135, 1975.

[7] M. C. Mazumder, S. K. Sen, and P. C. Das Gupta, "Processing of degummed ramie on jute machinery," *Indian Textile Journal*, vol. 86, p. 87, 1976.

[8] S. K. Dey and S. K. Bhattacharya, "Perspective use of Ramie Fibre in blends with jute," in *Proceeding of 24th Indian Jute Industries' Research Association Technological Conference*, p. 123, 2002.

[9] S. N. Pandey, "Ramie fibre: part II. Physical fibre properties. A critical appreciation of recent developments," *Textile Progress*, vol. 39, no. 4, pp. 189–268, 2007.

[10] S. O. Perum, B. N. Iliev, H. A. Zoneva, and B. L. Ilieva, *Method of Production of Fine (Hemp) Jute Yarns*, 1985.

[11] S. K. Bhaduri and P. K. Ganguly, Indian Patent No.-220787, 2007.

Hindawi Publishing Corporation
Conference Papers in Materials Science
Volume 2013, Article ID 171867, 5 pages
http://dx.doi.org/10.1155/2013/171867

Conference Paper

Characterization of Cellulose Microfibrils Obtained from Hemp

Anna Šutka,[1] Silvija Kukle,[1] Janis Gravitis,[2] and Laima Grave[1]

[1] *Institute of Textile Materials Technologies and Design, Riga Technical University, Riga 1048, Latvia*
[2] *Laboratory of Biomass Eco-Efficient Conversion, Latvian State Institute of Wood Chemistry, Dzerbenes Street 27, Riga 1006, Latvia*

Correspondence should be addressed to Anna Šutka; anna.putnina@rtu.lv

Received 4 July 2013; Accepted 2 October 2013

Academic Editors: R. Alagirusamy, R. Fangueiro, H. Hong, and A. T. Marques

This Conference Paper is based on a presentation given by Anna Šutka at "International Conference on Natural Fibers—Sustainable Materials for Advanced Applications 2013" held from 9 June 2013 to 11 June 2013 in Guimarães, Portugal.

Microfibrillated cellulose was extracted from hemp fibres using steam explosion pretreatment and high-intensity ultrasonic treatment (HIUS). The acquired results after steam explosion treatment and water and alkali treatments are discussed and interpreted by Fourier transform infrared spectroscopy (FTIR). Scanning electron microscopy (SEM) was used to examine the microstructure of hemp fibres before and after each treatment. A fibre size analyser was used to analyse the dimensions of the untreated and treated cellulose fibrils. SEM observations show that the sizes of the different treated fibrils have a diameter range of several micrometres, but after HIUS treatment fibres are separate from microfibrils, nanofibres, and their agglomerates.

1. Introduction

Hemp fibres have high strength, low density, and high sustainability; therefore they are used as reinforcement in composite materials. This usefulness of cellulose fibrils is because small fibrils have better mechanical properties than the individual macrofibres. Within their structure, small fibrils include more cellulose crystals, having a higher elastic modulus than fibres, which contribute to their increased strengths [1]. Microfibrillated cellulose (MFC) is cellulose fibril aggregates obtained through disintegration of the cell wall in cellulose fibres [2]. The diameter of MFC fibrils is usually at the range of 10–100 nm and can be up to several micrometres in length, depending on the preparation methods and material source [3].

This paper compares the preparation of cellulose micro- and nanofibers obtained from hemp bast fibres and shives using steam explosion and high-intensity ultrasonication treatments.

The steam explosion (SE) autohydrolysis is currently comprehensively studied as a promising green pretreatment technology [4, 5] to obtain microfibrils of cellulose and also to remove noncelluloses constitutes—lignin, hemicelluloses, pectins, and waxes.

The high-intensity ultrasonication technique is an environmentally benign method and a simplified process that conducts fibre isolation and chemical modification simultaneously and helps significantly reduce the production cost of cellulose nanofibre and its composites [3]. HIUS creates cavitation and high vibrational energy in the suspension, resulting in the separation of hemp cellulose micro- and nanofibre bundles and agglomerates [6]. In the present work SE and HIUS will be combined to obtain MFC fibrils.

2. Materials and Methods

Dew-retted hemp fibres of local variety "Purini" and shives of local variety "Bialobrzeskie" grown on the experimental fields of the Latgalian Agriculture Research Center LLZC (Latvia, district Vilani) and sodium hydroxide (NaOH) (Commercial grade) are used in this research. Hemp fibres were prepared by cutting into uniform size of approximately 1-2 mm length, whereas shives were prepared by milling into uniform size of approximately 1-2 mm length. This size of fibers and shives allows steam explosion process and ultrasound treatment taking place in the chemical and physical processes to

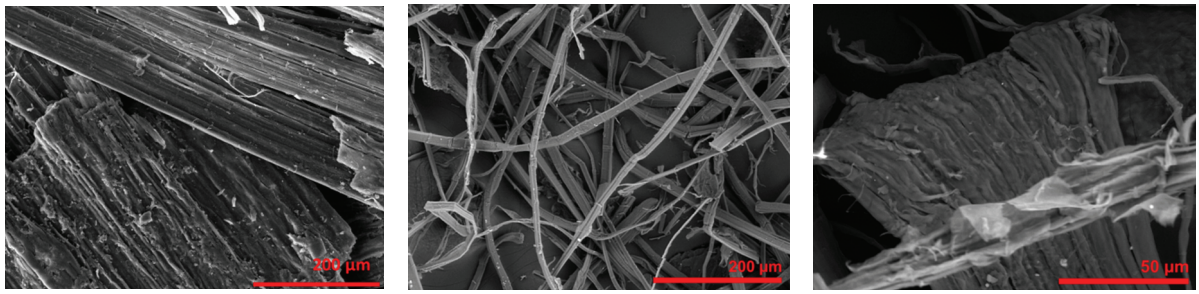

F F SE WA F SE WA

Figure 1: Untreated and steam-exploded hemp fibers.

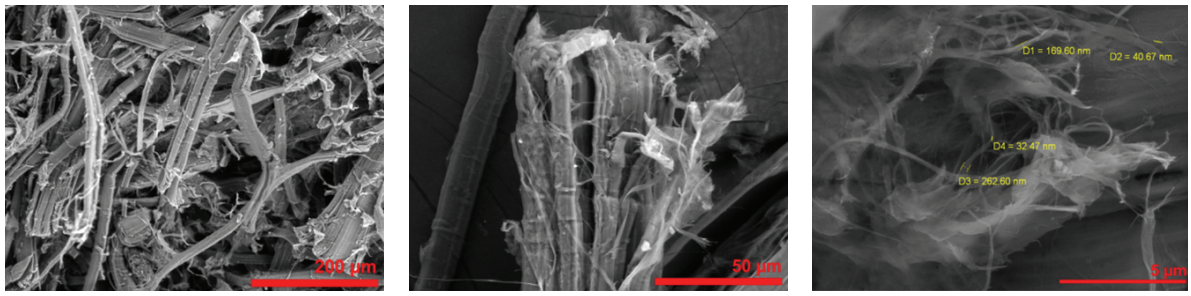

Figure 2: Ultrasonic-treated hemp fibers after steam explosion (F SE WA US).

penetrate deeper into the fibers in the inner layers. The samples variants under investigation are shown in Table 1.

2.1. Steam Explosion Treatment. Steam explosion treatment (SE) conditions are shown in Table 2. After SE treatment hydrothermal and alkali treatment follows that allows partial removal of constituents from hemp fibres including hemicelluloses, pectins/waxes, lignin, and oils covering the external surface of the fibres cell wall.

Severity parameter or the reaction ordinate R_0 can be expressed as

$$R_0 = t * \exp\left[\frac{(T-100)}{14.75}\right], \quad (1)$$

where duration of the value of treatment time (t, minutes) and temperature (T, °C) express the SE severity against the base temperature T_{base} or reference = 100°C [7].

2.2. High-Intensity Ultrasonication Technique (HIUS). The fibres were suspended in distilled water and treated with ultrasound (ultrasonic processor UP 200 Hp, 200 W, frequency 26 kHz, amplitude 90%, sonotrode S26d14, Ø14 mm) (HIUS) for 45 min. HIUS produces very strong mechanical oscillating power, so cellulose fibrils can be isolated from cellulose fibres by the action of hydrodynamic forces of ultrasound [8]. In order to control the process temperature, the beaker with the cellulose fibres in water was put in a water bath with controlled temperature. The fibres and shives suspensions were filtered and dried at room temperature, while there is no change in mass.

Table 1: Sample variants under investigation.

Sample	SE	Water extraction	0.4% NaOH extraction	HIUS
F (fibers)	−	−	−	−
F SE WA	+	+	+	−
F SE WA US	+	+	+	+
S (shives)	−	−	−	−
S SE WA	+	+	+	−
S SE WA US	+	+	+	+

Table 2: Steam explosion treatment parameters.

Variants	SE parameters			
	Temperature °C	Pressure bar	Time min	log R_0
Fibres ("Purini")	235	32	3	3.97
Shives ("Bialobrzeskie")	235	32	3	3.97

2.3. Fourier Infrared Spectroscopy (FTIR). Fourier transform infrared (FTIR) spectra of the samples under investigation were recorded in KBr pellets by Spectrum One (Perkin Elmer, UK) FTIR spectrometer in the range of 4000–400 cm^{-1} (resolution: 4 cm^{-1}). About 2 mg of sample was crushed into powder. The fibre or shive particles were then mixed with KBr and pressed into a disc about 1 mm thick.

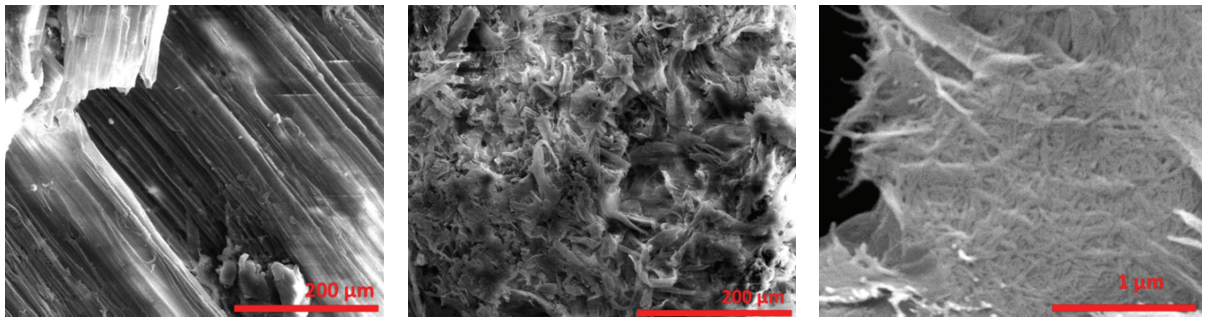

Figure 3: Untreated, steam-exploded, and ultrasonic-treated hemp.

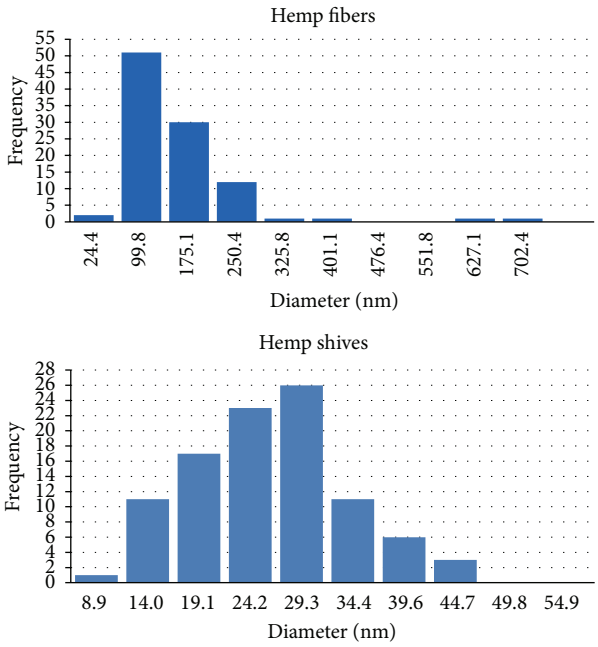

Figure 4: Size distribution of steam-exploded and ultrasonic-treated hemp fibers and shives diameter.

2.4. Scanning Electron Microscopy (SEM). SEM micrographs of fibres surface were taken using a scanning electron microscope VEGA Tescan 5136M (Czech Republic—UK). Prior to SEM evaluation, the samples were coated with gold by means of a plasma sputtering apparatus.

2.5. Static Image Analysis. CorelDRAW Graphics Suite X6 software was used to measure the diameters of fibres and shives from two dimensional images obtained from SEM micrographs.

3. Results and Conclusions

This study shows that there are substantial differences on the isolation of hemp microfibrils after various treatments (alkali treatment, steam explosion, and ultrasonic treatment), surface morphology, physical properties, and chemical composition of microfibrils.

Table 3: Diameters of fibers and shives particles after SE and HIUS treatments.

Diameter nm	Fibers (F SE WA US)	Shives (S SE WA US)
Average	125.2	24.0
Max	777.8	60.0
Min	24.4	8.9

The cellulose microfibrils made by steam explosion and HIUS treatment were light and dark brown depending on treatment conditions and severity parameter, still indicating the presence of residual organic substrates, including a small amount of lignin.

SEM is used to characterize properties of hemp fibers and shives such as fiber diameter, diameter distribution, fiber orientation, and morphology. Figures 1, 2, and 3 show SEM micrographs of untreated, steam-exploded, and ultrasonic treated hemp fibres. From micrographs we can see differences of surface morphologies and fibril sizes. SEM showing the presence of the individual cellulose micro- and nanofibres obtained from hemp on steam explosion together with ultrasonication is used. Rest of the samples did not show formation of MFC fibrils which could be explained by insufficient and uneven capacity of steam explosion treatment to form fibrils.

Shorter and finer fibrils were observed from the micrographs of shive S SE WA US sample (Figure 3), a combination of SE and HIUS treatments; however, fibrils were not individual but agglomerate during the sample drying process affected by the strong intermolecular hydrogen bonding [3].

Size distributions of the diameter of nanofibres obtained from shives (S SE WA US) and fibers (F SE WA US) by image analysis are compared in Figure 4. From these results, hemp fibers were found to have diameters ranging from 20 to 700 nm with average value ~125 nm, whereas shives range from 9 to 60 nm with average value 24 (Table 3). From Figure 4 we can see that nanofibres obtained from shives have more uniform distribution of diameters than nanofibres obtain from bast fibers.

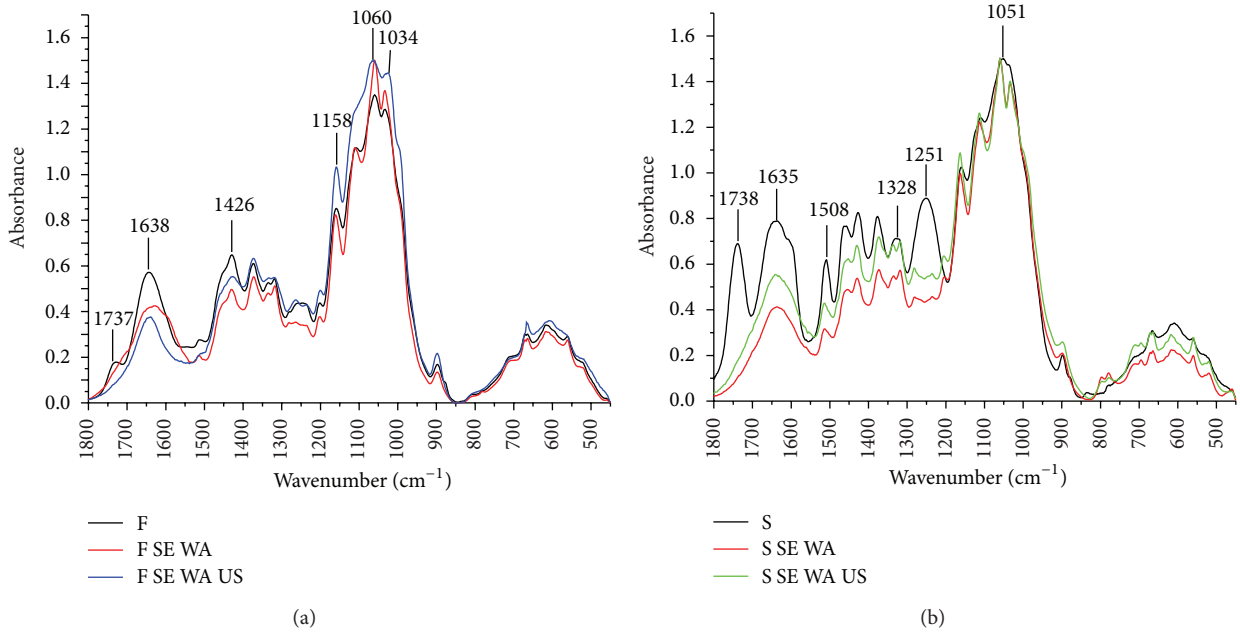

Figure 5: FTIR spectra of untreated, steam-exploded, and HIUS-treated hemp fibres (F) and shives (S).

Infrared Furrier spectroscopy allows revealing modifications of main structures; noncellulose compounds through identification of carboxylacids and esters found in pectin, lignin, and waxes were found in cellulose microfibrils [9]. The hemp fibres showed characteristic peaks at 1737 cm^{-1} (unconjugated C=O in hemicellulose) and 1638 cm^{-1} (absorbed O–H or carbonyl band) (Figure 5(a)). IR bands of hemp shives are found at 1738 cm^{-1} (unconjugated C=O in hemicellulose), 1635 cm^{-1} (absorbed O–H or carbonyl band), 1508 cm^{-1} (aromatic rings of lignin), and 1251 cm^{-1} (acetylated hemicellulose) (Figure 5(b)) [10, 11]. After SE, water and alkali extraction corresponding peaks are decreasing. HIUS treatment improves the extraction of lignin as evidenced by the disappearance of peak at 1508 cm^{-1}.

4. Conclusions

Hemp cellulose microfibrils are individualized from bast fibres and shives using steam explosion, hydrothermal and alkali treatment and high-intensity ultrasonication. Results of this study have shown that SE treatment combined with following hydrothermal and 0,4 wt.% NaOH treatment allows partial removal of constituents from hemp fibres. SEM observations show that the sizes of the different treated fibrils have a diameter range of several micrometres. It can be seen that after HIUS treatment fibres are separate from microfibrils, nanofibres, and their agglomerates. FTIR analysis showed differences between the spectra for the untreated, steam-exploded, and ultrasound-treated hemp fibres and shives. Further work should be performed in order to avoid agglomeration of microfibrils due to and after ultrasonic treatment for further nanotechnological processing.

Acknowledgment

This work has been supported by the European Social Fund within the project "support for the implementation of doctoral studies at Riga Technical University."

References

[1] I. Sakurada, Y. Nukushina, and T. Ito, "Experimental determination of the elastic modulus of crystalline regions in oriented polymers," *Journal of Polymer Science A*, vol. 57, no. 165, pp. 651–600, 1962.

[2] A. Svagan, *Bio-inspired polysaccharide nanocomposites and foams. doctor of philosophy [Ph.D. thesis]*, KTH Chemical Science and Engineering, Department of Fibre and Polymer Technology, Stockholm, Sweden, 2006.

[3] E. H. Qua, P. R. Hornsby, H. S. S. Sharma, and G. Lyons, "Preparation and characterisation of cellulose nanofibres," *Journal of Materials Science*, vol. 46, no. 18, pp. 6029–6045, 2011.

[4] B. Deepa, E. Abraham, B. M. Cherian et al., "Structure, morphology and thermal characteristics of banana nano fibers obtained by steam explosion," *Bioresource Technology*, vol. 102, no. 2, pp. 1988–1997, 2011.

[5] Q. Cheng and S. Wang, "A novel process to isolate fibrils from cellulose fibers by high-intensity ultrasonication, part 1: Process optimization," *Journal of Applied Polymer Science*, vol. 113, no. 2, pp. 1270–1275, 2009.

[6] N. Sano, M. Naito, M. Chhowalla et al., "Pressure effects on nanotubes formation using the submerged arc in water method," *Chemical Physics Letters*, vol. 378, no. 1-2, pp. 29–34, 2003.

[7] M. Heitz, E. Capek-Monard, P. G. Keoberle et al., "Fractionation of populus tremuloides at the pilot plant scale: optimization of steam pretreatment conditions using the STAKE II technology," *Bioresource Technology*, vol. 35, no. 1, pp. 23–32, 1991.

[8] Q. Cheng, *Fabrication and analysis of polymeric nanocomposites from cellulose fibrils [Ph.D. thesis]*, University of Tennessee, Knoxville, Tenn, USA, 2007.

[9] Q. Wang, X. R. Fan, W. D. Gao, and J. Chen, "Characterization of bioscoured cotton fabrics using FT-IR ATR spectroscopy and microscopy techniques," *Carbohydrate Research*, vol. 341, no. 12, pp. 2170–2175, 2006.

[10] D. M. Panaitescu, D. Donescu, C. Bercu, D. M. Vuluga, M. Iorga, and M. Ghiurea, "Polymer composites with cellulose microfibrils," *Polymer Engineering & Science*, vol. 47, no. 8, pp. 1228–1234, 2007.

[11] D. M. Panaitescu, D. Donescu, C. Bercu, D. M. Vuluga, M. Iorga, and M. Ghiurea, "Polymer composites with cellulose microfibrils," *Polymer Engineering and Science*, vol. 47, no. 8, pp. 1228–1234, 2007.

Hindawi Publishing Corporation
Conference Papers in Materials Science
Volume 2013, Article ID 750802, 5 pages
http://dx.doi.org/10.1155/2013/750802

Conference Paper

A Mechanical Analysis of *In Situ* Polymerized Poly(butylene terephthalate) Flax Fiber Reinforced Composites Produced by RTM

C. Romão,[1] C. M. C. Pereira,[2] and J. L. Esteves[3]

[1] *Department of Mechanical Engineering and Industrial Management (DEMGI), School of Technology and Management, Polytechnic Institute of Viseu, 3504-510 Viseu, Portugal*
[2] *Institute of Mechanical Engineering and Industrial Management (INEGI), University of Porto, 4200-465 Porto, Portugal*
[3] *Department of Mechanical Engineering (DEMec), Faculty of Engineering, University of Porto, 4200-465 Porto, Portugal*

Correspondence should be addressed to C. Romão; romao@estv.ipv.pt

Received 16 September 2013; Accepted 18 November 2013

Academic Editors: R. Fangueiro, H. Hong, and A. T. Marques

This Conference Paper is based on a presentation given by C. Romão at "International Conference on Natural Fibers—Sustainable Materials for Advanced Applications 2013" held from 9 June 2013 to 11 June 2013 in Guimarães, Portugal.

This work addresses mechanical characterization in tension of woven flax fabric reinforced *in situ* polymerized poly(butylene terephthalate) composites, produced by the RTM technique. A brief description of the developed RTM set-up is made and the composite manufacturing details are presented. A morphological analysis of the mechanically characterized materials by Scanning Electronic Microscopy (SEM) is also made. The produced neat polymer (pCBT) showed a brittle behavior and mechanical properties lower than those found in the literature. Its reinforcement with woven flax fabric resulted in an enhancement of both tensile strength and stiffness. The obtained results can be significantly improved by the polymer modifying chemically , optimizing the control of the processing parameters, and subjecting flax fibers to a surface treatment compatible with the CBT 160 resin.

1. Introduction

Thermoplastic composites offer some interesting advantages over thermosets counterparts, such as higher toughness and impact resistance, recyclability, and faster production cycles. The use of vegetable fibers as reinforcement, replacing glass fibers, further increases the range of benefits: they are renewable, less expensive, and not abrasive and have lower density, specific properties (σ_r/ρ and E/ρ) that can be comparable to those of glass fibers (e.g., hemp and flax) and have lower environmental impact, since they are biodegradable and easily recyclable. The thermoplastic matrix selection needs, however, to take into account the vegetal fibers low thermal resistance and the processing technique that will be used. The cellulosic component of the fibers experiences a fast and irreversible degradation at temperatures about 200°C [1, 2].

The common thermoplastic processing techniques do not allow the combination of engineering or high performance thermoplastics with vegetal fibers due to its high melting temperature. Reactive processing of thermoplastics is a recent technique, currently in development and optimization, which makes use of mono- or oligomeric precursors that, after heated and mixed with an activator system, impregnate the fibers and polymerize *in-situ* to form the desired matrix. Due to its low molecular weight the precursors have extremely low melt viscosity (in order of mPa.s) allowing appropriate impregnation of short and continuous reinforcement at lower processing pressures and moderate temperatures (180 to 250°C for PA12 and PBT). The traditional liquid molding technologies of thermoset composites (like RTM, VARTM, SRIM, and RRIM) can be used to process this new generation of thermoplastic materials. Though, attending to the existing

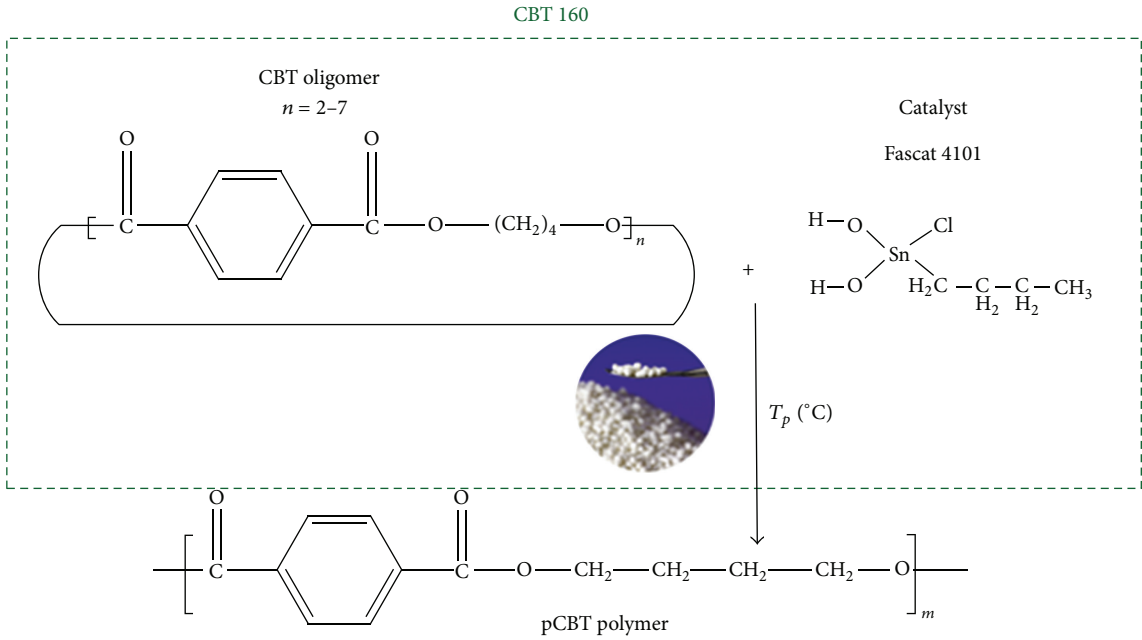

Figure 1: CBT 160 resin and its polymerization to pCBT (polymerized CBT).

differences in the processing of these two types of polymeric materials, it is necessary to make adjustments in the traditional RTM equipment [3, 4].

This paper describes the mechanical behavior in tension of neat and flax fiber reinforced *in-situ* polymerized poly(butylene terephthalate), produced by the isothermal RTM technique, starting from the precursor Cyclic Butylene Terephthalate (CBT resin). A morphological analysis of the mechanically characterized materials by Scanning Electronic Microscopy (SEM) is also made.

The main objective was to investigate the possible compatibility between these two kinds of materials, both very sensitive to humidity. Reactive processing of vegetal fiber reinforced thermoplastics, as far as the authors know, had not been tested so far.

2. Materials and Methods

2.1. Materials. The polymeric precursor used in this study is the one-component CBT 160 resin, a Cyclic Butylene Terephthalate oligomer mixture that already contains the catalyst (Figure 1), supplied by Cyclics Corporation (Schwarzheide, Germany). It is reinforced with nontreated flax woven fabric, supplied by Composites Evolution (Chesterfield, United Kingdom), suitable for processing by traditional liquid molding techniques such as hand lay-up, vacuum infusion, and RTM. The woven fabric type is 4×4 Hopsack, based on 250 tex yarns, with 7 warp ends/cm, 11 weft picks/cm, and a surface weight of 510 g/m^2 (Figure 2).

Figure 2: Biotex Flax 4 × 4 Hopsack, 510 g/m^2.

2.2. RTM Set-Up and Composite Manufacturing Details. The developed RTM set-up consists mainly of a heated mold, a system for melting the resin under nitrogen atmosphere (fusion system), a heated system to inject the resin into the fiber bed, and three different temperature control units connected to each of these thermal systems (Figure 3). The CBT 160 resin was heated under a nitrogen atmosphere to 190°C (aprox.) and then injected under a nitrogen pressure of 2–50 kPa into the closed mold, at the same temperature. Once the mold was completely filled, the temperature was maintained for 30 min, in order to complete the polymerization reaction and to allow for cold crystallization. In principle, the part could be demolded at this temperature. However, since demolding at such high temperatures is rather troublesome with the current mold set-up, the part was allowed to cool before demolding. Before processing, CBT 160 was dried at 80°C for 2 h. Composites were produced using a 32% volume fraction of 4×4 Hopsack woven flax fabric undried and dried at 80°C for 24 h.

2.3. Mechanical Properties. Tensile tests were performed according to ISO 527-4, on a universal INSTRON 3367

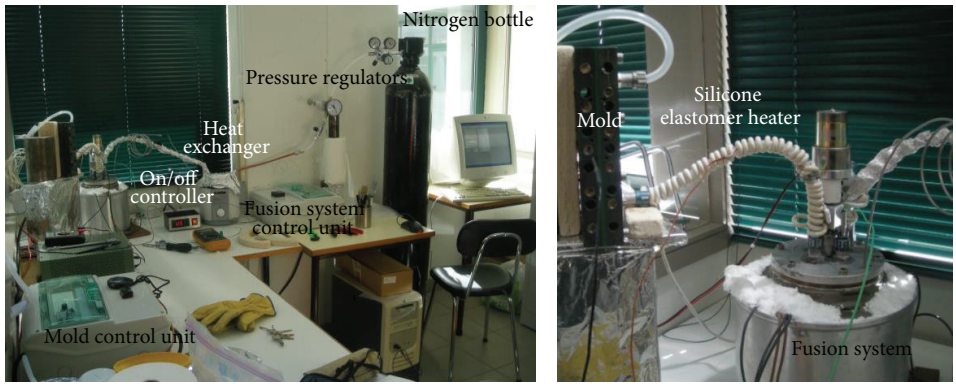

Figure 3: The developed RTM set-up.

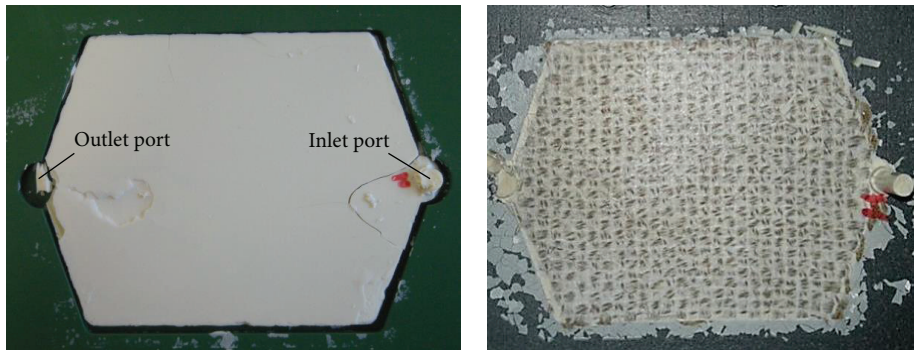

(a) (b)

Figure 4: Pure pCBT (a) and flax reinforced pCBT (b) plates produced by RTM.

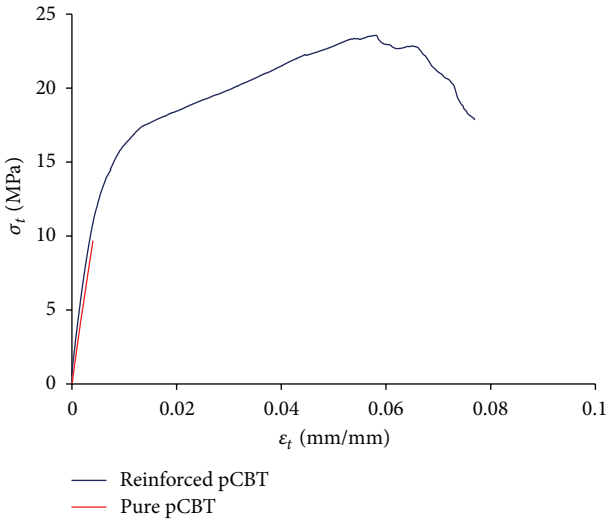

Figure 5: Typical tensile stress—strain plots for pure and reinforced pCBT.

machine equipped with a 30 kN load cell and an extensometer with a gauge length of 25 mm. The test speed was 2 mm/min.

2.4. Morphological Analysis. The morphology of the developed materials was analyzed by SEM, using a scanning electron microscope with integrated X-ray microanalysis: FEI QUANTA 400 FEG ESEM/EDAX PEGASUS.

3. Results and Discussion

3.1. Production. Flat plates ($100 \times 100 \times 4\,mm^3$) of neat and reinforced pCBT (polymerized Cyclic Butylene Terephthalate) were successfully produced using the RTM set-up and the production method described previously (Figure 4). The neat pCBT plates exhibit a higher mold shrinkage, during which fissuration also took place. The incorporation of the reinforcement reduced the matrix shrinkage; however, the presence of microcracks randomly distributed on the surface of the produced plates was observed. The presence of microcracks is also reported by other researchers for glass fiber reinforcements [5].

3.2. Mechanical Properties. Both neat and reinforced pCBT (polymerized Cyclic Butylene Terephthalate) were mechanically characterized. The results from the tensile tests are shown in Figure 5 and Table 1.

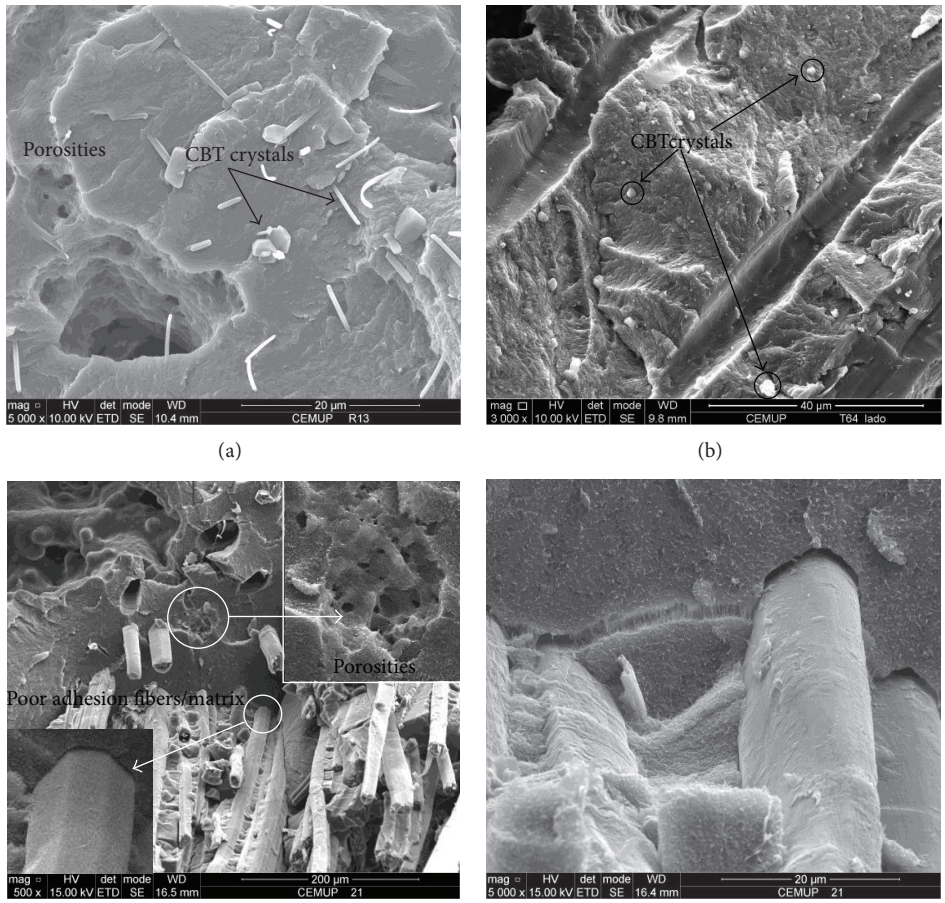

Figure 6: SEM micrographs of neat pCBT (a) and flax reinforced pCBT ((b), (c), and (d)).

Table 1: Uniaxial tension test results.

Samples		σ_t [MPa]	E_t [GPa]
Neat pCBT		15.0 ± 1.0	2.48 ± 0.26
pCBT/flax	Undried fibers	20.0 ± 0.5	3.89 ± 0.57
pCBT/flax	Dried fibers	26.1 ± 1.4	3.46 ± 0.91

Analyzing the results presented above, it is possible to conclude the following. (i) Neat pCBT isothermally processed at 190°C is brittle and has a tensile strength lower than that obtained by Mohd Ishak et al. [6] and Miller [7]. The pCBT brittleness has been already reported by several authors that investigate physical and/or chemical modification methods of pCBT [8, 9]. (ii) The reinforcement of pCBT with woven flax fabric results in an enhancement of both tensile strength and stiffness (iii) The use of dried fibers improves substantially the tensile strength of the composites.

3.3. Morphological Analysis. SEM micrographs are provided in Figure 6. Its analysis revealed (i) the presence of CBT oligomer crystals in both neat pCBT (Figure 6(a)) and reinforced pCBT (Figure 6(b)) samples; according to Abt et al. [9] these crystals act as a rigid filler and contribute to the brittleness of unmodified pCBT; the amount of CBT crystals apparently exceeds the equilibrium content (usually between 1 and 3%) which may have contributed to an increase in pCBT brittleness and to the decrease in its characteristic tensile properties; (ii) the presence of porosities in both neat (Figure 6(a)) and flax reinforced pCBT (Figure 6(c)) that influence, also, the mechanical properties; (iii) a low adhesion between the fibers and the matrix in most of the observed samples that can be improved by performing surface treatments on flax fibers.

4. Conclusions

The developed RTM production system enabled the successful production of the materials with the desired geometry. Notwithstanding, the neat polymer showed a brittle behavior and lower mechanical properties than those found in the literature. The analysis of the process and the results allowed concluding that neat pCBT mechanical properties can be further improved by optimizing the control of the processing parameters (pressure and temperature) and modifying chemically the pCBT polymer in order to decrease its brittleness. The composites exhibited better mechanical properties than those of pure polymer, although a weak

adhesion fibers/matrix that can be improved by subjecting flax fibers to a surface treatment compatible with the CBT 160 resin has been observed.

Acknowledgment

The authors gratefully acknowledge the funding by Ministério da Ciência, Tecnologia e Ensino Superior, FCT, Portugal, under the SFRH/BD/40522/2007 grant.

References

[1] C. Romão, *Estudo do Comportamento Mecânico de Materiais Compósitos de Matriz Polimérica Reforçados com Fibras Naturais*, Tese de Mestrado, Universidade do Porto, 2003.

[2] C. Bailie, *Green Composites: Polymer Composites and the Environment*, Woodhead, Canada, 2004.

[3] H. Parton, *Characterisation of the* in-situ *polymerisation production process for continuous fibre reinforced termoplastics [Ph.D. thesis]*, Katholieke Universiteit Leuven, 2006.

[4] K. van Rijswijk and H. E. N. Bersee, "Reactive processing of textile fiber-reinforced thermoplastic composites—an overview," *Composites A*, vol. 38, no. 3, pp. 666–681, 2007.

[5] R. T. D. Prabhakaran, T. L. Andersen, and A. Lystrup, "Glass/CBT laminate processing and quality aspects," in *Proceedings of the 10th International Conference on Flow Processes in Composite Materials (FPCM '10)*, Monte Verità, Switzerland, 2010.

[6] Z. A. Mohd Ishak, Y. W. Leong, M. Steeg, and J. Karger-Kocsis, "Mechanical properties of woven glass fabric reinforced *in situ* polymerized poly(butylene terephthalate) composites," *Composites Science and Technology*, vol. 67, no. 3-4, pp. 390–398, 2007.

[7] S. Miller, *Macrocyclic polymers from cyclic oligomers of poly(butylene terephthalate) [Ph.D. thesis]*, UMI, 1998.

[8] J. Baets, A. Godara, J. Devaux, and I. Verpoest, "Toughening of isothermally polymerized cyclic butylene terephthalate for use in composites," *Polymer Degradation and Stability*, vol. 95, no. 3, pp. 346–352, 2010.

[9] T. Abt, M. Sánchez-Soto, and A. Martínez de Ilarduya, "Toughening of *in situ* polymerized cyclic butylene terephthalate by chain extension with a bifunctional epoxy resin," *European Polymer Journal*, vol. 48, no. 1, pp. 163–171, 2012.

Hindawi Publishing Corporation
Conference Papers in Materials Science
Volume 2013, Article ID 274359, 5 pages
http://dx.doi.org/10.1155/2013/274359

Conference Paper

Spanish Broom (*Spartium junceum* L.) as New Fiber for Biocomposites: The Effect of Crop Age and Microbial Retting on Fiber Quality

Luciana G. Angelini, Silvia Tavarini, and Lara Foschi

Department of Food, Agriculture and Environment, University of Pisa, Via San Michele degli Scalzi, 2, 56124 Pisa, Italy

Correspondence should be addressed to Luciana G. Angelini; luciana.angelini@unipi.it

Received 26 July 2013; Accepted 8 September 2013

Academic Editors: R. Fangueiro and H. Hong

This Conference Paper is based on a presentation given by Luciana G. Angelini at "International Conference on Natural Fibers—Sustainable Materials for Advanced Applications 2013" held from 9 June 2013 to 11 June 2013 in Guimarães, Portugal.

Recently, there has been a revival of interest in Spanish broom (*Spartium junceum* L.) as a possible source of fibers to be used in biocomposite materials. The aim of this work was to evaluate the role of two selected strains of *Clostridium felsineum* (NCIMB 10690 and NCIMB 9539) in the retting of Spanish broom vermenes. Chemical composition and physical, mechanical, and morphological properties of fibers were investigated. The obtained results indicate that the process provides an ecofriendly method for Spanish broom retting and support the hypothesis that these fibers can be successfully used in composite materials.

1. Introduction

Since the last years, polymer composites reinforced with natural fibers are gaining ever more interest especially for industrial applications. Their low cost, high specific mechanical properties, and biodegradability represent the main advantages in their utilization as renewable alternatives instead of the majority of synthetic reinforcement, such as glass fibers [1]. The sources of raw material used in composites as reinforcement or fillers are mainly represented by flax, cotton, hemp, jute, kenaf, sisal, and coconut fiber.

Spanish broom (*Spartium junceum* L.), a member of the Leguminosae family, has been considered a potential interesting source of natural, sustainable, and renewable fiber for textile and technical applications [2, 3]. These fibers derived from the plant branchlets (known as vermenes) show extraordinary tensile resistance and flexibility and are able to produce materials in combination with biodegradable and plastic matrices [1, 4]. Spanish broom (*Spartium junceum* L.) is a perennial shrub growing in hot and dry climate throughout the Mediterranean area, where it naturally occurs in hilly soils, contributing to lower erosion and risks of nutrient leaching. This plant is somewhat adapted to alkaline and salty soils. The name *Spartium* is from the Greek word denoting "cardage," in allusion to the use of the plant. The stem fibers have been used since ancient time as hemp substitute, being used mainly for coarse fabrics and cordage. Spanish broom cortical fibers are multiple elementary fibers (ultimates) arranged in bundles. The elementary fibers are bound together by lignin. A thick secondary cell wall indicates a high cellulose content. The diameter of ultimates varies from 5 to 10 μm while the diameter of the whole bundle is about 50 μm [4].

The retting process is the major limitation to efficient and high-quality fiber production. In the last years, pectinolytic enzymes produced by microorganisms have gained most attention. These enzymes degrade the pectin of the middle lamella and primary cell wall, leading to separation of the cellulose fibers [5]. Microorganisms of the genus *Clostridium* are primarily involved in retting under anaerobic conditions. The aim of this work was to evaluate the role of two selected strains of *Clostridium felsineum* (NCIMB 10690 and

NCIMB 9539) in the retting of Spanish broom fibers obtained from 2- and 7-year-old crops (establishment year excluded). Morphology and the chemical, physical, and mechanical properties of the derived fibers were examined in order to evaluate the feasibility to use them in biocomposites.

2. Materials and Methods

2.1. Field Experiment. The vermenes were obtained from cultivation trials carried out at the Department of Agriculture, Food and Environment of University of Pisa (Italy, 43°40′ N; 10°19′ E; 5 m elevation) on a deep silt loam soil (sand 15.5%; silt 65.5%; clay 18.0%; organic matter 1.62%; pH 8.1; total nitrogen 0.12%; available P_2O_5 29.2 mg kg^{-1}; exchangeable K_2O 137 mg kg^{-1}). The soil was characterised by a water table rather superficial with a depth of 120 cm during the driest season. The soil displayed the following hydrological characteristics: field capacity 27.3% dw, wilting point 9.4% dw. A selected clone (PI DAGA92) of *Spartium junceum* from local population was used in this evaluation. Stump sprouts were transplanted at the end of April 2002. A plant density of 20.000 plants ha^{-1} with an interrow spacing of 1 m and an intrarow spacing of 0.5 m was adopted. Plot size was 48 m^2 (8×6 m). During the establishment year, plants were cut at the end of the growing season to allow the vegetative regrowth in the second year. Thereafter it was possible to harvest *Spartium junceum* one time in each year during autumn. In order to evaluate maximum crop yield, plants were maintained in optimum water supply conditions. All plots received the same amount (100 kg ha^{-1}) of preplanting fertilization of N, P, and K. The nitrogen dose was split into two equal preplanting and late-spring applications. From the second growing season, plots received only 50 kg ha^{-1} of N at the end of winter. Plots were kept weed-free by harrowing in the interrow and hand hoeing in the intrarow. The experiment was laid out in a randomised block design with four replicates. Productive determinations were performed on a minimal area of 6 m^2 in the inner part of each plot. After harvest, all plants in the plots were cut 15 cm above ground for allowing uniform vegetative regrowth. Dry vermenes were decorticated by hand, in order to remove the outer bark/epidermis and the bast from the woody core of the stems.

2.2. Retting Process. 100 g of bark, obtained from manually decorticated vermenes, was placed in 9 L of water tanks constantly heated at 30°C for 7 days. Tanks were inoculated with anaerobic bacteria *Clostridium felsineum* strains NCIMB 10690 and NCIMB 9539 selected for high pectinolytic activity, using a 1 : 8 ratio between broth culture and water. Finally, fiber bundles were washed with water under pressure and oven-dried at 60°C until constant weight.

2.3. Chemical and Mechanical Characterization. In accordance with the TAPPI OM 250 method, the lignin content was determined as the sum of insoluble and soluble lignin, the latter being determined spectrophotometrically at 205 nm. Pentosan content was determined according to the TAPPI T 223 hm 84 and ash content according to the TAPPI 15 OS 58 method. The TAPPI 284 OM 82 method was used to assess the extractives content and the UNI 8282 method to determine the degree of cellulose polymerization in cuprietylenediamine (CED) after delignifying the material with sodium chlorite. The index of crystallinity is given by the ratio to the area of the (002) peak to the intensity of the amorphous background [6]. Fibre bundles were confined in small plastic sleeves and then cross-sectioned. Scanning microscopy (SEM) was carried out on gold coated cross-sections. The tensile properties of selected filaments were determined with an Instron 1185 (load cell 10 N) at the cross-head speed of 1 mm min^{-1} at room temperature (20 ± 2°C) and 70 ± 5% relative humidity. Since the diameter of filaments was not uniform, selection of suitable samples was made with the help of a low magnification microscope; the diameter for each filament was taken at different places with the help of a precision gauge meter and the average value was used. To measure the strength and the elongation of fibers, different gauge lengths were used, in the range 10–50 mm; a minimum of 50 filaments was taken for each gauge length to give data statistical meaning. The elastic modulus (E) was measured by the slope of the conventional stress-strain curves taking the distance between grips as the gauge length.

2.4. Statistical Analysis. All the variables were subjected to the analysis of variance (ANOVA) using the statistical software CO-STAT Cohort V6.201-2002. A factorial design with crop age and microbial strain as main treatments was used. Means were separated on the basis of least significance difference (LSD) test only when the ANOVA F-test per treatment was significant at the 0.05 or 0.01 probability level [7].

3. Results and Conclusions

The agronomic characteristics of Spanish broom were investigated for seven years in the pedoclimatic conditions of Central Italy. The dry yield components, evaluated after 2 and 7 years of cultivation, were reported in Table 1. The dry yield was composed of 53% new branches, representing the economic yield. The average yield per annum of dry vermenes was 10.5 and 7.8 t ha^{-1} after 2 and 7 years of cultivation, respectively. The moisture content of branchlets averaged 60% and it is important for the necessity to store raw material with low moisture content and to maximise the marketable products. The cultivation trials, carried out for 7 years, showed that this species was drought tolerant; moreover, being a nitrogen fixing plant, it could be cultivated on marginal lands due to its low input requirements.

The vermenes were manually decorticated and the obtained bast was processed using *Clostridium felsineum* strains NCIMB 10690 and NCIMB 9539 for microbial retting. The fiber yield was significantly affected by the crop age, microbial strains, and their interaction. The highest yield was obtained in the vermenes from the younger crop degummed with NCIMB 10690 while the ones derived from older plants degummed using NCIMB 9539 have given about 20%

Table 1: Effect of crop age on dry yield components (t ha^{-1} year^{-1}) and bast/vermenes ratio in Spanish broom crops.

Crop age	Total above-ground dry yield (t ha^{-1} year^{-1})	Vermenes dry yield (t ha^{-1} year^{-1})	Bast dry yield (t ha^{-1} year^{-1})	Bast/vermenes ratio
1-2 years†	20.0 ± 2.7^{a}	10.5 ± 2.5^{a}	4.2 ± 1.1^{a}	0.40 ± 0.05^{a}
1–7 years†	14.9 ± 5.5^{a}	7.8 ± 3.0^{a}	3.5 ± 1.2^{a}	0.47 ± 0.08^{a}

Mean values followed by the same letters are not significantly different for $P \leq 0.05$ following a one-way ANOVA test with crop age as variability factor. †Establishment year excluded.

Table 2: Effect of crop age and microbial strain on chemical composition and crystallinity of broom fibers.

	Humidity (%)	Extractives (%)	Lignin (%)	Ash (%)	Pentosans (%)	Cellulose†† (%)	X-ray index of crystallinity (%)
2-year-old NCIMB10690	5.47^{a}	6.34^{a}	15.15^{bc}	0.37^{a}	4.55^{a}	73.94^{ab}	77.2^{a}
2-year-old NCIMB9539	5.10^{a}	6.47^{a}	13.01^{c}	0.30^{a}	4.04^{a}	76.48^{a}	73.7^{b}
7-year-old NCIMB10690	5.26^{a}	7.02^{a}	17.11^{b}	0.32^{a}	4.75^{a}	71.12^{b}	73.4^{b}
7-year-old NCIMB9539	5.05^{a}	7.32^{a}	21.71^{a}	0.23^{a}	4.42^{a}	66.55^{c}	70.3^{c}
Analysis of variance							
Crop age (A)	n.s.	n.s.	**	n.s.	n.s.	*	*
Strain (S)	n.s.	n.s.	n.s.	n.s.	n.s.	n.s.	n.s.
A × S	n.s.	n.s.	*	n.s.	n.s.	*	*

Mean values followed by the same letters are not significantly different for $P \leq 0.05$ following a two-way ANOVA test with crop age and microbial strain as variability factors. $^{*}P \leq 0.05$; $^{**}P \leq 0.01$; n.s.: not significant ($P \geq 0.05$). ††Determined as difference.

Table 3: Effect of crop age and microbial strain on fiber diameter: mean, minimum, and maximum values.

	Mean diameter†† (μm)	Min (μm)	Max (μm)
2-year-old NCIMB10690	63.1 ± 18.2^{a}	30	140
2-year-old NCIMB9539	53.0 ± 9.3^{b}	25	70
7-year-old NCIMB10690	48.8 ± 8.6^{c}	30	80
7-year-old NCIMB9539	48.6 ± 8.7^{c}	20	70

Mean values followed by the same letters are not significantly different for $P \leq 0.05$ following a two-way ANOVA test with crop age and microbial strain as variability factors. ††Mean value for $n = 133$–148.

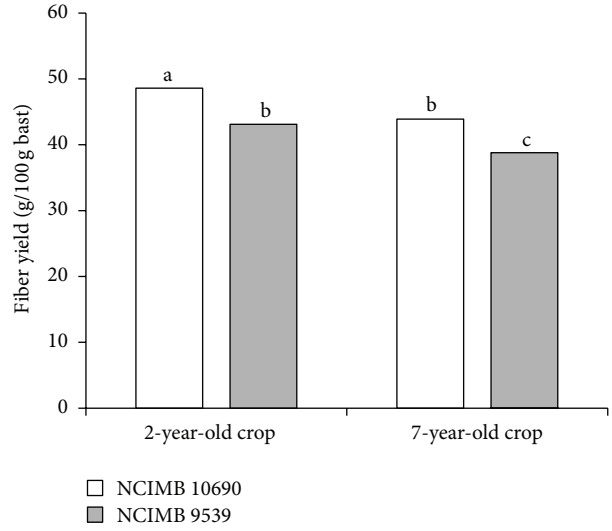

Figure 1: Influence of crop age and microbial strain on fiber yield. Mean values followed by the same letters are not significantly different for $P \leq 0.05$ following a two-way ANOVA test with crop age and microbial strain as variability factors.

less fibers (Figure 1). The chemical composition and the crystallinity index of the derived fibers were shown in Table 2. The results outlined a high content of cellulose (67–76%), while lignin (13–22%), pentosans (4-5%), and extractives (6-7%) were low (Table 2). The microorganisms used for the retting carried out a selective attack against pectins and cellulose, with the lowest percentage of lignin and the highest value of cellulose in the 2-year-old fibers after retting with NCIMB 9539 (Table 2). The fibers obtained from younger plants generally provided a fiber characterized by a higher tensile strength (Figure 2(a)), a lower lignin content (Table 2), and a greater diameter (Table 3). In these plants the retting with NCIMB 10690 presented a lesser percentage of cellulose compared to retting with NCIMB 9539, which would suggest a greater strength of the fiber. In spite of this, the use of strain NCIMB 10690 provided a greater crystallinity index that gives a higher resistance (tensile strength) to the fiber compared to ones obtained with strain NCIMB 9539 which are characterized by an intermediate crystalline/amorphous ratio (Figure 2(a)). By definition, the elastic modulus, shown in Figure 2(b), is a quantity independent of the length of the fiber, as it represents the initial slope of the stress-strain curve. The elastic modulus of Spanish broom processed with microbial retting is 13.2 GPa (as overall mean) and it is yet greater than that of most rigid nonoriented polymers (1–3 GPa) making it possible to stiffen commodity plastics such as, polyolefins [4]. It is interesting to note that the value of the Spanish broom fibers obtained by mechanical retting in a study conducted in the same field by Angelini et al. [4]

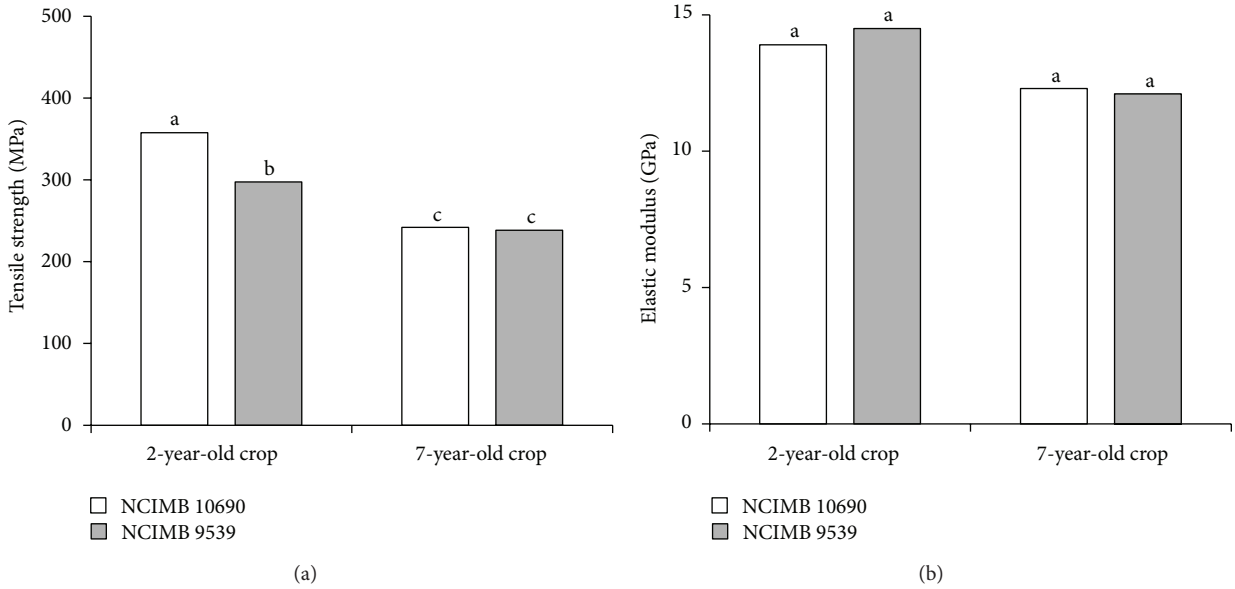

Figure 2: Influence of crop age and microbial strain on tensile strength (a) and elastic modulus (b). Mean values followed by the same letters are not significantly different for $P \leq 0.05$ following a two-way ANOVA test with crop age and microbial strain as variability factors.

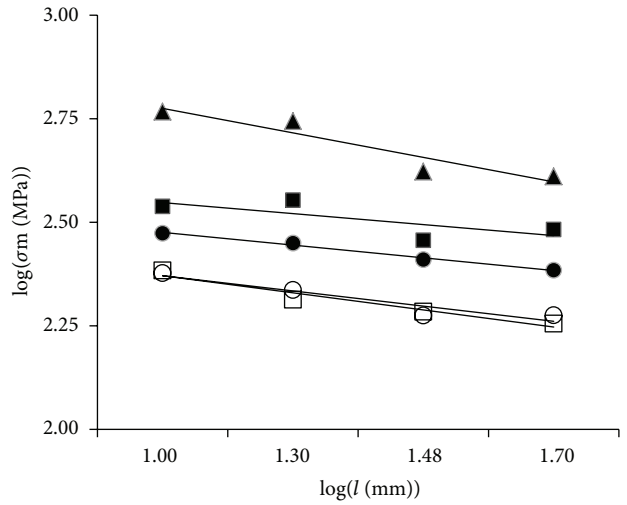

Figure 3: Comparison of the influence of gauge length on strength of Spanish broom fibers obtained from two different crop ages and two different rettings (mechanical and microbial). ■: retting of 2-year-old broom with NCIMB 10690; •: retting of 2-year-old broom with NCIMB 9539; □: retting of 7-year-old broom with NCIMB 10690; ○: retting of 7-year-old broom with NCIMB 9539; ▲: mechanical retting [4].

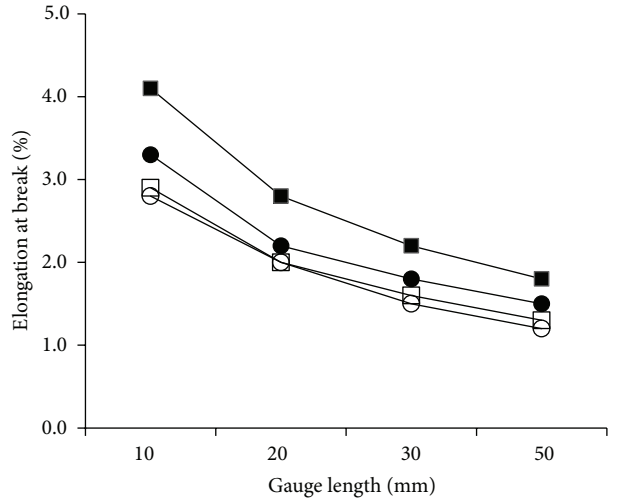

Figure 4: Influence of gauge length on elongation at break of broom fibers. ■: retting of 2-year-old broom with NCIMB 10690; •: retting of 2-year-old broom with NCIMB 9539; □: retting of 7-year-old broom with NCIMB 10690; ○: retting of 7-year-old broom with NCIMB 9539.

was 21.5 GPa, greater than those obtained in the present study and thus would present a greater tensile strength. This result is confirmed also by the analysis reported in Figure 3 where the plots of log (mean stress) versus log (gauge length) for Spanish broom fibers are shown (the solid line represents the regression line). It is observed that for all treatments, the fiber strength increased with the decrease of gauge length. Consequently, the strength of fibers obtained from vermenes of 2-year-old crop degummed with NCIMB 10690 was the highest. The comparison of regression lines confirms that the strength of fibers obtained by mechanical retting was higher than those observed in this study. This could be due to the cellulose degradation operated by the microbes that confers a greater weakness to fibers. However, we can point out that the slope of the line obtained in this work was lower than that reported in the literature [4]. This highlights a higher reliability of these fibers as the slope of the regression line deals with the speed with which the tensile strength

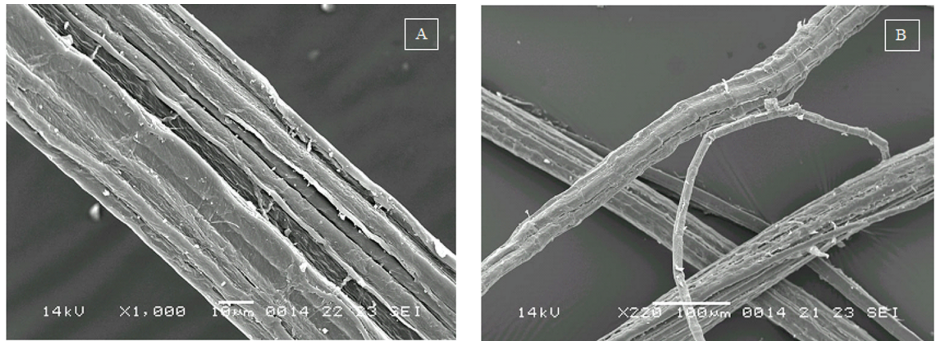

(a) (b)

Figure 5: Longitudinal view of Spanish broom fibers obtained by SEM. (a) retting of 2-year-old broom with NCIMB 10690; (b) retting of 2-year-old broom with NCIMB 9539.

decreases. Furthermore these results confirm that the natural fibers can reach a good reliability in the mechanical behaviour comparable with the artificial ones, although the natural fibers are characterized by greater surface irregularities. In Figure 4 the influence of gauge length on elongation at break is shown. The range of variation in the average elongation at break (strain) was comprised between 1.2% and 4.1%, for fibers of 5 and 1 cm long, respectively. According to the theory of Weibull [8], the shorter fibers exhibited a higher value of elongation at break due to a lower number of defects. As the length increases, the probability that the fiber section contains a defect is higher and, therefore, the mean value of elongation decreases. The longitudinal SEM view of the Spanish broom bundles (Figures 5(a) and 5(b)) clearly showed these irregularities and defects.

In conclusion, the obtained results showed the good agronomic characteristics of Spanish broom with low environmental impact of its cultivation and a good fiber productivity during the years. The microbial retting here tested provided fibers characterised by a good reliability in the mechanical behaviour.

The two microorganisms used in the retting showed a different activity depending on crop age and the considered parameter, such as lignin and cellulose content or crystallinity index. As general trend, the NCIMB 10690 strain provided a greater index of crystallinity in fibers from both crops, even if a higher tensile strength was observed only in the vermenes from the younger crop. The chemical and mechanical properties of the obtained fibers are promising and support the hypothesis that these fibers can be a potential replacement for man-made fibers in composite materials. The importance of the microbial retting in the degumming of Spanish broom as well as the choice of the most suitable microbial strain awaits elucidation on the basis of these preliminary results.

References

[1] R. Cassano, S. Trombino, E. Bloise et al., "New broom fiber (*Spartium junceum* L.) derivatives: preparation and characterization," *Journal of Agricultural and Food Chemistry*, vol. 55, no. 23, pp. 9489–9495, 2007.

[2] B. Gabriele, T. Cerchiara, G. Salerno et al., "A new physical-chemical process for the efficient production of cellulose fibers from Spanish broom (*Spartium junceum* L.)," *Bioresource Technology*, vol. 101, no. 2, pp. 724–729, 2010.

[3] D. Katović, A. Katović, and M. Krnčević, "Spanish broom (*Spartium junceum* L.)—history and perspective," *Journal of Natural Fibers*, vol. 8, pp. 81–98, 2011.

[4] L. G. Angelini, A. Lazzeri, G. Levita, D. Fontanelli, and C. Bozzi, "Ramie (*Boehmeria nivea* (L.) Gaud.) and Spanish broom (*Spartium junceum* L.) fibres for composite materials: agronomical aspects, morphology and mechanical properties," *Industrial Crops and Products*, vol. 11, no. 2-3, pp. 145–161, 2000.

[5] F. Brühlmann, M. Leupin, K. H. Erismann, and A. Fiechter, "Enzymatic degumming of ramie bast fibers," *Journal of Biotechnology*, vol. 76, no. 1, pp. 43–50, 2000.

[6] L. Segal, J. J. Creely, A. E. Martin Jr., and C. M. Conrad, "An empirical method for estimating the degree of crystallinity of native cellulose using the X-ray diffractometer," *Textile Research Journal*, vol. 29, no. 10, pp. 786–794, 1962.

[7] K. A. Gomez and A. A. Gomez, "Two factor experiments," in *Statistical Procedures for Agricultural Research*, K. A. Gomez and A. A. Gomez, Eds., pp. 84–130, John Wiley & Sons, New York, NY, USA, 1984.

[8] W. Weibull, "A statistical distribution function of wide applicability," *Journal of Applied Mechanics*, vol. 18, pp. 293–297, 1951.

Hindawi Publishing Corporation
Conference Papers in Materials Science
Volume 2013, Article ID 738741, 6 pages
http://dx.doi.org/10.1155/2013/738741

Conference Paper

Polylactic Acid (PLA) Composite Films Reinforced with Wet Milled Jute Nanofibers

Vijay Baheti, Jiri Militky, and S. Z. Ul Hassan

Department of Material Engineering, Technical University of Liberec, Liberec, Czech Republic

Correspondence should be addressed to Vijay Baheti; vijaykumar.baheti@gmail.com

Received 1 August 2013; Accepted 8 September 2013

Academic Editors: R. Fangueiro and H. Hong

This Conference Paper is based on a presentation given by S. Z. Ul Hassan at "International Conference on Natural Fibers—Sustainable Materials for Advanced Applications 2013" held from 9 June 2013 to 11 June 2013 in Guimarães, Portugal.

In the present study, waste jute fibers formed in textile industries were wet pulverized to nanoscale using high energy planetary ball milling. The rate of refinement of uncleaned jute fibers having noncellulosic contents was found slower than the cleaned jute fibers. This behavior is attributed to the strong holding of fiber bundles by noncellulosic contents which offered resistance to the defibrillation during wet milling. In addition, the pulverization of fibers in the presence of water prevents the increase in temperature of mill which subsequently avoided the sticking of material on the milling container. After three hours milling, the diameter of nanofibers was observed around 50 nm. In the further stage, obtained nanofibers were incorporated under 1 wt%, 5 wt%, and 10 wt% loading into polylactic acid composite films. The potentials of jute nanofibers were investigated for improvement in mechanical and barrier properties of films. The maximum improvement in mechanical properties was observed in case of 5 wt% composite film where Young's modulus was increased to 3.3 GPa from 1.0 GPa as compared with neat PLA film.

1. Introduction

The demand for textiles has increased significantly in the last decade due to the rise in the living standards of people. However, increased demands of textiles also brought the challenges to dispose significant amount of wastes, generated during the processing and end of life textile materials [1, 2]. In recent years, research on recycling and reuse of textile wastes, instead of landfilling or incineration, has gained a lot of importance due to the increased awareness of environmental concerns. Traditionally, textile wastes have been converted to individual fiber stage through cutting, shredding, carding, and other mechanical processes. The fibers are then rearranged into products for applications in garment linings, household items, furniture upholstery, automotive carpeting, automobile sound absorption materials, carpet underlays, building materials for insulation and roofing felt, and low-end blankets [1, 2]. However, recent increased competition and reduced profit margins of such industries have forced the researchers to find alternative more profitable applications of textile wastes. One such interesting way is to separate the nanofibrils or nanocrystals from the textile wastes and subsequently incorporate them into high performance functional products.

The lists of the previous literature articles have reported the remarkable mechanical properties of cellulose nanofibers in the range of 130–160 GPa that resulted from parallel arrangement of molecular chains without folding [3–5]. As a result, cellulose nanofibers have been used in value added applications such as reinforced biodegradable nanocomposites, foams, aerogels, optically transparent functional materials, and oxygen-barrier layers [6–8].

The noncellulosic substances in waste jute fibers (i.e., lignin, hemicelluloses, and waxy materials) hinder the reaction between hydroxyl groups of fibers and polymer matrices and consequently deteriorate the mechanical properties of composites [9–11]. In order to have better bonding between fibers and matrix, the noncellulosic contents must be removed from the waste jute fibers. In the present study, pretreatment of waste jute fibers with a sequential

action of alkali and bleaching was carried out, due to its inexpensive nature [12, 13], for the removal of lignin and hemicelluloses. In the subsequent stage, cleaned waste jute fibers were subjected to wet pulverization in high energy planetary ball milling process to separate jute nanofibers. During the process of ball milling, fibers tend to defibrillate under the shearing action of frictional force of balls and subsequently refine to nanosegments due to the impact force [7, 8]. In fact, ball milling technique has been found to be simple, economical, and ecofriendly, over commonly preferred strong acid hydrolysis used for the separation of cellulose nanocrystals.

The present paper deals with the wet pulverization of waste jute fibers to nanoscale using high energy planetary ball milling process. The prepared nanofibers were then incorporated into polylactic acid to improve their mechanical, thermal, and barrier properties. The biodegradable nanocomposite films can be expected to serve in food packaging films, agriculture mulch cover, and so forth.

2. Experimental

2.1. Materials. Short waste jute fibers were obtained from India. The fibers were measured to have a density of 1.58 g/cm^3, modulus of 20 GPa, tensile strength of 440 MPa, and elongation of 2%. Polylactic acid (PLA) was purchased from NatureWorks LLC, USA, through local supplier Res-inex, Czech Republic. The PLA had a density of 1.25 g/cm^3 and the average molecular weight (Mw) of 200,000. Chloroform which was used as solvent was purchased from Thermo Fisher, Czech Republic.

2.2. Pulverization of Jute Fibers to Nanofibers. In the beginning, chemical pretreatment of jute fibers was carried out sequentially with 4 wt% sodium hydroxide (NaOH) at 80°C for 1 hour and with 7 g/L sodium hypochlorite (NaOCl) at room temperature for 2 hours under pH 10-11. Subsequently, the fibers were antichlor treated with 0.1% sodium sulphite (Na_2SO_3) at 50°C for 20 min [7].

High energy planetary ball milling (Fritsch pulverisette 7, Germany) was used for wet pulverization of waste jute fibers in distilled water. The sintered corundum container of 80 mL capacity and zirconium balls of 3 mm diameter were chosen for 3 hours of wet milling. The ball to material ratio (BMR) was kept at 10 : 1, and the speed was kept at 850 rpm with reverse rotation of containers. At the end of wet milling, jute particles were separated from water by centrifugation at 4000 rpm and simultaneously transferred to isopropanol to avoid hornification during drying [7].

Particle size distribution of wet milled jute particles was studied after each hour of milling on a dynamic light scattering instrument (Malvern zetasizer nanoseries). Deionized water was used as a dispersion medium, and it was ultrasonicated for 5 min with bandelin ultrasonic probe before particle size measurement. Refractive index of 1.52 for water was used to calculate particle size of wet milled jute fibers.

In addition, morphologies of wet milled jute particles were observed on scanning electron microscope (SEM) of TS5130-Tescan at 30 KV accelerated voltage and on field emission scanning electron microscope (FESEM) of Zeiss at 5 kV accelerated voltage. The amount of 0.01 g of jute particles was dispersed in 100 mL acetone, and then a drop of the dispersed solution was placed on aluminum foil and gold coated after drying.

2.3. Preparation of Nanocomposite Thick Films. PLA/jute nanofiber composite films with 1, 5, and 10 wt% filler content were prepared by mixing the calculated amount of jute nanofibers with 5% PLA in chloroform using a magnetic stirrer. The stirring was performed at room temperature for 3 hours. The composite mixture was further ultrasonicated for 10 min on Bandelin Ultrasonic probe mixer with 50-horn power. The final mixtures were then cast on a Teflon sheet in order to prevent sticking of the nanocomposite film. The films were kept at room temperature for 2 days until they were completely dried and then removed from the Teflon sheet. Neat PLA film was also prepared as a reference control sample for comparison purpose.

2.4. Characterization

2.4.1. Differential Scanning Calorimetry (DSC). The melting and crystallization behaviors of the neat and composite films were investigated on DSC 6 Perkin Elmer instrument using Pyris software under nitrogen atmosphere with sample weight of 7 mg. The sample was heated from 25°C to 200°C at a rate of 5°C/min. The crystallinity (%) of the PLA was estimated from the following equation:

$$\%\text{Crystallinity} = \left(\frac{\Delta H_f}{w \times \Delta H_0}\right) \times 100\%, \quad (1)$$

where ΔH_f is heat of melting of sample, ΔH_0 is heat of melting 100% crystalline PLA 93 j/g [8], and w is mass fraction of PLA in nanocomposite.

2.4.2. Tensile Properties. Tensile testing was carried out using a miniature material tester Rheometric Scientific MiniMat 2000 with a 1000 N load cell at a crosshead speed of 10 mm/min. The samples were prepared by cutting strips from the films with a width of 10 mm. The length between the grips was kept 100 mm. Ten samples were measured for each sample. Further, the morphology of nanocomposite films was investigated using scanning electron microscope TS5130-Tescan SEM at 20 KV accelerated voltage.

2.4.3. Oxygen Barrier Properties. Oxygen barrier property (mL/m^2·24 h·0.1 MPa) of 10 cm circular sample was measured by manometric method using permeameter Lyssy L100–5000 on Systech Instrument, USA at 23°C and 0% RH, respectively.

2.4.4. Water Vapour Barrier. Water vapour barrier property (g/m^2·d) of 6.5 cm circular sample was measured using the gravimetric method ZM-23 at 38°C and 85% RH, respectively.

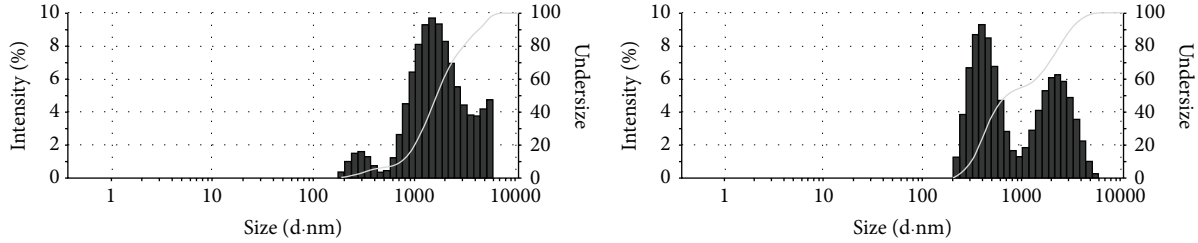

Figure 1: (a) Particle size distribution of one hour dry milling. (b) Particle size distribution of one hour wet milling.

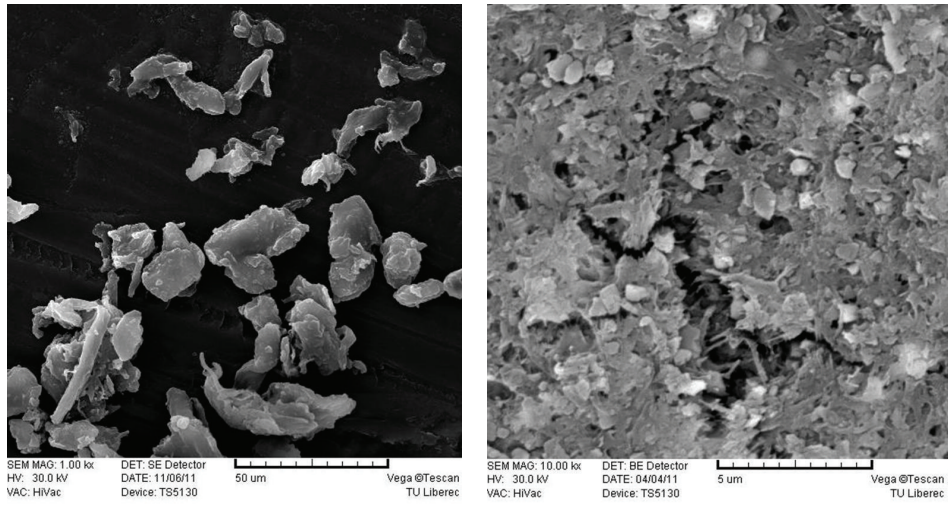

Figure 2: (a) SEM image of one hour dry milling. (b) SEM image of one hour wet milling.

3. Results and Conclusions

3.1. Effect of Milling Condition on Particle Size Reduction of Jute Fibers. Under one hour of dry milling, jute fibers were pulverized to microparticles with an average size of 1480 nm in wider particle size distribution as shown in Figures 1(a) and 2(a). The multimodal distribution of particles is attributed to the increase in temperature within the mill because of continuous impact of balls [7]. The increase in temperature of mill resulted in the deposition of jute particles on the surface of milling container and balls. In case of wet milling, the increase in temperature was slowed down by deionised water which consequently resulted in narrow particle size distribution with an average particle size of ~640 nm after one hour of wet milling as shown in Figures 1(b) and 2(b). In other words, uniformity in impact action of balls on every individual particle can be guaranteed during milling in wet condition [7].

3.2. Effect of Wet Milling Time on Particle Size Reduction of Jute Fibers. When waste jute fibers were subjected to extended duration of wet milling, the average particle size reached to 443 nm after 3 hours of wet milling, and the particle size distribution changes slowly from multimodal nature to unimodal nature as shown in Figure 3(a). This showed the consistency and homogeneity in milling action on every individual particle as milling continued for longer time. However, the surface of milling balls which are of expensive materials also started to get deteriorated with the increase in the wet milling time [7].

The shape of jute particles was observed in the form of nanofibers having diameter around 50 nm as shown in Figure 3(b). It was also possible to see few particles without aspect ratio which might be considered as agglomerates of hundreds of individual jute nanofibers.

3.3. Thermal Behavior of Nanocomposite Films. Table 1 shows that T_g and T_m values of PLA increased with the increased loading of jute nanofibers. The maximum improvement was observed in case of 10 wt% of jute nanofibers where T_g was increased from 42°C to 49°C, and T_m was increased from 147°C to 153°C as compared to the neat PLA film. The higher values of T_g are attributed to the delay in polymer relaxation due to the restriction in chain mobility caused by the presence of nanofibers. On the other hand, the increased value of T_m can be attributed to the formation of bigger crystals. The wider peak of crystallization temperature for nanocomposite films shown in Figure 4 indicated an enhanced crystallization

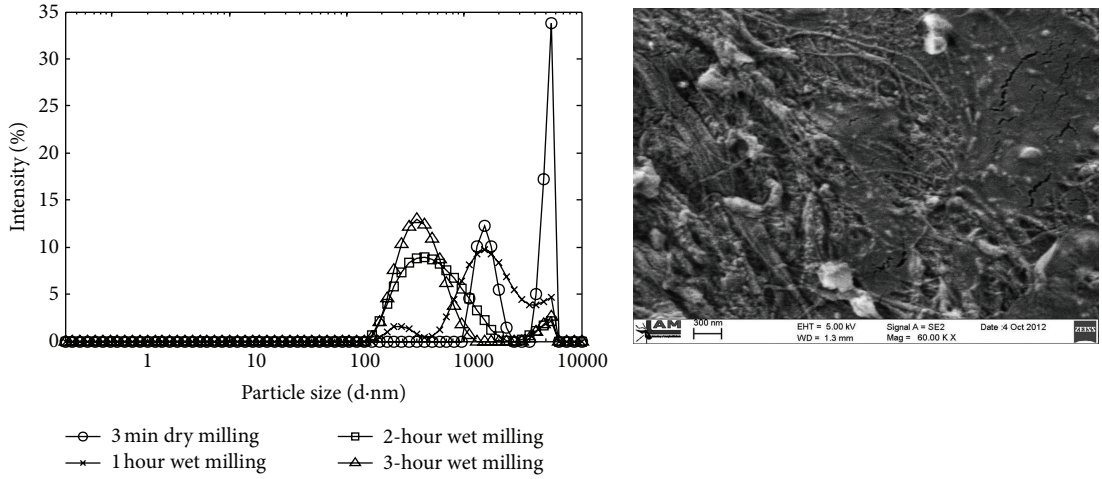

Figure 3: (a) Effect of extended wet milling time on pulverization. (b) FESEM image of particle size after 3-hour wet milling.

Table 1: Behavior of PLA/JNF composite films on application of heat.

Sample	T_g (°C)	T_c (°C)	T_m (°C)	ΔH (J/g)	Crystallinity %
Neat PLA	42.35	98.85	147.49	17.33	18.63
1% JNF + PLA	42.84	97.90	153.15	20.52	22.28
5% JNF + PLA	46.01	97.70	153.14	24.74	26.84
10% JNF + PLA	49.00	96.43	153.97	26.38	30.21

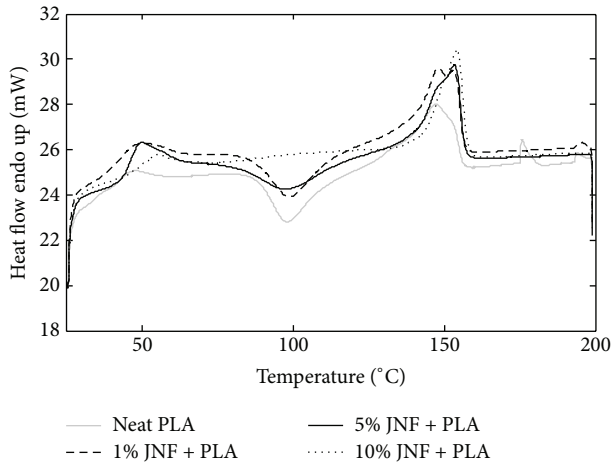

Figure 4: DSC of neat PLA and nanocomposite films.

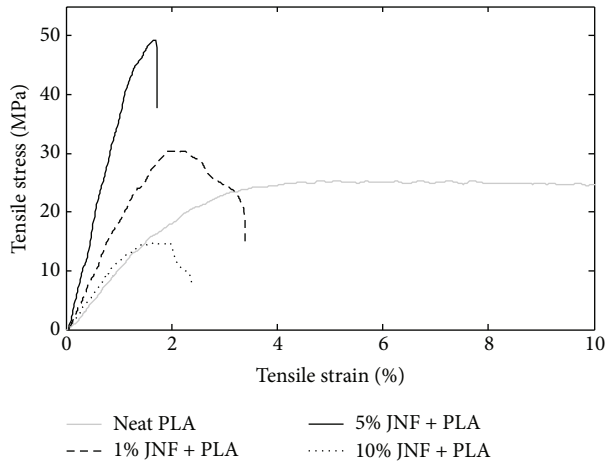

Figure 5: Stress-strain curve of neat PLA and nanocomposite films.

rate of PLA molecules in the presence of jute nanofibers due to their nucleating ability. The increase in crystallinity of PLA after addition of jute nanofibers was confirmed from the increase in heat of melting values given in Table 1.

3.4. Mechanical Properties of Nanocomposite Films. Figure 5 shows that the modulus of the PLA films increased significantly from 1.04 GPa to 3.3 GPa with the addition of 5 wt% jute nanofibers. The improved interaction between nanofibers and matrix, together with higher crystallinity of PLA in composites, can be attributed to the increase in modulus of the composites as compared to neat PLA. In order to understand the interaction between PLA and jute nanofibers, the morphology of fractured surfaces were studied under the SEM as shown in Figure 6. The fractured surface of 5 wt% nanocomposites (Figure 6(c)) shows the presence of wrinkles in contrast to the smooth surface of 1 wt% nanocomposite (Figure 6(b)). The wrinkles and roughness on the surface indicated greater stress transfer from matrix to jute nanofibers and consequent improvement in the

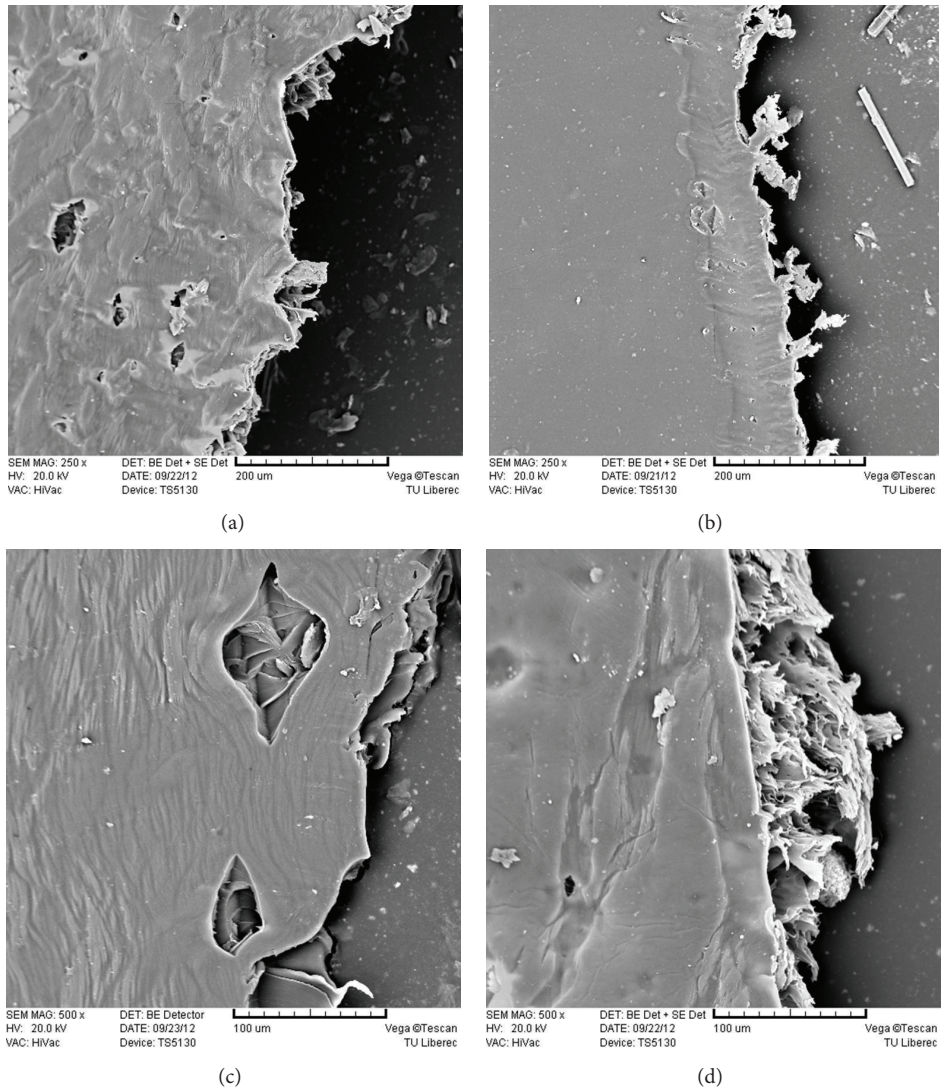

Figure 6: (a) Neat PLA film. (b) 1% JNF/PLA film. (c) 5% JNF/PLA film. (d) 10% JNF/PLA film.

modulus of 5 wt% nanocomposite. Similarly, less number of voids around filler and matrix explained very good interfacial adhesion between them. With further increase in the loading of jute nanofibers to 10 wt%, the modulus of composite films dropped significantly to 1.0 GPa. This could be explained by the clustering of nanofibers at higher loading, which results in the formation of voids at the interface of filler-matrix as shown in Figure 6(d).

3.5. Barrier Properties of PLA/JNF Composite Film. Previous studies reported that improvement in barrier properties is directly related to the tortuosities created by nanoparticles. The tortuous nature of path depends on the shape and aspect ratio of the filler, degree of exfoliation or dispersion, filler loading and orientation, adhesion to the matrix, moisture activity, filler-induced crystallinity, polymer chain immobilization, filler-induced solvent retention, degree of purity, porosity, and size of the permeate [9, 11].

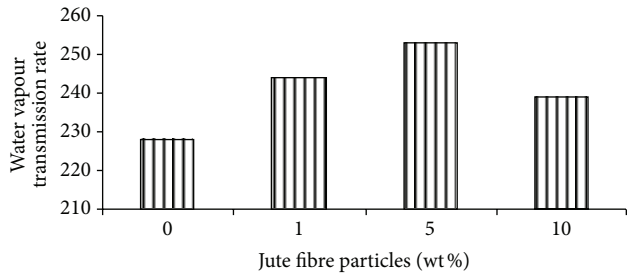

Figure 7: Moisture barrier of neat PLA and nanocomposite film.

PLA films after addition of jute nanofibers showed poor performance in water vapor and gas barrier behaviors at lower loading. Permeation rate of water vapor was found to increase in composite PLA films loaded with 1 wt% and 5 wt% jute nanofibers, and maximum permeation was observed in 5 wt% loading as shown in Figure 7. Similarly, the permeation

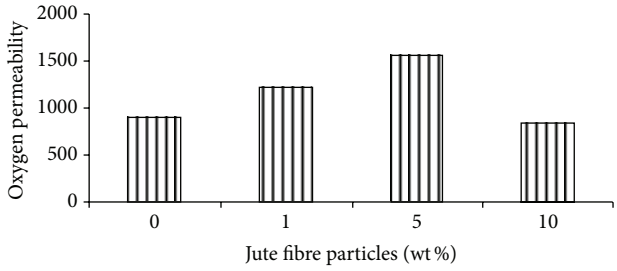

Figure 8: Oxygen barrier of neat PLA and nanocomposite film.

rate of oxygen was also observed higher in 1 wt% and 5 wt% composite films than neat PLA films from Figure 8. The main reasons behind poor barrier properties at lower loading can be related to the least improvement in crystallinity of matrix. In this way, the improvement in barrier performance at higher filler loading (i.e., 10 wt%) is attributed to the maximum improvement in crystallinity of matrix.

4. Conclusion

The pulverization of jute fibers by high energy wet milling process is a simple, economical, and environment friendly approach for separation of nanofibers. The diameter of nanofibers reached 50 nm after 3 hours of wet milling. This technique has a very good scope on industrial scale for the refinement of large amount of waste fibers generated in the textile industry. When jute nanofibers were incorporated into PLA matrix for preparation of biodegradable nanocomposite films, the maximum improvements in mechanical properties were observed at 5 wt% loading of nanofibers. The improvements in properties are attributed to the increased interaction of nanofibers along with increased crystallinity of PLA. However, the deterioration in properties at 10 wt% loading of jute nanofibers is attributed to the nonhomogeneous stress transfer from matrix to fillers due to poor dispersion and agglomerations of nanofibers at higher filler loading. Further, the poor barrier performance of PLA films at lower loading of nanofibers is related with the least improvement of crystallinity of matrix.

Acknowledgment

The present study was supported by SGS Project number 48011 at the Technical University of Liberec, Czech Republic.

References

[1] W. Wang, *Recycling in Textiles*, Woodhead Publishing, Cambridge, UK, 2006.

[2] R. Horrocks, *Recycling Textile and Plastic Waste*, Woodhead Publishing, Cambridge, UK, 1996.

[3] T. Zimmermann, N. Bordeanu, and E. Strub, "Properties of nanofibrillated cellulose from different raw materials and its reinforcement potential," *Carbohydrate Polymers*, vol. 79, no. 4, pp. 1086–1093, 2010.

[4] H. Wang, L. Huang, and Y. Lu, "Preparation and characterization of micro- and nano-fibrils from jute," *Fibers and Polymers*, vol. 10, no. 4, pp. 442–445, 2009.

[5] V. Baheti, R. Abbasi, and J. Militky, "Ball milling of jute fibres wastes to prepare nanocellulose," *World Journal of Engineering*, vol. 9, no. 1, pp. 45–50, 2012.

[6] J. K. Pandey, W. S. Chu, C. S. Kim, C. S. Lee, and S. H. Ahn, "Bio-nano reinforcement of environmentally degradable polymer matrix by cellulose whiskers from grass," *Composites B*, vol. 40, no. 7, pp. 676–680, 2009.

[7] V. Baheti and J. Militky, "Reinforcement of wet milled jute nano/micro particles in polyvinyl alcohol films," *Fibers and Polymers*, vol. 14, no. 1, pp. 133–137, 2013.

[8] V. Baheti, R. Abbasi, J. Militky, and J. Dobias, "Barrier properties of poly lactic acid packaging films reinforced with jute micro/nano particles," *Vlakna a Textil*, vol. 19, no. 3, pp. 10–16, 2012.

[9] M. D. Sanchez-Garcia, E. Gimenez, and J. M. Lagaron, "Morphology and barrier properties of solvent cast composites of thermoplastic biopolymers and purified cellulose fibers," *Carbohydrate Polymers*, vol. 71, no. 2, pp. 235–244, 2008.

[10] T. Yu, J. Ren, S. Li, H. Yuan, and Y. Li, "Effect of fiber surface-treatments on the properties of poly(lactic acid)/ramie composites," *Composites A*, vol. 41, no. 4, pp. 499–505, 2010.

[11] G. Rodionova, M. Lenes, O. Eriksen, and O. Gregersen, "Surface chemical modification of microfibrillated cellulose: improvement of barrier properties for packaging applications," *Cellulose*, vol. 18, no. 1, pp. 127–134, 2011.

[12] M. S. Islam, K. L. Pickering, and N. J. Foreman, "Influence of alkali treatment on the interfacial and physico-mechanical properties of industrial hemp fibre reinforced polylactic acid composites," *Composites A*, vol. 41, no. 5, pp. 596–603, 2010.

[13] T. H. Nam, S. Ogihara, N. H. Tung, and S. Kobayashi, "Effect of alkali treatment on interfacial and mechanical properties of coir fiber reinforced poly(butylene succinate) biodegradable composites," *Composites B*, vol. 42, no. 6, pp. 1648–1656, 2011.

Hindawi Publishing Corporation
Conference Papers in Materials Science
Volume 2013, Article ID 141204, 10 pages
http://dx.doi.org/10.1155/2013/141204

Conference Paper

Looking for Links between Natural Fibres' Structures and Their Physical Properties

Nicola M. Everitt, Nesma T. Aboulkhair, and Mike J. Clifford

Materials, Mechanics & Structures Division, Faculty of Engineering, University of Nottingham, Nottingham NG7 2RD, UK

Correspondence should be addressed to Nicola M. Everitt; nicola.everitt@nottingham.ac.uk

Received 1 August 2013; Accepted 8 September 2013

Academic Editors: R. Fangueiro and H. Hong

This Conference Paper is based on a presentation given by Nicola M. Everitt at "International Conference on Natural Fibers—Sustainable Materials for Advanced Applications 2013" held from 9 June 2013 to 11 June 2013 in Guimarães, Portugal.

Natural fibres have excited growing attention in the last decade since they offer the potential to act as candidates substituting for man-made fibres as composite reinforcements. Their superiority over synthetic fibres is that they are environmentally friendly and biodegradable. Numerous industrial sectors are interested in such composites, including but to name a few the aeronautical and the automotive fields. However natural fibres tend to suffer from large variability in properties compared to the "traditional" man-made fibres, and the performance of their composites often does not conform to that theoretically predicted from single-fibre tests. This study investigates the properties of the single fibres. The mechanical properties of the fibres were correlated to their microstructure. There are factors that were found to contribute to the reported variability, some of which are inherent in the fibres and some are related to testing parameters.

1. Introduction

Fibre reinforced composite materials are gaining popularity in the industry day by day for their superiority over individual materials [1]. Synthetic fibres, such as glass and carbon fibres, are most commonly used in this area. However, there are lots of motivators to shift to renewable sustainable materials, such as rising oil prices and its depletion, in addition to the aim of living in a cleaner environment. Moreover, producing all natural/green composites is becoming more popular as environmental regulations are being initiated in response to the international calls for renewable/recyclable sources for materials. Hence comes the industrial interest in ecofriendly composite materials [2, 3]. Therefore, there is interest in studying the feasibility of using natural fibres in composite materials. Documentation of the structural properties of natural fibres is difficult because of the wide range of variability in the reported properties (Table 1). For engineers, this variation within the mechanical properties of natural fibres is a challenge towards designing reliable components for industry since they are accustomed to the accurate, precise, and repeatable properties of synthetic fibres. Variability of properties of natural fibres is caused by several factors, some are already inherent in the fibres (due to maturity, age, location, source, fibre extraction technique, and fibre's microstructure), and some are related to the testing/characterization techniques [4–6].

When designing a composite material, it is important to be able to have an estimate of the expected mechanical properties. The rule of mixtures is a key tool for predicting the tensile properties of composites. However, it is not always found to be suitable when using natural fibres as reinforcements although its predictions in some cases are close to the experimental results depending on the constituents [7]. There are different forms of modified rules of mixtures that are being developed to fill the gap of deviation from the ROM [8–10]. This deviation could be attributed to several factors such as the variability within the mechanical properties of each fibre [5, 6] or poor adhesion between the fibre and the matrix that does not allow a homogeneous load transfer from

Table 1: Ranges of mechanical properties of natural fibres from the literature compared to man-made fibres.

Fibre type	Tensile strength (MPa)	Young's modulus (GPa)	Elongation to failure %
E-glass [33]	200–2400	68.9	3
S-glass [11, 33]	2400–4500	73–86	2.8–3
Carbon [33]	4000	227–241	1.4–1.8
Coir [11, 20, 33, 34]	130–580	4–6.2	15–40
Flax [6, 11, 20, 33–35]	345–1500	28–100	1.2–3.2
Jute [6, 11, 20, 33, 34]	380–800	10–30	1.16–1.8
Hemp [11, 20, 33]	550–900	68.9–70	1.6–4

one entity to the other for the load to be carried by the stiffer constituent [11, 12].

Despite the difficulties that face research exploring the uses of natural fibres, it is becoming more and more important to invest in this field. One of the pros of using natural fibres to substitute man-made fibres is the fact that they are not only environmentally friendly during their growth but also after using them, since natural fibres are biodegradable [12–18]. However, the setbacks of using natural fibres cannot be overlooked, for example, their poor wettability, being incompatible with some polymers, and high moisture absorption [11, 14]. In addition, from an environmental sustainability point of view, natural fibres reinforced composites are not yet recyclable. This is not a problem that is specific to natural fibre reinforced composites but to all composite materials due to the difficulty of separating the different entities building up the composite [19].

Lots of work is being carried out in order to enhance the mechanical behaviour of composite materials in which natural fibres act as reinforcements whether by using different coupling agents or fibre treatments prior to composite processing. However, not much work is directed towards understanding the root cause behind this unpredictability. This study aims at understanding the fibre-related factors that make accurate predictions of the mechanical properties such as Young's modulus of natural fibre reinforced composites challenging [20, 21].

A natural fibre is itself a composite material by nature of the fact that it consists of cellulose fibrils embedded in a lignin matrix [6]. This complex structure could contribute to the factors affecting the accurate prediction of their mechanical properties. For single fibre testing (SFT), special arrangements are needed to handle and align these ultrafine fibres. Consequently, the testing systems are usually custom made to accommodate the small load and elongation required for the deformation of the ultrafine fibres. Examples of these systems are precision load cells, cantilevers, and atomic force microscope-based nanoindentation system. However, this setup is not an easy one for testing since it requires high skills for manipulation of individual fibres [22]. The commonly followed standard test methods are ASTM D3822-07 and the BS 3411-1971. There is also the ASTM D3379-79 that was used by Sathishkumar et al. [23].

The results from a single fibre test are affected by several factors such as the clamping length, area measurement, elongation measurement, and modulus calculation. Osorio et al. [12] and Nechwatal et al. [24] reported that the clamping length has an inversely proportional relationship to the strength of the fibre due to the increase in the existing defects that weaken the fibre. The reason behind the inverse relation between the fibre length and its mechanical strength was clearly explained by Defoirdt et al. [15]. The probability of breakage is expected to be at the weakest point of the fibre. The longer the fibre, the higher the probability of existence of a weak section that is prone to failure at a certain load. Defroidt et al. [15] also stated that the strain to failure of the fibre is inversely proportional to its length, which they attributed to the same factors.

The area measurement highly affects the stress calculations in SFT, and according to some of the literature it is the main contributor to the variation in the reported properties. It is usually determined either through density measurement and backcalculation of the fibre fineness/diameter [25], or through direct measurement along the gauge length from microscope images, or measuring the diameter at the point of failure [25, 26]. The problem with the first method is that it is not accurate as it depends on the apparent density and that with the latter is that it assumes the fibre to be of circular cross-section, which is rarely the case. Nechwatal et al. [24] reported that the correlation between using the two methods is significantly high. Hu et al. [25] dedicated a full study to the different methodologies of diameter measurements. In agreement with lots of previous research, it was established that increasing the diameter of the fibres leads to a depression in the tensile properties. Thomason et al. [4] compared the optical average diameter method with measuring imaged cross-sections for natural fibre diameter determination. The reported results showed that the calculated average diameter from optical microscopy is always at least double the measured diameter since the former technique ignores the cross-section irregularities and assumes a circular cross-section. This finding shows how much the reported Young's modulus values are influenced since the majority of the published data relies on the calculated average diameter method. However, they did demonstrate that the variation in diameter along the length did not have a major effect on the mechanical properties variation. Tomczak et al. [27] reported that increasing the fibre diameter results in depressing the tensile strength of the fibre. Similar behaviour was reported for the influence of the length on the strength, as they are also inversely proportional.

Another factor affecting the SFT results is the measurement of the elongation, which is an issue bearing in mind the effect of the fibre slippage from the adhesive that cannot be monitored directly [24].

Polarized optical microscope images showed the structure of hemp fibres to contain series of dislocations [25]. Sawpan et al. [28] also observed the kinks in the structure

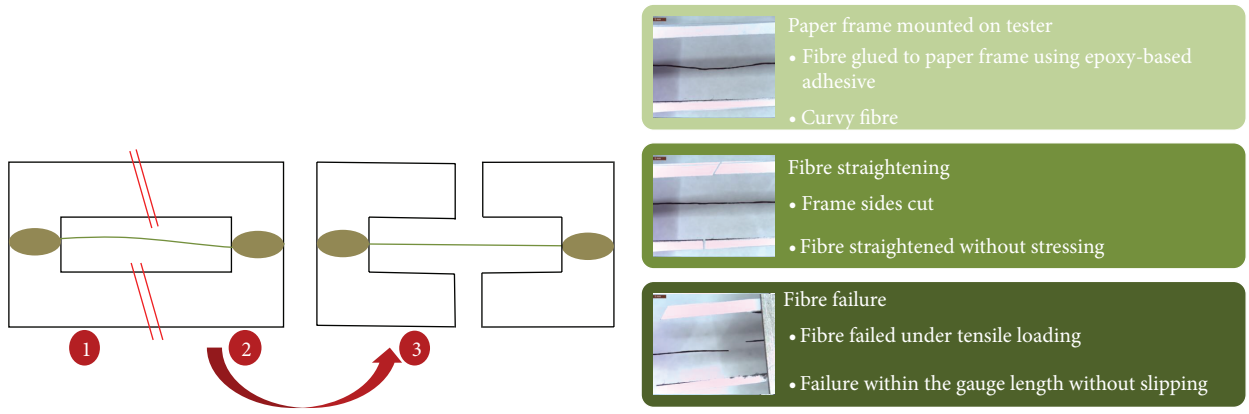

(a) (b)

Figure 1: Schematic presentation showing preparing the fibre for tensile testing and optical microscope images taken during the process.

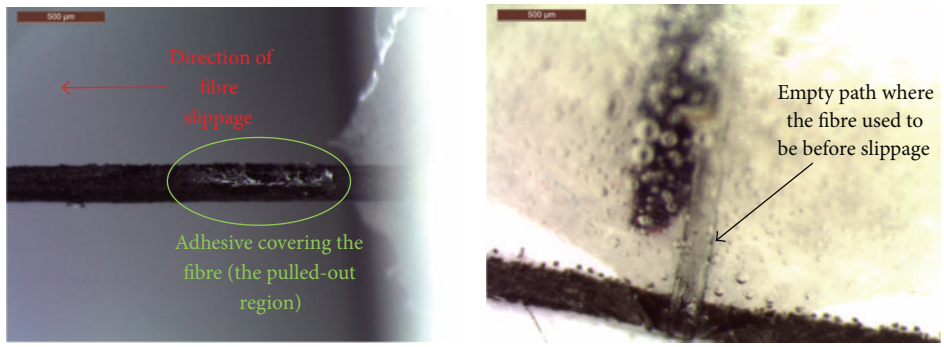

(a) (b)

Figure 2: Optical microscope images of coir fibre under tensile loading slipping out of the adhesive (a), and the adhesive after the fibre has slipped out with its empty space clearly obvious (b).

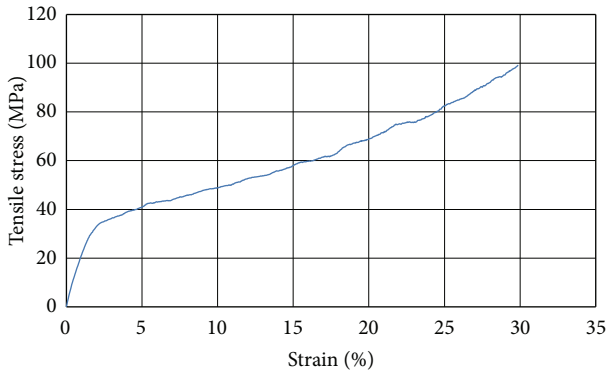

Figure 3: Representative stress-strain curve showing the tensile behavior of coir fibres.

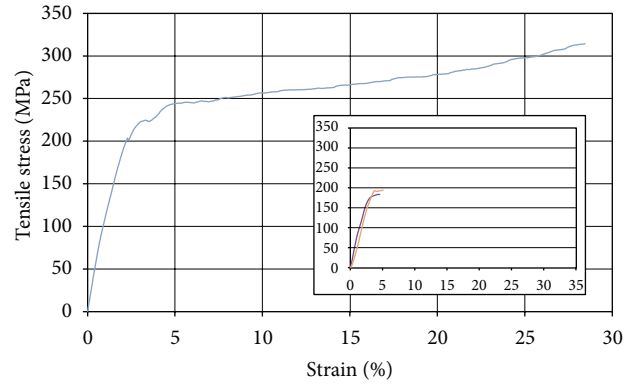

Figure 4: Representative curves for tensile behaviour of some of the tested cattle hair fibres with the inset showing samples with early premature failure.

of hemp fibres and attributed the variation in the mechanical properties to their presence. Kompella and Lambros [29] concluded that the strength of the fibre is highly dependent on the amount of surface flaws in the fibre. Studies of the fracture surface of the fibre showed that failure took place through fracture of fibre cells, delamination within the fibre cells, and delamination between the fibre cells [5].

Materials are built up of smaller elements that are linked together. A material would fail at the weakest point, which is where dislocations, kink bands, or defects exist, or where

diameter variation occurs, or even both simultaneously. Dislocations do not only affect the tensile behaviour of single fibres but also, from a broader perspective, affect the behaviour of the composite material since debonding between the fibre and matrix usually takes place at a dislocation as it is considered a location for stress concentration [30, 31]. This study aims at correlating the structure of the fibres with their mechanical properties and the influence of the abovementioned defects on the tensile behaviour of the fibres.

2. Experimental Work

Cattle hair, horsetail hair, hemp, flax, jute, and coir fibres were supplied by ENKEV (UK) Ltd. A Deben microtensile tester using a 200 N load cell was used to test all the single fibres. The testing speed employed was 1.5 mm/min. The gauge length of the fibres was 30 mm. The tension tests were conducted in accordance with the ASTM D3822-07. Each fibre was glued to a paper frame using Araldite adhesive, which is left for 24 hours in the laboratory before testing for the adhesive to cure and the fibres to be conditioned. The frame would then be mounted to the tensile tester clamps. After that the sides of the frames are cut for the load to be fully carried by the fibre. Some of the fibres exhibited a curly structure and so they had to be straightened by the tester without stressing the fibre before running the test. The test procedure is shown in the schematic presentation in Figure 1.

The type of adhesive to use for mounting the fibres was investigated at the start of the experimental work to prevent the fibre from slipping out of the adhesive during testing. Figure 2 shows a coir fibre under tensile loading with evidence of slipping. The epoxy-based adhesives were found to be the most satisfactory for minimizing slippage. Using epoxy-based adhesive did not yield a 0% slippage of fibres, but it was diminished to the minimum and the fibres that slipped during the test were discarded.

Images along the length of the fibre were taken using an optical microscope before testing the fibre. The cross-section of the fibre was assumed to be circular and hence the diameter was directly measured from the images using ImageJ software. To consider the variation along the length of the fibre, the diameter was measured at 20 different locations and an average value was then calculated.

A Phillips XL30 scanning electron microscope SEM was used to characterize the longitudinal and cross-sectional surfaces of the fibres. Moreover, the fracture surfaces of the tensile test specimens were investigated. Since natural fibres are not conductive materials, the fibres were first coated with platinum for successful imaging.

3. Results and Discussion

Representative curves for the stress-strain behaviour of coir fibres are demonstrated in Figure 3. The behaviour of coir is seen to start with a nearly linear elastic region that is followed by a second phase showing a more gradual increase in force per % increase in strain. This two-phase phenomenon

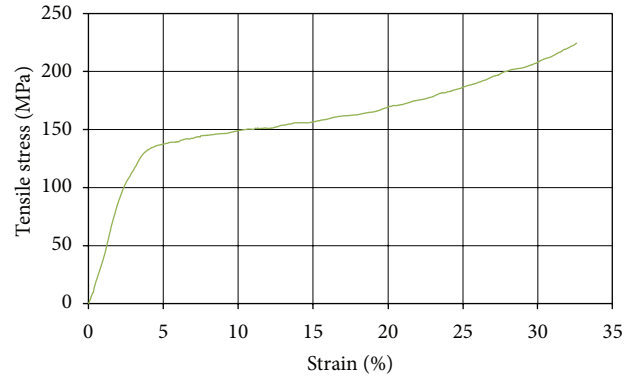

Figure 5: Representative curves for tensile behaviour of some of the tested horsetail hair fibres.

led to a relatively high elongation to failure [32], and it could be attributed to stress relaxation taking place during loading the fibres for residual stresses already existing in the fibres or microfibrils self-alignment during deformation. The diameter variation along the gauge length was found to be a factor affecting the measured tensile strength of the fibre. As the variation in diameter (standard deviation of diameter measurements) increases for a particular fibre, the mechanical behaviour, in terms of strength and modulus, is depressed considerably. However, when designing for industry it will not be feasible to check the diameter variation for each single fibre embedded in the composite. But this should be generally considered as a factor that is highly affecting the modulus of elasticity.

The changing slope of the tensile curve was also observed for the cattle and horsetail hair (Figures 4 and 5); the slope of the curve changes at a specified strain value. It is possible to make rough estimates for the strain value after which the slope of the curve changes, and these are 2.5%, 3.2%, and 3.5% for coir, cattle, and horsetail fibres, respectively. Although the mentioned three types of fibres behave in the same manner, white cattle hair is seen to have both the least scatter of data and the highest tensile strength parameters. It is important to note that both hair types tend to be highly ductile as most of the tested specimens have not failed/fractured at the specified strain. For those reaching an elongation equal or greater than 30%, the test was stopped before failure because the tester reached its maximum travel limit. On the other hand, some of the hair samples failed prematurely right after the slope change, that is, the transition from one form of deformation to another. Representative tensile stress-strain curves for the fibres that failed prematurely are shown in the inset in Figure 4. The reason behind this early failure would be better understood by witnessing the difference in morphology of both fibres that behave differently in such a different manner.

Unlike coir, cattle, and horsetail fibres, flax, hemp, and jute fibres stress-strain curves show only one stage, which is almost linearly elastic, in agreement with Müssig et al. [32]. Representative stress-strain curves of hemp, flax, and jute are

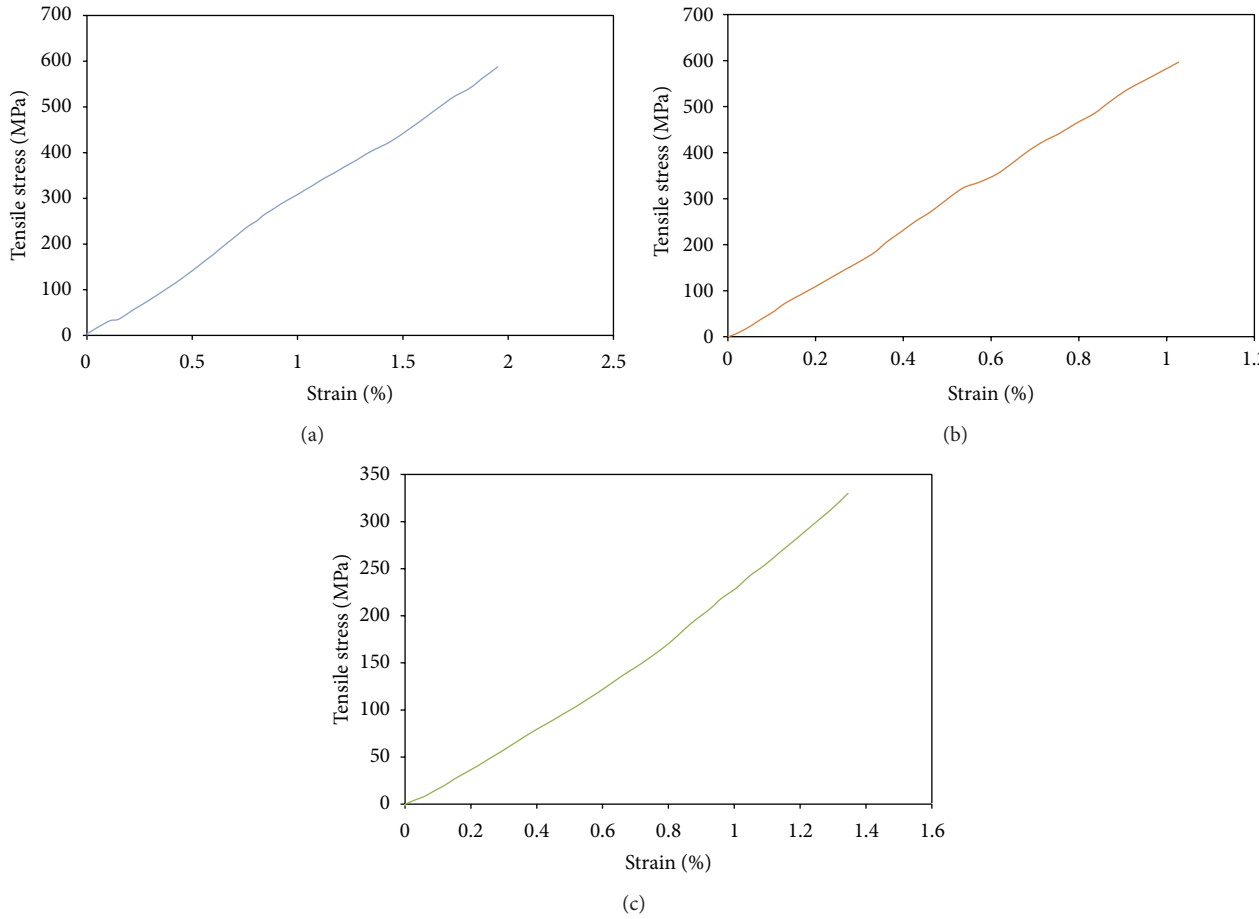

Figure 6: Representative curves for tensile behaviour of (a) hemp single fibres, (b) flax single fibres, and (c) Jute single fibres.

demonstrated in Figure 6. The scatter in the tensile behaviour of hemp, flax, and jute fibres is quite large. This is expected for natural fibres as suggested by the literature. Despite the scatter, the overall behaviour of these three fibres is superior to that of coir, cattle hair, and horsetail hair when considering the modulus of elasticity. But it is evident that the ductility of the plant fibres (excluding coir) is much lower than that of hair. The stiffness of both types of fibres is quite comparable though.

A summary of the tensile properties of cattle hair is shown in Figure 7. These graphs show the large scatter within each property. However, a general trend for the behaviour can be determined and the significance of this trend is established through the R-squared values on the plots. The measured Young's modulus shows no statistical trend with measured diameter. However, it can be concluded that the measured stiffness (force per unit elongation) of cattle hair increases with increasing the fibre diameter, whereas its strength to failure shows a slight tendency to decrease with increasing the diameter. The graphs for hemp fibres (Figure 8) show weak correlation between the fibre diameter and the different mechanical properties. It could be observed that the higher population of the fibre's properties tend to be at the lower range for Young's modulus and strength at failure.

Figure 9 shows SEM images of the cross-section of coir fibre. This image points out the dilemma that has been reported to be a factor affecting the mechanical properties of natural fibres through biased calculations, that is, the method used for diameter measurement. Although using optical microscope images to determine the diameter of the fibre has been stated to be an adequate technique, still the assumption that the cross-section of the fibre is circular influences the estimation of the cross-sectional area. For instance, the maximum diameter measurements for the fibre in Figure 9(a) are almost double the minimum diameter. This means that depending on the view observed in the optical microscope image, an error of up to 50% can exist. Nevertheless, this statement cannot be generalized since some of the fibres do have circular cross-sections such as the coir fibre shown in Figure 9(b). Moreover, measuring the diameter using this method and calculating the failure stress of the material are not only ignoring the fact that the fibre is not circular but also assuming a uniform density across the cross-section. This is not the case for lots of the natural fibres as can be seen in SEM images of coir fibres (Figures 9 and 10) since the fibre cross-section shows a large amount of hollowness in the fibre that is not considered in diameter measurement. This means that the strength measurements

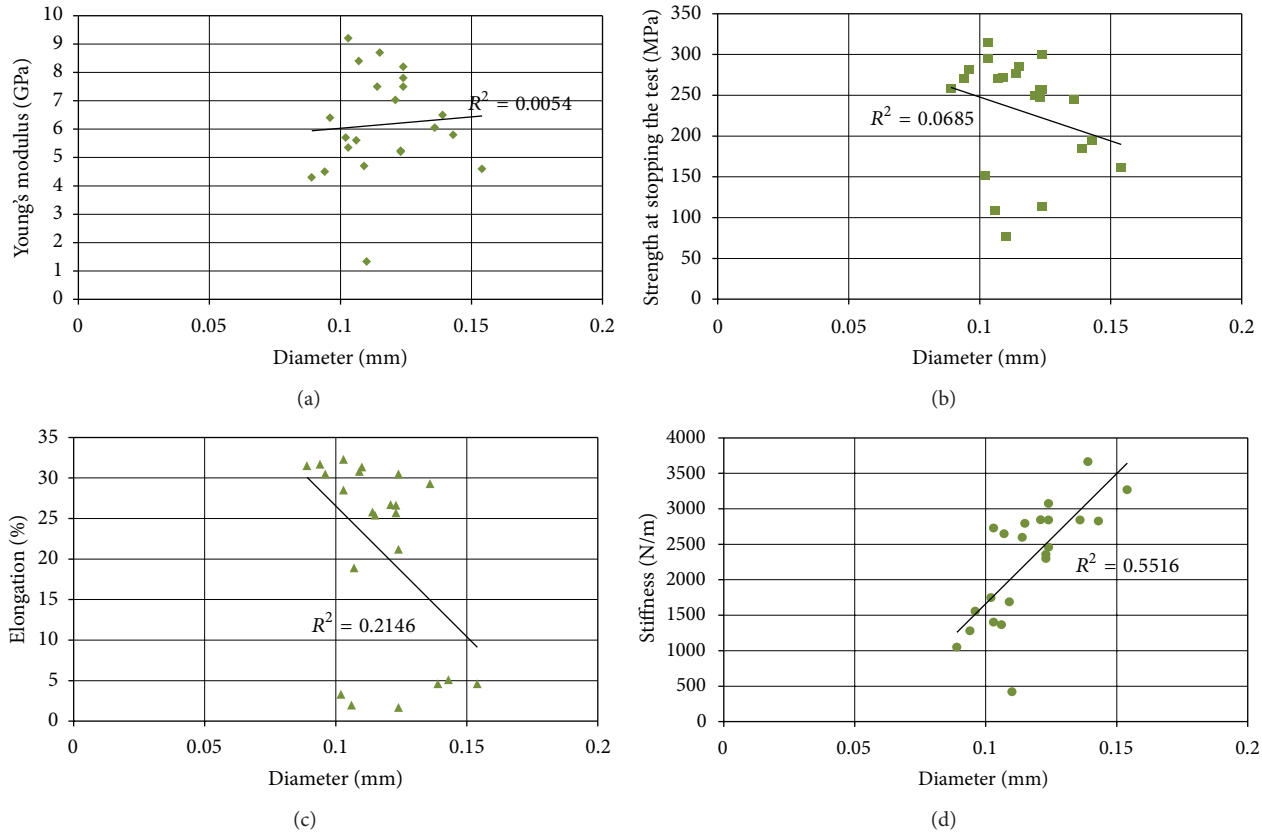

Figure 7: Summary of cattle hair tensile properties.

are misled as the area effectively carrying the load is well less than the measured one.

The high magnification SEM image in Figure 8(a) suggests that the microfibrils towards the centre of the fibre tend to have a coiled spring-like structure, with this spring being lined with a thin layer as shown in the inset in the same figure. The scenario of failure could be that this thin layer first is stretched (bearing the load), then it fails, and that would represent the first stage in the stress-strain curve. After that the spring itself is carrying the load and this is the second part of the curve until it fails, which means that the whole fibre failed. This hypothesis was also suggested by the SEM image in Figure 8(b) of the fracture surface of a tensile test coir fibre. Observation of the deformation of the fibre under tensile loading in an SEM could help verify this hypothesis.

A characteristic feature that was noticed in the structure of cattle hair (as shown in Figure 11) is that, unlike other hair types (keratinous), it has a smooth surface. This is clearly demonstrated by comparing the surface of the cattle hair to that of Merino wool. Moreover, some of the observed hair samples contained a hole in the middle and others did not (as shown in Figure 12). This observation needs further investigation and better understanding of the anatomy of the cattle hair. Another feature that was noticed in the cattle hair is the presence of kink bands that could act as structural defects leading to the premature failure that was observed in tensile stress-strain curves. This kind of defect/feature can be seen in Figure 12 as well.

The structure of jute fibres shown in Figure 13 is similar to that of most plant fibres (flax and hemp in this study); each fibre is a bundle of microfibrils waxed together. The abovementioned statement about the inaccuracy of assuming the cross-section of the fibre to be circular is also supported by the SEM images of jute fibres here.

4. Conclusions

Natural fibres have the potential to be candidates to replace synthetic fibres in lots of applications. There are barriers that are hindering their progress into industry [2]. First and foremost is the variability within the properties of the fibres, which affects the final properties of them when used as reinforcements in composite materials. There are two sorts of variability: the apparent variability that is caused by measurement and testing techniques and the actual property variability of the fibre by nature. The former type of variability is caused by experimental methods such as the diameter measurements as well as variability in microstructure.

It has already been well established by previous work that the use of plant fibres such as hemp, flax, jute, and coir in composite materials is beneficial from an engineering perspective as well as the environmental impact scope. There

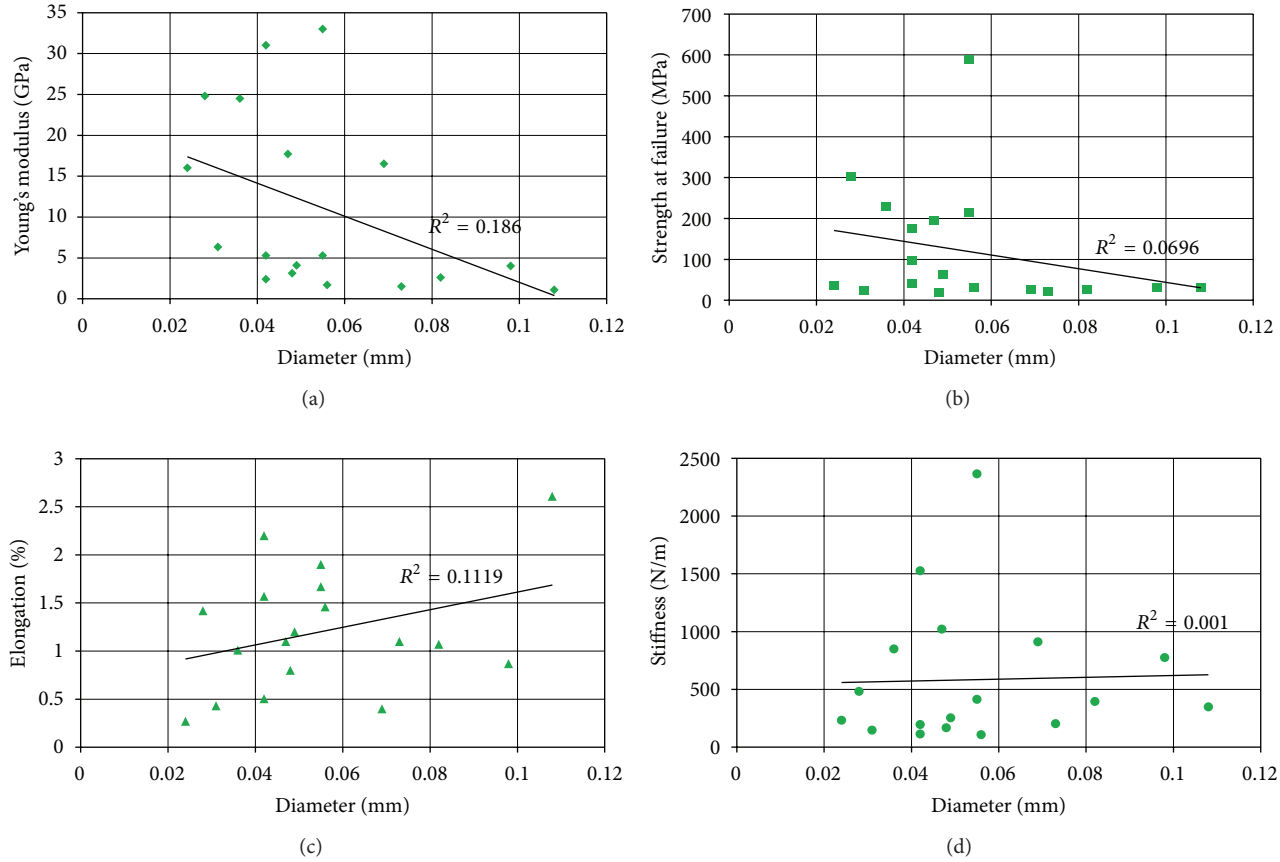

Figure 8: Summary of hemp tensile properties.

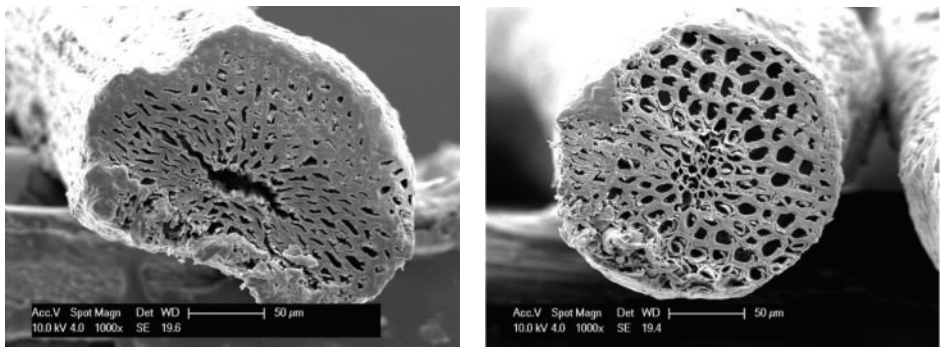

(a) (b)

Figure 9: SEM images of the cross-sections of coir fibres.

are no relevant published investigations for the properties of cattle hair and horsetail hair. This study has shown the animal hairs to have good mechanical properties, in terms of ductility (in the range of 20% elongation on the average) and strength to failure (in the range of 250–300 MPa on the average), suggesting that they could be utilized in several applications.

Natural fibres usually have the mechanical properties suitable for their role in nature. For instance, coir fibres are expected to have high impact strength/resistance as their role in nature is to protect the nut from breakage upon falling. Understanding the role of each fibre in nature could help utilizing them in the suitable applications. In addition, the structural defects in the fibres cannot be overlooked as they seem to be playing a vital role in the deformation of the fibres. Further investigation is required in order to monitor the microstructural evolution of the fibres while deformation is under tensile loading.

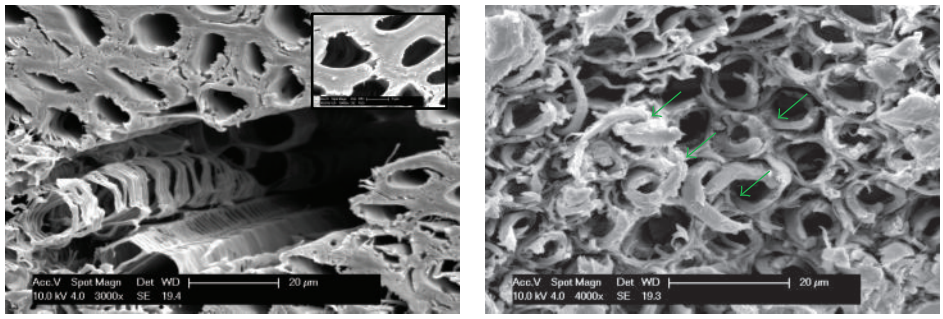

(a) (b)

Figure 10: SEM images showing (a) coir microfibrils at higher magnification with the spring-like structure and the interconnecting layer and (b) fracture surface of a coir fibre that failed under tensile loading (the arrows point towards features demonstrating spirality of the microfibrils).

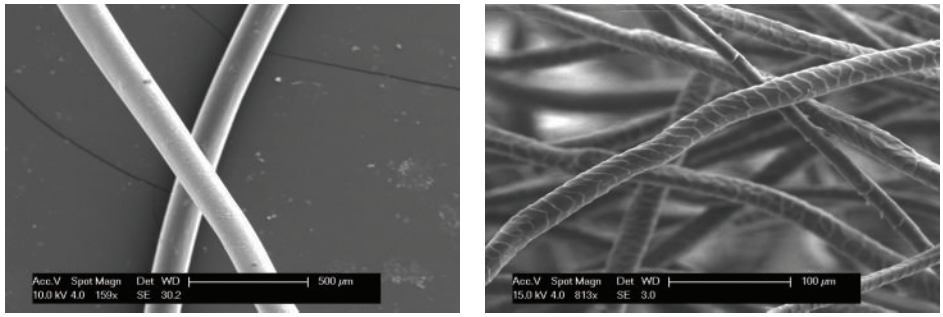

(a) (b)

Figure 11: SEM images showing the smooth surface of cattle hair (a) versus keratinous structure of wool (b).

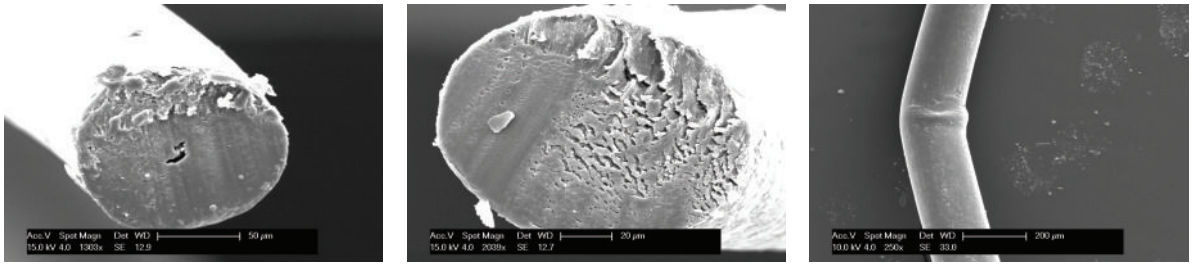

(a) (b) (c)

Figure 12: SEM images showing different features of cattle hair (with and without a hole in the middle, kink bands).

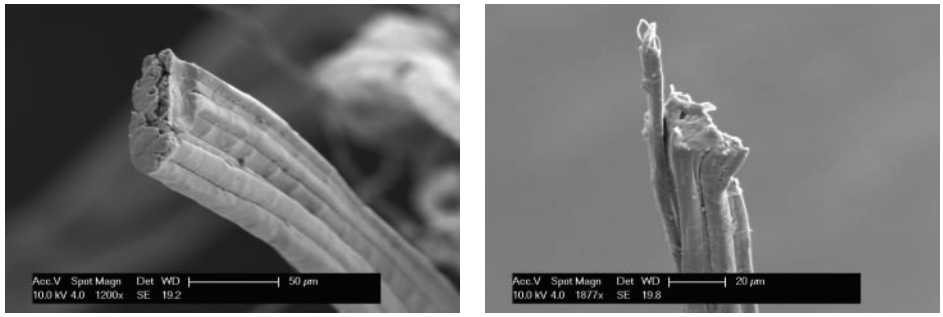

(a) (b)

Figure 13: Jute fibres shown to consist of several elementary fibres waxed together.

Conflict of Interests

The authors declare that there is no conflict of interests regarding the publication of this paper.

Acknowledgments

Nesma T. Aboulkhair gratefully acknowledges funding provided by the Dean of Engineering scholarship for International Research Excellence, Faculty of Engineering, University of Nottingham. Nicola M. Everitt thanks the Bioengineering Research group and The Faculty of Engineering for travel funding to present this research at the International Conference on Natural Fibers-Sustainable Materials for Advanced Applications, Portugal, 2013. The fibres used were kindly donated by ENKEV natural fibres.

References

[1] M. Kuranska and A. Prociak, "Porous polyurethane composites with natural fibres," *Composites Science and Technology*, vol. 72, no. 2, pp. 299–304, 2012.

[2] M. Assarar, D. Scida, A. El Mahi, C. Poilâne, and R. Ayad, "Influence of water ageing on mechanical properties and damage events of two reinforced composite materials: flax-fibres and glass-fibres," *Materials and Design*, vol. 32, no. 2, pp. 788–795, 2011.

[3] A. O'Donnell, M. A. Dweib, and R. P. Wool, "Natural fiber composites with plant oil-based resin," *Composites Science and Technology*, vol. 64, no. 9, pp. 1135–1145, 2004.

[4] J. L. Thomason, J. Carruthers, J. Kelly, and G. Johnson, "Fibre cross-section determination and variability in sisal and flax and its effects on fibre performance characterisation," *Composites Science and Technology*, vol. 71, no. 7, pp. 1008–1015, 2011.

[5] F. D. A. Silva, N. Chawla, and R. D. D. T. Filho, "Tensile behavior of high performance natural (sisal) fibers," *Composites Science and Technology*, vol. 68, no. 15-16, pp. 3438–3443, 2008.

[6] K. Oksman, A. P. Mathew, R. Långström, B. Nyström, and K. Joseph, "The influence of fibre microstructure on fibre breakage and mechanical properties of natural fibre reinforced polypropylene," *Composites Science and Technology*, vol. 69, no. 11-12, pp. 1847–1853, 2009.

[7] N. Venkateshwaran, A. Elayaperumal, and G. K. Sathiya, "Prediction of tensile properties of hybrid-natural fiber composites," *Composites B*, vol. 43, no. 2, pp. 793–796, 2012.

[8] A. G. Facca, M. T. Kortschot, and N. Yan, "Predicting the tensile strength of natural fibre reinforced thermoplastics," *Composites Science and Technology*, vol. 67, no. 11-12, pp. 2454–2466, 2007.

[9] A. S. Virk, W. Hall, and J. Summerscales, "A new rule of mixtures for natural fibre composites," 2013, http://www.tech.plym.ac.uk/sme/composites/C2011_EcoComp_Virk.ppt.

[10] A. S. Virk, W. Hall, and J. Summerscales, "Modulus and strength prediction for natural fibre composites," *Materials Science and Technology*, vol. 28, no. 7, pp. 864–871, 2012.

[11] P. Wambua, J. Ivens, and I. Verpoest, "Natural fibres: can they replace glass in fibre reinforced plastics?" *Composites Science and Technology*, vol. 63, no. 9, pp. 1259–1264, 2003.

[12] L. Osorio, E. Trujillo, A. W. Van Vuure, and I. Verpoest, "Morphological aspects and mechanical properties of single bamboo fibers and flexural characterization of bamboo/epoxy composites," *Journal of Reinforced Plastics and Composites*, vol. 30, no. 5, pp. 396–408, 2011.

[13] N. Sgriccia, M. C. Hawley, and M. Misra, "Characterization of natural fiber surfaces and natural fiber composites," *Composites A*, vol. 39, no. 10, pp. 1632–1637, 2008.

[14] D. Dai, M. Fan, and P. Collins, "Fabrication of nanocelluloses from hemp fibers and their application for the reinforcement of hemp fibers," *Industrial Crops and Products*, vol. 44, pp. 192–199, 2013.

[15] N. Defoirdt, S. Biswas, L. D. Vriese et al., "Assessment of the tensile properties of coir, bamboo and jute fibre," *Composites A*, vol. 41, no. 5, pp. 588–595, 2010.

[16] K. Charlet, C. Baley, C. Morvan, J. P. Jernot, M. Gomina, and J. Bréard, "Characteristics of Hermès flax fibres as a function of their location in the stem and properties of the derived unidirectional composites," *Composites A*, vol. 38, no. 8, pp. 1912–1921, 2007.

[17] D. C. O. Nascimento, A. S. Ferreira, S. N. Monteiro, R. C. M. P. Aquino, and S. G. Kestur, "Studies on the characterization of piassava fibers and their epoxy composites," *Composites A*, vol. 43, no. 3, pp. 353–362, 2012.

[18] W. Wang and G. Huang, "Characterisation and utilization of natural coconut fibres composites," *Materials and Design*, vol. 30, no. 7, pp. 2741–2744, 2009.

[19] A. Bourmaud and C. Baley, "Investigations on the recycling of hemp and sisal fibre reinforced polypropylene composites," *Polymer Degradation and Stability*, vol. 92, no. 6, pp. 1034–1045, 2007.

[20] O. Faruk, A. K. Bledzki, H. P. Fink, and M. Sain, "Biocomposites reinforced with natural fibers: 2000–2010," *Progress in Polymer Science*, vol. 37, no. 11, pp. 1552–1596, 2012.

[21] K. G. Satyanarayana, J. L. Guimarães, and F. Wypych, "Studies on lignocellulosic fibers of Brazil—part I: source, production, morphology, properties and applications," *Composites A*, vol. 38, no. 7, pp. 1694–1709, 2007.

[22] E. P. S. Tan, S. Y. Ng, and C. T. Lim, "Tensile testing of a single ultrafine polymeric fiber," *Biomaterials*, vol. 26, no. 13, pp. 1453–1456, 2005.

[23] T. P. Sathishkumar, P. Navaneethakrishnan, and S. Shankar, "Tensile and flexural properties of snake grass natural fiber reinforced isophthallic polyester composites," *Composites Science and Technology*, vol. 72, no. 10, pp. 1183–1190, 2012.

[24] A. Nechwatal, K. P. Mieck, and T. Reußmann, "Developments in the characterization of natural fibre properties and in the use of natural fibres for composites," *Composites Science and Technology*, vol. 63, no. 9, pp. 1273–1279, 2003.

[25] W. Hu, M. Ton-That, F. Perrin-Sarazin, and J. Denault, "An improved method for single fiber tensile test of natural fibers," *Polymer Engineering and Science*, vol. 50, no. 4, pp. 819–825, 2010.

[26] V. Placet, F. Trivaudey, O. Cisse, V. Gucheret-Retel, and M. L. Boubakar, "Diameter dependence of the apparent tensile modulus of hemp fibres: a morphological, structural or ultrastructural effect?" *Composites A*, vol. 43, no. 2, pp. 275–287, 2012.

[27] F. Tomczak, T. H. D. Sydenstricker, and K. G. Satyanarayana, "Studies on lignocellulosic fibers of Brazil—part II: morphology and properties of Brazilian coconut fibers," *Composites A*, vol. 38, no. 7, pp. 1710–1721, 2007.

[28] M. A. Sawpan, K. L. Pickering, and A. Fernyhough, "Effect of various chemical treatments on the fibre structure and tensile properties of industrial hemp fibres," *Composites A*, vol. 42, no. 8, pp. 888–895, 2011.

[29] M. K. Kompella and J. Lambros, "Micromechanical characterization of cellulose fibers," *Polymer Testing*, vol. 21, no. 5, pp. 523–530, 2002.

[30] L. G. Thygesen and P. Hoffmeyer, "Image analysis for the quantification of dislocations in hemp fibres," *Industrial Crops and Products*, vol. 21, no. 2, pp. 173–184, 2005.

[31] D. Dai and M. Fan, "Investigation of the dislocation of natural fibres by Fourier-transform infrared spectroscopy," *Vibrational Spectroscopy*, vol. 55, no. 2, pp. 300–306, 2011.

[32] J. Müssig, H. Fischer, N. Graupner, and A. Drieling, "Testing methods for measuring physical and mechanical fibre properties (plant and animal fibres)," in *Industrial Applications of Natural Fibres*, pp. 267–309, John Wiley & Sons, New York, NY, USA, 2010.

[33] S. W. Beckwith, "Natural fibers: nature providing technology for composites," *SAMPE Journal*, vol. 44, no. 3, pp. 64–65, 2008.

[34] M. M. Rahman and M. A. Khan, "Surface treatment of coir (*Cocos nucifera*) fibers and its influence on the fibers' physico-mechanical properties," *Composites Science and Technology*, vol. 67, no. 11-12, pp. 2369–2376, 2007.

[35] C. Baley, A. le Duigou, A. Bourmaud, and P. Davies, "Influence of drying on the mechanical behaviour of flax fibres and their unidirectional composites," *Composites A*, vol. 43, no. 8, pp. 1226–1233, 2012.

Hindawi Publishing Corporation
Conference Papers in Materials Science
Volume 2013, Article ID 873692, 5 pages
http://dx.doi.org/10.1155/2013/873692

Conference Paper

The Effect of Fibre Composition and Washing Conditions upon Hand Properties of Knitted Materials

Gita Busilienė, Eugenija Strazdienė, and Virginijus Urbelis

Department of Clothing and Polymeric Products Technology, Faculty of Design and Technologies, Kaunas University of Technology, Studentu Street 56, 51424 Kaunas, Lithuania

Correspondence should be addressed to Gita Busilienė; gita.busiliene@gmail.com

Received 4 July 2013; Accepted 8 September 2013

Academic Editors: R. Fangueiro and H. Hong

This Conference Paper is based on a presentation given by Gita Busilienė at "International Conference on Natural Fibers—Sustainable Materials for Advanced Applications 2013" held from 9 June 2013 to 11 June 2013 in Guimarães, Portugal.

The behaviour of knitted plated jersey materials made from natural and man-made fibres was tested after certain washing conditions. Surface density and thickness of investigated materials differed insignificantly, from 206 g/m^2 up to 222 g/m^2 and from 0.56 mm up to 0.79 mm, respectively. Special device for textile materials hand evaluation based on the principle of pulling of a disc-shaped specimen through a rounded hole was used. The aim of this study was to investigate the effect of materials' fibre composition and washing conditions upon the changes of hand properties of knitted materials. Analysis of obtained results showed that, during washing, textile materials shrink and become more dense and rough, and their rigidity increases as well. Thus, the most significant effect of 5-cycle washing was obtained for knitted material with bamboo fibres.

1. Introduction

The objective evaluation of textile hand is based on physical parameters, that is, numeric values, which are estimated with the help of specialised devices. Objective evaluation of textile hand is performed on the basis of the dependency (deflection height-force), which is obtained when tested sample is pulled through the hole [1–3]. The advantage of such method is the possibility to define one complex criterion for textile hand characterization which is obtained on the basis of pulling curves' characteristic zones. In previous studies, it was established that KTU-Griff-Tester deviceis suitable for investigating the changes of fibrous materials behaviour and hand variations [4, 5].

2. Materials and Methods

Knitted fabrics with the different fibre compositions and the same type of weave were chosen as the objects of the investigation. Table 1 shows the characteristics of investigated knitted fabrics.

For the investigation, knitted materials after five cycles of the washing process were used. One cycle of the washing process was at water temperature of 40°C, washing duration of 31 minutes, and centrifugation duration of 10 minutes (number of rotations: 600), following the standard ISO 6330:2002. After washing a knitted materials were dried in a horizontal position (duration >10 hours). In this study, the washing agent BEICLEAN RG-N which is a detergent and emulsifier was applied. For better performance, it was used together with washing intensifier BEIMPLEX NWS, which acts upon alkaline ions and heavy metals by preventing the formation of deposits, that is, allowing the avoidance of the formation of plaque on washed materials and sediments in washing machines. In other words, BEIMPLEX NWS strengthens the feature of BEICLEAN RG-N to disperse the contaminants. In this research, the water of average hardness (pH 7–14) was used, and washing conditions were selected corresponding to laundry state which is slight soiling. Table 2 shows the chemical composition of the used washing agent.

Tests were performed using KTU-Griff-Tester device, which was fixed in standard tensile testing machine [6–8]. Disc-shaped samples with the radius $R = 56.5$ mm

Table 1: The characteristics of investigated knitted fabrics.

Fabric symbol	Composition	Pattern	Density		Surface density, g/m^2	Thickness δ_1, mm	Thickness change $\Delta\delta$, %
			Wale dir. P_w, dm^{-1}	Course dir. P_c, dm^{-1}			
M1	95% CO, 5% EL	Plated jersey	265	160	222	0.77	3.9
M2	95% Bo, 5% EL		215	170	215	0.56	3.6
M3	95% CV, 5% EL		215	155	206	0.79	8.9
M4	92% CV, 8% EL		230	160	208	0.62	9.7
M5	88% CV, 12% EL		310	175	210	0.59	11.9

CV: viscose; CO: cotton; Bo: bamboo; EL: elastane.

Table 2: Chemical composition of washing agent.

Washing agent	Chemical composiotion	Ionic character	pH value of a 10% solution	Specific weight at 20°C
BEICLEAN RG-N	Modified fatty alcohol ethoxylates	Nonionic	6.0–7.0	1.0
BEIMPLEX NWS	Polycarboxylates, phosphates	Anionic	5.5–6.5	1.27

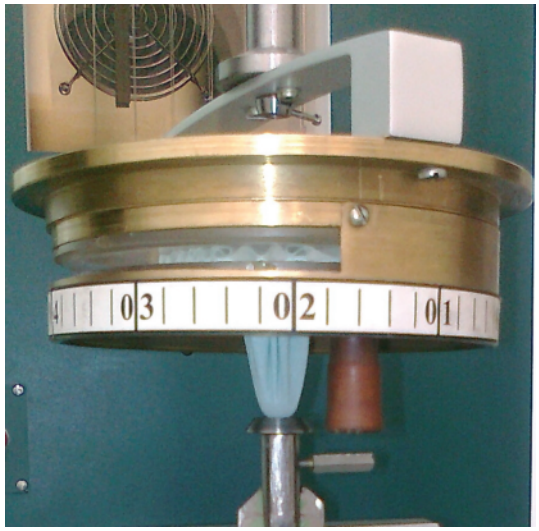

(a)

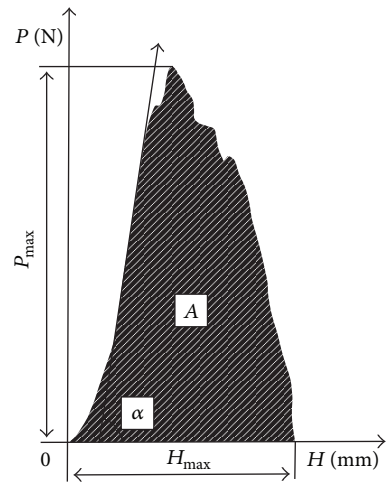

(b)

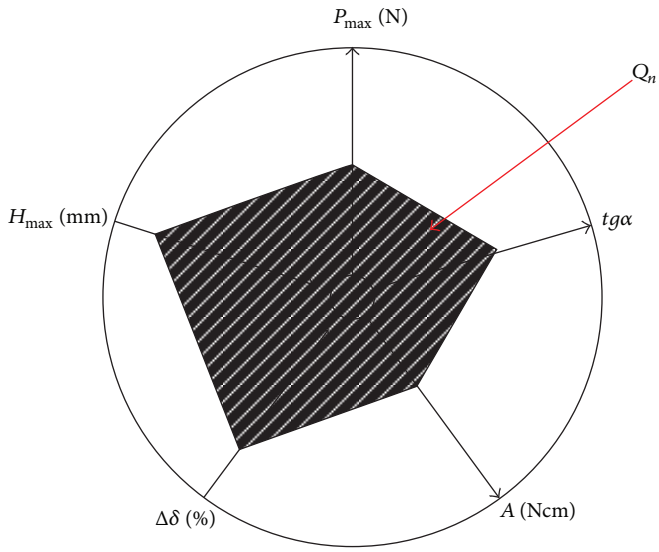

(c)

Figure 1: KTU-Griff-Tester device (a); typical extraction curve H-P (b); the optimisation diagram (c).

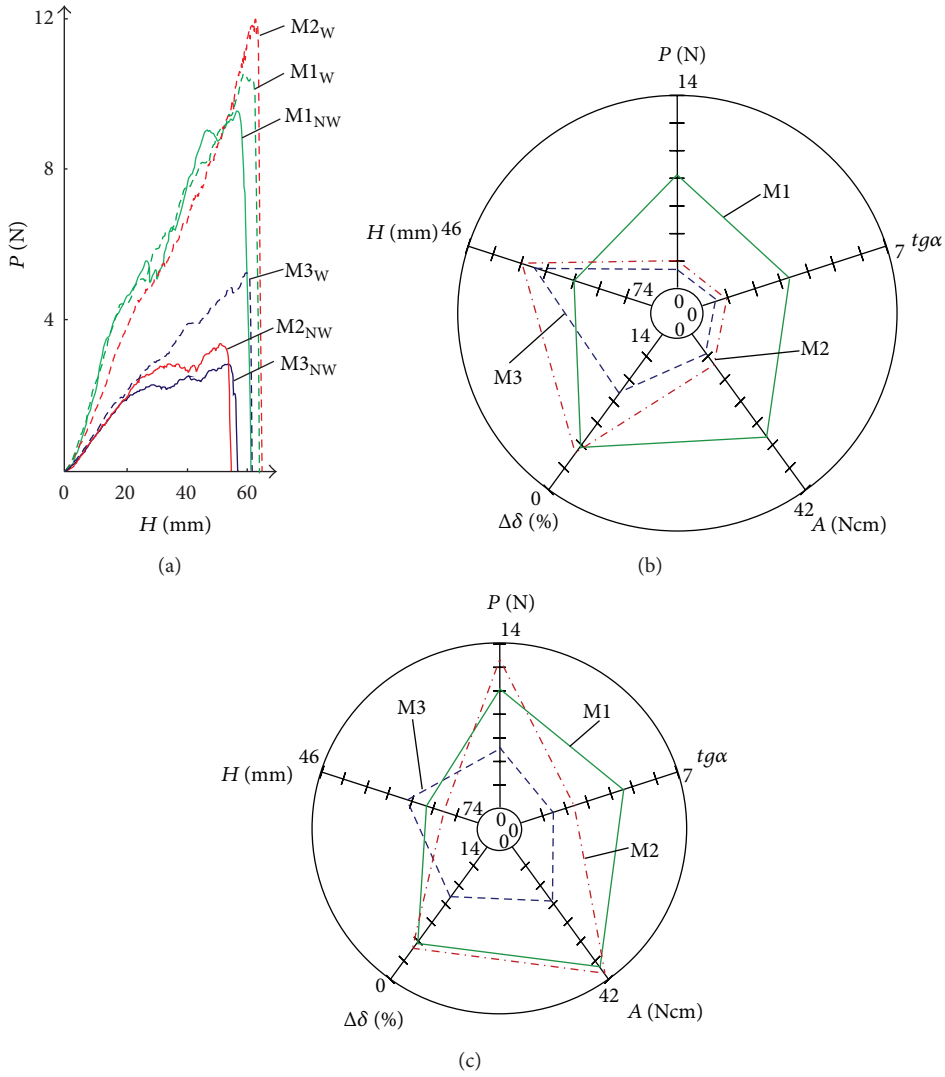

FIGURE 2: Typical pulling curves of knitted materials with different fibre content (a); the diagram of complex hand rates Q_{NW} calculation for nonwashed specimen (b); the calculation of complex hand rates Q_W after sample washing (c).

were pulled by spherical punch $\varphi = 5$ mm with the needle through the central hole of the device. Extraction speed was 100 mm/min. The distance between the limiting plates $h = 5.6 \cdot \delta$ mm and radius $r = 10$ mm of the hole was chosen according to the tested fabric thickness $0.5 < \delta < 1.0$. The distance between the plates was calculated for each tested material and was kept constant for nonwashed samples and after washing.

During testing pulling curves H-P (deflection height force) were registered on the basis of which such parameters were defined: maximum extraction force P_{max}, maximum deflection height H_{max} and the tangent of nominal slope angle of the H-P curve $tg\alpha$. The pulling work A, Ncm, and complex hand rate Q_n also were calculated. The changes of thickness $\Delta\delta$ were defined using thickness gauge SCMIDT DPT 60 DIGITAL; under two different loads (ratio 1:5) [6, 8, 9]. Knitted samples were tested and evaluated under controlled environmental conditions ($\varphi = 65 \pm 2\%$, $T = 20 \pm 2^{\circ}$C). For each sample, six specimens were tested, and the error level was within the limits of 5%. KTU-Griff-Tester device, typical extraction curve H-P, and optimisation diagram on the basis of the complex hand rate are shown in Figure 1.

3. Results and Conclusions

Seeking to define the effect of fibre composition upon the rate of hand evaluation of knitted materials of different fibre content and having a certain percent of elastane were investigated. The characteristics of knitted materials pulling through a hole process are shown in Table 3.

Typical pulling curves of knitted materials with different fibre content and the diagrams of complex hand rates Q_{NW} calculation for nonwashed specimens are shown in Figures 2(a) and 2(b). Obtained results revealed that viscose knitted material M3 has the best hand rate: $Q_{NW} = 2.30$. Hand rates of material M2 from bamboo fibres are worse by 27%.

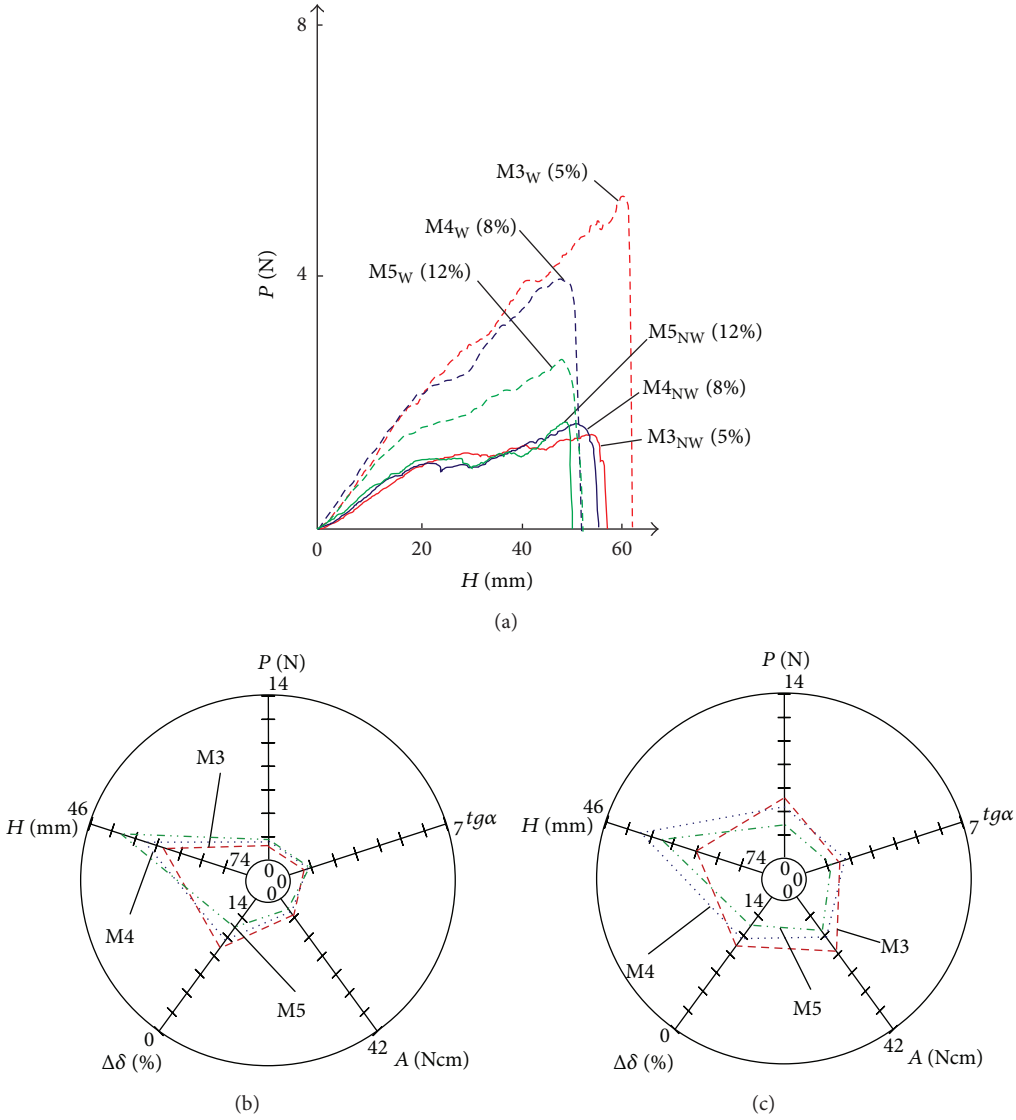

FIGURE 3: Typical pulling curves of viscose knitted materials with different elastane content (a); the diagrams of complex hand rates Q_{NW} calculation for nonwashed specimens (b); the calculation of complex hand rates Q_W after sample washing (c).

The values of hand rates of constituent parts for materials M3 and M2 are also close: P_{max} varied from 1.37 N to 2.00 N (the difference is 46%) N; $tg\alpha$ varied from 0.68 to 0.86 (the difference is 26%); H_{max} varied from 54.0 mm to 56.2 mm (the difference is 4%). The material with cotton fibres M1 (Q_{NW} = 11.50) differs mostly by poor hand results. Its complex hand rate Q_{NW} is more than 4 times higher compared to those of the other investigated materials. Pulling force P_{max}, the rigidity described by $tg\alpha$, and pulling work A of M1 material are also up to 5 times higher compared to corresponding values of M3 material. The value H_{max} which describes the deformability of tested samples is higher by 14%. According to the character of pulling curves and taking into account the determined values of hand rates, it can be stated that knitted materials from viscose and bamboo fibres are soft, thin, smooth, and easily slipping.

Analysis of obtained results has shown that the washing process of knitted materials reduces their hand rates; that is, the ratio Q of hand rates Q_W/Q_{NW} for all investigated fabrics after 5 washing cycles became worse from 1.3 times for material from cotton fiber with 5% elastane up to 5.4 times for material from bamboo fiber with 5% elastane (Table 3). The same results were also obtained in earlier research works, which showed that hand rates after washing became worse by 2.5 ÷ 4.1 times [5]. This phenomenon is illustrated by typical pulling through hole curves H-P which are shown in Figure 2(a) and the optimisation diagrams of hand rates Q_{NW} and Q_W calculation for samples after washing which are shown in Figures 2(b) and 2(c).

During washing, textile materials shrink and become more dense and rough, and their rigidity increases as well. Thus, constituent values of hand rate, P_{max}, $tg\alpha$, and A,

Table 3: The characteristics of knitted materials pulling through a hole.

Symbol, treatment	P_{max}, N	$tg\alpha$	A, Ncm	H_{max}, mm	Q_{NW} and Q_W	Q
M1						
NW	8.20 ± 0.73	3.36 ± 0.11	28.89 ± 1.35	62.00 ± 0.60	11.50 ± 0.54	1.30
W	10.53 ± 0.33	4.67 ± 0.27	37.66 ± 1.72	65.00 ± 1.43	14.99 ± 0.69	
M2						
NW	2.00 ± 0.07	0.86 ± 0.02	7.30 ± 0.22	54.00 ± 0.49	2.91 ± 0.09	5.42
W	12.72 ± 0.18	2.36 ± 0.11	39.65 ± 0.92	68.00 ± 0.73	15.78 ± 0.37	
M3						
NW	1.37 ± 0.06	0.68 ± 0.03	5.78 ± 0.09	56.20 ± 0.84	2.30 ± 0.03	3.05
W	5.28 ± 0.23	1.44 ± 0.06	17.62 ± 0.58	62.50 ± 1.78	7.02 ± 0.23	
M4						
NW	1.62 ± 0.07	0.83 ± 0.04	5.44 ± 0.17	54.26 ± 0.26	2.16 ± 0.07	2.23
W	4.04 ± 0.26	1.60 ± 0.07	12.09 ± 0.50	52.50 ± 0.84	4.81 ± 0.22	
M5						
NW	1.64 ± 0.09	0.84 ± 0.04	4.79 ± 0.20	50.50 ± 0.44	1.91 ± 0.08	1.83
W	2.72 ± 0.15	1.31 ± 0.07	8.79 ± 0.30	55.00 ± 0.54	3.50 ± 0.12	

NW: nonwashed specimen, W: specimen after washing; the hand ratio Q was determined as ratio Q_{NW}/Q_W, where Q_W is the area of washing treatment and Q_{NW} is the area of nonwashed specimen.

increase. Pulling force P_{max} increased from 1.28 for material from cotton fiber with 5% EL up to 6.36 for material from bamboo fiber with 5% EL times, $tg\alpha$ up to 2.74 for material from bamboo fiber with 5% EL, and pulling work A from 1.3 for material from cotton fiber with 5% EL up to 5.43 for material from bamboo fiber with 5% EL times. The values of pulling height H_{max} vary in the limits of 0.25% ÷ 3.75%, except for M2 knitted material, for which H_{max} increases up to 26%. Thus, the most significant effect of 5-cycle washing was obtained for knitted material M2 from bamboo fiber with 5% EL.

Comparative analysis performed with viscose knitted materials M3, M4, and M5 has revealed that, with the increase of elastane in their content from 5% to 12%, pulling force P_{max} and slope angle $tg\alpha$ increase by 20%, but pulling work A and pulling height H_{max} decrease by 18% and 11%, respectively. Typical pulling curves of viscose knitted materials with different fibre content and the diagrams of complex hand rates Q_{NW} calculation for nonwashed samples are shown in Figures 3(a) and 3(b). The curves of viscose materials M3, M4, and M5 pulling through a hole show that the behaviour of these materials is similar; that is, the increase of elastane in their content perfected their hand property insignificantly—Q_{NW} decreased only by 17%.

Typical pulling curves of viscose knitted materials with different elastane content and the diagrams of complex hand rate Q_W calculation for samples after washing are shown in Figures 3(a) and 3(c). The results of the investigation of the washing effect upon hand rates Q_W confirmed previous conclusions for the materials with different elastane content; the decrease of hand rate Q_W varies form 32% (for 8% EL) to 51% (for 12% EL) when compared to knitted material from viscose with 5% EL. The most significant effect of 5-cycle washing process was defined for knitted material from viscose, having 5% of elastane in its content. Hand ratio Q becomes worse by 3 times in this case. The lowest effect of 5-cycle washing is defined for material from viscose with 12% elastane. Its hand rate Q_W became worse by 51%.

References

[1] A. Seidel, "Griffbewertung von strumpfwaren mit dem ITV-griff-tester," *Melliand Textilberichte*, vol. 82, no. 6, pp. 491–494, 2001.

[2] G. Martišiūtė and M. Gutauskas, "A new approach to evaluation of textile fabric handle," *Materials Science*, vol. 7, no. 3, pp. 186–190, 2001.

[3] H. A. Kim and H. S. Ryu, "Hand and mechanical properties of stretch fabrics," *Fibers and Polymers*, vol. 9, no. 5, pp. 574–582, 2008.

[4] D. Juodsnukytė, M. Gutauskas, and S. Krauledas, "Influence of fabric softeners on performance stability of the textile materials," *Materials Science*, vol. 11, no. 2, pp. 179–182, 2005.

[5] D. Truncytė and M. Gutauskas, "The influence of the technological treatment regime on the mechanical properties of textile fabrics," *Materials Science*, vol. 12, no. 4, pp. 350–354, 2006.

[6] V. Daukantienė, L. Papreckienė, and M. Gutauskas, "Simulation and application of the behaviour of a textile fabric while pulling it through a round hole," *Fibres and Textiles in Eastern Europe*, vol. 11, no. 2, pp. 37–41, 2003.

[7] E. Strazdienė, S. B. Saïd, M. Gutauskas, L. Schacher, and D. C. Adolphe, "The evaluation of fabric treatment by Griff tester and sensory analysis," *International Journal of Clothing Science and Technology*, vol. 18, no. 5, pp. 326–334, 2006.

[8] D. Truncytė, L. Papreckienė, and M. Gutauskas, "Behaviour of textile membranes while being pulling through a hole by the constrained methods," *Fibres and Textiles in Eastern Europe*, vol. 15, no. 1, pp. 50–54, 2007.

[9] D. Grinevičiūtė, L. Papreckienė, and M. Gutauskas, "The optimization of complex hand rate determination," *Materials Science*, vol. 12, no. 1, pp. 79–83, 2006.

Hindawi Publishing Corporation
Conference Papers in Materials Science
Volume 2013, Article ID 253913, 5 pages
http://dx.doi.org/10.1155/2013/253913

Conference Paper

A Qualitative Study of Residual Pesticides on Cotton Fibers

Syed Zameer Ul Hassan,[1] Jiri Militky,[1] and Jan Krejci[2]

[1] *Department of Textile Materials, Technical University of Liberec, Studentská 2, 46117 Liberec, Czech Republic*
[2] *BVT Technologies, a.s., Hudcova 78c, 61200 Brno, Czech Republic*

Correspondence should be addressed to Syed Zameer Ul Hassan; zameer_51214@hotmail.com

Received 1 August 2013; Accepted 16 September 2013

Academic Editors: R. Fangueiro and H. Hong

This Conference Paper is based on a presentation given by Syed Zameer Ul Hassan at "International Conference on Natural Fibers—Sustainable Materials for Advanced Applications 2013" held from 9 June 2013 to 11 June 2013 in Guimarães, Portugal.

Two different methods are utilized for this study. The first method covers the measurement of bioelectrical signals caused by enzymatic inhibition of acetyl cholinesterase (AChE) for the detection of pesticides. Biosensor toxicity analyzer (BTA) was used for the testing and the monitoring of changes in bioelectrical signals caused by the interaction of biological substances, and residues were evaluated. The second method is based on measurement of the oxygen level caused by photosynthetic inhibition of residual pesticides by the interaction with green algae, *Scenedesmus* (Chlorophyta). Algae growth analyzer (AGA) equipped with miniature sensitive oxygen electrode, a light source and cover to model light and dark phases was used enabling us to follow the lifecycle of algae producing oxygen. The test, conducted under the guideline of faster analogy of DIN 863 toxicity test, alga growth inhibition test (OECD TG 201) was and ISO standard (ISO: 8692). Two samples of cotton were analyzed. Cryogenic homogenization was carried out for sample pretreatment. Soxhlet extraction method (SOX) and ultrasound assisted extraction (USE) were used for extraction. Both methods show reasonable results and can successfully be utilized for the detection of residual pesticides on different types of cotton and especially to compare the classical conventional and organic cotton.

1. Introduction

Cotton has always been a major part of the textile industry and today provides almost 38% of the world textile consumption, second only to polyester, which recently took the lead [1]. Cotton production is highly technical and difficult because of pest pressures and environment, for example, drought, temperature, and soil nutritional conditions. The total area dedicated to cotton production accounts for approximately 2.4% of arable land globally, and cotton accounts for an estimated 16% of the world's pesticide consumption [2]. Around 2.5 million tons of pesticides are used annually, and the number of registered active substances is higher than 500. Humans can be exposed to pesticides by direct or indirect means. Direct or primary exposure normally occurs during the application of these compounds, and indirect or secondary exposure can take place through the environment or the ingestion of food [3].

This is why development of natural biological methods of insect control was initiated. Cotton grown without the use of any synthetically compounded chemicals (i.e, pesticides, fertilizers, defoliants, etc.) is considered as "organic" cotton. It is produced under a system of production and processing that seeks to maintain soil fertility and the ecological environment of the crop [4].

Benzoylureas, carbamates, organophosphorus compounds, pyrethroids, sulfonylureas, and triazines are the most important groups [5]. The organophosphates and carbamates are powerful inhibitors of acetyl cholinesterase [6]. They can irreversibly inhibit acetyl cholinesterase (AChE) which is essential for the function of the central nervous system [7], resulting in the buildup of the neurotransmitter acetylcholine which interferes with muscular responses and in vital organs produces serious symptoms and eventually death [8]. Inhibition of AChE by any xenobiotic compound is used as a tool for assessment of toxicity of some pesticides

such as organophosphates and carbamates [9]. As the pesticide residue is a potentially serious hazard to human health, the control and detection of pesticide residue play a very important role in minimizing risk. Many methods have been developed in the last few years for the detection of pesticides. The most widely used methods are gas chromatography (GC), high-performance liquid chromatography (HPLC), gas chromatography-mass spectrometry (GC-MS), immune assay, and fluorescence. However, these techniques, which are time consuming, expensive, and requiring highly trained personnel, are available only in sophisticated laboratories [10].

Biosensors based on the inhibition of acetylcholine esterase (AChE) have been widely used for the detection of OP compounds [11]. Electroanalytical sensors and biosensors provide an exciting and achievable opportunity to perform biomedical, environmental, food, and industrial analysis away from a centralized laboratory due to their advantages such as high selectivity and specificity, rapid response, low cost of fabrication, possibility of miniaturization, and ease of integration in automatic devices [12]. Electrochemical biosensors for measurement of these pesticides are based on the inhibition of AChE, and the inhibition degree is proportional to the pesticide concentration [13].

Assessment of human exposure to pesticides and other toxicants through biological monitoring offers one means to evaluate the magnitude of the potential health risk of these chemicals [14]. Algae occupy an important position as the primary producers in aquatic ecosystems, and they are the basis of many aquatic food chains. For this reason, they are used in environmental studies for assessing the relative toxicity of various chemicals and waste discharges [15].

The term algae refers to both macro algae and a highly diversified group of microorganisms known as microalgae. The number of algal species has been estimated to be one to ten million, and most of them are microalgae [16]. Algae are eukaryotic and predominantly aquatic, photosynthetic organisms. They range in size from the tiny flagellate *micromonas* that is 1 micrometer (0.000039 inch) in diameter to giant kelps that reach 60 meters (200 feet) in length [17].

Single celled microalgae are among the most productive autotrophic organisms in nature due to their high photosynthetic efficiencies and the lack of heterotrophic tissues [18]. The green pigment chlorophyll (which exists in three forms: chlorophyll a, b, and c) is present in most photosynthetic organisms and provides an indirect measure of algal biomass [19]. Even though all algae species combined represent only 0.5% of total global biomass by weight, algae produce about 66% of the net global production of oxygen on earth—more than all the forests and fields [20].

Algae possess a number of distinct physical and ecological features, and their ability to proliferate over a wide range of environmental conditions reflects their diversity [17, 20].

The action of toxic substances on algae is therefore not only important for the organisms themselves but also for the other links of the food chains [21]. Algal toxicity tests and life-cycle toxicity tests are increasingly being used in bioassay test batteries, and it has been observed in several studies that for a large variety of chemical substance algal tests are relatively sensitive bioassay tools [22, 23]. Thus, inhibition of photosynthetic performance could also be used as a tool to evaluate the presence of pollutants [15].

Figure 1: Biosensor toxicity analyzer with microflow unit.

Keeping in mind the above-mentioned factors, the goal of the present work was to study two different methods for the detection of pesticides and hazardous compounds based on acetyl cholinesterase inhibition and the monitoring of changes in the oxygen level caused by the interaction of residual analytes and the green algae, *Scenedesmus* (Chlorophyta). Both methods are simple, fast, and more sensitive for pesticide determination with much lower detection limit.

2. Materials and Methodology

Two samples of Egyptian cotton Giza 86 (G86) and Pakistani cotton MNH 93 were collected from the cultivation season 2011/2012. Both varieties have classical conventional cotton and organic cotton. HPLC grade acetonitrile solvent was used for the extraction procedure. Green algae of the family Scenedesmaceae and genus *Scenedesmus* was arranged by Bvt Technologies, Czech Republic.

The determination of pesticides in samples at low concentrations is always a challenge. The main aim of any extraction process is the isolation of analytes of interest from the selected sample by using an appropriate extracting phase. The development of an appropriate sample preparation procedure involving extraction, enrichment, and cleanup steps becomes mandatory to obtain a final extract concentrated on target analytes. Cryogenic homogenization was carried out for all the samples, and Soxhlet extraction method along with ultrasonic extraction was used for extracting the analytes.

2.1. Principle of BTA. The target for many insecticides is an enzyme called acetyl cholinesterase (AChE) [24]. Acetyl cholinesterase's (AChE) biological role is the termination of impulse transmissions at cholinergic synapses within the nervous system of the insects and mammals by rapid hydrolysis of the neurotransmitter acetylcholine. Pesticides block the catalytic activity of the active center, thus, acting as inhibitors of AChE. This results in the accumulation of acetylcholine in the synaptic membrane, which blocks the nerves from processing the signals properly [25].

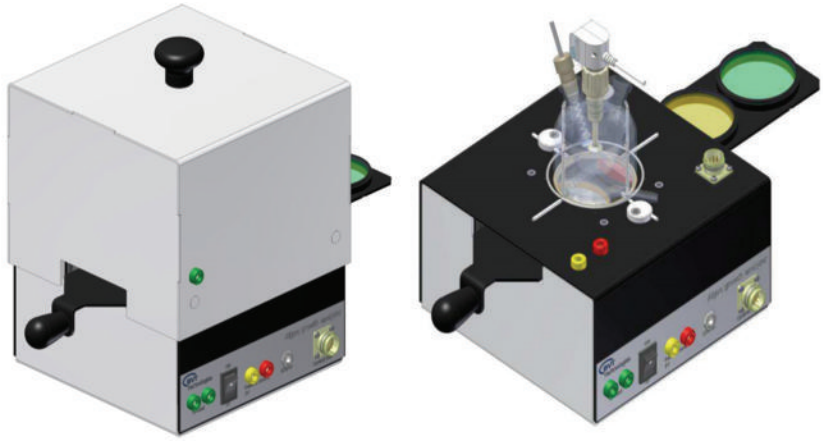

Figure 2: Algae growth analyzer.

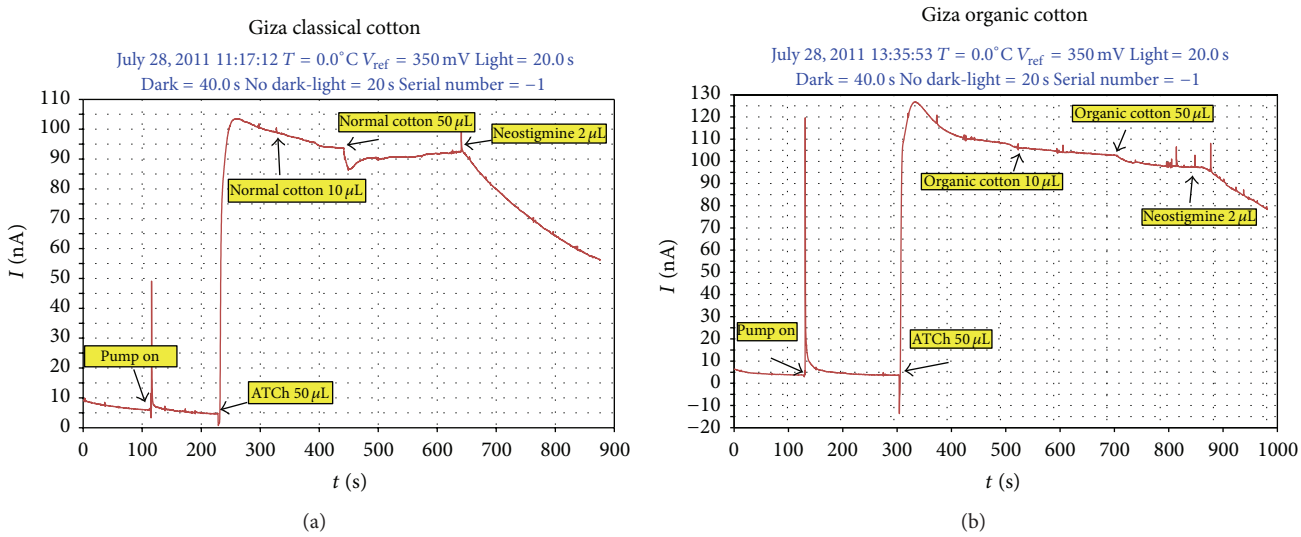

Figure 3: Enzymatic inhibition of Giza classical cotton and organic cotton.

Biosensor toxicity analyzer (BTA) works on the above-mentioned principle and monitors the activity of the inhibition of AChE with the help of sensors which are equipped with an enzymatic membrane of AChE enzyme which is immobilized.

It consists of two major parts, one of which is the microflow unit and the other is Bioanalyzer. The micro flow unit has the capillary arrangement which allows precise and constant flow of the liquid onto the active surface of the AChE sensor for a high level of repeatability and sensitivity in the measurements. The module has an integrated chamber in which the sensor can easily be placed or replaced as shown in Figure 1.

2.2. Principle of Algae Growth Analyzer. Algae growth analyzer is universal device enabling us to follow the lifecycle of algae or other biological objects producing oxygen. The device bears light source, exchangeable color filters, sensitive oxygen electrode, and cover to model dark phase as shown in Figure 2. It is controlled by Bioanalyzer potentiostat that allows user to program light and dark phases, measure, and evaluate the oxygen electrode response. The device provides faster analogy of DIN 863 toxicity test that takes about 1 hour.

Initially, calibration of the device is done with 1 gm Na_2SO_4 and 5 mL distilled water to consume all the oxygen inside the glass cell repeatedly for three times. Then, it is washed with distilled water for three times.

As all the resulted extracts were extracted by the solvent, acetonitrile, so as to ignore the impact of solvent on the communication of analytes with algae, this solvent was evaporated completely at room temperature, and then, the pure extracts were treated directly with 5 mL algae samples in Petri dishes. We allowed them to cultivate for one hour, and then, the samples were tested in algae growth analyzer.

3. Results and Conclusions

The results of the enzymatic inhibition are shown in Figure 3 for Giza classical cotton and organic cotton, respectively.

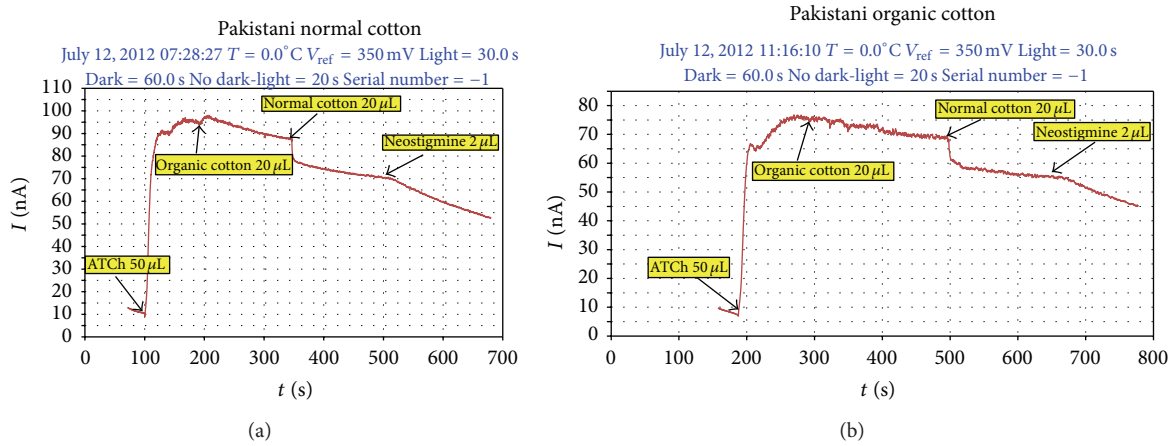

Figure 4: Enzymatic inhibition of Pakistani classical cotton and organic cotton.

In these graphs, the response of current (nanoamperes) is on y-axis, and the time (seconds) is on x-axis.

It can be observed that although both classical and organic cotton samples show the change in the intensity of the current, but the organic cotton sample shows more response and more inhibition in case of Egyptian cotton, whereas in case of Pakistani cotton samples (Figure 4), the normal cotton shows more response and more inhibition as compared to the organic one.

Although the use of synthetic pesticides and sprays is prohibited in the cultivation of organic cotton, but the presence of these xenobiotic compounds indicates the improper storage, organic fields surrounded by the conventional cotton fields, or maybe some negligence in the organic cotton production line.

All the above-mentioned extracts were analyzed by AGA for duration of 30 minutes each. With the help of miniature oxygen electrode, we have obtained the oxygen production activity of the algae in presence of the extracts by recording the oxygen produced in medium.

The results of Giza cotton from Egypt were shown in Figure 5. There are differences in the oxygen production, but in each case the addition of extract increases the production of oxygen, whereas if we compare the classical and organic cotton, the stimulating agents in classical cotton are more, and this is the reason of increase of oxygen production. Also, it may be the possibility that the hazardous compounds in classical cotton are less than the organic one.

The results in Figure 6 contain the Pakistani classical and organic cotton. In this case, we can see that there are differences in the oxygen production with the addition of extracts, whereas if we compare the classical and organic cotton, the stimulating agents in organic cotton are more and this is the reason of increase of oxygen production.

In case of Giza cotton, the organic cotton shows the inhibitory effect on photosynthetic activity of the algae, whereas in the case of Pakistani cotton this inhibition is caused by the classical cotton.

This study is based on the development of two different methods for the detection of pesticides and hazardous

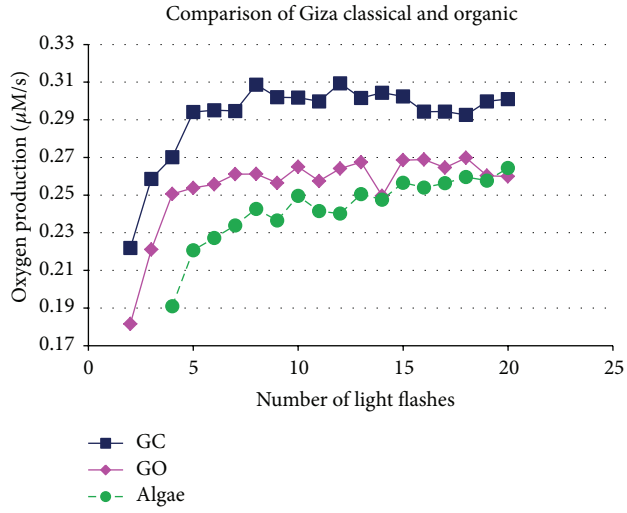

Figure 5: Comparison of Giza classical and organic cotton.

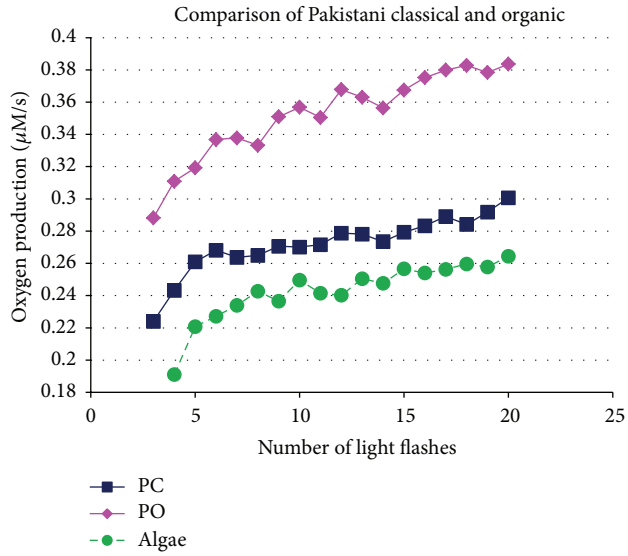

Figure 6: Comparison of Pakistani classical and organic cotton.

compounds based on acetyl cholinesterase inhibition and the monitoring of changes in the oxygen level caused by the interaction of residual analytes and the green algae, *Scenedesmus* (Chlorophyta).

Contrary to other sophisticated methods, acetyl cholinesterase inhibition test is an easier, faster, and cheaper method. It is a method that offers to different investigators an easy way to detect the presence of organo phosphorus and carbamate pesticides.

The results obtained with the laboratory algal test indicate a reasonable interaction of the analytes and the photosynthetic activity of the algae. Clearer picture of this interaction may be observed by prolonging these tests. Further research may be needed to verify the usefulness of the method presented here for the screening of pesticides on some more varieties of cotton of different regions.

Acknowledgment

The authors would like to thank Professor Dr. Ing. Zdeněk Kůs, Rector, from Technical University of Liberec, Czech Republic, for providing the grants not only to conduct these experiments but also for the presentations.

References

[1] D. Myers, "Organic cotton," in *Organic Cotton*, D. Myers, Ed., Intermediate Technology Publications Limited, London, UK, 1999.

[2] R. S. Blackburn, "Life cycle and environmental impact," in *Sustainable Cotton Production*, L. Grose, Ed., Wood Head Publishing Limited, Cambridge, UK, 2009.

[3] E. Turiel, "Sample handling of pesticides in food and environmental samples," in *Analysis of Pesticides in Food and Environmental Samples*, J. L. Tadeo, Ed., CRC Press, 2008.

[4] S. Gordon and Y. L. Hsieh, Eds., *Cotton: Science and Technology*, Wood Head Publishing Ltd, Cambridge, UK, 2007.

[5] L. Alder, K. Greulich, G. Kempe, and B. Vieth, "Residue analysis of 500 high priority pesticides: better by GC-MS or LC-MS/MS?" *Mass Spectrometry Reviews*, vol. 25, no. 6, pp. 838–865, 2006.

[6] A. Naggar, "Clinical findings and cholineste rase levels in children of organ ophosphate s and carbamates poisoning," *European Journal of Pediatrics*, vol. 168, pp. 951–956, 2009.

[7] H. Hu, X. Liu, F. Jiang, X. Yao, and X. Cui, "A novel chemiluminescence assay of organophosphorous pesticide quinalphos residue in vegetable with luminol detection," *Chemistry Central Journal*, vol. 4, no. 1, article 13, 2010.

[8] A. Mulchandani, W. Chen, P. Mulchandani, J. Wang, and K. R. Rogers, "Biosensors for direct determination of organophosphate pesticides," *Biosensors and Bioelectronics*, vol. 16, no. 4-5, pp. 225–230, 2001.

[9] M. L. Hannam, J. A. Hagger, M. B. Jones, and T. S. Galloway, "Characterisation of esterases as potential biomarkers of pesticide exposure in the lugworm *Arenicola marina* (Annelida: Polychaeta)," *Environmental Pollution*, vol. 152, no. 2, pp. 342–350, 2008.

[10] P. Mulchandani, A. Mulchandani, I. Kaneva, and W. Chen, "Biosensor for direct determination of organophosphate nerve agents—1. Potentiometric enzyme electrode," *Biosensors and Bioelectronics*, vol. 14, no. 1, pp. 77–85, 1999.

[11] R. P. Deo, J. Wang, I. Block et al., "Determination of organophosphate pesticides at a carbon nanotube/organophosphorus hydrolase electrochemical biosensor," *Analytica Chimica Acta*, vol. 530, no. 2, pp. 185–189, 2005.

[12] D. G. Buerk, *Biosensors: Theory and Applications*, Technomic Publishing Company, 1995.

[13] A. Arvinte, "Development of a pesticides biosensor using carbon-based electrode systems," in *Chemicals as Intentional and Accidental Global Environmental Threats*, L. Simeonov and E. Chirila, Eds., pp. 337–343, Springer, 2006.

[14] J. Ma, "Differential sensitivity to 30 herbicides among populations of two green algae *Scenedesmus obliquus* and *Chlorella pyrenoidosa*," *Bulletin of Environmental Contamination and Toxicology*, vol. 68, no. 2, pp. 275–281, 2002.

[15] S. Sánchez-Fortún, F. Marvá, A. D'Ors, and E. Costas, "Inhibition of growth and photosynthesis of selected green microalgae as tools to evaluate toxicity of dodecylethyldimethylammonium bromide," *Ecotoxicology*, vol. 17, no. 4, pp. 229–234, 2008.

[16] L. Barsanti and P. Gualtieri, *Algae Anatomy, Biochemistry, and Biotechnology*, CRC Press, Boca Raton, Fla, USA, 2006.

[17] K. Rogers, Ed., *Fungi, Algae AND Protists*, Britannica Educational Publishing, New York, NY, USA, 1st edition, 2011.

[18] Z. Perrine, S. Negi, and R. T. Sayre, "Optimization of photosynthetic light energy utilization by microalgae," *Algal Research*, vol. 1, no. 2, pp. 134–142, 2012.

[19] D. Chapman, Ed., *Water Quality Assessments*, E & Fn Spon, London, UK, 2nd edition, 1996.

[20] M. Edwards, *Green Algae Strategy End Oil Imports and Engineer Sustainable Food and Fuel*, Mark R. Edwards, Tempe, Ariz, USA, 2008.

[21] M. D. Ferrando, E. Sancho, and E. Andreu-Moliner, "Chronic toxicity of fenitrothion to an algae (*Nannochloris oculata*), a rotifer (*Brachionus calyciflorus*), and the cladoceran (*Daphnia magna*)," *Ecotoxicology and Environmental Safety*, vol. 35, no. 2, pp. 112–120, 1996.

[22] J. Ma, R. Zheng, L. Xu, and S. Wang, "Differential sensitivity of two green algae, *Scenedesmus obliqnus* and *Chlorella pyrenoidosa*, to 12 pesticides," *Ecotoxicology and Environmental Safety*, vol. 52, no. 1, pp. 57–61, 2002.

[23] K. J. Buhl, S. J. Hamilton, and J. C. Schmulbach, "Chronic toxicity of the bromoxynil formulation Buctril to *Daphnia magna* exposed continuously and intermittently," *Archives of Environmental Contamination and Toxicology*, vol. 25, no. 2, pp. 152–159, 1993.

[24] J. L. Tadeo, "Pesticides: classification and properties," in *Analysis of Pesticides in Food and Environmental Samples*, J. L. Tadeo, Ed., CRC Press, 2008.

[25] A. Mulchandani and R. Rajesh, "Microbial biosensors for organophosphate pesticides," *Applied Biochemistry and Biotechnology*, vol. 165, no. 2, pp. 687–699, 2011.

Hindawi Publishing Corporation
Conference Papers in Materials Science
Volume 2013, Article ID 956072, 6 pages
http://dx.doi.org/10.1155/2013/956072

Conference Paper

Influence of Hydroxyethyl Cellulose Treatment on the Mechanical Properties of Jute Fibres, Yarns, and Composites

Ranajit K. Nag, Andrew C. Long, and Michael J. Clifford

Faculty of Engineering, University of Nottingham, Nottingham NG7 2RD, UK

Correspondence should be addressed to Ranajit K. Nag; emxnr1@nottingham.ac.uk

Received 2 August 2013; Accepted 8 September 2013

Academic Editors: R. Fangueiro and H. Hong

This Conference Paper is based on a presentation given by Ranajit K. Nag at "International Conference on Natural Fibers—Sustainable Materials for Advanced Applications 2013" held from 9 June 2013 to 11 June 2013 in Guimarães, Portugal.

Jute yarns were treated by tap water with and without tension at room temperature for 20 minutes and then dried. Fibre and yarn strength were measured before and after treatment. Unidirectional (UD) composites were made by both treated and untreated yarns with and without applying hydroxyethyl cellulose (HEC) as size material. Water-treated jute yarns without tension and composites made of those yarns showed decreased strength, and water treated jute yarns with tension and composites made of those yarns showed increased strength with respect to raw yarns and composites made of raw yarns. However, no specific trend was noticed for fibre tensile strength and tensile modulus. HEC sized yarns showed up to 12% higher failure load with respect to unsized yarns, and composites made of HEC sized yarns showed up to 17% and 12% increase in tensile strength and tensile modulus, respectively, compared to composites made of similar types of unsized yarns.

1. Introduction

Cellulose-based fibres can be an ideal source of reinforcement material for composite production due to their abundant production and supply. Cellulose fibres are plant-based, and nearly 1000 types of plants produce useable cellulose fibres [1]. Each year plants produce about 180 billion tons of cellulose around the world [2]. Cellulose has excellent specific properties (tensile modulus 138 GPa and tensile strength >2 GPa [3]). However, natural fibre composites (NFC) suffer some limitations such as lower tensile and impact strength [4]. Plant-based fibres contain different quantity of cellulose (Table 1 [1]). Cotton contains a very high percentage of cellulose, and it secures the first position according to production among the important cellulosic fibres. However, it has limited use in composite production due to moderate mechanical properties [5] and high level of ecological impact for cultivation of cotton [6]. Cultivation of jute needs little or no fertilizer and almost no use of pesticides. Jute is a cheap fibre, and the position of jute is second according to yearly production worldwide (Table 1) among important usable cellulosic fibres. It has very good mechanical properties (tensile modulus 32 GPa and tensile strength 550 MPa [7]) and has the versatility to use in different textile preforms. All these attractive properties developed interest to choose jute fibre for this research work.

All natural fibres are discontinuous except silk, which makes them challenging to use directly for composite production. Therefore, a preform is helpful to use staple natural fibres in composite manufacture. Different textile preforms such as yarn [8], nonwoven fabric [9], woven fabric [10], knitted fabric [11], multiaxial fabric [12], and 3D fabric [13] are very common for composite production. To explore the strength of reinforcement in composites, proper alignment of fibre is very important [8]. Among different types of preforms, unidirectional (UD) fibre matt gives better alignment of fibres [8]. Textile yarn is generally used to make the UD fibre matt. Sewing, use of adhesive, and lino weaving may be some possible ways of forming UD matt from textile yarn. In this work hydroxyethyl cellulose (HEC), an adhesive material, was used to bind the UD matt. It is a natural cellulose-based product which is soluble in water. It is cheap, nontoxic, and

Table 1: Annual production of some of the commercially important fibre sources and their chemical composition [1].

Fibre type	World annual production (10^3 Tonnes)	Cellulose %	Hemicellulose %	Lignin %	Pectin %
Cotton	18,450	92	6	—	<1
Jute	2,850	72	13	13	
Flax	830	81	14	3	4
Sisal	378	73	13	11	2
Hemp	214	74	18	4	1
Coir	650	43	<1	45	4
Ramie	170	76	15	1	2
Straw	—	40	28	17	8
Kapok	123	13			

easy to apply [4]. Stirring by mechanical stirrer for 10 minutes gives a homogenous viscous solution to use as binding material. Before applying this binding material extensively, it is important to investigate its effect on composite properties.

Natural fibre composites (NFC) are now used for non-structural or semistructural purposes and find limited use in structural application. To improve mechanical properties, researchers have studied fibre surface modification, matrix modification, and the use of coupling agents [14]. Among these well-established methods, physical or chemical fibre surface modification is very popular. Physical methods include stretching, calendaring, thermal treatment [14], and production of hybrid yarns [15]; chemical treatments include alkali treatment and the use of coupling agents [16]. To perform chemical treatment on natural fibre, researchers normally treat it in a water-based chemical solution. As water-based treatments are popular, it is very important to understand if there is any effect on natural fibre composites due to water treatment under different conditions.

2. Materials and Methods

2.1. Materials. In this experimental work, tossa jute yarn was used, supplied by Janata Sadat Jute Mills Ltd., Bangladesh. Unsaturated polyester, trade name polylite 420-100 by Reichhold UK Ltd., was used as the matrix material.

2.2. Preparation of Yarn for Water Treatment, Sizing, and Composites. Yarns were lightly wound on a perforated plastic tube under tension neither to allow any slackness nor to apply any stretching. Yarn winding tension was approximately 1.5 gm/Tex. After water treatment, these yarns were described as water-treated yarn with tension. Loose yarns dipped in water were described as water-treated yarn without tension. All yarns to be sized were wrapped closely together on a plastic sheet in a single ply. Sizing enabled yarns to form UD matt. UD matt of unsized yarns was made by wrapping it on a square steel frame. The dimension of the frame was 260 mm × 260 mm × 1 mm. Width of the arms of frame was 10 mm, and yarns were wrapped on it closely together. Care was taken to avoid under tension or overtension to minimise any slack and to avoid stretching of the yarns.

2.3. Water Treatment. Loose yarns and yarns wrapped on the perforated tube were dipped in tap water at room temperature for 20 minutes. Yarns were then taken out of the water bath, squeezed and pressed gently, and dried in an oven at 105°C for one hour.

2.4. HEC Sizing. HEC solution was made with 0.6% HEC (*w/w*) with tap water. A homogenous solution was made with the help of a mechanical stirrer. Stirring was done for 10 minutes at 200 revolutions per minute. This solution was then applied to the wrapped yarns on plastic sheet by brush. Yarns were then dried at 105°C for one hour.

2.5. Preparation of Composites. Vacuum assisted resin transfer moulding (VARTM) was used to manufacture composites in this work. In VARTM, resin is infused in a closed mould with vacuum which helps to avoid trapped air bubbles. Fibre volume fraction and dimensions of the composite plaque can be closely controlled. This is a compatible and relatively cheap method for infusing long fibre like jute. Considering the advantages, VARTM was chosen.

UD matt of sized yarn was cut according to the inside dimension of a picture frame (250 mm × 250 mm), and the weight of the UD yarn sheet was measured to calculate fibre volume fraction. Unsized yarns were infused whilst wrapped on the frame. A different inside dimension (260 mm × 260 mm) picture frame was used to form the edge of the mould. 0.20% (by weight) accelerator NL-49P (cobalt (11) (2-ethylhexanoate) 1% CO in diisobutyl phthalate) and 0.8% (by weight) butanox catalyst (methyl ethyl ketone peroxide 35% in phthalate plasticizer) were mixed with resin.

In this experiment, first accelerator was mixed with resin with a hand stirrer and then catalyst to avoid any accident. After infusion the tool was closed overnight for cure. The composite plaque was then postcured for 6 hours at 60°C inside an oven. To avoid any sort of deformation during postcuring, the composite plaque was placed between two pieces of glass fibre composite with some weight added to it.

2.6. Single Fibre Preparation for Tensile Test. Single jute fibre extracted from yarns was attached on a rectangular paper frame with araldite adhesive. The dimension of the paper

frame was 35 mm × 20 mm. A rectangular hole having dimension 25 mm × 10 mm was cut inside the paper frame with reference to BS ISO 11566: 1996. The diameter of each fibre was measured using an optical microscope. The diameter was measured at three places (both the ends and middle) of each fibre to be tested, and the mean value was taken as the effective fibre diameter. Practically, the width was considered as fibre diameter assuming that the fibre has circular cross-section.

3. Testing

3.1. Single Fibre Tensile Test. Single fibres were tested in tension according to BS ISO 11566: 1996. The fibre attached on rectangular paper with araldite was mounted to the jaws of a Hounsfield machine. Vertical arms of the rectangle were burnt carefully by an electric burner after mounting. 5N load cell was used with 1 mm extension/min. Load and extension were then recorded up to failure. 25 specimens were tested for each sample. Mean values were calculated for tensile strength and tensile modulus.

3.2. Single Yarn Tensile Test. HEC sized and unsized raw yarns and water treated yarns with and without tension were used for tensile testing. This test was done with reference to BS ISO 3341: 2000. The specimen length was 250 mm, and the result was calculated from 10 tests.

3.3. Composite Test. The tensile tests for composites were carried out with reference to BS EN ISO 527-4: 1997. Plaques were tested along the longitudinal direction of yarn. The dimension of sample for tensile test was 250 mm × 15 mm. After cutting the composite plaque to the required size for testing, both cut edges were polished by sand paper. Then, width and thickness of the composite strip were measured at three places (both the ends and middle) to find the mean value of width as well as thickness of the strip, to calculate the stress. Strain was measured by using an extensometer. 50 KN load cell was used, and the rate of extension was 1 mm/min. 5 tests were done for each sample to calculate the mean values of tensile strength and tensile modulus. Tensile modulus was calculated at 0.025 to 0.1 percent strain range, as this region exhibited the highest value of stiffness for plant-based composites [4].

4. Results and Discussion

4.1. Fibre Test Result. Tensile strength and stiffness of single jute fibres are presented in Figures 1 and 2, respectively. These results did not show any specific trend; however, a large value of standard deviation was noticed in all cases. Experimental results showed that the surface treatment studied in this research work did not affect the tensile properties of jute fibre. High values of standard deviation may be due to inherent properties of single jute fibres [17].

A large variation of jute fibre diameter, tensile strength, and tensile modulus has been observed in previous studies [7, 18].

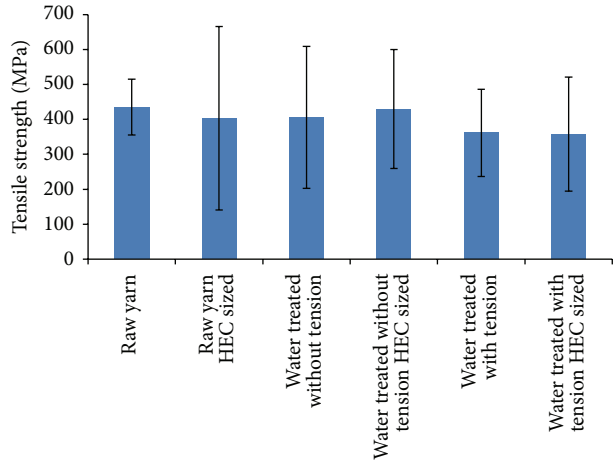

Figure 1: Tensile strength of single jute fibre (error bars indicate standard deviation).

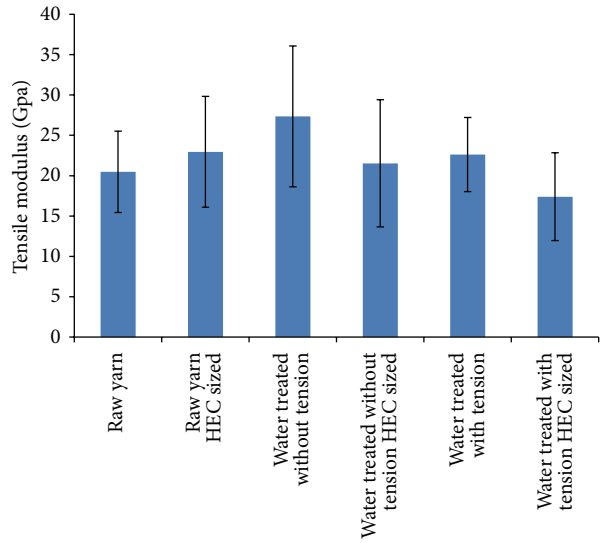

Figure 2: Tensile modulus of single jute fibre (error bars indicate standard deviation).

4.2. Yarn Test Result. Yarn test results (Figure 3) showed an increase in failure load for HEC sized yarn apart from respective unsized yarn. This is a well-cited [19, 20] phenomenon since the size material has an adhesive property which binds fibres in the yarn close together (Figures 4, 5, and 6) making the yarn stronger. However, HEC sized raw yarn did not show any increase in failure load. This may be due to some deficiencies such as variations in linear density, incursion of faults, variation of fibre quality, or impurities in the yarn. A decrease in yarn failure load was found for water-treated yarn without tension, whilst water-treated yarn with tension showed an increase in failure load with respect to raw yarn. This behaviour may be due to some reorientation of fibres in the yarn as a result of water treatment. The jute spinning process involves a series of operations including drawing, drafting, and twisting. All of these operations induce a level of stretching on fibres, and stretched fibres tend to relax

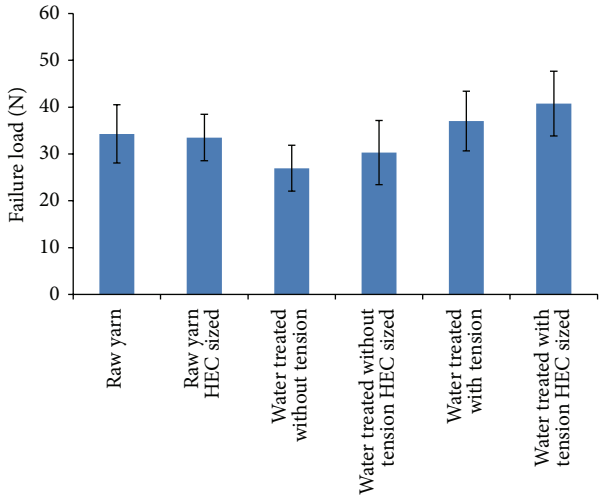

Figure 3: Failure load of single jute yarn (error bars indicate standard deviation).

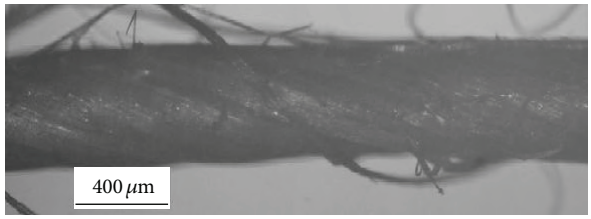

Figure 4: Water-treated yarn without tension and HEC sized.

Figure 5: Raw yarn HEC sized.

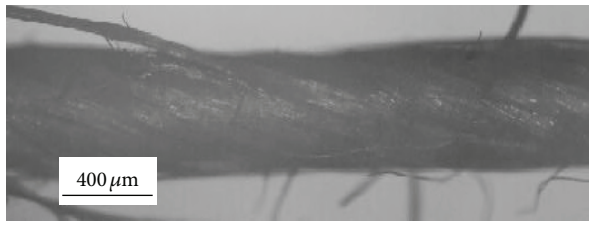

Figure 6: Water-treated yarn with tension.

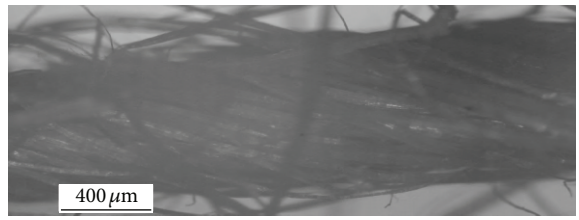

Figure 7: Water-treated yarn without tension.

Figure 8: Raw yarn.

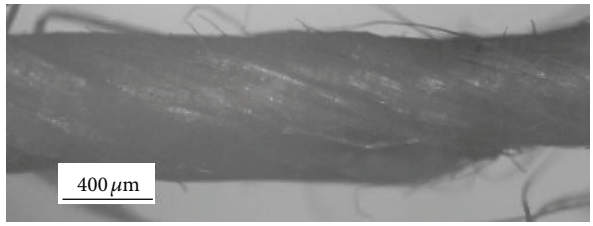

Figure 9: Water-treated yarn with tension.

when load is removed. Dipping yarn without tension in water enabled fibres to achieve this relaxed state, and at this stage fibres shrank but all fibres did not shrink to the same extent, and the result was an open structure yarn (Figure 7) with respect to raw yarn (Figure 8), and yarn also got wavy configuration. Due to this open structure, cohesive force reduced, and this may be the reason for the lower yarn failure load for water-treated yarn without tension. During water treatment of yarn under tension (Figure 9), yarns could not shrink, but tendency to shrink may have helped fibres to become oriented towards the yarn axis which increased yarn failure load.

4.3. Composites Test Result. From the test results good correlation was found between failure load of yarn and tensile strength of composites, supporting the observations by other researchers [21] that composites follow the yarn property rather than fibre property. Composites made of sized yarns showed 9–17% higher tensile strength (Figure 10) and 5–10% higher tensile modulus (Figure 11) with respect to composites made of the same type of unsized yarns. Use of sizing material increased the strength of yarns, and stronger yarns produced stronger composites. As mentioned earlier, water-treated yarns without tension exhibited an open structure as well as a wavy configuration. Composites made of these yarns without applying HEC size showed 10% lower tensile strength (Figure 10) and 11% lower tensile modulus (Figure 11) with respect to composites made of raw yarns. The change in yarn structure affected the alignment of fibres in the yarn, and fibres became wavy and curly, which may have reduced composite properties. Composites made of water-treated yarns applying tension but no HEC size showed 7% higher

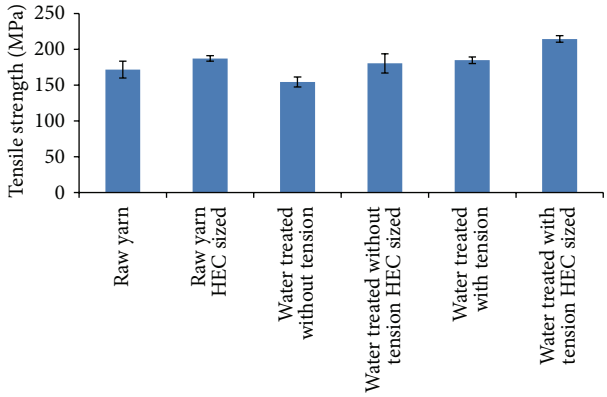

Figure 10: Tensile strength of composites (error bars indicate standard deviation).

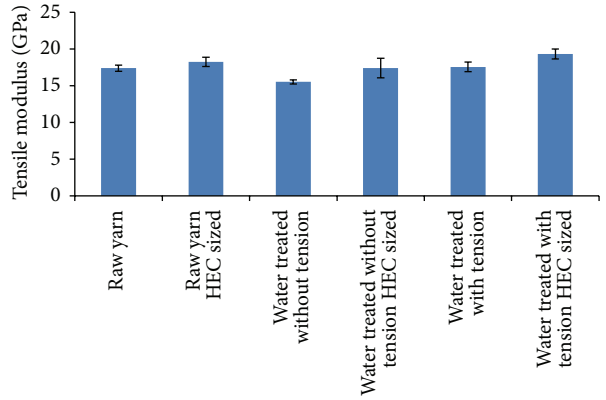

Figure 11: Tensile modulus of composites (error bars indicate standard deviation).

tensile strength (Figure 10) and 1% higher tensile modulus (Figure 11) with respect to composites made of raw yarns. As mentioned earlier, due to application of tension during yarn wetting, fibres may aligned better towards yarn axis, and composites made of these yarns showed higher tensile properties.

5. Conclusion

Application of HEC size and water treatment had no effect on the properties of jute fibre.

All types of HEC sized yarn studied in this research showed higher failure load with respect to similar types of unsized yarn. Water treatment of jute yarn without tension reduced yarn failure load, and water treated yarn under tension showed higher failure load with respect to raw yarn.

Composites made of HEC sized yarn showed higher tensile strength and tensile modulus in all cases with respect to composites made of similar types of unsized yarn. Composites made of water treated yarn without tension showed lower tensile strength and tensile modulus, and composites made of water-treated yarn with tension showed higher tensile strength and tensile modulus with respect to composites made of raw yarn. This behaviour is very important for water-based chemical treatment of natural textile yarn for composite manufacture. As yarn properties and composites properties are affected due to wetting yarn with and without tension.

Acknowledgment

This research is funded by "Bangabandhu Fellowship on Science and ICT," Government of Bangladesh. The authors are grateful to this funding authority.

References

[1] L. Y. Mwaikambo and M. P. Ansell, "Chemical modification of hemp, sisal, jute, and kapok fibers by alkalization," *Journal of Applied Polymer Science*, vol. 84, no. 12, pp. 2222–2234, 2002.

[2] R. A. Festucci-Buselli, W. C. Otoni, and C. P. Joshi, "Structure, organization, and functions of cellulose synthase complexes in higher plants," *Brazilian Journal of Plant Physiology*, vol. 19, no. 1, pp. 1–13, 2007.

[3] K. L. Pickering, *Properties and Performance of Natural Fibre Composites*, Woodhead Publishing Limited, 2008.

[4] D. U. Shah, P. J. Schubel, P. Licence, and M. J. Clifford, "Hydroxyethylcellulose surface treatment of natural fibres: the new "twist" in yarn preparation and optimization for composites applicability," *Journal of Materials Science*, vol. 47, no. 6, pp. 2700–2711, 2012.

[5] H. Lilholt and J. M. Lawther, "Natural organic fibres," in *Comprehensive Composite Materials (6 vols.)*, A. Kelly and C. Zweben, Eds., vol. 1, chapter 10, pp. 303–325, Elsevier Science, 2000.

[6] R. Robinson, *The Great Book of Hemp*, Park Street Press, South Paris, Me, USA, 1996.

[7] A. S. Virk, W. Hall, and J. Summerscales, "Multiple data set (MDS) weak-link scaling analysis of jute fibres," *Composites A*, vol. 40, no. 11, pp. 1764–1771, 2009.

[8] B. Madsen, P. Hoffmeyer, and H. Lilholt, "Hemp yarn reinforced composites—II. Tensile properties," *Composites A*, vol. 38, no. 10, pp. 2204–2215, 2007.

[9] N. D. Yilmaz, N. B. Powell, P. Banks-Lee, and S. Michielsen, "Multi-fiber needle-punched nonwoven composites: effects of heat treatment on sound absorption performance," *Journal of Industrial Textiles*, pp. 1–16, 2012.

[10] N. A. Fleck, P. M. Jelf, and P. T. Curtis, "Compressive failure of laminated and woven composites," *Journal of Composites Technology and Research*, vol. 17, no. 3, pp. 212–220, 1995.

[11] D. Falconneta, P. E. Bourbana, S. Panditab, J. A. E. Månson, and I. Verpoest, "Fracture toughness of weft-knitted fabric composites," *Composites B*, vol. 33, pp. 579–588, 2002.

[12] Y. Wang, "Mechanical properties of stitched multiaxial fabric reinforced composites from mannual layup process," *Applied Composite Materials*, vol. 9, no. 2, pp. 81–97, 2002.

[13] L. Ciobanu, "Development of 3D knitted fabrics for advanced composite materials," in *Advances in Composites Materials Ecodesign and Analysis*, B. Attaf, Ed., pp. 161–192, 2011.

[14] A. K. Bledzki and J. Gassan, "Composites reinforced with cellulose based fibres," *Progress in Polymer Science*, vol. 24, no. 2, pp. 221–274, 1999.

[15] H. Gu and L. Liyan, "Research on properties of thermoplastic composites reinforced by flax fabrics," *Materials and Design*, vol. 29, no. 5, pp. 1075–1079, 2008.

[16] M. M. Thwe and K. Liao, "Tensile behaviour of modified bamboo-glass fibre reinforced hybrid composites," *Plastics, Rubber and Composites*, vol. 31, no. 10, pp. 422–431, 2002.

[17] H. S. Sen, "Quality improvement in jute and kenaf fibre," in *Proceedings of the International Conference on Prospects of Jute & Kenaf as Natural Fibres*, International Jute Study Group, Dhaka, Bangladesh, February 2009.

[18] J. Summerscales, W. Hall, and A. S. Virk, "A fibre diameter distribution factor (FDDF) for natural fibre composites," *Journal of Materials Science*, vol. 46, no. 17, pp. 5875–5880, 2011.

[19] W. T. Schreiber, M. N. V. Geib, and O. C. Moore, "Effect of sizing, weaving, and abrasion on the physical properties of cotton yarn," *Journal of Research of the National Bureau of Standards*, vol. 18, pp. 559–563, 1937.

[20] Ž. Penava and S. Kovačević, "Impact of sizing on physico-mechanical properties of yarn," *Fibres & Textiles in Eastern Europe*, vol. 4, no. 48, pp. 32–36, 2004.

[21] B. Madsen, P. Hoffmeyer, A. B. Thomsen, and H. Lilholt, "Hemp yarn reinforced composites—I. Yarn characteristics," *Composites A*, vol. 38, no. 10, pp. 2194–2203, 2007.

Hindawi Publishing Corporation
Conference Papers in Materials Science
Volume 2013, Article ID 878014, 7 pages
http://dx.doi.org/10.1155/2013/878014

Conference Paper

Microstructural Characterization of Natural Fibers: *Etlingera elatior*, *Costus comosus*, and *Heliconia bihai*

Cláudia I. T. Navarro, Sidnei Paciornik, and José R. M. d'Almeida

Materials Engineering Department, Pontifícia Universidade Católica do Rio de Janeiro, Rua Marquês de São Vicente, 225 Gãvea, 22451-900 Rio de Janeiro, RJ, Brazil

Correspondence should be addressed to José R. M. d'Almeida; dalmeida@puc-rio.br

Received 1 August 2013; Accepted 8 September 2013

Academic Editors: R. Fangueiro and H. Hong

This Conference Paper is based on a presentation given by José R. M. d'Almeida at "International Conference on Natural Fibers—Sustainable Materials for Advanced Applications 2013" held from 9 June 2013 to 11 June 2013 in Guimarães, Portugal.

This work describes the structural and morphological characteristics of fibers obtained from the stem of three ornamental plants, namely, *Etlingera elatior*, *Costus comosus*, and *Heliconia bihai*. The stems of these plants are long and nowadays do not have any use, being disregarded. The results obtained showed that the three fibers have a crystalline index of around 58% and are thermally stable to approximately 230°C, 240°C, and 255°C for *E. elatior*, *C. comosus*, and *H. bihai*, respectively. The fibers present an average humidity amount of less than 9% and the thermal degradation peak for the cellulose component varies from 358°C for *E. elatior* to 379°C for *C. comosus*. The morphological analysis showed that the fibers present a large variability of the shape of their cross-sections, which are preferentially elongated. These morphological characteristics were used to estimate the error made when one considers the fibers having a circular cross-section.

1. Introduction

From very ancient times natural fibers were used in several applications, such as sacks, but starting at the middle of the XX century they began to be largely replaced by synthetic fibers. These man-made fibers present several advantages such as uniformity of properties, including the mechanical ones. However, the increasingly concern of the society with a sustainable development promoted a come back to lignocellulosic materials, and today natural fibers are replacing synthetic ones, such as glass fibers, for example, at the automotive industry [1].

In fact, lignocellulosic fibers are a very attractive option both economically and ecologically, since they are not toxic, have normally a low price, have low density, and are less abrasive to the molds and processing equipment. Besides, they consume less energy to be produced and are biodegradable and neutral with respect to CO_2 emission [2].

Although one can cite several advantages, as above, the use of lignocellulosic fibers also presents several disadvantages. One can highlight the hydrophilic behavior of these fibers, which can hinder the fiber to matrix adhesion, once several common polymeric matrices are hydrophobic in character. Also, the hydrophilic nature of the lignocellulosic fibers can contribute to fast humidity absorption, leading to a consequent loss of dimensional stability of the manufactured part.

Another disadvantage of using lignocellulosic fibers is the intrinsic variability of their properties, due to several causes, encompassing variables ranging from the age of the plant and its harvesting time, to soil fertility and weather variations. Besides, due to the fact that they have a natural origin, the cross-section shape and size can largely vary from fiber to fiber and also along the length of a single fiber. This is an important aspect, since it is usual to determine a typical fiber "diameter" and to assume that the fibers have a circular

Figure 1: Procedure used to obtain sharp cross-section. After soaking the fibers in water, the use of a doctor blade enables a cut without deformation artifacts due to the cutting procedure.

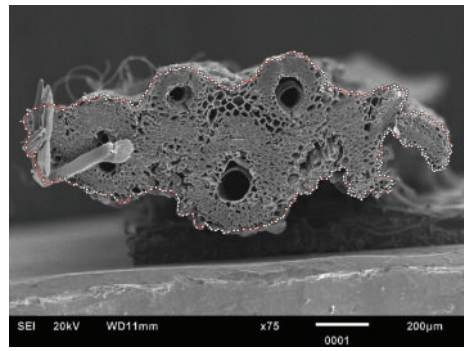

Figure 2: Manual outline of the fiber's perimeter. Example for a *C. comosus* fiber.

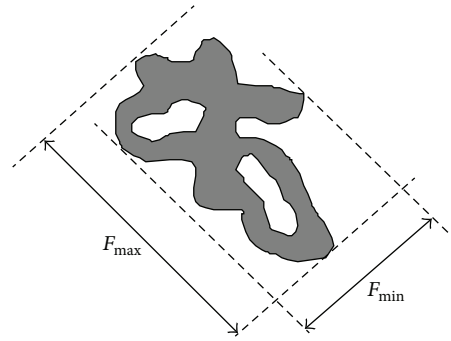

Figure 3: Definition of the size parameters of an object.

cross-section when one wants to characterize the cross-section of a lignocellulosic fiber [3]. This approach can be a crude one and can have influence on the evaluation of the mechanical properties of the fibers, since it can generate cross-section areas far apart from the real ones [4–6].

Besides the more common lignocellulosic fibers, largely studied and in many instances already used in several commercial products, such as jute (*Corchorus capsularis*), sisal (*Agave sisalana*), and flax (*Linum usitatissimum*), several other less common fibers also have a great potential to be used as reinforcement in polymer matrix composites. Less common fibers here meaning fibers that are not yet largely exploited due to being restrict to a certain ecosystem and/or region or simply because they are only obtained as a by-product of other harvests. Several examples can be cited here, such as fibers extracted from palms (piassava (*Attalea funifera*) [7] or *Borassus flabellifer* [8]) or from other plants (e.g., from *Urtica dioica* [9]). Another source of lignocellulosic fibers is the vast market of ornamental plants and flowers. In Brazil this is a growing market with a financial turnover amounting around 2.2 billion dollars per year. As many ornamental plants have stalks as long as 1.5 m and since only their top part is commercialized, the leftover residues have a great potential to be processed to obtain long or short fibers that can be used as reinforcement in polymer matrix composites.

In this work the structural and morphological characteristics of fibers obtained from three ornamental plants (*Etlingera elatior*, *Costus comosus*, and *Heliconia bihai*) are studied. The morphological aspects of the fibers were studied by both scanning electron microscopy and digital image analysis, and the structural characteristics were accessed by X-rays diffraction and thermogravimetric analysis. Special emphasis was given to the digital image analysis technique to characterize the true cross-section shape and area of these fibers and to discuss the results obtained with those calculated considering the fibers as with a circular and uniform cross-section.

2. Methods and Materials

The fibers used in this work came from a farm located at Rio Bonito county, RJ State, Brazil. These fibers were obtained from the leftover stems of the following ornamental plants: *Etlingera elatior*, *Costus comosus*, and *Heliconia bihai*. The common names of these plants are, respectively, torch ginger, red tower ginger, and heliconia. The fibers were obtained using a manual molasses mill. This simple device removes very efficiently the sap of the residues, has a very low energetic consume, and produces fibers as long as the processed residue. Fibers averaging about 40 mm were obtained in this work. This equipment was already successfully used to process fibers from the leftover residue of pejibaye palms [10].

These fibers were then suitably processed to the analysis to be performed. They were powdered to the thermogravimetric and X-rays diffraction analysis. The X-rays analysis was performed from $2\theta = 5^{\circ}$ to $2\theta = 80^{\circ}$, with increments of 0.02°, using Cu-$\kappa\alpha$ radiation ($\lambda = 1{,}5406$ Å). The analysis was performed using an equipment setup of 40 kV and 30 mA. The crystalline index, CI, of the fibers was calculated using the following relationship [11]:

$$\mathrm{CI} = \left[\frac{(I_{002} - I_{\mathrm{am}})}{I_{002}}\right] \times 100, \quad (1)$$

where I_{002} is the intensity of (002) plane reflection and I_{am} is the intensity of the amorphous material at $2\theta = 18^{\circ}$.

The thermogravimetric analysis was performed from 28°C e 750°C, using a heating rate of 10°C/min, N_2 atmosphere, and a gas flow of 20 mL/min. The mass of the samples ranged from 8.67 mg to 11.79 mg.

To be analyzed at the scanning electron microscope (SEM), fibers 25 mm long were used. These fibers were first

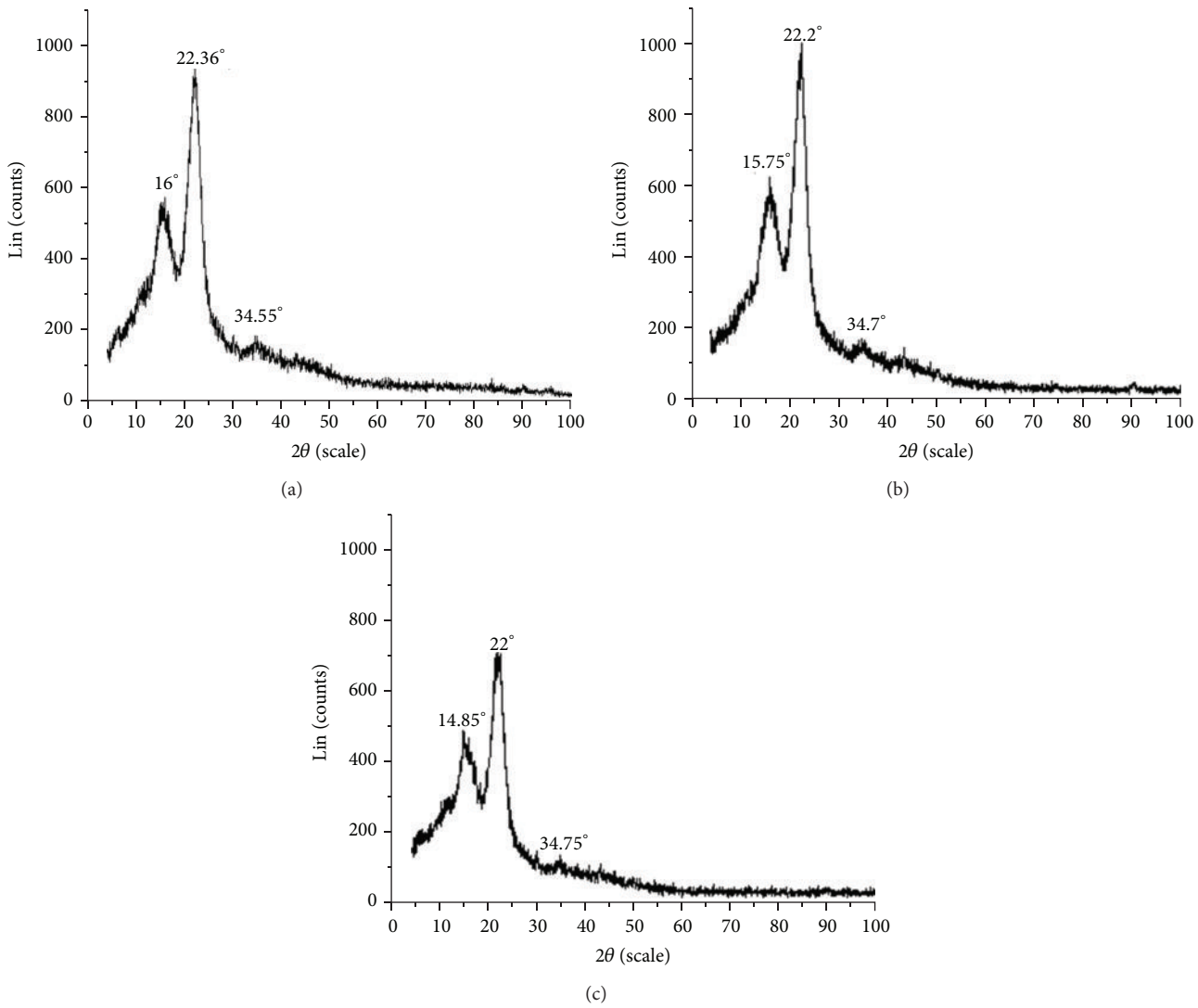

Figure 4: X-rays diffractogram of the fibers: (a) *E. elatior*; (b) *C. comosus*; and (c) *H. bihai*.

immersed in water for around 6 hours and were then cut using a doctor blade, as depicted in Figure 1. This simple procedure guarantees a smooth cross-section, without deformation artifacts usually observed when dry fibers are cut. The cut fibers were dried at 70°C ± 5°C until constant weight and were subsequently mounted vertically at a specimen holder to have their cross-section analyzed at the SEM. At this step, the fibers were individually mounted at the side of the cylindrical SEM specimen holder with a double face tape, carefully aligning them with the vertical axis of the specimen holder. This guarantees that the fibers' cross-section rests transversally to the microscope axis, since the specimen holder is perfectly aligned with this axis.

Although this was a very time-consuming step it proved to be feasible, and the cross-section of the vast majority of the fibers was at a horizontal plane perpendicular to the microscope vertical axis. Therefore, measurements errors at the fibers cross-sections geometrical parameters were minimized.

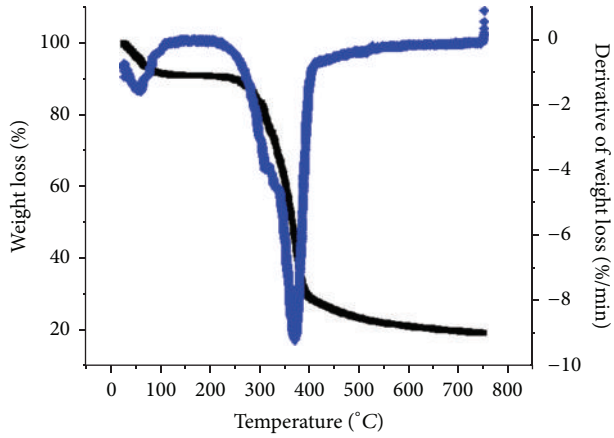

Figure 5: Thermogravimetric behavior of the *H. bihai* fiber. The same overall behavior was also observed for *E. elatior* and *C. comosus* fibers.

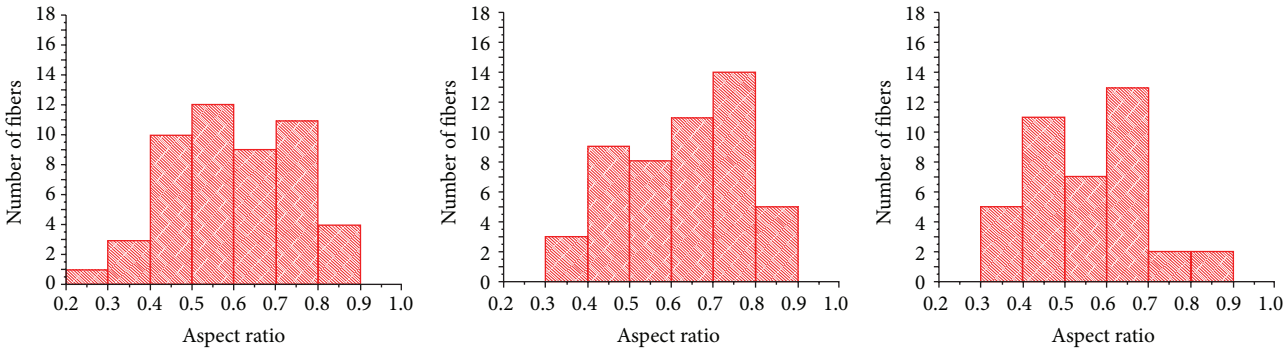

FIGURE 6: Aspect ratio histograms from (a) *E. elatior*, (b) *C. comosus,* and (c) *H. bihai* fibers.

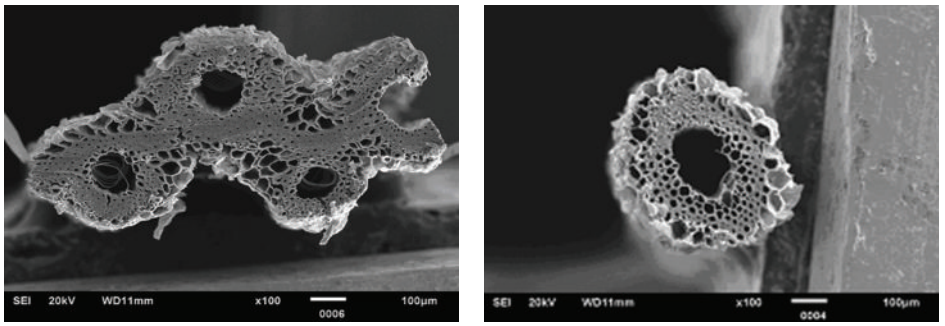

FIGURE 7: Examples of the large fibers' cross-section variability found for *C. comosus*.

SEM images were captured using a beam electron voltage of 20 kV on gold sputtered samples and at the secondary electrons imaging mode.

Digital image analysis was used to characterize the fiber cross-sections. However, due to the very irregular shape of the fibers and to the fact that their images were collected separately—one by one—it was not possible to use a completely automated analysis process, as described in a previous work [6]. Here, the first step of the digital image analysis was a manual outline of the fiber's perimeter, as shown in Figure 2. After this border was delineated all the following analyses of the fibers could be fully automated. Fifty fibers from *E. elatior* and *C. comosus* and 40 from *H. bihai* were analyzed.

The parameters used to the morphometric analysis of the fibers were the true fiber area (A_T), obtained just by counting the image pixels contained inside the outlined perimeter; the maximum and minimum calipers ($F_{\max}$) and ($F_{\min}$), corresponding, respectively, to the longest and to the shortest projection of the fiber, Figure 3 [12]; and the aspect ratio (AR) defined as the ratio between ($F_{\max}$) and ($F_{\min}$), considered as a good measure of the cross-section elongation.

The measurement of both maximum and minimum calipers has also the objective to estimate a circular area of the cross-sections, since it is a common place to assume that the fibers have a circular cross-section when traditional measurements methods, such as when micrometers or other calipers, are used. Since the image analysis methodology permits the direct measurement of the true area of the cross-section it is also possible to estimate the error commited when the maximum or the minimum calipers are used as representative measures of an "apparent fiber diameter." These errors can be calculated using the following equations [6]:

$$E_{F_{\max}} = \left| \frac{A_T - A_{F_{\max}}}{A_T} \right| \times 100,$$
$$E_{F_{\min}} = \left| \frac{A_T - A_{F_{\min}}}{A_T} \right| \times 100, \quad (2)$$

where $A_{F_{\max}}$ and $A_{F_{\min}}$ are the circular areas calculated, respectively, using $F_{\max}$ or $F_{\min}$ as the fiber diameters.

3. Results and Discussion

Figure 4 shows the results of the X-rays analysis. The spectra of the three fibers are, as expected, similar and show the presence of the three characteristic peaks of native cellulose; namely, [13, 14] (i) the peak with the highest intensity at 22.2° corresponds to the diffraction of the (002) plane; (ii) a broad peak between 14° and 16° corresponds to the diffraction of

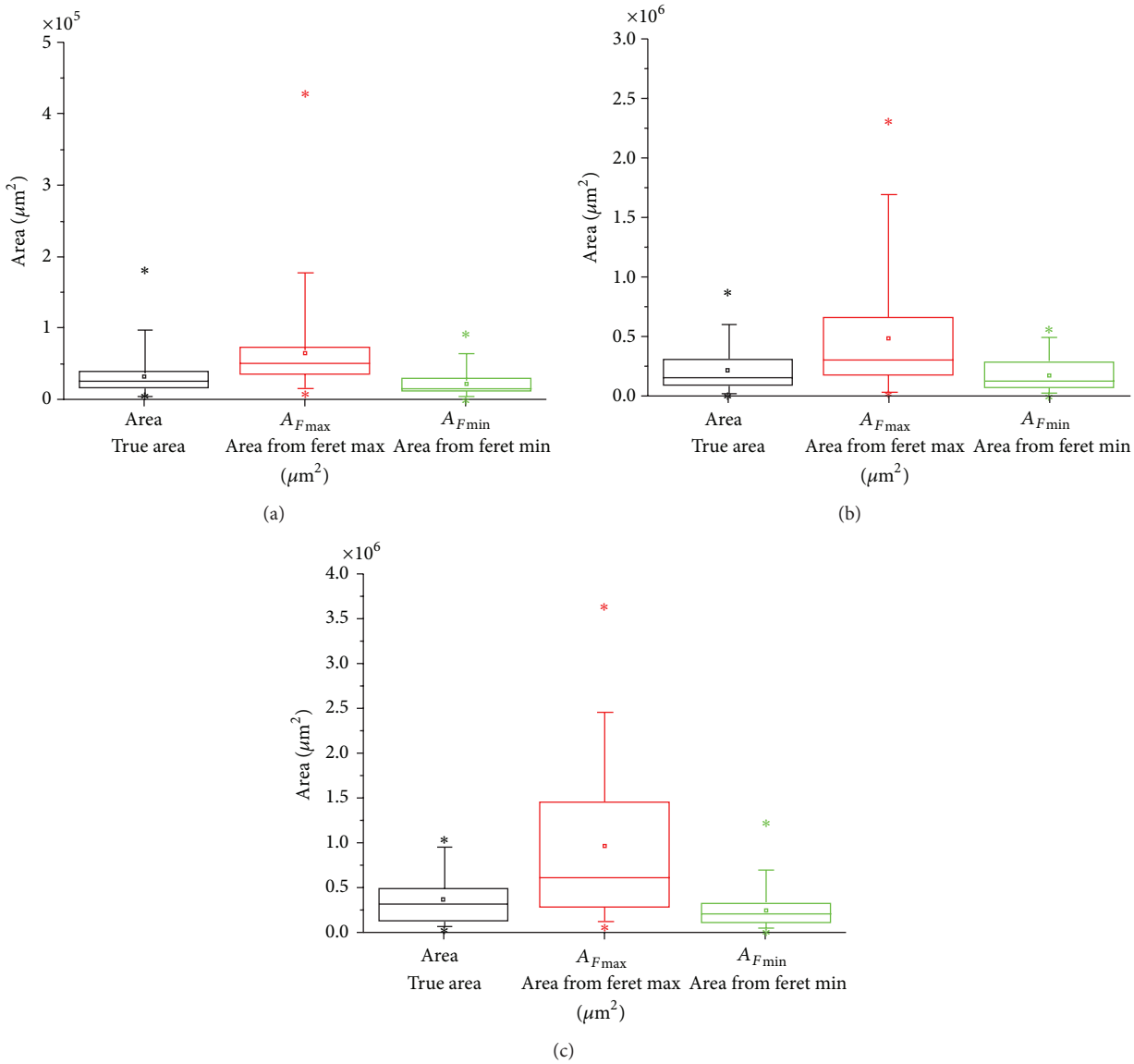

Figure 8: Comparison between the true fiber area directly measured by image analysis and the areas calculated assuming circular cross-sections: (a) *E. elatior*, (b) *C. comosus*, and (c) *H. bihai* fibers.

both (101) and (10$\bar{1}$) planes; and (iii) the peak around 34° corresponds to the (040) plane.

The crystalline index of the fibers, evaluated from (1), showed no significant statistical difference between the fibers. The values obtained were 58.5%, 57.8%, and 58.5% for, respectively, *E. elatior*, *C. comosus* and *H. bihai* fibers. These values are similar to values reported for several other lignocellulosic fibers [15].

Figure 5 shows the thermogravimetric behavior observed for the *H. bihai* fiber, and it is also representative of the behavior of the other two fibers. At the temperature range between around 30°C and 90°C there is a mass loss attributed to loss of humidity. The values measured for the three types of fibers are listed in Table 1 and agree with the values reported for several other lignocellulosic fibers [7, 16, 17].

Table 1: Humidity loss and peak temperature of the cellulose decomposition of *E. elatior*, *C. comosus,* and *H. bihai* fibers.

Fiber	Humidity loss, %	Peak temperature, °C
E. elatior	8.9	358
C. comosus	7.8	379
H. bihai	8.8	370

The onset of the thermal degradation of the fibers, defined as the temperature where a mass loss of 1% occurs at the plateau following the humidity mass loss, began at around 230°C for *E. elatior*, 240°C for *C. comosus*, and 255°C for *H. bihai*. The subsequent mass loss is mainly attributed to the thermal

Table 2: Statistical comparison between the true area and the circular areas calculated using the maximum and minimum caliper values. Student's t-test between the average values.

	Area calculated using the maximum caliper	Area calculated using the minimum caliper
E. elatior	Yes ($P = 1.8E-7$)	Yes ($P = 2.5E-6$)
C. comosus	Yes ($P = 9.4E-7$)	Yes ($P = 4.2E-5$)
H. bihai	Yes ($P = 7.1E-7$)	Yes ($P = 2.5E-5$)

95% confidence interval. Yes means a statistically significant difference.

decomposition of hemicellulose, as well as to the rupture of glycoside link of the cellulose molecule and the rupture of α and β aryl-alkyl-ether linkages originated from the thermal degradation reactions of lignin [18, 19].

The last thermal degradation step is associated to the degradation of cellulose and the value where the peak temperature of the cellulose thermal degradation occurred—obtained from the DTG curve—is also listed in Table 1. The values obtained closely agree with the values reported for the thermal degradation of cellulose from other several lignocellulosic fibers [20].

Figure 6 shows the histograms of the aspect ratio of the fibers obtained from digital image analysis results. These histograms show that the fibers' cross-section has a large variety of forms, since AR presents a large range of values. In fact, one can observe that for *E. elatior* values ranging from 0.2 to 0.9, with an average of 0.60 and a standard deviation (SD) of 0.15, were obtained. *C. comosus* fibers showed a similar trend with AR values ranging from 0.3 to 0.9, with an average of 0.63 and a SD of 0.14. *H. bihai* fibers also showed values from 0.3 to 0.9. The average value here was of 0.55 with a SD of 0.13. Figure 7 shows some cross-sections, where one can clearly observe the very different shape of the fibers. Besides, the histograms of Figure 6 show that the cross-section of the fibers is preferentially elongated, since AR values are smaller than 1. AR values approaching unity mean a more equiaxial fiber' cross-section.

In Figure 8 the graphs compare the true area, measured by image analysis, with the circular areas calculated from the minimum and maximum calipers. The Student's t-test was applied assuming a 95% confidence interval and has indicated that there exists a significant difference between the true area and the calculated circular areas for the three analyzed fibers. These results are listed in Table 2 and show that the circular area calculated both from the maximum or from the minimum caliper is statistically different from the true measured cross-section area.

The errors between the circular areas inferred using the calipers as "diameters" and the true area were calculated using (2). Therefore, for each specimen of each fiber two errors were calculated, namely, $E_{F_{max}}$ and $E_{F_{min}}$, when the maximum caliper and the minimum caliper were used, respectively. For the population of each fiber, maximum, minimum, and average values of each error were then calculated. These values are listed in Table 3, where one can see that errors as large as 300% can be generated assuming the fibers as circular objects.

Table 3: Values of $E_{F_{max}}$ and $E_{F_{min}}$ for the three fibers species.

		E. elatior	*C. comosus*	*H. bihai*
$E_{F_{max}}$ (%)	Maximum	273	267	337
	Minimum	28	37	48
	Average	108	116	142
$E_{F_{min}}$ (%)	Maximum	69	59	61
	Minimum	2	5	2
	Average	31	23	31

4. Conclusions

The thermal and structural characteristics of fibers obtained from the stems of three ornamental plants were analyzed in this work. These stems are, nowadays, considered just as waste at the economic branch represented by the flower and ornamental plants market. However, the obtained results indicate that these fibers have thermal stability and crystalline index similar to the values found for other lignocellulosic fibers already used as reinforcement in polymer matrix composites. Therefore, from their structural characteristics, these fibers are possible candidates to be used as reinforcement in composites, for example, at interior door panels.

The fibers' cross-section morphology was also analyzed, and the results indicate that the values obtained by digital image analysis can be strongly different from the ones obtained when the fibers' cross-sections are considered as circular. Determination of the aspect ratio showed that the fibers have, in fact, an elongated shape, meaning that the circular cross-section hypothesis can be a crude approximation. The image analysis approach was shown to be an important tool, since its use significantly increases the accuracy of the measurements made on each fiber, and also enhanced the statistical significance of the morphometric parameters measured, since the number of fibers analyzed can be increased without a considerable increase on the analysis time requested. This is a key point about digital image analysis, since using usual techniques involves time-consuming steps, and the number of parameters measured and/or the number of objects analyzed is usually low.

Conflict of Interests

The authors declare that there is no conflict of interests regarding the publication of this paper.

Acknowledgment

The authors acknowledge the financial support from the Brazilian Funding Agency CNPq.

References

[1] J. Holbery and D. Houston, "Natural-fiber-reinforced polymer composites in automotive applications," *JOM*, vol. 58, no. 11, pp. 80–86, 2006.

[2] A. K. Mohanty, M. Misra, and L. T. Drzal, "Sustainable bio-composites from renewable resources: opportunities and challenges in the green materials world," *Journal of Polymers and the Environment*, vol. 10, no. 1-2, pp. 19–26, 2002.

[3] C. Bergfjord and B. Holst, "A procedure for identifying textile bast fibres using microscopy: flax, nettle/ramie, hemp and jute," *Ultramicroscopy*, vol. 110, no. 9, pp. 1192–1197, 2010.

[4] J. L. Thomason, J. Carruthers, J. Kelly, and G. Johnson, "Fibre cross-section determination and variability in sisal and flax and its effects on fibre performance characterisation," *Composites Science and Technology*, vol. 71, no. 7, pp. 1008–1015, 2011.

[5] X. W. Xu and K. Jayaraman, "An image-processing system for the measurement of the dimensions of natural fibre cross-section," *International Journal of Computer Applications in Technology*, vol. 34, no. 2, p. 115, 2009.

[6] J. R. M. d'Almeida, M. H. P. Mauricio, and S. Paciornik, "Evaluation of the cross-section of lignocellulosic fibers using digital microscopy and image analysis," *Journal of Composite Materials*, vol. 46, no. 24, pp. 3057–3065, 2012.

[7] J. R. M. d'Almeida, R. C. M. P. Aquino, and S. N. Monteiro, "Tensile mechanical properties, morphological aspects and chemical characterization of piassava (*Attalea funifera*) fibers," *Composites A*, vol. 37, no. 9, pp. 1473–1479, 2006.

[8] K. O. Reddy, B. R. Guduri, and A. V. Rajulu, "Structural characterization and tensile properties of Borassus fruit fibers," *Journal of Applied Polymer Science*, vol. 114, no. 1, pp. 603–611, 2009.

[9] S. M. Mortazavi and M. K. Moghadam, "Introduction of a new vegetable fiber for textile application," *Journal of Applied Polymer Science*, vol. 113, no. 5, pp. 3307–3312, 2009.

[10] B. C. Temer and J. R. M. d'Almeida, "Characterization of the tensile behavior of Pejibaye (Bactris gasipaes) fibers," *Polymers from Renewable Resources*, vol. 3, no. 2, p. 33, 2012.

[11] V. Tserki, N. E. Zafeiropoulos, F. Simon, and C. Panayiotou, "A study of the effect of acetylation and propionylation surface treatments on natural fibres," *Composites A*, vol. 36, no. 8, pp. 1110–1118, 2005.

[12] S. Paciornik and M. H. P. Maurício, "Digital imaging," in *ASM Handbook: Metallography and Microstructures*, G. F. V. Voort, Ed., pp. 368–402, ASM International, Materials Park, Ohio, USA, 2004.

[13] M. Z. Rong, M. Q. Zhang, Y. Liu, G. C. Yang, and H. M. Zeng, "The effect of fiber treatment on the mechanical properties of unidirectional sisal-reinforced epoxy composites," *Composites Science and Technology*, vol. 61, no. 10, pp. 1437–1447, 2001.

[14] D. M. R. Georget, P. Cairns, A. C. Smith, and K. W. Waldron, "Crystallinity of lyophilised carrot cell wall components," *International Journal of Biological Macromolecules*, vol. 26, no. 5, pp. 325–331, 1999.

[15] J. F. Revola, A. Dietrich, and D. A. I. Goring, "Effect of mercerization on the crystallite size and crystallinity index in cellulose from different sources," *Canadian Journal of Chemistry*, vol. 65, no. 8, pp. 1724–1725, 1987.

[16] J. R. M. d'Almeida, A. L. F. S. d'Almeida, and L. H. de Carvalho, "Mechanical, morphological, and structural characteristics of caroa (*Neoglaziovia variegata*) fibres," *Polymers and Polymer Composites*, vol. 16, no. 9, pp. 589–595, 2008.

[17] A. Bismarck, A. K. Mohanty, I. Aranberri-Askargorta et al., "Surface characterization of natural fibers; surface properties and the water up-take behavior of modified sisal and coir fibers," *Green Chemistry*, vol. 3, no. 2, pp. 100–107, 2001.

[18] B. Wielage, T. Lampke, G. Marx, K. Nestler, and D. Starke, "Thermogravimetric and differential scanning calorimetric analysis of natural fibres and polypropylene," *Thermochimica Acta*, vol. 337, no. 1-2, pp. 169–177, 1999.

[19] K. C. M. Nair, S. Thomas, and G. Groeninckx, "Thermal and dynamic mechanical analysis of polystyrene composites reinforced with short sisal fibres," *Composites Science and Technology*, vol. 61, no. 16, pp. 2519–2529, 2001.

[20] A. L. F. S. d'Almeida, V. Calado, D. W. Barreto, and J. R. M. d'Almeida, "Effect of surface treatments on the dynamic mechanical behavior of piassava fiber-polyester matrix composites," *Journal of Thermal Analysis and Calorimetry*, vol. 103, no. 1, pp. 179–184, 2011.

Hindawi Publishing Corporation
Conference Papers in Materials Science
Volume 2013, Article ID 651787, 6 pages
http://dx.doi.org/10.1155/2013/651787

Conference Paper

Preparation of Cellulosic Fibers from Sugarcane for Textile Use

Davina Michel,[1] Bruno Bachelier,[2] Jean-Yves Drean,[1] and Omar Harzallah[1]

[1] *Laboratoire de Physique et de Mécanique Textiles-EAC CNRS 7189, Université de Haute Alsace 11 rue Alfred, Werner, 68093 Mulhouse, France*
[2] *Centre de Coopération Internationale en Recherche Agronomique, pour le Développement, Avenue Agropolis, 34398 Montpellier Cedex 5, France*

Correspondence should be addressed to Davina Michel; dav.michel@live.fr

Received 30 April 2013; Accepted 8 September 2013

Academic Editors: R. Fangueiro and H. Hong

This Conference Paper is based on a presentation given by Davina Michel at "International Conference on Natural Fibers—Sustainable Materials for Advanced Applications 2013" held from 9 June 2013 to 11 June 2013 in Guimarães, Portugal.

The production of natural fibers is not sufficient to accommodate the textile needs of the growing world population. Therefore, textile research is exploring alternative natural resources to produce fibers. Though typically known for its nutritional use, the sugarcane can also be used for textile production because of its high fiber content. The aim of our study was to extract fibers from sugarcane and to analyze their mechanical behavior. Cane particles were treated with an alkaline solution in order to get cellulosic fibers. Physical and mechanical characterizations were carried out on these fibers: linear density, fineness, tensile properties, and bending rigidity. Their microstructure was analyzed to better understand their behavior. The results showed a strong influence of extraction parameters on the characteristics of fibers. Depending on these parameters, fibers fineness ranged from 8 to 80 tex, length ranged from 19 to 62 mm, and tenacity ranged from 7 and 25 cN/tex.

1. Introduction

Sugarcane (*Saccharum spp.*) is a Poaceae commonly cultivated in tropical areas. In 2011, 1.7 billion tons of sugarcane was produced worldwide [1]. Cane stalk is crushed in sugar mills and alcohol mills, generating 30% of residue left after crushing: bagasse. Nowadays, the valorization of such byproducts is crucial for environmental and sustainable reasons. A transformation of byproducts at low environmental impact is of interest for the creation of new products, for instance, in the textile, composite, or geotextile industries. Small tropical islands, like Martinique in the Caribbean, are seeking new methods to revalorize their byproducts. In 2009, sugarcane production in Martinique was about 220 000 tons; sugarcane is the staple second crop of this French island, after banana. Sixty percent of this production was converted to 86.6 hl of pure alcohol, and the remaining forty percent was converted to 5,600 tons of sugar. Nearly, 70,000 tons of bagasse was produced [2]. In Martinique, bagasse is used as a combustible material to generate energy for the local industries. Depending on the year and on the volume of production, surplus of bagasse is mainly used to feed animals.

Bagasse comes from different parts of the cane stalk comprising the outside rind crushed with the inner pith. It contains 45% of fiber and composed of 45% cellulose, 33% hemicelluloses, and 20% lignin [3]. Long and fine fibers are located in the rind part of the stalk and short fibers in the inside part known as the pith as discussed by Van Dillewijn [4]. As bagasse is a mixture of both parts, the fibers have uneven and uncontrolled lengths. However, because of its high fiber content and particularly because of its cellulose rate, bagasse can be used to produce sustainable fibers. Previous research has shown the chemical extraction of sugarcane fibers from the rind part of the cane stalk [5]. Costa has produced lyocell after an alkaline pulping process on sugarcane bagasse [6]. From different studies on sugarcane, valorizations of bagasse particles have not been characterized for textile application.

The aim of our study was firstly to evaluate the feasibility of extracting fibers from bagasse of sugarcane and secondly

Table 1: Identification of extracted fibers according to the extraction conditions.

Prehydrolysis	Sodium hydroxide concentration	
	1 N	0.1 N
With salty water	BPS-1 N	—
With distilled water	—	BPD-0.1 N
Without prehydrolysis	B-1 N	B-0.1 N

to define the process to convert these fibers into yarn, in a sustainable way.

2. Materials and Methods

2.1. Raw Material Preparation. Samples of bagasse of sugarcane from 12 varieties of *Saccharum ssp.* were collected from the Galion sugar mill in Martinique (a French Caribbean island), in 2011 and 2012. There was no significant difference between these varieties in the chemical composition and morphological structure of the basic components as established by [7, 8]. Wet bagasse was collected at the exit of the sugar mill in Martinique with 50% moisture content. This bagasse was oven-dried at 105°C for 24 hours and then exported by plane to the Laboratory of Textile Physics and Mechanics in Mulhouse (France). The granulometric method was used for sizewise classification of the dry bagasse particles. 25% of particles was collected in the 4 mm mesh of the sieve and used for experimental purposes.

2.2. Extraction of Cellulosic Fibers. Contrary to the kraft process which use high concentrated alkaline solution (at 17% of sodium hydroxide) to obtain cellulosic pulp [9], the extraction was conducted at lower alkaline concentration in order to obtain fine fibers.

Four types of fibers were extracted by chemical processing at different alkaline concentrations, with or without prehydrolysis, in a pilot scale. These parameters were studied to determine their effects on the fiber properties. From different combinations of the parameters of extraction, results were shown for the fibers obtained in conditions showing comparable properties, in this present work.

As pretreatment, prehydrolysis was performed in an autoclave at 130°C for one hour with either distilled or salty water. The whole alkaline extraction was carried out at 130°C for one hour in an autoclave. For each extraction, samples were prepared in groups of five with one gram of untreated dry bagasse. Table 1 presents the identification of the obtained fibers.

To neutralize the pH of fibers, several washing processes were conducted to eliminate the excess of soda in the fibers. After all alkaline extraction, fibers were oven-dried at 105°C for 24 hours, then conditioned at standard lab conditions [10], that is, a temperature of 20°C ± 2°C and a relative humidity of 65% ± 2% for at least 48 hours.

2.3. Fiber Fineness and Fiber Diameter. Tests were conducted to calculate the fiber fineness (linear density). Among each of the four types of fibers extracted, samples of 100 conditioned fibers were chosen randomly to be measured. The length of each fiber was measured using a knitmeter, and its weight was obtained by using an electronic scale. Micrographs of fiber cross sections were taken with a scanning electron microscope (SEM), and the diameter was calculated using Image J software. Twenty samples of each of the four types of fibers were tested.

2.4. Tensile Properties. Tensile tests were conducted on each individual fiber and attached to a cardboard layer by its extremities, to avoid any displacement during the test. MTS 20 M tensile tester was used to find out the tensile load and the elongation of the fibers. From several length classes of fibers, the tests were carried out at a rate of 1 mm/min using a 100 N load cell up to the breakup and 25 mm initial length.

2.5. Bending Rigidity. The fiber flexibility was determined by testing the bending rigidity and hysteresis with KAWABATA (KES FB2-SH). This device bent the entire fiber, placed between a fixed and a mobile grip, according to a constant curvature, which produced an ideal bending behavior as shown in Figure 1. Thirty fibers for each of the four types of fibers were tested with an intergrip distance about 35 mm. To avoid air-flow disturbance, the device was isolated in a PMMA booth.

2.6. Observations by Scanning Electron Microscopy (SEM). SEM was performed with a Hitachi S-2360 N apparatus operated at different voltages from 15 to 20 kV. Fibers were pasted onto a carbon tape to fix them on aluminum stubs. Fibers were coated with gold to make them conductive prior to SEM observation. The longitudinal surface and cross-section of fibers were analyzed and measured by microscopic observation.

3. Results

In the raw material, cellulose, hemicelluloses, and lignin were bonded together with small amounts of extraneous components. Chemical extraction was the most common way to remove the lignin and, consequently, to separate the individual fibers. By alkaline treatment, fiber bundles were isolated however, individual fibers were not reached and remained stuck together. Prior to the study of the extraction of individual fibers, the work focused on the characterization of the extracted fiber bundles as technical fibers.

3.1. Length and Fineness of the Extracted Fiber Bundles. The dimensions of the extracted fiber bundles were determined including fiber length and fiber fineness. Because of the heterogeneous length fiber distribution, the adjusting parameters "Barbe" as the weighted mean and "Hauteur" as the mean of apparent length (commonly used for cotton fibers) have been calculated. Mean results of fiber length, fiber diameter, and fiber fineness are reported in Table 2 (with values of standard deviation).

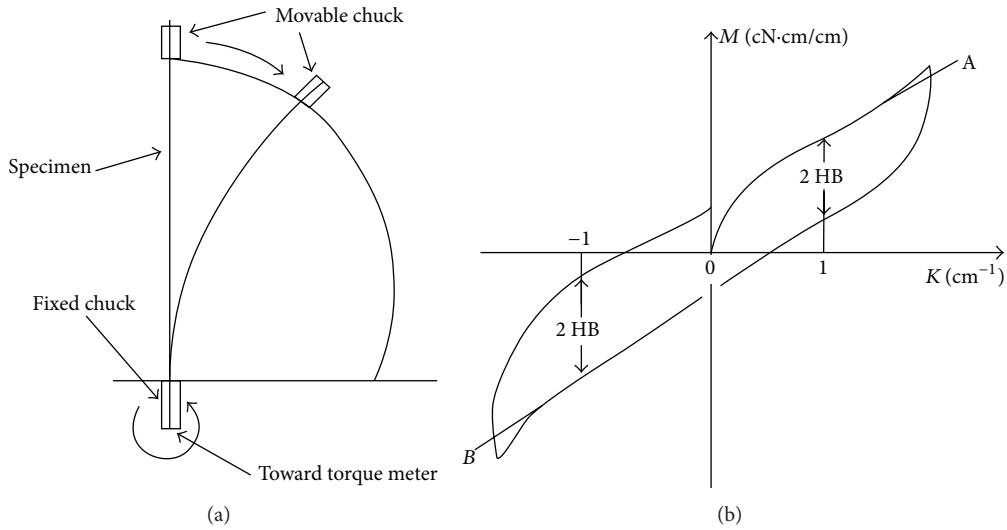

Figure 1: KES-FB2 diagram (a) and bending diagram (b) [11].

Table 2: Mean length and fineness of the four types of extracted fibers.

Bagasse fibers	Mean length (mm)	Barbe (mm)	Hauteur (mm)	Mean diameter (μm)	Fiber fineness (tex)
BPS-1 N	29.8 ± 6.7	35.6	33.3	117 ± 60	32 ± 24
BPD-0.1 N	45.6 ± 16.3	33.9	27.4	189 ± 100	39 ± 28
B-1 N	37.7 ± 9.9	31.6	27.6	181 ± 90	35 ± 21
B-0.1 N	37.6 ± 9.7	34.2	29.6	156 ± 45	49 ± 32

The fiber length selection should be determined around these adjusting fiber lengths. Diagrams of weighted mean are presented in Figure 2.

Fiber bundles obtained present large length dispersion independently of the extraction conditions. Reported measures present high variance coefficient values (over 50% for whole). This dispersion—common to unconventional natural fibers—was due to the heterogeneity of the raw material. There was no evidence on the effect of extraction process on the either fiber length or on the fiber fineness [11].

3.2. Tensile Properties. Mean tenacity values ranged from 7 cN/tex to 22 cN/tex. Results are reported in Table 3. Fiber bundles extracted at highest alkaline concentration had lower tenacity values than those extracted with 0.1 N NaOH solution, especially after a prehydrolysis.

The loss of tenacity is likely dependent on the fiber dimension. Similar trends of the alkaline effects on tenacity properties have been reported by Collier et al. [5], from the rind part of the sugarcane.

3.3. Bending Rigidity. BPS-1 N treatment produced fibers with a bending rigidity similar to agave fibers [12]. At the same alkaline concentration, fibers extracted with prehydrolysis had the lowest bending rigidity as shown in Table 4, with most of the lignin being removed. Also, fiber dimensions such as diameter and fineness influenced the fiber bending behavior.

Table 3: Tensile properties of fiber bundles.

Bagasse fibers	Tenacity (cN/tex)	Extension to break (%)	Energy to break (mJ)
BPS-1 N	7.5 ± 4.4	1.97 ± 1.3	1.2 ± 2
BPD-0.1 N	14 ± 3.8	3.86 ± 1.8	2.9 ± 4.2
B-1 N	11 ± 6.3	4.2 ± 4.3	2.2 ± 3.4
B-0.1 N	22 ± 11.7	3.24 ± 1	4.7 ± 4.4

Table 4: Tenacity of fiber bundles by treatment.

Bagasse fiber bundle	Bending rigidity gf·cm^2/fiber bundle	Bending hysteresis gf·cm/fiber bundle
BPS-1 N	0.027 ± 0.03	0.056 ± 0.03
B-1 N	0.116 ± 0.122	0.165 ± 0.166
BPD-0.1 N	0.190 ± 0.184	0.200 ± 0.151
B-0.1 N	—	—

Fibers extracted at high alkaline concentration after salty prehydrolysis (BPS-0.1 N) presented the lower bending rigidity because of the high lignin content-removed. Bending rigidity and hysteresis values showed the effect of the prehydrolysis on the fiber bending properties. In fact, at the same

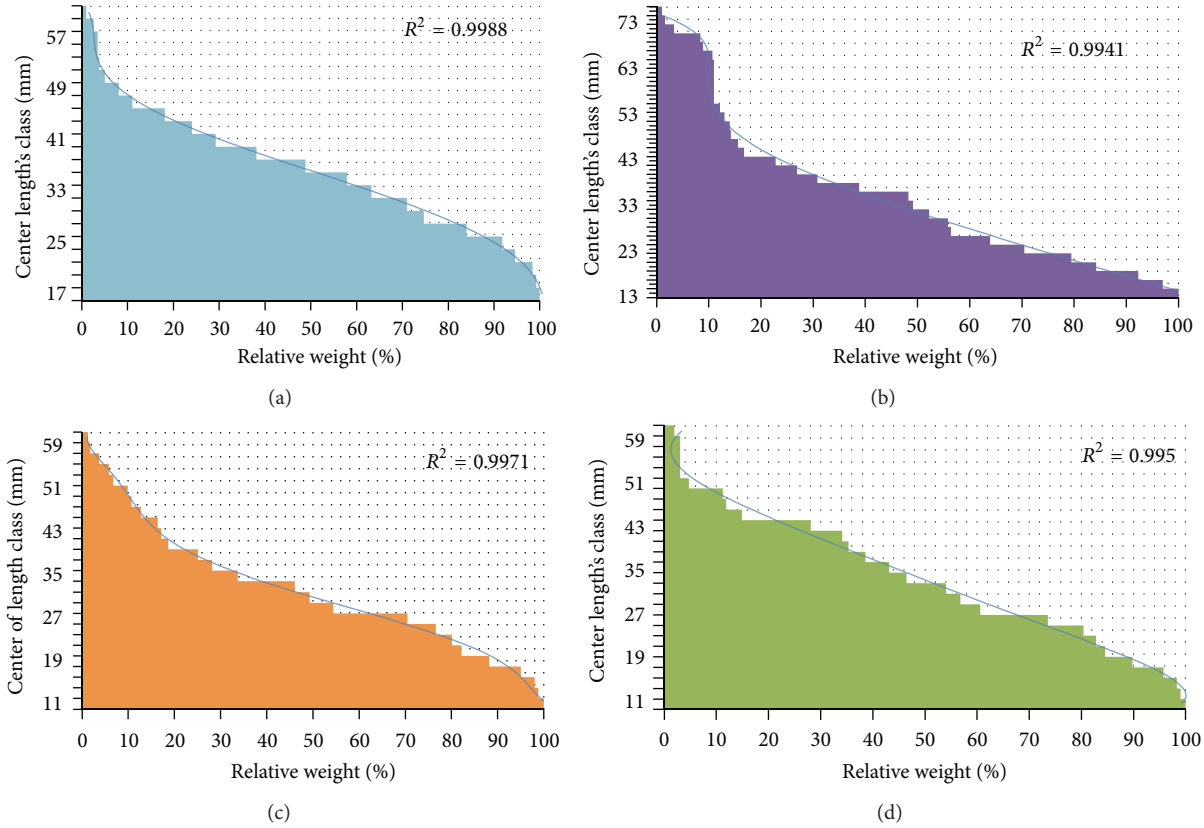

Figure 2: Length's repartition of each extracted fibres, BPS-1 N (a), BPD-0.1 N (b), B-1 N (c), and B-0.1 N (d).

alkaline concentration, prehydrolyzed BPS-1 N fibers get less rigid than the other B-1 N. The prehydrolysis facilitated the attack of the alkaline solution on the polymeric structure by inflating the cellulosic fiber structures as reported for other natural fibers [13]. Fibers extracted under conditions B-0.1 N at low alkaline concentration without prehydrolysis were not able to be bent by the Kawabata device. The concentration was the most effective parameter influenced that the fiber bending properties.

3.4. Observations by SEM. The SEM analysis of extracted fiber bundles allowed for observing the influence of the extraction conditions on the surface of fibers. In comparison with the raw material in Figure 3, the microscopic analysis of extracted fibers, as shown in Figures 4 and 5 demonstrated that all treatments removed various quantities of lignin. The longitudinal view of treated fibers at high concentration in Figure 4 shows a smooth surface. For fibers treated at a low alkaline concentration seen in Figure 5, incrusting materials like pectin are visible between the cells despite the treatment [5]. The presence of these materials showed the limits and the inadequacy of an extraction at low alkaline concentration.

4. Discussions

Due to the previous mechanical action in the sugar mill, different lengths of fiber bundles were obtained with a relative

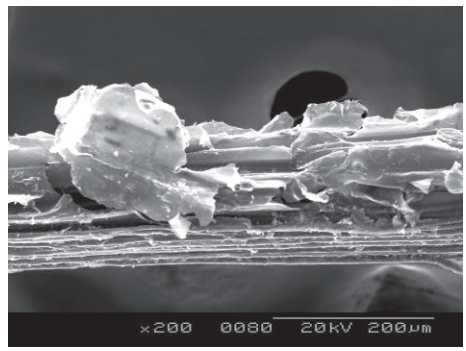

Figure 3: Longitudinal view of raw particle of sugarcane bagasse.

standard deviation of over 50%. Depending on the alkaline concentration as the main factor of severity, fine fibers could be obtained. It was observed that salty prehydrolysis and alkaline concentrations are the parameters that most affect the fiber dimensions. The preference for the salty prehydrolysis as opposed to distilled water was obvious by a visual examination of the color of the bath left after the pretreatment, due to its impact on fiber swelling.

On the one hand, tenacity values of the treated fibers were quite low (7–22 cN/tex) compared to those of other natural fibers like jute (25–53 cN/tex), linen (24–70 cN/tex), or agave (10–28 cN/tex) as discussed elsewhere [14, 15]. On the other hand, the observed values of breaking elongations of

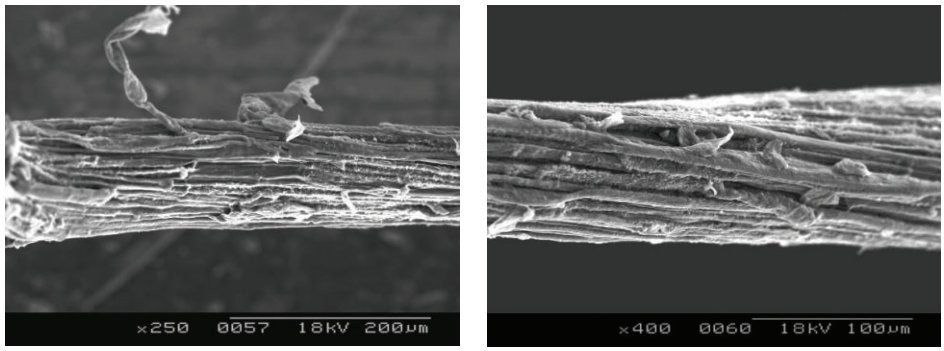

Figure 4: Fiber bundle extracted at 1 N NaOH on longitudinal view: with prehydrolysis on left and without prehydrolysis on right.

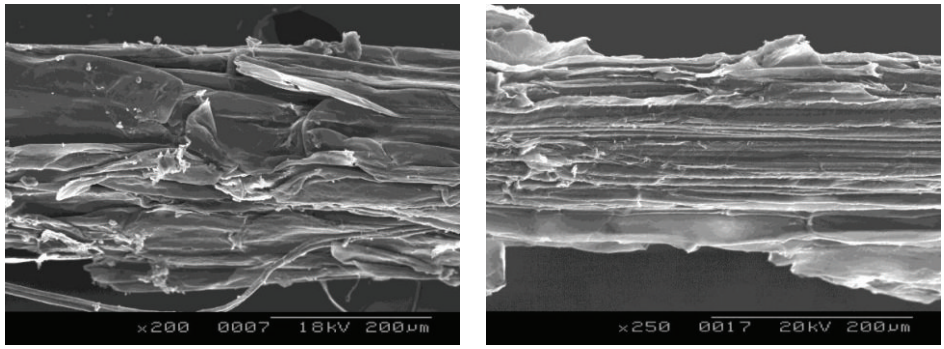

Figure 5: Longitudinal view of fiber bundle extracted at 0.1 N NaOH with prehydrolisis on left and without prehydrolysis on right.

bagasse fibers are similar to those of natural fibers mentioned below. Fiber elongation partially reflects the extent of ease of stretching a fiber. In this case, the extracted sugarcane fibers exhibit a very low value of breaking elongation with respect to breaking strength. Similar results have been reported elsewhere [6] from sugarcane straw lyocell with tenacity of 4.1 cN/tex and elongation rate of 1.80 ± 1.12. Thus, these fibers are not easily stretchable under small loads, which mean in essence that these are fibers with low flexible abilities [16].

This characterization is also supported by results obtained during the bending test. Flexible fibers were obtained due to their bending rigidity [17]. The low elastic recuperation of these fibers could be responsible for the bending hysteresis value obtained. A particular behavior was the irregular displacement of the fiber which could be increased by the irregularity of the sections all along the fiber.

5. Conclusions

Fiber bundles were chemically extracted from raw bagasse of sugarcane. The alkaline extraction was the best and most efficient way to remove lignin since the solution was more concentrated. A prehydrolysis in salty water inflated fibers that facilitated the impregnation of chemical reagent. Alkaline extraction affected the dimensions as well as the mechanical properties of the fibers in bundles. However, the use of alkaline alone or combined with prehydrolysis did not produce ultimate individual fibers. The use of concentrated solution was limited because of the severity of the extraction which prematurely can affect the cellulosic content. Thin fibers were obtained at high alkaline concentration with a lack of tenacity, of bending rigidity, and of bending hysteresis. These parameters could be improved by changing extraction conditions, using additional tools like ultrasounds and mechanical action after the chemical extraction. All in all, fiber bundles dimensions and properties can be controlled by the extraction condition according to the use wanted.

Acknowledgments

The research team has no financial or commercial relations with any of the commercial identities mentioned in this paper. The authors gratefully acknowledge the Region of Martinique and CIRAD Montpellier for the financial support, as well as Dominique PETIT from the CTCS Martinique for the technical support.

References

[1] FAOSTAT, 2012, http://faostat.fao.org/site/567/DesktopDefault.aspx?PageID=567#ancor.

[2] Technical Center of Sugar and Sugarcane of Martinique, "Chiffres de la filière canne: Production agricole et industrielle sur les 10 dernières campagnes. Internal documentation," 2012.

[3] Instituto de investigaciones de la caña de azúcar, "La industria de los derivados de la caña de azúcar," Editorial Científico-Técnica la Habana 111, 1980.

[4] C. Van Dillewijn, *Botany of Sugarcane. Chronica Botanica*, Stechert-Hafner, Waltham, Mass, USA, 1952.

[5] B. J. Collier, J. R. Collier, P. Agarwal, and Y.-W. Lo, "Extraction and evaluation of fibres from sugar cane," *Textile Research Journal*, vol. 62, no. 12, pp. 741–748, 1992.

[6] S. M. Costa, P. G. Mazzola, J. C. A. R. Silva, R. Pahl, A. Pessoa, and S. A. Costa, "Use of sugarcane Straw as a source of cellulose for textile fiber production," *Industrial Crops and Products*, vol. 42, pp. 189–194, 2013.

[7] Cuba9, *Atlas del Bagazo de la Caña de Azúcar*, Geplacea/Pnud, Mexico City, Mexico, 1990.

[8] G. J. M. Rocha, A. R. Gonçalves, B. R. Oliveira, E. G. Olivares, and C. E. V. Rossell, "Steam explosion pretreatment reproduction and alkaline delignification reactions performed on a pilot scale with sugarcane bagasse for bioethanol production," *Industrial Crops and Products*, vol. 35, no. 1, pp. 274–279, 2012.

[9] J. F. Rodriguez, "I taller sobre cellulosa, papel y derivados del bagazo," Filial De La ATAC Cuba 9, 1994.

[10] "Kato Tech Co., LTD. KES-FB2-SH Single Hair Bending Tester: User's Manual," katotech@kestako.co.jp.

[11] D. Michel, *Evaluation du potentiel textile et fibreux des fibres de Saccharum Officinarum [Ph.D. thesis]*, LPMT, University of Haute Alsace, Mulhouse Cedex, France, 2013.

[12] Y. Chaabouni, J. Drean, S. Msahli, and F. Sakli, "Morphological characterization of individual fiber of Agave americana L.," *Textile Research Journal*, vol. 76, no. 5, pp. 367–374, 2006.

[13] M. Dallel, A. Lallam, M. Leon, and M. Renner, "Physical and mechanical characterization of Alfa (stipa tenacissima l.) fibres for textile applications," in *Proceedings of the 12th AUTEX World Textile Conference*, Zadar, Croatia, 2011.

[14] M. Harris, *Handbook of Textile Fiber*, Harris Research Laboratories, Washington DC, USA, 1954.

[15] S. Msahli, J. Y. Drean, and F. Sakli, "Evaluating the fineness of agave Americana L. fibers," *Textile Research Journal*, vol. 75, no. 7, pp. 540–543, 2005.

[16] A. R. Bunsell, *Handbook of Tensile Properties of Textile and Technical Fibers*, vol. 91, Woodhead Publishing Series in Textiles No. 91, Cambridge, UK, 2009.

[17] R. Meredit, *Proceedings of Fifth International Congress on Rheology*, vol. 1, University of Tokyo Press, Tokyo, Japan, 1969.

Hindawi Publishing Corporation
Conference Papers in Materials Science
Volume 2013, Article ID 402372, 7 pages
http://dx.doi.org/10.1155/2013/402372

Conference Paper

Neglected Wools: Fundamental Steps to Counteract the Loss of Potentially Valuable Materials Derived from Native Sheep Breeds

Laura Bacci,[1] Francesca Camilli,[1] Sara Di Lonardo,[1] Pierpaolo Duce,[2] Enrico Vagnoni,[2] and Antonio Mauro[3]

[1] *Institute of Biometeorology, National Research Council (IBIMET-CNR), Via G. Caproni 8, 50145 Firenze, Italy*
[2] *Institute of Biometeorology, National Research Council (IBIMET-CNR), Traversa la Crucca 3, 07100 Li Punti, Italy*
[3] *Ricerche e Servizi (R.S.), Via A. Volta 42, 50041 Calenzano, Italy*

Correspondence should be addressed to Francesca Camilli; f.camilli@ibimet.cnr.it

Received 31 July 2013; Accepted 8 September 2013

Academic Editors: R. Fangueiro and H. Hong

This Conference Paper is based on a presentation given by Laura Bacci at "International Conference on Natural Fibers—Sustainable Materials for Advanced Applications 2013" held from 9 June 2013 to 11 June 2013 in Guimarães, Portugal.

In order to enhance the textile value of Italian native and local wools, research projects were carried out by starting mapping wools from some Italian sheep breeds through a preliminary morphological characterization of wool fibres. Furthermore, textile processing procedures differing from the commonly used woolling techniques have been set up. The results have shown that, at national level, native and local wools, beyond being more widely employed in the carpets production, could be also used in the higher added value sector of clothing and fashion.

1. Introduction

Many of the European livestock breeds have been greatly altered, and today a high percentage of local or traditional breeds are extinct or marginalized. As about 30% of the farm-animal breeds are currently at high risk of extinction [1], it is essential for their efficient and sustainable use, development, and conservation to understand the diversity, distribution, basic characteristics, comparative performance, and the current status of the animal genetic resources for each country [2].

Despite this situation, which is common to many wool producers all over Europe, local and autochthonous wools could be exploited to make them profitable for both wool producers and textile industries. However, it should be noted that it would be very difficult to develop a market because EU does not recognize wool as an agricultural product, as reported by Harmsworth [3]. Even so, in November 2011, Shetland wool produced in the Shetlands gained Protected Geographical Status with Protected Designation of Origin (PDO) classification as "Native Shetland Wool" after accreditation from EU.

The focus on autochthonous wools is justified by economic, environmental, and cultural reasons. According to FAO [4], the consistency of autochthonous sheep breeds, which are characterized by different productive attitudes, has strongly decreased in recent years with severe consequences on rural areas.

The consensus concerning the conservation of animal genetic resources by maintaining a certain variation of local breeds within their production systems is large [5]. Genetic resources conservation is also one of the strongest reasons for breed preservation [6], with the purpose of meeting future market demands as well as being an insurance against future changes in production circumstances [4].

Furthermore, at global level, the sheep industry is currently undergoing major breed adjustments as climate changes can affect changes in pasture yields [7]. According

to Harle et al. [7], the quality of coarser (merinos) wools is less vulnerable to the impact of drier conditions than finer wools, as future scenarios due to climate changes show. Although research on wool production should integrate climate changes with factors such as market influences and socioeconomic dynamics [7], also at global dynamics level there could be reasons for textile industries to focus on local resources represented by autochthonous wools.

It is well known that fiber diameter, among other quality parameters, is crucial in determining the economic value of, for example, Merino wool [8, 9]. Whiteley [10] has graded the 10 major raw wool characteristics for processing importance. A number of processing trials indicated that 80–90% of variation in processing performance and yarn and fabric quality may be explained by its variation [9]. Variation in fiber diameter accounting for 61% wool characteristics for processing importance was also found by Atkins et al. [11] and Wuliji et al. [12].

Understanding the diversity of sheep breeds can facilitate understanding different quality and quantity of wools produced. In fact, the high variability of wools (usually produced by small herds located in sparse mountain areas) represents a difficulty in terms of logistics and adequate amount of wool supply to the manufacturing system. Furthermore, the lack of wool selection and difficulties in wool management, at agricultural level, as well as technical difficulties in the textile industrial processing, make coarse wool market very weak with consequences on sheep breeding economies. In this respect, local wools are a practical and economic burden for breeders, as the income from wool sale does not even cover shearing expenses.

This situation is also framed in the European regulation context with EC 1069/2009 and EU 142/2011 ruling wool production and management and defining wool as an animal byproduct that must be thrown into landfill, if it is not directed towards the textile supply chain. Italian local wools often either are thrown into landfill or even incorrectly disposed of in the environment.

Italian native and local wools (the production is estimated about 14.000 tons/year) are mostly assessed as "coarse wools" and are not enough appraised by clothing and fashion market that requires fibers of such quality standards as those provided by Merinos wool.

The full utilization of Italian wool in all the different branches of the textile industry (from green building to the clothing-fashion sector) could contribute to reducing the import of wool, thus benefiting rural economies and the environment with the decrease of raw materials import (Merinos wool) and export (e.g., local wools are often directed towards Asian countries). The utilization could also help textile producers in more easily tracing products, thus providing consumers with better knowledge about the origin of textile products.

In this sense, the multifunctional and innovative use of local wools could support the protection of autochthonous sheep breeds that is also directly associated with sustainable agriculture with all the benefits on the adaptation of animal populations to adverse environmental conditions, high biological efficiency, and traditional management.

In the larger perspective to grant Italian wool, an economic and environmental value, assuring both a right profit to sheep breeders and benefits to the environment, research was carried out by verifying the feasibility of a local textile production chain that could generate additional income for all the stakeholders involved in the textile sector (from farmers to apparel manufacturers).

In particular, the present work aims at showing that, at national level, native and local wools, beyond being more widely employed in the textile furnishing (for instance, carpets production) or green building sectors, could be also used in the higher added value sector of clothing and fashion.

In order to achieve this purpose, a basic qualitative characterization of wool from different Italian native sheep breeds has been carried out, and the results obtained from the study of the industrial processing of the Sardinian wool, the most significant coarse wools in terms of potential available amounts of raw material, are discussed. Furthermore, textile processing woolling techniques have been set up and tested on Sardinian sheep breed in Tuscany.

2. Material and Methods

2.1. Wool Samples. Wool samples were collected from the following sheep breeds.

(1) The Sardinian sheep, an autochthonous dual-purpose sheep (milk and meat) breed of Sardinia Island (more of 3 million ewes). Wool production is approximately 1,3–1,5 kg per capita. Sardinian sheep is also raised in other Italian regions, such as Tuscany.

(2) The Arbus black sheep, a small-sized animal. About 1.000 ewes are located in the Medio-Campidano district (Sardinia). The ancestral traits suggest that the population escaped the selection process that was mainly oriented toward milk yield and the white color of the fleece, for which the predominant white strain of Sardinian sheep was established [13].

(3) The Vissana sheep, a white medium-small sized autochthonous sheep breed coming from Visso in Mount Sibillini (Marche) and belongs to the Apennine group. It is reared in the central Umbrian Apennine, in Marches, Latium, and some areas of southern Tuscany (http://eng.agraria.org/). The production attitudes are meat, milk, and wool.

(4) The Amiata sheep or "sheep from Crete Senesi and the Amiata Mountain". It derives from the Vissana sheep widely diffused in the central and southern Tuscany since the first half of the XIX century. It is a large-sized animal showing triple production attitudes: meat, milk, and wool. Most of the studied population is white.

(5) The Appennine sheep, a medium-large sized animal from Central Italian Appennine. It is a rustic breed, able to exploit forage available resources, even in disadvantaged areas of the Centre-South Italian Appennine.

(6) The Bergamasca sheep, a large-sized animal mainly selected for meat production. It is an Alpine breed that is not only mainly spread in the area around Bergamo (Lombardy) but, nowadays, also diffused in other Italian areas.

(7) The Biellese sheep, mainly selected for meat production, even if it has also a good wool and milk production. The wool quality is adapted for bedding and carpet manufacturing. It is similar to the Bergamasca sheep and is diffused in the region of Piedmont.

(8) The Gentile di Puglia sheep (or Apulian Merinos), mainly selected, in the past, for wool production, even if nowadays it is used for meat production. It is mainly spread in the Apulia, Calabria, and Basilicata regions. It is a Merinos sheep crossbreed from local and Spanish Merinos sheep breeds.

(9) The Altamurana sheep (or Murge sheep), bred mainly for milk production (in the past it was used also for meat and wool productions). It comes from Altamura in the province of Bari (Apulia).

(10) The Massese sheep (or Formese sheep) bred mainly for milk production. It is a native sheep breed coming from Massa (Tuscany). Nowadays, it is diffused in Tuscany and Liguria regions. Its fleece is dark and cannot be dyed. This could result in a benefit for the textile production of natural colored wools.

(11) The white Garfagnina sheep. It probably derives from the Appennine strain. It shows triple production attitudes: meat, milk, and wool. It is typical of the Garfagnana area in the province of Lucca (Tuscany), even though it was spread in different areas of Tuscany and Emilia Romagna.

(12) The Villnoesser Schaf (or Fiemmese or Tingola) sheep, a crossbreed between Bergamasca sheep and Padovaner Seidenschaf, that is spread in the Dolomiti Valleys and the Trentino province. Some sheep breeders are working in order to exploit wool and produce traditional clothing.

(13) The Zerasca sheep. It derives from an Apennine strain that has been isolated for a long time in the Zeri area in Lunigiana (Tuscany) and in the areas close to Liguria. After the II World War, it has been crossed with other local breeds, such as the Massese.

2.2. Wool Fibers Fineness and Wool Fibers Length Measurements. Wool fibers fineness measurements were performed according to UNI 5423-64 rules. A subsample of carded and combed fibers weighing between 1,2 and 1,5 g was placed in parallel according to length classes with an aligned extreme (comb sorter system). Groups of fibers were extracted according to classes of length expressed in millimeters. Every group of fibers was weighed in order to obtain a distribution based on weight. Length measurements were reported as mean and maximun values, together with standard deviation.

Figure 1: Dyed Sardinian wool flocks.

Figure 2: Dyed Sardinian wool cones.

2.3. Wool Processing Procedures. 50 kg of scoured Sardinian wool (bred in Tuscany) was spun by woolen ring through the standard carding cycle.

100 kg of scoured Sardinian wool (bred in Tuscany) was carded by the combed cycle, and a card sliver with parallel fibers was obtained. After some spinning test, the wool sliver was then cut every 5 cm so as to remove >10 cm fibers that emerged from the web divider during the production of roving to be spun on the woolen ring. The material obtained was carded again.

A small amount of combed carded wool was processed into roving without being cut. The uncut roving was combed, and >10 cm fibers (almost 40%) were discarded. The obtained combed roving was spun by using a hollow spindle spinning machine suited for processing high titred fancy yarns directed to the interior decoration sector.

In order to obtain the final fabrics, the yarn underwent the following steps: weaving; bleaching (this step is particularly important for light colors dying); calendaring; dyeing procedures. With regard to the latter, wools were dyed as flock (Figure 1), yarn cones (Figure 2), and fabric ("inflow" procedure, Figure 3).

Both 5.6 Nm titred yarn (100% wool) and 8,5 Nm titred yarn (70% wool and 30% nylon) were dyed. Synthetic dyes satisfying the GOTS specifications (the mark regarding textile commodities produced by organic material) were used following spring-summer 2102 color trends. Natural dyes were applied only on flock wools.

Table 1: Morphological characteristics of wool fibers of some Italian native sheep breeds.

Sheep breed	Mean diameter (μm)	CV%	Average length fibers (mm)	CV%
Sardinian sheep (Tuscany region)	18.9	143.5	109.7	25.0
Sardinian sheep (Sardinia region)	41.0	39.1	125.2	68.4
Tingola (or Fiemmese)	39.7	99.2	96.3	18.8
Bergamasca	39.0	117.9	88.0	50.2
Arbus black sheep	35.7	42.8	125.7	72.5
Zerasca	34.7	179.8	63.9	19.1
Brianzola	34.2	122.0	58.5	18.8
Vissana	32.7	108.5	35.8	17.8
Apennine	30.6	131.3	56.1	20.3
Amiata	30.4	125.7	41.4	20.1
Gentile di Puglia	26.7	133.4	40.0	21.2
Biellese	25.5	231.4	92.1	24.0
Altamurana or Murge	26.7	158.6	65.2	20.8
Massese nera	22.6	184.2	43.4	16.9
Garfagnina Bianca	18.1	116.2	85.5	25.9

Figure 3: "Inflow" dyeing procedure for fabric dyeing.

Figure 4: Scoured white Sardinian wool.

Figure 5: Wool fabrics obtained from white Sardinian sheep wool.

Figure 6: Tailoring phase.

3. Results and Discussion

3.1. Native Wool Characterization. Table 1 reports standard parameters (mean diameter and length) of wool fibres quality of some Italian native sheep breeds. The few available wool samples collected did not allow statistical elaborations. Among all the analysed wools, Sardinian wool showed the highest mean diameter, representing the maximum extreme of this wool range where the Garfagnina Bianca resulted in the lowest.

Nevertheless, values of wool fibres diameters from the Sardinian sheep grown in Tuscany showed a very high variability and seemed to be much thinner than those from

(a) (b)

Figure 7: Jacket for woman (a) and gilet for man (b) made by fabrics produced with Sardinian wool.

(a) (b)

Figure 8: Jackets (a) and gilet (b) for man made by fabrics produced with Sardinian wool.

native Sardinian. Moreover, values of length of Sardinian wool fibres tended to be higher than those detected in other wools. As length negatively affected the processing phase, only the wool from Sardinian white sheep (from Tuscany region) was tested for yarn production.

3.2. Implementation of Textile Industrial Processing Method for Coarse Wools. The wool derived from Sardinian sheep breed forms the highest amount of local wool produced in Italy by sheep breed, compared to other local and native wools. Because of that, the object of the study has been the textile industrial processing of this type of wool. Research on methods for improving the Sardinian wool processing—its most critical being the spinning phase—can help understand the technical problems that can be common to other coarse wools.

One of the major problems faced in this study was represented by kemp fibers, as nowadays, in the Italian textile manufacturing industry, no technical device is available to remove them.

Kemp fibers, either as long or short fibers, are very coarse and can be found in large amounts in Sardinian wools. During spinning, they are hard to be aligned together with the other fibers, thus resulting in an unpleasant stinging sensation when touching threads and fabrics. Furthermore, kemp fibers are difficult to dye, thus causing inhomogeneous colors as results of the dyeing phase.

In this study, ca. 150 kg of Sardinian wool (Figure 4) was used, and 250 m of carded fabric weighing between 300 and 350 g/m^2 was produced (Figure 5).

These fabrics were made with different weave patterns. They were used in the manufacturing of garments, such as

Figure 9: Weaving phase.

Figure 10: Ink jet printing applied on wool fabrics.

clothing for men and women that passed tailoring (Figure 6) and wearing testing, after being worn in winter time (Figures 7 and 8).

3.3. Yarn Obtained through Woollen Cycle. The yarn obtained through woollen cycle resulted in a coarse irregular, quite furry, shaggy yarn, and 3.5–3.7 Nm titred, thus, not suitable to obtain fabrics to be employed in the clothing garments industry. One of the causes for yarn irregularity was the inhomogeneous fiber length ranging from 2-3 cm to 15 cm, and resulting hard to process through the post carder divider and, afterwards, the spinning phase.

3.4. Yarn Obtained through a Mixed Cycle (Combing Cycle + Woollen Cycle). Yarn obtained through a mixed cycle (combing cycle + woollen cycle) resulted as being very regular, little furry yarns, 5.6 Nm titred (100% wool) yarn.

8.5 Nm titred yarn was also obtained using 70% wool and 30% nylon.

Combing roving using a hollow spindle spinning machine produced high titred fancy yarns to be possibly employed in the interior decoration sector.

Part of the yarn was bleached and depigmented. After several tests, high quality standard yarns were obtained.

Following the weaving phase (Figure 9), the carded fabrics underwent carbonization in order to remove almost all vegetal residues (they could not be completely removed from the fleece).

Dyes applied on fabrics not always showed pleasant results due to the high frequency of black hair. Furthermore, in order to dye with light colors, these fabrics needed to be bleached to take off the yellowish colored background. Calendering was applied to evaluate the level of "smoothing of rather rough textile surfaces." Such good levels have been also demonstrated by the good results obtained by ink jet printing such fabrics (Figure 10).

4. Conclusions

The achievement of 5.6 Nm titred (100% wool) and 8.5 Nm titred (70% wool and 30% nylon) yarns obtained from applying a mixed cycle processing procedure on coarse wools, such as those derived from the Sardinian sheep breed, opens new horizons towards the use of this type of wool.

All the dyeing, printing, weaving, and finishing tests confirmed that yarns and fabrics produced with coarse wools can undergo the same textile processing phases as those applied to wools commonly used in the clothing-fashion sector.

The tests, developed at laboratory and industrial scale, have shown that, from a technical point of view, wools from native sheep breeds can be employed for several textile productive purposes including those regarding the textile furniture sector and also the clothing-fashion industry ones.

Therefore, in order to further improve the results obtained, coarse wools and native sheep breeds deserve more attention and investment on behalf of the textile industries as well as of the textile and animal production research.

If this will be accomplished, coarse wools will be no more neglected—being, nowadays, considered almost as a waste material—and will rise to be properly acknowledged and defined as feedstock of interest of the manufacturing industry.

Conflict of Interests

The authors declare that they have no conflict of interests with regard to the paper.

Acknowledgments

The results presented in this study have been supported by the following projects: MEDLaine "À la recherche des couleurs et des tissus de la Méditerranée" cofunded by ERDF, Operating Programme IT-FR Maritime, 2007–2013, and "Sustainable Textile Chain" (FTS) funded by the CNR (National Research Council). Special thanks are due to Ms. Irma L. Schwegler for making garments and tailoring feedbacks.

References

[1] B. D. Scherf, *World Watch List for Animal Diversity*, FAO, Rome, Italy, 3rd edition, 2000.

[2] FAO, "Global plan of action for animal genetic resources and the Interlaken Declaration adopted by the international technical conference on animal genetic resources for food and agriculture," FAO, 2007, http://www.fao.org/docrep/010/a1404e/a1404e00.htm.

[3] A. Harmsworth, "The role of livestock products in the economic development of a remote island community," In Collected papers from workshops of the European Network for livestock systems in integrated rural development. A concerted action of the Commission of the European Union, pp. 150–155. EU Commission, DG VI FAIR1 CT95-0114, 1997.

[4] FAO, "Primary guidelines for development of national animal genetic resources management plans," 1998, http://dad.fao.org/cgi-bin/getblob.cgi?sid=-1,50006248.

[5] G. C. Gandini and J. K. Oldenbroek, "Choosing the conservation strategy," in *Genebanks and the Conservation of Farm Animal Genetic Resources*, J. K. Oldenbroek, Ed., pp. 11–31, ID-DLO, Lelystad, The Netherlands, 1999.

[6] G. C. Gandini and E. Villa, "Analysis of the cultural value of local livestock breeds: a methodology," *Journal of Animal Breeding and Genetics*, vol. 120, no. 1, pp. 1–11, 2003.

[7] K. J. Harle, S. M. Howden, L. P. Hunt, and M. Dunlop, "The potential impact of climate change on the Australian wool industry by 2030," *Agricultural Systems*, vol. 93, no. 1–3, pp. 61–89, 2007.

[8] L. Hunter and E. Gee, "The effect of staple crimp. resistance to compression and fibre diameter and length characleristics on the physical properties of wool worsted yarns," in *Proceedings of the 6th Quinquennial International Wool Textile Research Conference*, pp. 327–347, Pretoria, South Africa, September 1980.

[9] L. Hunter, D. W. F. Turpie, and E. Gee, "The effect of wool fibre properties and breed of sheep on worsted processing performance and on yarn and fabric properties," in *Proceedings of the 2nd World Congress Sheep Beef Cattle Breed*, pp. 703–710, Pretoria, South Africa, April 1984.

[10] K. J. Whiteley, "Wool processing wool tech," *Sheep Breeding*, vol. 35, pp. 109–113, 1987.

[11] K. D. Atkins, K. A. Coelli, A. E. Casey, and S. J. Semple, "Genetic differences among merino bloodlines from NSW and Victorian wether comparisons (1983–1993)," *Wool Technology and Sheep Breeding*, vol. 43, no. 1, pp. 1–14, 1995.

[12] T. Wuliji, K. G. Dodds, J. T. J. Land, R. N. Andrews, and P. R. Turner, "Response to selection for ultrafine Merino sheep in New Zealand. I. Wool production and wool characteristics of ultrafine fibre diameter selected and control Merino yearlings," *Livestock Production Science*, vol. 58, no. 1, pp. 33–44, 1999.

[13] M. Piras, S. Casu, S. Salaris, M. G. Usai, and A. Carta, "The Pecora Nera di Arbus: a new sheep breed in Sardinia, Italy," *Animal Genetic Resources Information*, vol. 45, pp. 91–92, 2009.

Hindawi Publishing Corporation
Conference Papers in Materials Science
Volume 2013, Article ID 243023, 3 pages
http://dx.doi.org/10.1155/2013/243023

Conference Paper

Anaerobic Biodegradability of Agricultural Renewable Fibers

Bo Shi, Peter Lortscher, and Doris Palfery

Corporate Research and Engineering, Kimberly-Clark Corporation, Neenah, WI 54956, USA

Correspondence should be addressed to Bo Shi; bshi@kcc.com

Received 18 June 2013; Accepted 8 September 2013

Academic Editors: R. Fangueiro and H. Hong

This Conference Paper is based on a presentation given by Bo Shi at "International Conference on Natural Fibers—Sustainable Materials for Advanced Applications 2013" held from 9 June 2013 to 11 June 2013 in Guimarães, Portugal.

Natural fiber-based paper and paperboard products are likely disposed of in municipal wastewater, composting, or landfill after an intended usage. However, there are few studies reporting anaerobic sludge digestion and biodegradability of agricultural fibers although the soiled sanitary products, containing agricultural fibers, are increasingly disposed of in municipal wastewater or conventional landfill treatment systems, in which one or more unit operations are anaerobic digestion. We conducted a series of biodegradation studies using corn stalk and wheat straw pulp fibers to elucidate biodegradability and biodegradation kinetics under anaerobic sludge digestion conditions. The degradation results indicate that corn stalk achieved 78.4% biodegradation and wheat straw 72.4% biodegradation, all within 56 days of the study. In comparison, corn stalk generated more biogas than wheat straw. Unlike any raw agricultural crop residues, anaerobic biodegradation of agricultural fibers is largely unaffected by the presence of lignin, physical sizes of crop stalks, and plant cell wall constitutes.

1. Introduction

Commodity fibrous materials have been mostly pulped from softwood or hardwood trees, which are a main source of virgin raw material for pulp and paper. In recent years, society has become more conscious of environmental concerns and responsible resource utilization. Nonwood alternative natural materials such as agricultural residues (corn stover, rice or wheat straw, bagasse and cotton stalk, etc.) are increasingly being explored to temper the supply and cost fluctuations of conventional wood-based pulp fibers despite the challenges of nonwood material collection, transportation, storage, and pulping as discussed by Chandra [1]. It is commercially attractive to integrate agricultural fiber manufacturing together with bioenergy and biofuel production. An example of such a processing integration is based on a novel hot water treatment and subsequent mechanical refining explored by Raymond and Closset [2], Kelley [3], and Leponiemi et al. [4]. The fiber fraction derived from such a low cost processing option can be utilized for printing, writing or specialty grades paper outlined by Won and Armed [5], bathroom tissue, and containerboard applications exemplified by Hurter [6]. Sustainable packaging industries (http://www.s-packaging.com/) use natural fibers such as wheat straw for protective packaging applications, which is a great eco-friendly alternative to traditional Styrofoam (EPS) and plastic packaging. Many developing countries such as China and India, where the forest resources are limited, have turned to nonwood plants and agrobased materials for papermaking reported by Chandra [1] and Atchison [7]. Currently, the use of agricultural residues for pulp and papermaking in the United States is negligible. However, Ahmed and Zhu [8] pointed out there are abundant agricultural remnants which are available annually for fiber-based product manufacturing.

The aforementioned products, after being soiled or used, would be likely disposed of either in a municipal wastewater treatment system, composting, or conventional landfill. Today's containerboard recycling activity may delay final disposal fate but it cannot be avoided since the recycled fibers have a limited useful lifespan. This paper addresses anaerobic sludge digestion of corn stalk and wheat straw pulp fibers to assess their anaerobic biodegradability.

2. Experimental

2.1. Materials. Corn stalk pulp was provided by USDA Forest Products Laboratory (Madison, WI, USA). The FQA data indicate the fiber length is 0.699 mm (fiber length weighted), fiber width or diameter is 22.1 μm, and its carbon content is 42.6%. Wheat straw pulp was obtained from Shandong Pulp and Paper Co. Ltd. (Jinan, China). The fiber length is 1.769 mm (fiber length weighted), fiber width or diameter is 28.7 μm, and its carbon content is 40.0%. The reference material is cellulose powder, which was purchased from Sigma-Aldrich (St. Louis, MO, USA).

Anaerobically digested sludge was collected from the Neenah-Menasha Sewerage Commission (Neenah, WI, USA) for the proposed investigation, which operates single-stage digestion with sludge residence time estimated to be about 14 days. Sludge solids content in the digested sludge was 2.5% and the pH for the digested sludge was within a range from 7.4 to 7.8. The sludge colour is black because of the presence of organic matter.

2.2. Methods. American Society for Testing and Materials—ASTM D5210-92 [9]—was used to carry out experiments to assess agricultural fiber biodegradation under anaerobic conditions. The sample volume for anaerobic sludge digestion is 100 mL with 25 mL as headspace in each serum bottle, which contained 10% sludge inoculum by volume and about 0.2 grams of the pulp material. The gas samples were taken using a burette apparatus by water displacement in the 100 mL burette and time intervals varied during the course of sample anaerobic digestion. In the first couple of weeks, sampling intervals were three days or shorter and one week apart towards the end of the sample anaerobic digestion. The temperature during sample sludge digestion was fixed at 35°C throughout the experiment. A specific bacteria genus name is not available because this is a consortium of anaerobic bacteria that are responsible for pulp sample biodegradation. Cellulose powder was used as a reference material to check the activity of the inoculum rather than using bacteria count. If less than 70% biodegradation is observed with the reference (on the basis of CO_2 and CH_4 production), the test must be regarded as invalid and should be repeated with fresh inoculum.

2.3. Biodegradability Estimate. The fiber sample weight was about 0.2 grams for each anaerobic sludge digestion experiment reported in this paper. The potential total gas production from a fibre sample, $V_{\text{Theoretical}}$, can be estimated using a carbon content in actual fiber composition analysed and one mole of gaseous carbon occupying 22.4 L under standard conditions. For experiments other than standard conditions, a correction factor has been considered in calculations for a percentage of algal biodegradation, as shown in ASTM 5210-92 [9].

The accumulated net CO_2 and CH_4 gas generation, $\sum V_{\text{Sample}}$, was obtained from an average of three samples after the accumulated CO_2 and CH_4 gases, generated from three blanks that are just anaerobically digested sludge inoculum without the presence of the agricultural fiber sample, $\sum V_{\text{Blank}}$, are subtracted. Equation (1) is then used to estimate agricultural fiber sample biodegradability, which is outlined by Shi and Palfery [10]:

$$\text{Biodegradability} = \frac{\sum V_{\text{Sample}} - \sum V_{\text{Blank}}}{V_{\text{Theoretical}}} \times 100\%. \quad (1)$$

Cellulose is normally used as the reference material so that biodegradation of carbohydrate samples can be compared. The evolved gas (CO_2 + CH_4) volume is dependent on only the carbon amount regardless of the CO_2 and CH_4 ratio stated by Itävaara and Vikman [11].

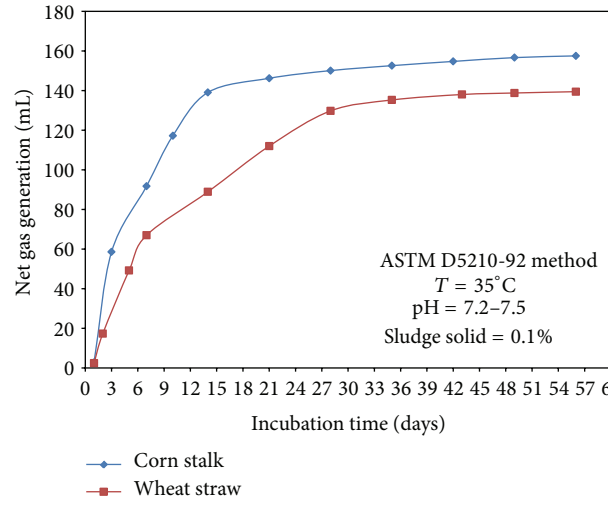

Figure 1: Corn stalk and wheat straw fiber anaerobic sludge digestion results.

3. Results

ASTM D5210-92 [9] as described above was followed to assess agricultural fiber anaerobic biodegradability. Each sample weight was about 0.2 grams with three replicates. The average results from anaerobic sludge digestion of corn stalk and wheat straw fibers are shown in Figure 1, which indicates that corn stalk fiber produced more biogases (157.5 mL) than wheat straw fiber (139.5 mL). Biodegradability of corn stalk fiber is estimated to be 78.4% according to (1). For wheat straw fiber, it achieved 72.4% biodegradation. The testing duration for all samples was 56 days and cellulose powder, used as a reference material, achieved 73.2% biodegradation. Unlike any raw agricultural crop residues, anaerobic biodegradation of agricultural fibers is largely unaffected by the presence of lignin studied by Singh et al. [12], chemical pretreatments by Song et al. [13], and plant cell wall constitutes, which complicates biodegradability calculations by Richard [14].

This study shows that corn stalk fiber biodegraded faster than wheat straw fiber, especially within the first 30 days of sludge digestion. The rate of anaerobic biodegradation can be modeled according to the first-rate kinetic model outlined by Shi et al. [15], which is to be covered separately. The difference in fiber biodegradability and biodegradation kinetics is due

to accessibility of anaerobic bacteria to internal structures of a cellulosic component in each type of the fiber studied.

4. Conclusions

The data presented above provide a new understanding of the fate of agricultural fibers in the environment, which is important to facilitate product design for the environment, particularly for those of wastewater treatment facilities and bioreactor/conventional landfills.

Agricultural residues remaining from the harvest of food-based crops such as wheat straw, rice, and corn stalk are important sources of papermaking fiber. Judicious choices will be inherently driven by relative abundance and delivered cost, compatibility with existing manufacturing infrastructure, contribution to product characteristics and manufacturing efficiency, environmental sustainability objectives, economic viability, and success of products in the marketplace. Kimberly-Clark announced ambitious sustainable development goals to reduce its forest fiber footprint at Rio+20 United Nations Conference on Sustainable Development in 2012, which included a goal of 50% reduction of wood fiber sourced from natural forests by 2025. Agricultural crop remnants fit well with corporate sustainability strategy and more product research and development activities using nonwood natural fibers are expected in the future.

Acknowledgments

The authors gratefully acknowledge corn stalk pulp sample from USDA Forest Products Laboratory, Madison, WI, USA, and wheat straw pulp sample from Shandong Pulp and Paper Co. Ltd., Jinan, China.

References

[1] M. Chandra, *Use of nonwood plant fibers for pulp and paper industry in Asia: potential in China [M.S. thesis]*, Virginia Polytechnic Institute and State University, Blacksburg, VA, USA, 1998.

[2] D. Raymond and G. Closset, "Forest products biorefinery: technology for a new future," *Solutions*, vol. 87, no. 9, pp. 49–53, 2004.

[3] S. S. Kelley, "Forest biorefineries: reality, hype or something in between?" *Paper Age*, vol. 122, no. 2, pp. 46–48, 2006.

[4] A. Leponiemi, A. Johansson, and K. Sipilä, "Assessment of combined straw pulp and energy production," *BioResources*, vol. 6, no. 2, pp. 1094–1104, 2011.

[5] J. M. Won and A. Armed, "Corn stalk as a raw material for papermaking," in *Proceedings of the 58th Appita Annual Conference and Exhibition*, pp. 5–11, Melbourne, Australia, April 2004.

[6] R. W. Hurter, *Nonwood Plant Fiber Uses in Papermaking*, 2001.

[7] J. Atchison, "Update on global use of non-wood plant fibers and some prospects for their greater use in the United States," in *Proceedings of the North American Non-wood Fiber Symposium*, Atlanta, GA, USA, 1998.

[8] A. Ahmed and J. Y. Zhu, "Cornstalk as a source of fiber and energy," in *Proceedings of the 3rd International Symposium on Emerging Technology of Pulping and Papermaking*, Guangzhou, China, 2006.

[9] "Standard test method for determining the anaerobic biodegradation of plastic materials in the presence of municipal sewage sludge," ASTM D5210-92, American Society for Testing and Materials, Philadelphia, PA, USA, 1992.

[10] B. Shi and D. Palfery, "Temperature-dependent polylactic acid (PLA) anaerobic biodegradability," *International Journal of Environment and Waste Management*, vol. 10, no. 2-3, pp. 297–306, 2012.

[11] M. Itävaara and M. Vikman, "An overview of methods for biodegradability testing of biopolymers and packaging materials," *Journal of Environmental Polymer Degradation*, vol. 4, no. 1, pp. 29–36, 1996.

[12] D. Singh, J. Zeng, D. D. Laskar, L. Deobald, W. C. Hiscox, and S. Chen, "Investigation of wheat straw biodegradation by Phanerochaete chrysosporium," *Biomass and Bioenergy*, vol. 35, no. 3, pp. 1030–1040, 2011.

[13] Z. Song, G. Yang, Y. Guo, and T. Zhang, "Comprison of two chemical pretreatments of rice straw for biogas production by anaerobic digestion," *Bioresources*, vol. 7, no. 3, pp. 3223–3236, 2012.

[14] T. Richard, "The effect of lignin on biodegradability," Cornell Composting, 1996, http://compost.css.cornell.edu/calc/lignin.html.

[15] B. Shi, C. Bunyard, and D. Palfery, "Plant polymer biodegradation in relation to global carbon management," *Carbohydrate Polymers*, vol. 82, no. 2, pp. 401–404, 2010.

Hindawi Publishing Corporation
Conference Papers in Materials Science
Volume 2013, Article ID 136861, 6 pages
http://dx.doi.org/10.1155/2013/136861

Conference Paper

Impact Property of PLA/Flax Nonwoven Biocomposite

Shah Alimuzzaman,[1] R. H. Gong,[1] and Mahmudul Akonda[2]

[1] *Textiles and Paper, School of Materials, University of Manchester, Manchester M13 9PL, UK*
[2] *Tilsatec Advanced Materials, Tilsatec Ltd., Wakefield WF2 9ND, UK*

Correspondence should be addressed to Shah Alimuzzaman; sazaman_2006@yahoo.com

Received 25 June 2013; Accepted 28 August 2013

Academic Editors: R. Alagirusamy and H. Hong

This Conference Paper is based on a presentation given by Shah Alimuzzaman at "International Conference on Natural Fibers—Sustainable Materials for Advanced Applications 2013" held from 9 June 2013 to 11 June 2013 in Guimarães, Portugal.

Flax fibre reinforced polylactic acid (PLA) biocomposites were fabricated by using a new technique incorporating an air-laying nonwoven web forming process and compression moulding technologies. The relationship between the main process variables and the properties of the biocomposite was investigated. The results show that with the increasing of flax content, the notched Izod impact strength increased. The maximum value of 28.3 KJ/m^2 was achieved at 60% flax fibre content. As the moulding temperature and moulding time increased, the impact strength decreased. The physical properties of the biocomposites were also evaluated. As the flax fibre content increased, the void content of the biocomposites increased. This was further confirmed by the surface morphology of the composite material. The appropriate processing parameters for the biocomposites were established.

1. Introduction

Natural fibre-reinforced polymer composites are of great importance in the end-use applications [1–3]. The combined behaviour of the stiffness, elastic matrix, and strong fibrous reinforcement is achieved by these composites. The developments of fibre reinforced composites have made materials that are stiffer than steel and harder than aluminium available [4]. Natural fibres and their composites offer environmental advantages such as lower pollutant emissions and lower greenhouse gas emissions. During the last few years, many conventional materials are replaced by polymer based materials in various applications. The productivity, ease of processing, and cost reduction are the most significant advantages which the polymers offer over other traditional materials [5–7]. Biocomposites are widely used for automotive interior parts, structural parts, and interior and exterior decoration materials [8]. Biodegradable composites are becoming more popular due to their low cost and low density, and also because of the increase in oil price and recycling and environment necessities. In this project, PLA is used as a matrix, and flax fibre is used as a reinforcing material. PLA is a synthetic aliphatic polyester from renewable agriculture products; it is biodegradable and with properties comparable to some fossil-oil-based polymers [9]. Flax fibres exhibit some unique mechanical properties. Baley [10] and Charlet et al. [11] showed that flax fibres can have mechanical properties greater than those of E-glass fibres.

To make fibre reinforced composite materials, the film stacking [12, 13], injection moulding [14, 15], and compression moulding [9, 15, 16] are the most widely used manufacturing methods. In the present study, the flax fibres were blended with staple PLA fibres to form a homogenous fibre mixture. This enhances the delamination resistance of composites made from film stacking. The mixed fibres were converted to fibre webs using an air-laying nonwoven process. A unique feature of air-laid nonwoven process is to produce the webs with isotropic fibre orientation distribution [17], leading to isotropic composites. The fibre webs were thermally consolidated before finally converted to composites. This avoids any potential fibre damage caused by the widely used needle punching method for nonwoven composites [18, 19]. The

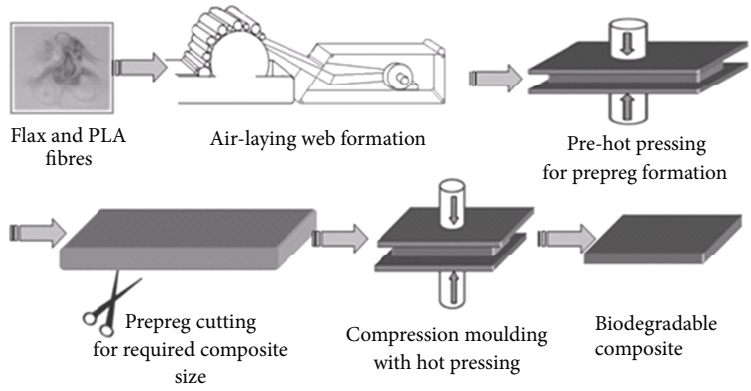

Figure 1: Schematic diagram of composite manufacturing steps.

nonwoven web was converted into biocomposites by the compression moulding process. The compression moulding method has the ability to mould large, fairly intricate parts and is cost effective.

The tensile, flexural, and thermal properties of the biocomposites manufactured by this project are reported in a previous paper [20]. The present report is mainly focused on the impact strength and physical properties of the biocomposites. The relationships between the main process variables and the performance of the composite material were investigated; the various factors that influence the performance of the composite were analyzed to determine the optimal parameters.

2. Experimental

2.1. Materials. Both PLA and flax fibres were supplied by Tilsatec Advanced Materials, Tilsatec Ltd., Wakefield, UK, in sliver form of commercial grade. The PLA was in staple fibre form with an average length of 75 mm, an average diameter of 28.46 μm, and a density of 1.25 g/cm^3. The flax fibre had an average length of 65 mm, an average diameter of 21.59 μm, and a density of 1.40 g/cm^3.

2.2. Composite Preparation. The PLA/Flax biocomposites were prepared by using the air laying web formation technique. The weights of PLA and flax fibres were measured so as to determine the weight percentage of fibre and matrix polymer of the resulting composite. The flax and PLA fibres were mixed during the web forming process. The nonwoven web was then folded to the required thickness. In order to facilitate handling, the folded web was then prepressed, cut to the required size, and finally hot pressed to form the composite material. Figure 1 shows a schematic diagram of the manufacturing steps of the biocomposites.

The biocomposites containing different weight percentages of fibres were produced. The thickness of the composites with one layer of nonwoven prepreg of 1065 g/m^2 and compression moulding pressure of 50 bar was found to be 1.00 ± 0.1 mm. Depending on the thickness of composite material required, a number of prepregs can be doubled to make the required thickness. The biocomposite samples were then cut to desired shape according to the standard for testing and evaluation. To ensure that all absorbed moisture was removed, the prepregs containing PLA and flax fibres were dried at 80°C under vacuum for 10 hours before final hot pressing. Fibre-matrix composition, the moulding temperature, and the moulding time were selected as process variables which are illustrated in Table 1.

Table 1: Process variables.

Levels	Factors			
	Fibre composition (%) PLA/Flax	Moulding temperature (°C)	Moulding time (min.)	Moulding pressure (bar)
1	60P/40F	180	05	50
2	50P/50F	190	10	50
3	40P/60F	200	15	50

2.3. Impact Strength. Izod impact tests were conducted on notched samples according to ISO 180: 2001 at room temperature using a pendulum of 4.2 J energy. The dimensions of the test specimen were 80 mm × 10 mm × 4 mm with 2 mm notched at the centre of the vertical edge. The direction of the blow in the Izod test was "edgewise parallel" with a striking velocity of 2.44 m/sec. Each value reported is the average of at least five tests, and the error bars correspond to plus or minus one standard deviation.

2.4. Fibre Volume Fraction and Void Content. Since the mechanical property of the biocomposites depends on their real fibre volume fractions, they were measured after the consolidation operation, in order to ensure the fibre-matrix ratio in the prepreg according to the initial selection of the fibre fraction by weight. Composites were dissolved in a solvent, dichloromethane (DCM), at room temperature by stirring to obtain complete dissolution of the PLA matrix. The fibre volume fraction and void content of the PLA/Flax biocomposites were determined using the digestion method

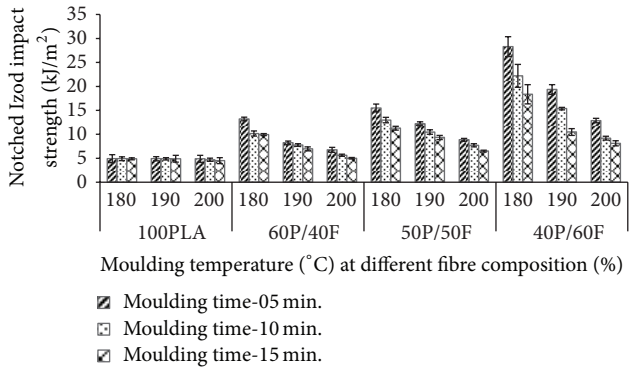

Figure 2: Effect of process variables on the notched Izod impact strength.

in accordance with BS EN 2564: 1998. The void content by volume (V_o) was calculated according to

$$V_o = 100 - \left[W_f \times \frac{\rho_c}{\rho_f} + \left(100 - W_f\right) \times \frac{\rho_c}{\rho_r} \right], \quad (1)$$

where V_o is the void content as a percentage of the initial volume; W_f is the fibre content as a percentage of the initial mass; ρ_c is the specimen density, in grammes per cubic centimetre; ρ_f is the fibre density, in grammes per cubic centimetre; ρ_r is the density of the resin, in grammes per cubic centimetre.

2.5. Surface Morphology. Fractographic studies with scanning electron microscopy (SEM) were carried out in detail on the impact fracture surfaces and the surfaces of the PLA/Flax biocomposites. The samples were viewed perpendicular to the fractured surface. A SEM (Philips, XL 30) with field emission gun and accelerating voltage of 5.00 kV was used to obtain images for the biocomposite specimen. The nonconducting surface of the biocomposite was coated with carbon in Edwards coating system (E306A, USA) before being subjected to SEM in order to prevent electrical discharge.

3. Results and Discussion

3.1. Impact Strength. Impact strength of a composite is directly related to the toughness of the material. The fibres play an important role in the impact resistance of fibre reinforced biocomposites as they interact with the crack formation and act as stress-transferring medium. The notched Izod impact strength of the neat PLA and its biocomposites as the function of process variables is depicted in Figure 2.

As can be seen, impact strength increased with increased flax fibre content for all moulding temperature and time. This was because as the fibre content increased, more interfaces exist on the crack path and more energy was consumed. In fact, the concentration of flax fibres would have increased with increased fibre content, which could lead to increased pull-out and also increased impact strength. From the thermal analysis, it was found that the crystallinity of the biocomposites decreased with increased fibre content [20].

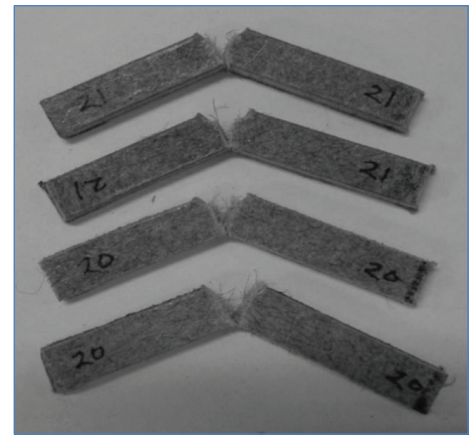

Figure 3: Photograph of the impact tested biocomposite samples with 60 wt% flax fibre.

In principle, the lower the crystallinity is, the lower the brittleness becomes. At the fracture surface, it can be seen that flax fibres were broken in the case of more brittle sample, whereas fibres were pulled out from the surface in the cases of less brittle samples.

The image of the impact tested biocomposites is illustrated in Figure 3, which shows that the samples were not completely separated into two pieces but flax fibres bridged the gap. This mode of failure was associated with high energy absorption [15]. In addition, examination of the impact fracture surfaces showed fibre pull-out due to the fracture of flax fibre during impact loading (Figure 4(a)). Good impact strength is mainly due to the energy absorption when the fibres are pulled out of the matrix. It is assumed that the weaker bonding leads to better impact strength than very strong bonding which can cause a sudden failure [21, 22]. This can also be explained by the voids in the biocomposites. Voids in the biocomposites increased with increased flax fibre content. Voids may be the cause for weaker bonding.

It was found that the notched Izod impact strength of the 60P/40F biocomposite was 13.2 KJ/m^2 at 180°C moulding temperature and 5-minute moulding time. The maximum impact strength 28.3 KJ/m^2 was obtained at 180°C moulding temperature and 5-minute moulding time with 40P/60F biocomposite. The neat PLA (100 PLA) shows very low impact strength (approximately 5 KJ/m^2), and it is not significantly affected by the moulding temperature and time. So it can be seen that addition of 40, 50, and 60% of flax fibre content increased the impact strength by about 170%, 216%, and 477%, respectively, at 180°C moulding temperature and 5-minute moulding time.

It was also observed that the impact strength decreased with increased moulding time and temperature. It might be that the longer period and higher temperature of moulding increased the crystallinity, that is, brittleness of the composites, resulting in reduced impact strength.

3.2. Fibre Volume Fraction and Void Content. The void contents of the biocomposites are illustrated in Figure 5. It is clear that the voids in the biocomposites increased as the

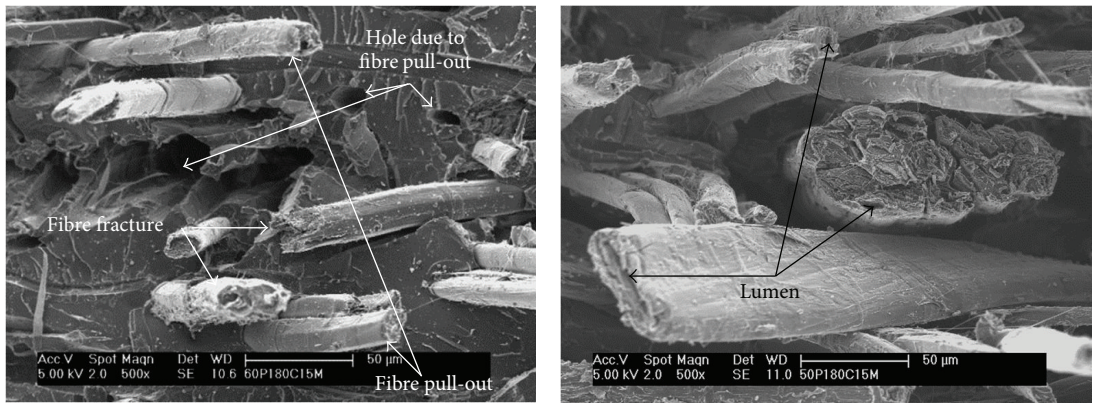

Figure 4: SEM micrograph of the impact fracture surface of the biocomposite. (a) The fibre fracture and fibre pull-out. (b) The lumen in the flax fibre.

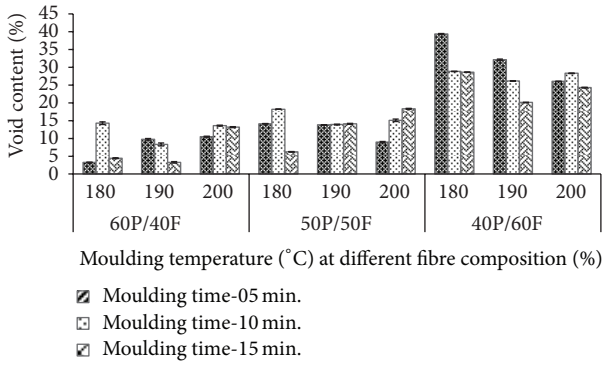

Figure 5: Effect of process variables on the void content of the biocomposites.

nominal fibre fraction by weight increased. In general, the voids are closely related to the processing conditions because they can be formed by gases which may be generated in the thermal process. Since this study adopted thermoplastic PLA and there are few possible sources of gas, the voids may be formed due to the discontinuous resin matrix inside the composites, resulting from the uneven distribution of the PLA fibres or their failure to form a continuous phase in the biocomposites.

The elementary flax fibres consist of a primary cell wall, a secondary cell wall, and a lumen. The lumen is an open channel in the centre of the fibre, and it can be as small as 1.5% of the cross-section of the fibres [23]. The size of the lumen mainly depends on the maturity of the fibres. Generally the lumen size (cross-section of the lumen) is larger for immature fibre and smaller for matured fibres. The lumens can be observed in the fracture surface of the biocomposites and are shown in Figure 4(b). These lumens also act as a void portion. Therefore, the flax fibres themselves are carrying the voids naturally. It might be the cause for increased voids with increasing flax fibre weight percentage. From Figure 5, it can be seen that there is no significant trend of void content with changing processing (moulding) temperature and time.

Figures 6(a)–6(c) represent the SEM micrographs of the impact fracture surfaces of the biocomposites. From the investigation, it can be seen that the amount of voids increases with increasing flax fibre content. The amount of voids is consistent with the quantitative analysis of the void content (Figure 5).

3.3. Surface Morphology. Figures 7(a)–7(c) show the SEM images of the surface of the PLA/Flax biocomposites with different flax fibre content. It can be seen that the number of pores gradually increases with increasing flax fibre content in the composites, and a large number of pores are clearly visible in the biocomposite with 60% flax fibres (40P/60F) (Figure 7(c)). In a previous study, it was found that the water absorption of the biocomposites increased with increased flax fibre content [24]. The increasing trend of water absorption may be because of increasing void content through which water may ingress into the materials.

It was also found that the water absorption of biocomposites increased with increased moulding temperature and time [24]. A large number of pores were created between the fibre and matrix interface due to the fibre degradation at higher moulding temperature and time. The pores act as passage for water into the biocomposites, and it may be the cause of higher water absorption. This indicates that it is very important to control the moulding temperature and time to decrease the water absorption of biocomposites when the fibre content is higher. The higher fibre content is desired in biocomposites to achieve good mechanical properties, and in this case, it is important to control the moulding temperature and time for decreasing water absorption. Therefore, the moulding temperature and time are recommended to be about 180°C and 5 minutes for manufacturing PLA/Flax biocomposites. These processing conditions are also recommended for the high tensile and flexural properties, reported in the previous paper [20].

4. Conclusions

This paper reports the mechanical, physical, and morphological properties of flax fibre reinforced PLA biocomposites

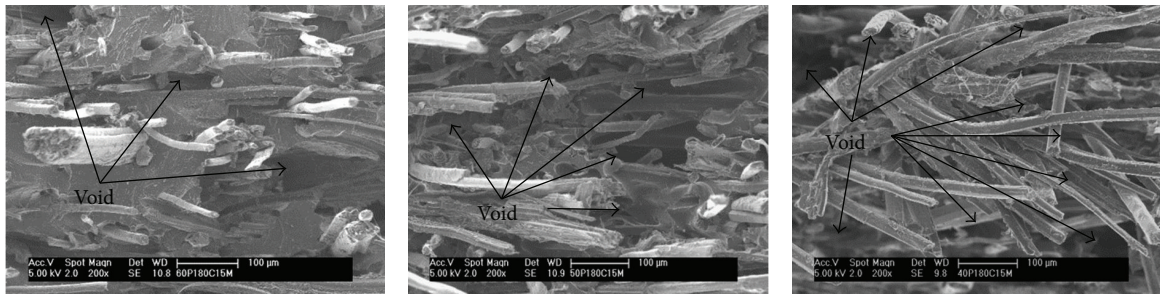

(a) (b) (c)

Figure 6: SEM micrographs of impact fracture surface of 40% (a), 50% (b), and 60% (c) flax fibre reinforced composites.

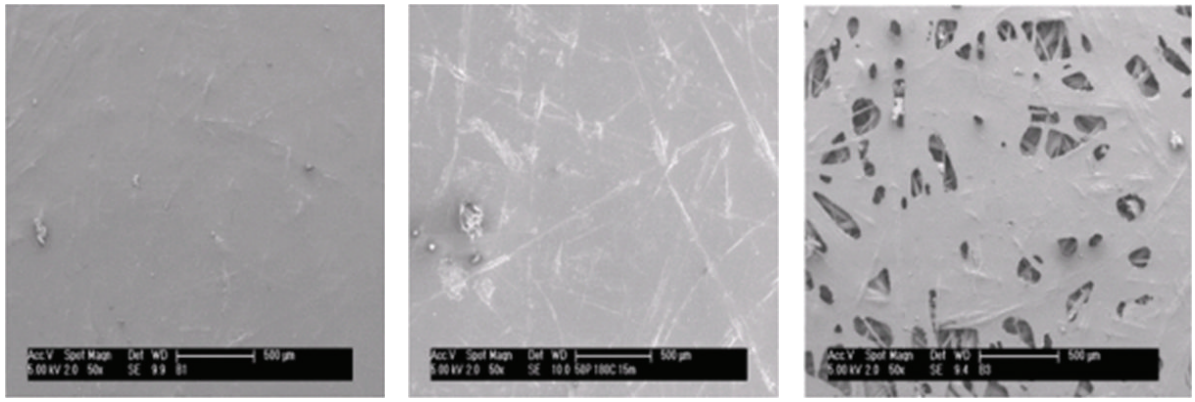

(a) 60P/40F (b) 50P/50F (c) 40P/60F

Figure 7: SEM micrographs of the biocomposite surfaces with different flax fibre content.

based on air-laid nonwoven web forming method. Factors including flax fibre content, moulding temperature, and moulding time were investigated. Flax fibre content is the most significant factor influencing the physical and mechanical properties of the biocomposites. It is found that increasing flax fibre content in the biocomposites increases the mechanical properties, and the maximum notched Izod impact strength is 28.3 KJ/m^2. The notched Izod impact strength increased with increased flax fibre content, but it decreased with increased moulding temperature and time. The void content of the biocomposites also increases with increasing flax fibre content. The best processing conditions for the highest PLA/Flax biocomposite performance according to notched Izod impact strength was 60% flax fibre, 180°C moulding temperature, and 5-minute moulding time. 180°C moulding temperature and 5-minute moulding time are also recommended as the processing conditions for the highest PLA/Flax biocomposite performance according to the tensile and flexural properties reported in the previous paper [20].

Conflict of Interests

The authors of the paper have no direct financial relation or any other conflict of interests related to the paper with the company mentioned in this paper.

Acknowledgments

The authors gratefully acknowledge the funding by the Bangabandhu Fellowship on Science and ICT project under the Ministry of Science and Technology of the Government of The People's Republic of Bangladesh. The authors also express their appreciation to Tilsatec Advanced Materials, Tilsatec Ltd., UK, for supplying PLA and flax fibres.

References

[1] H. Li and M. M. Sain, "High stiffness natural fiber-reinforced hybrid polypropylene composites," *Polymer-Plastics Technology and Engineering*, vol. 42, no. 5, pp. 853–862, 2003.

[2] A. S. Singha and V. K. Thakur, "Morphological, thermal, and Physicochemical characterization of surface modified Pinus fibers," *International Journal of Polymer Analysis and Characterization*, vol. 14, no. 3, pp. 271–289, 2009.

[3] A. S. Singha and V. K. Thakur, "Chemical resistance, mechanical and physical properties of biofibre based polymer composites," *Polymer-Plastics Technology and Engineering*, vol. 48, no. 7, pp. 736–744, 2009.

[4] V. K. Thakur and A. S. Singha, "Mechanical and water absorption properties of natural fibers/polymer biocomposites," *Polymer-Plastics Technology and Engineering*, vol. 49, no. 7, pp. 694–700, 2010.

[5] A. S. Singha and V. K. Thakur, "Synthesis and characterization of Grewia optiva fiber-reinforced PF-based composites," *International Journal of Polymeric Materials*, vol. 57, no. 12, pp. 1059–1074, 2008.

[6] A. S. Singha and V. K. Thakur, "Fabrication and characterization of S. cilliare fibre reinforced polymer composites," *Bulletin of Materials Science*, vol. 32, no. 1, pp. 49–58, 2009.

[7] A. S. Singha and V. K. Thakur, "Synthesis and characterization of S. cilliare fibre reinforced green composites," *International Journal of Plastics Technology*, vol. 11, pp. 835–851, 2007.

[8] C. Clemons, "Wood-plastic composites in the United States: the interfacing of two industries," *Forest Products Journal*, vol. 52, no. 6, pp. 10–18, 2002.

[9] K. Oksman, M. Skrifvars, and J.-F. Selin, "Natural fibres as reinforcement in polylactic acid (PLA) composites," *Composites Science and Technology*, vol. 63, no. 9, pp. 1317–1324, 2003.

[10] C. Baley, "Analysis of the flax fibres tensile behaviour and analysis of the tensile stiffness increase," *Composites A*, vol. 33, no. 7, pp. 939–948, 2002.

[11] K. Charlet, C. Baley, C. Morvan, J. P. Jernot, M. Gomina, and J. Bréard, "Characteristics of Hermes flax fibres as a function of their location in the stem and properties of the derived unidirectional composites," *Composites A*, vol. 38, no. 8, pp. 1912–1921, 2007.

[12] P. Ouagne, L. Bizet, C. Baley, and J. Bréard, "Analysis of the film-stacking processing parameters for PLLA/flax fiber biocomposites," *Journal of Composite Materials*, vol. 44, no. 10, pp. 1201–1215, 2010.

[13] Y. Yuan, M. Guo, and Y. Wang, "Flax fibres as Reinforcement in Poly(Lactic acid) biodegradable composites," in *Proceedings of the ICICIS*, R. Chen, Ed., vol. 134, pp. 547–553, CCIS, 2011.

[14] B. Bax and J. Müssig, "Impact and tensile properties of PLA/Cordenka and PLA/flax composites," *Composites Science and Technology*, vol. 68, no. 7-8, pp. 1601–1607, 2008.

[15] M. A. Sawpan, K. L. Pickering, and A. Fernyhough, "Improvement of mechanical performance of industrial hemp fibre reinforced polylactide biocomposites," *Composites A*, vol. 42, no. 3, pp. 310–319, 2011.

[16] D. Plackett, T. L. Andersen, W. B. Pedersen, and L. Nielsen, "Biodegradable composites based on L-polylactide and jute fibres," *Composites Science and Technology*, vol. 63, no. 9, pp. 1287–1296, 2003.

[17] J. W. S. Hearle and P. J. Stevenson, "Nonwoven fabric studies—part III: the anisotropy of nonwoven fabrics," *Textile Research Journal*, vol. 33, pp. 877–888, 1963.

[18] S. H. Lee and T. J. Kang, "Mechanical and impact properties of needle punched nonwoven composites," *Journal of Composite Materials*, vol. 34, no. 10, pp. 816–840, 2000.

[19] S. Tejyan, A. Patnaik, A. Rawal, and B. K. Satapathy, "Structural and mechanical properties of needle-punched nonwoven reinforced composites in erosive environment," *Journal of Applied Polymer Science*, vol. 123, no. 3, pp. 1698–1707, 2012.

[20] S. Alimuzzaman, R. H. Gong, and M. H. Akonda, "Nonwoven polylactic acid and flax biocomposites," *Polymer Composites*, vol. 34, no. 10, pp. 1611–1619, 2013.

[21] J. Ganster and H.-P. Fink, "Novel cellulose fibre reinforced thermoplastic materials," *Cellulose*, vol. 13, no. 3, pp. 271–280, 2006.

[22] N. Graupner and J. Müssig, "A comparison of the mechanical characteristics of kenaf and lyocell fibre reinforced poly(lactic acid) (PLA) and poly(3-hydroxybutyrate) (PHB) composites," *Composites A*, vol. 42, no. 12, pp. 2010–2019, 2011.

[23] H. L. Bos, "The potential of flax fibres as reinforcement for composite materials," Technische Universiteit Eindhoven, 2004.

[24] S. Alimuzzaman, R. H. Gong, and M. H. Akonda, "Biodegradability of nonwoven flax fibre reinforced polylactic acid biocomposites," *Polymer Composites*. In press.

Hindawi Publishing Corporation
Conference Papers in Materials Science
Volume 2013, Article ID 539856, 6 pages
http://dx.doi.org/10.1155/2013/539856

Conference Paper

Experimental Behavior of Natural Fiber-Based Composites Used for Strengthening Masonry Structures

Rosamaria Codispoti,[1] Daniel V. Oliveira,[2] Raul Fangueiro,[2] Paulo B. Lourenço,[2] and Renato S. Olivito[1]

[1] *Department of Civil Engineering, University of Calabria, 87036 Rende (CS), Italy*
[2] *Department of Civil Engineering, University of Minho, P-4800-058 Guimarães, Portugal*

Correspondence should be addressed to Rosamaria Codispoti; rosamaria.codispoti@unical.it

Received 15 July 2013; Accepted 22 August 2013

Academic Editors: R. Alagirusamy and H. Hong

This Conference Paper is based on a presentation given by Rosamaria Codispoti at "International Conference on Natural Fibers-Sustainable Materials for Advanced Applications 2013" held from 9 June 2013 to 11 June 2013 in Guimarães, Portugal.

This paper deals with the experimental characterization of the tensile behavior of fiber-based composites and flexural strength of natural fiber-reinforced polymer (NFRP) sheets externally glued on masonry bricks, in terms of load capacity and stress distribution along the bonded length. The bricks adopted for this experimentation are solid clay bricks, typically used in ancient masonry structures. Nonimpregnated and impregnated flax, hemp, jute, and sisal fibers were examined. Two types of matrices have been used, polymer matrices and mortar-based matrices. Composite materials defined as NFRP (Natural Fiber Reinforced Polymer) and NFRG (Natural Fiber Reinforced Grout) were obtained.

1. Introduction

In the last few years, the scientific community has shown a particular interest in the use of natural composite materials, focusing on themes related to recyclable, renewable, and environmentally sustainable materials as substitutes of some of the most common man-made fibers. In the civil construction area, several attempts have been done in this field [1]. Recently, the attention has been paid to the possibility of using natural fibers to strengthen masonry structures [2].

Historic masonry buildings show specific challenges when compared to ordinary buildings regarding conservation issues, because of their cultural heritage value and low-strength substrate. Consequently, choosing appropriate strengthening techniques is extremely important and complex. Attention has to be focused on limiting interventions to a minimum, avoiding unnecessary strengthening. This goal is clearly in agreement with the principles of sustainable development.

2. Experimental Plan

The experimental program was organized into two main phases, mechanical characterization of natural materials and study of adhesion between composite systems and masonry. Bidirectional fabrics of flax, hemp, sisal, and jute fibers were used. Tensile tests on fabrics were carried out on impregnated and nonimpregnated fabrics. Two types of matrices were used, polymer matrices and mortar-based matrices. The polymer thermosetting matrices used were epoxy resin and polyester resin in order to produce Natural Fiber Reinforced Polymer (NFRP), while, mortar-based matrices were used in order to produce Natural Fiber Reinforced Grout (NFRG) [3]. In the second part of the experimental plan, three point bending tests and pull-off tests were carried out in order to study the behavior between NFRP composites and the masonry system [4–6]. In this case, flax-based composites and hemp-based composites were used with a thermosetting matrix in epoxy resin, following the results achieved from the tensile tests.

Table 1: Average mechanical properties of matrices (CoV is provided inside parentheses).

	Epoxy resin	Polyester resin	Mortar
Tensile strength [MPa]	53.8 (9.7%)	29.0 (17%)	—
Flexural strength [MPa]	—	—	0.19 (5%)
Compressive strength [MPa]	—	—	11.3 (5%)

Table 2: Stress and Young's Modulus of the NF, NFRP, and NFRG (CoV is provided inside parentheses).

Matrix/fiber	Nonimpregnated		NFRP-Epoxy		NFRP-Polyester		NFRG	
	f_t [MPa]	E [MPa]	f_t [MPa]	E [MPa]	f_t [MPa]	E [MPa]	f_t [MPa]	E [MPa]
Jute	32.9 (14%)	691.5 (11%)	87.3 (31%)	1382.2 (17%)	80.3 (10%)	4135.3 (20%)	25.9 (7%)	531.3 (10%)
Sisal	55.2 (17%)	863.3 (15%)	73.5 (15%)	748.1 (20%)	64.3 (21%)	1431.5 (18%)	35.6 (8%)	345.5 (13%)
Hemp	46.7 (8%)	618.7 (7%)	63.1 (12%)	1674.7 (9%)	58.2 (13%)	1535.0 (9%)	33.1 (8%)	268.2 (5%)
Flax	68.8 (7%)	1746.9 (10%)	117.4 (17%)	1866.6 (20%)	109.8 (17%)	4393.3 (9%)	57.2 (3%)	774.2 (7%)

Table 3: Average of results obtained from three point bending tests (CoV is provided inside parentheses).

Material	F_{max} [kN]	ε [μm/m]	$f_{flexural}$ [kPa]
Brick	4.81 (14%)	—	800 (14%)
Flax	6.49 (2%)	1284 (17%)	1050 (3%)
Hemp	6.18 (4%)	1142 (44%)	980 (3%)

Table 4: Average of results obtained from pull-off tests.

Fiber type	F_{max} [kN]	Tensile strength [kPa]
Flax	2.28 (9%)	1208 (9%)
Hemp	2.38 (4%)	1265 (4%)

2.1. Tensile Tests. Tensile tests on non-impregnated and impregnated fabrics were performed using natural materials, in particular bidirectional fabrics based on flax (w = 388 g/m^2, CoV = 1%), hemp (w = 455 g/m^2, CoV = 2%), jute (w = 254 g/m^2, CoV = 2%), and sisal (w = 1099 g/m^2, CoV = 4%). These four types of natural materials were examined because they have relatively good mechanical proprieties. All the specimens were cut in the warp direction (90°) and in weft direction (0°) with size equal to 300 × 50 mm^2. The test length is equal to 200 mm. Specimens were tested with and without the consideration of the matrix. Each specimen has been equipped with special steel plates on the edges, in order to ensure a uniform distribution of the load and to avoid the specimen from slipping during the test [7]. Specimens with polymer matrix were tested after 15 days from the preparation in order to ensure the proper curing of the matrix, while in the case of the mortar, the experimental tests were carried out after 28 days. Moreover, in the first part of the experimental program, mechanical characterization tests were performed on the matrices used for the production of NFRP and NFRG. Table 1 summarizes the mechanical properties obtained.

2.2. Three Point Bending Tests. To carry out three point bending tests, Portuguese traditional solid clay bricks were used as substrate. These bricks have a compressive strength of 14.3 MPa (CoV = 4%). In particular flax fiber-based composites and hemp-based composites were prepared using a matrix-based thermosetting epoxy resin, which is commonly used in the field of civil applications.

The testing machine is composed of the fixing of three points (Figure 1(a)), two lower supports and striking edge and the load at midspan, with a radius of 125 mm. The sizes of the specimens are schematically indicated in Figure 1(b). Natural fiber-based composites under study have a thickness of t_{fiber} = 3 mm for flax (six specimens, CoV = 16%) and t_{fiber} = 2.5 mm for hemp (six specimens, CoV = 11%). One layer of fabric, previously cut in the warp direction (90° direction) with dimensions equal to 140 × 50 mm^2, for each specimen that was applied to the brick, after the cleaning of the substrate and the primer application. To measure the displacements, two LVDTs were applied to the specimen, one in the midpoint of the brick and another, of control, corresponding to the load cell. However, to know the value of the strain, one strain gage was bonded at the centerline of the composite [8].

2.3. Pull-off Tests. Also for pull-off tests, the same solid clay bricks were used. This type of test was carried out in order to assess the direct tensile strength (mode I) of the composite system. In particular, failure will occur along

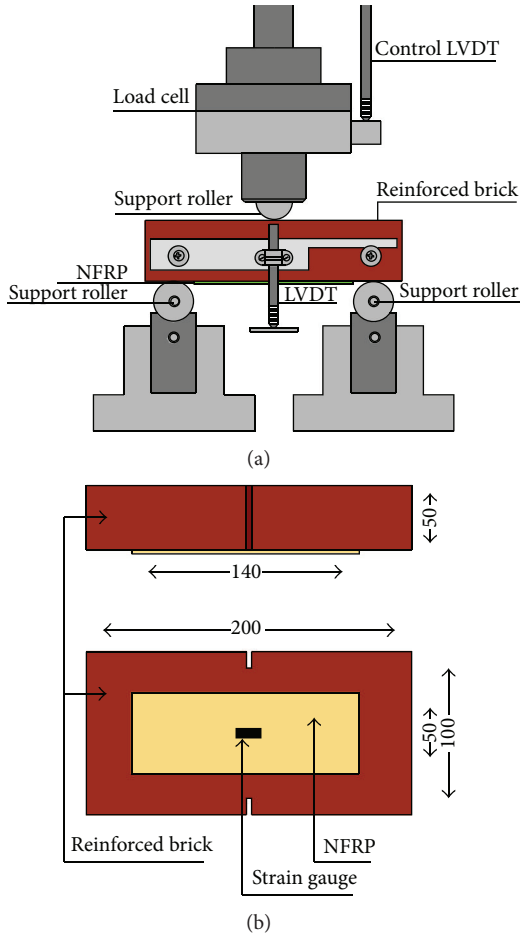

FIGURE 1: Three points bending test: (a) schematic representation for TPBT and (b) specimen's size, plan view and elevation view.

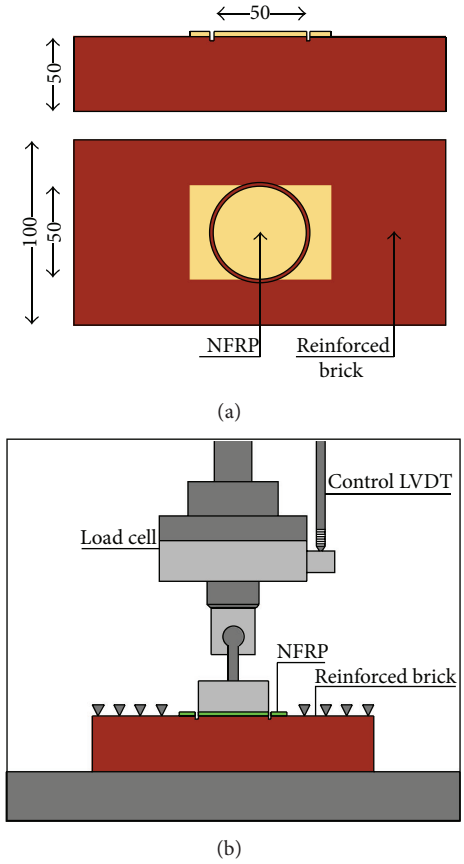

FIGURE 2: Pull-off tests: (a) specimen's size (plan view and elevation view) and (b) schematic representation.

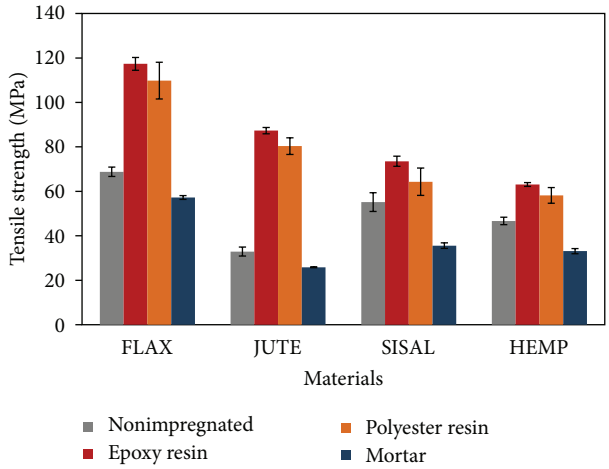

FIGURE 3: Tensile strength-Materials diagram.

the weakest plane within the system composed of the test fixture, adhesive, coating system, and substrate, and will be exposed by the fracture surface. The tests were carried out only on bricks strengthened with flax and hemp fibers. For each type of fabrics, 5 specimens were tested. Following the cleaning of the bricks, the composite system was applied. After primer application, a fiber strip of 70 mm width was glued on the brick (Figure 2(a), plan view). Afterwards, a partial-depth core with 49 mm diameter and 10 mm depth was drilled, see Figure 2(a) (elevation view), which leads to the creation of circular strengthened areas where rigid steel plates were glued. The testing machine is schematically indicated in Figure 2(b). In this case, only the LVDT control was considered, in correspondence to the load cell.

3. Results

3.1. Tensile Tests Results. Experimental tensile tests were carried out according to EN ISO 13934-1/2 [9]. All tensile tests were conducted in a normal atmosphere on specimens previously acclimatized, by means of a high-precision universal testing machine and conducted under displacement control. Before each test, a preload of 10 N (NFRP) and 1.5 N (NFRG) was applied and a velocity equal to 100 mm/min (NFRP) and 25 mm/min (NFRG) was used. The results obtained from the tensile tests are listed in Table 2. It is possible to note that the flax is the material with higher mechanical properties, followed by jute and sisal. Fabrics impregnated with epoxy resin (NFRP) present greater tensile strength than polyester resin, so consequently it can be stated that the epoxy resin is the most suitable from the mechanical point of view as a matrix of the natural fiber composite materials

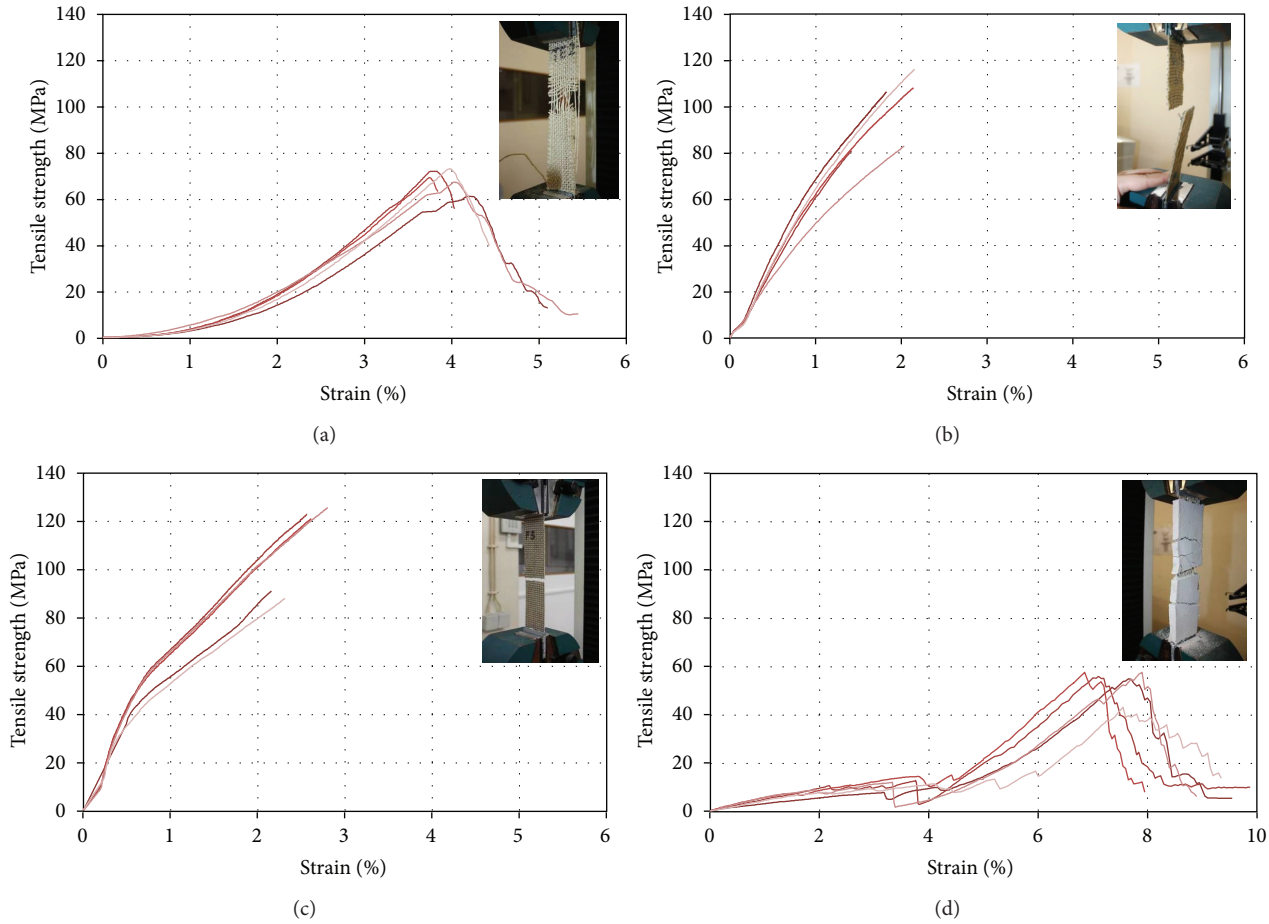

FIGURE 4: Failure modes for the flax-based composites, (a) nonimpregnated fabrics, (b) NFRP-epoxy, (c) NFRP-polyester, and (d) NFRG.

was tested. Concerning the fabrics with the cement-based matrix, further studies are still needed, especially regarding the thickness of the mortar which is to be applied to the specimen and the relation between water and the fibers. The results can also be observed in Figure 3. In previous tests done by the authors [10], it was observed that the fabrics have a higher strength at 90° (warp), rather than at 0° (weft), for this reason Table 2 shows the relative values obtained in the warp direction only. Figure 3 shows the different levels of strength of the natural fiber composite examined with the different matrices used.

For the different strengthening systems used, it is ofprimary importance to discuss the failure modes of the specimens. In the case of non-impregnated specimens, there is a reduction of the area of the individual yarns that makes up the fabric (Figure 4(a)) with a softening final part, while in the impregnated specimens with the polymer matrix, epoxy (Figure 4(b)), and polyester (Figure 4(c)), it is possible to notice an instantaneous and uniform break of the specimen with a particular hardening final part. Finally, in the case of the cement-based composite, the failure mode occurs slowly marked by the rupture of the mortar at the beginning and follows the break/stretching of single yarns that make up the fabric (Figure 4(d)). Figure 4 is relative to flax-based composites, but a similar behavior was found for the other three types of fibers tested.

3.2. Three Point Bending Tests Results. Experimental tests were carried out according to BS EN 1015-11:1999 [10]. However, the tests carried out in this present work differ from the tests described in the standard procedure; in the current test, the specimens are bigger ($200 \times 100 \times 50\,\text{mm}^3$) and they are masonry bricks externally strengthened with natural fiber-reinforced sheets.

These tests were carried out in order to analyze the load capacity between unreinforced and reinforced masonry bricks. The results obtained demonstrate that the reinforced bricks are more resistant when compared to unreinforced bricks, as expected. Indeed, it is possible to note that the reinforced bricks are characterized by an increment of flexural resistance of almost 38% with flax and 32% with hemp (see also Table 3).

The failure mode of the specimens is characterized by the breakage of the specimen in the section at the mid-span. This mode is the same for both flax-based reinforced and hemp-based reinforced bricks (Figures 5(a) and 5(b)).

3.3. Pull-off Tests Results. Experimental pull-off tests were performed under displacement control. These tests were performed following the guideline ASTM D4541-02 [11]. Table 4 illustrates the average pull-off test results for the two types of fibers used (flax and hemp). The results indicate that the pull-off strength is practically independent of the

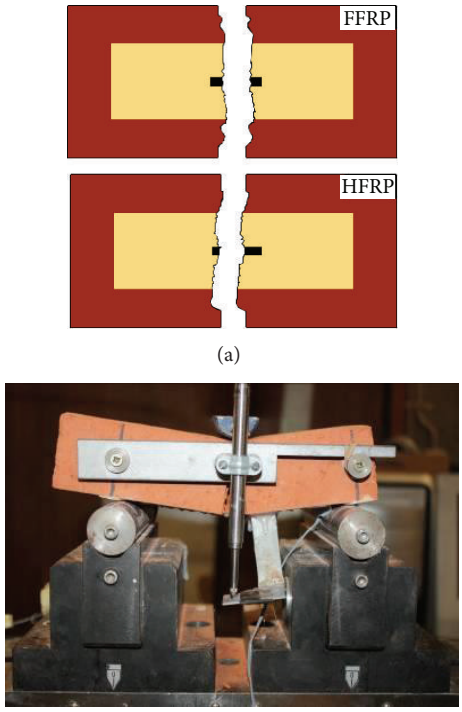

(a)

(b)

Figure 5: (a) Schematic failure modes for TPBT and (b) testing machine.

fiber, in fact the same value of tensile bond strength can be observed. This feature can be explained based on the failure behavior registered. For all specimens tested, failure was characterized by the ripping of a thin layer of brick (peeling), as illustrated in Figure 6. Indeed, the results show that the tensile strength of the interfaces depends on the tensile strength of the substrate, and therefore of the bricks, which is the weakest element of the NFRP-resin-substrate composite system under direct tensile loading.

4. Main Conclusions

Natural fiber-based composite materials have a wide variety of mechanical properties. This is a consequence of the fact that the properties of natural materials are influenced by several variables, as the type of fiber, the diameter of the fibers, the environmental conditions, and possible methods of fiber treatment [5, 7, 8]. This is also confirmed by the variety of the results obtained and shown in this paper, especially in the case of tensile tests. It is possible to note that flax is the material with higher mechanical properties, followed by jute and hemp; low performances were obtained with sisal fibers. However, these first data obtained, confirm the significant development that the natural materials are acquiring in the function of their biodegradability, low cost, low relative density, adequate specific resistance, and renewable nature.

Experimental tensile, three point bending, and pull-off results provided an effective base to deal with a more detailed study of the adhesion between the NFRP composites and the masonry substrates. The primary problem always present is

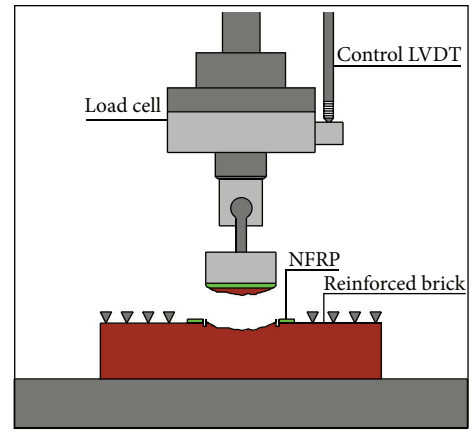

(a)

(b)

Figure 6: (a) Schematic failure modes for PT and (b) specimens tested.

the interfacial adhesion between the natural fiber and the matrix. It determines the final properties of a composite. The results obtained from the tests carried out show that the composites produced with epoxy or polyester resin matrixes increase considerably the mechanical properties of the composite systems based on natural fibers, even more than composites produced with inorganic-based matrices (mortar).

Acknowledgments

Authors would like to thank the Laboratory of Structures and Fibrous Materials Laboratory at the University of Minho. The first author also thanks engineer M. Jorge that contributed greatly to the preparation of the specimens and the carrying out of the experimental tests. The fibers used were kindly provided by LUSOTUFO and FIDIA s.r.l., to whom the authors are grateful.

References

[1] R. Fangueiro, "Textile structures," in *Fibrous and Composite Materials for Civil Engineering Applications*, Woodhead Publishing, 2011.

[2] D. Chandramohan and K. Marimuth, "A review on natural fibers," *International Journal of Research and Reviews in Applied Sciences*, vol. 8, no. 2, pp. 194–206, 2011.

[3] R. S. Olivito, R. Codispoti, and F. A. Zuccarello, "Applicazione di materiali compositi in fibre naturali e malta cementizia a strutture murarie," in *Atti del XX Congresso Nazionale Associazione Italiana di Maccanica Teorica ed Applicata (AIMETA '11)*, Bologna, Italia, 2011.

[4] R. S. Olivito, A. Venneri, and F. A. Zuccarello, "An experimental equipment for delamination tests of FRP reinforced bricks," in *III Convegno Nazionale Meccanica delle Strutture in Muratura Rinforzate con Compositi (MURICO '09)*, Venezia, Italia, 2009.

[5] D. V. Oliveira, I. Basilio, and P. B. Loureņo, "Experimental bond behavior of FRP sheets glued on brick masonry," *Journal of Composites for Construction*, vol. 15, no. 1, pp. 32–41, 2011.

[6] D. V. Oliveira, I. Basilio, and P. B. Loureņo, "Experimental behavior of FRP strengthened masonry arches," *Journal of Composites for Construction*, vol. 14, no. 3, pp. 312–322, 2010.

[7] R. Codispoti, D. V. Oliveira, R. Fangueiro, R. S. Olivito, and P. B. Lourenço, "Study on natural fiber based composites for strengthening of masonry structures," in *Conferenza Nazionale Analisi delle Sollecitazioni (AIAS '12)*, Vicenza, Italia, 2012.

[8] M. Giglio, A. Gilioli, and A. Manes, "Numerical investigation of a three point bending test on sandwich panels with aluminum skins and Nomex™ honeycomb core," *Computational Materials Science*, vol. 56, pp. 69–78, 2012.

[9] "Tensile properties of fabrics, part 1: determination of maximum force and elongation at maximum force using the strip method, Part 2: determination of maximum force using the grab method," EN ISO, 13934-1 and EN ISO, 13934-2, 1999.

[10] "Methods of test for mortar for masonry, part 11: determination of flexural and compressive strength of hardened mortar," BS EN, 1015-11, 1999.

[11] "Standard test method for pull-off strength of coatings using portable adhesion testers," ASTM D4541-02.